

**Subcellular and functional analyses
of two small heat shock proteins
and protein kinases
from peroxisomes of *Arabidopsis thaliana* L.**

Dissertation
zur Erlangung des Doktorgrades
der Mathematisch-Naturwissenschaftlichen Fachbereiche
der Georg-August-Universität zu Göttingen

vorgelegt von
Changle Ma
aus Zibo, China

Göttingen 2005

D7

Referent: Prof. Dr. Hans-Walter Heldt

Korreferent: Prof. Dr. Ivo Feußner

Tag der mündlichen Prüfung:

1.	INTRODUCTION	
1.1	Peroxisome functions	1
1.1.1	Metabolism of reactive oxygen species	1
1.1.2	Photorespiration and fatty acid β -oxidation	3
1.1.3	Peroxisomes and embryogenesis	5
1.2	Peroxisome biogenesis and degradation	6
1.2.1	Known signals for targeting of matrix proteins to peroxisomes	6
1.2.1.1	The peroxisome targeting signal type 1 (PTS1)	6
1.2.1.2	The peroxisome targeting signal type 2 (PTS2)	8
1.2.2	The mechanism of protein import into the peroxisome matrix	9
1.2.3	Peroxisome degradation	12
1.3	Peroxisome research in post-genome era	14
1.4	Heat shock proteins associated with peroxisomes	15
1.4.1	Plant heat shock proteins in general	15
1.4.2	Heat shock proteins involved in peroxisomal protein import	18
1.5	Protein kinases associated with peroxisomes	20
1.6	Objectives of the present investigation	22
2.	MATERIALS and METHODS	
2.1	Materials	24
2.1.1	Biochemicals	24
2.1.2	Enzymes	24
2.1.3	Kits	25
2.1.4	<i>E. coli</i> and yeast strains	25
2.2	Plant growth conditions	26
2.2.1	Standard growth	26
2.2.2	Stress treatments	26
2.2.3	Growth of <i>Arabidopsis</i> seedlings on agar plates	26
2.3	Molecular cloning	27
2.3.1	RNA isolation	27
2.3.2	Genomic DNA isolation	28
2.3.3	Estimation of the concentration of nucleic acids	29
2.3.2.1	Photometric method	29
2.3.2.2	Gel-electrophoretic method	29

2.3.4	Agarose gel electrophoresis, gel staining and documentation	29
2.3.5	Synthesis of cDNA by reverse transcription	30
2.3.6	Polymerase chain reaction	31
2.3.7	Semi-quantitative RT-PCR	32
2.3.8	PCR-based site-directed mutagenesis	33
2.3.9	Elution of resolved nucleic acid fragments from agarose gel	33
2.3.10	Ethanol precipitation of nucleic acid fragments	33
2.3.11	Ligation of cDNA fragments into destination vectors	34
2.3.12	Preparation of competent cells	34
2.3.12.1	Preparation of DH5 α and XL1-Blue competent cells	34
2.3.12.2	Preparation of <i>Agrobacterium tumefaciens</i> DHA105 competent cells	35
2.3.13	Transformation of competent cells	36
2.3.13.1	Transformation of <i>E.coli</i>	36
2.3.13.2	Transformation of yeast	36
2.3.13.3	Transformation of <i>Agrobacterium tumefaciens</i>	37
2.3.14	PCR screening of transformants	37
2.3.15	Isolation of plasmid DNA	38
2.3.16	Restriction digestion	38
2.3.17	Sequencing	39
2.4	Subcellular localization studies in <i>S.cerevisiae</i> and <i>Allium cepa</i> L.	40
2.4.1	cDNA constructs of peroxisomal small heat shock proteins	40
2.4.2	cDNA constructs of putative peroxisomal protein kinases	41
2.4.3	Subcellular localization studies in <i>S.cerevisiae</i>	42
2.4.4	Subcellular localization analysis in <i>Allium cepa</i> L.	43
2.4.5	Fluorescence microscopy	43
2.5	Yeast two-hybrid analyses	43
2.5.1	cDNA constructs for protein-protein interaction studies using yeast two-hybrid system	43
2.5.2	protein-protein interaction studies by yeast two-hybrid analyses	44
2.5.3	LiAc-mediated yeast co-transformation	44
2.5.4	Colony-lift filter assay	45
2.6	Plant transformation	45
2.6.1	Transformation of <i>Arabidopsis thaliana</i> with <i>Agrobacterium tumefaciens</i>	45
2.6.2	Transformation of onion epidermal cells	46

2.6.2.1	DNA precipitation onto gold particles	46
2.6.2.2	Transformation of onion epidermal cells by bombardment	46
2.7	Southern blotting	47
2.7.1	Digestion of genomic DNA with restriction enzymes	48
2.7.2	Transfer of digested genomic DNA to nylon membrane	48
2.7.3	Hybridization of DNA gel blots	49
2.7.3.1	Labelling of probes	49
2.7.3.2	Hybridization	49
2.8	Yeast complementation studies	50
2.9	Characterization of <i>Arabidopsis</i> T-DNA knock-out mutants	51
2.10	Protein analysis in <i>Arabidopsis</i> peroxisomes	51
2.10.1	Isolation of leaf peroxisomes from <i>Arabidopsis</i>	51
2.10.2	Protein determination-The Lowry Method	52
2.10.3	Protein precipitation	53
2.10.4	Sodium dodecyl sulphate polyacrylamide gel electrophoresis (SDS-PAGE)	53
2.11	Western blotting	54
3. RESULTS		55
3.1	Identification and characterization of two small heat shock proteins targeted to the matrix of plant peroxisomes	55
3.1.1	Protein identification, polypeptide structure, and peroxisome targeting prediction	55
3.1.2	Localization of AtHsp15.7 to the peroxisome matrix	58
3.1.2.1	Subcellular targeting analysis of EYFP fusion proteins	58
3.1.2.2	Biochemical identification of AtHsp15.7 in leaf peroxisomes isolated from <i>Arabidopsis</i>	61
3.1.3	Localization of AtAcd31.2 to the peroxisome matrix	63
3.1.4	Complementation of a yeast mutant deficient in cytosolic sHsps	67
3.1.5	Expression analysis of peroxisomal sHsps	70
3.1.5.1	Tissue and developmental specific expression of <i>Arabidopsis</i> sHSPs	70
3.1.5.2	Differential expression of <i>AtHSP15.7</i> and <i>AtACD31.2</i> under temperature stress conditions	72
3.1.5.3	Differential expression of <i>AtHSP15.7</i> and <i>AtACD31.2</i> under oxidative stress	73

3.1.6	<i>Arabidopsis</i> T-DNA insertion mutants deficient in one or both peroxisomal sHsps	76
3.1.6.1	Isolation of <i>hsp15.7</i> T-DNA insertion mutants	76
3.1.6.2	Isolation of an <i>acd31.2</i> T-DNA insertion mutant	79
3.1.6.3	Isolation of a sHsp double mutant	80
3.1.7	<i>hsp15.7-3</i> mutant shows a germination defect under heat stress	81
3.2.	Identification and characterization of putative peroxisomal protein kinases (PPPKs) in <i>Arabidopsis</i>	83
3.2.1	Identification of PPPKs in <i>Arabidopsis</i> genome by bioinformatics tools	83
3.2.2	Subcellular targeting analysis of PPPKs in <i>Saccharomyces cerevisiae</i>	85
3.2.3	Subcellular targeting analysis of PPPKs in <i>Allium cepa</i> L. (onion) epidermal cells	89
3.2.4	Analysis of the peroxisome targeting ability of putative peroxisome targeting domain (PTD) of PPPKs <i>in planta</i>	90
3.2.5	Definition of auxiliary and inhibitory elements for peroxisome targeting	92
3.2.6	PPPK7 does not interact with the PTS1 receptor PEX5 in the yeast two-hybrid system	94
3.3.	Characterization of two ATG proteins that may be involved in peroxisome degradation	96
3.3.1	Identification of a potential regulatory subunit of PPPK4 (AtAtg1a)	97
3.3.2	Expression profile of <i>Arabidopsis</i> homologs of <i>AtATG1</i> and <i>AtATG13</i>	99
3.3.3	Peroxisome targeting analysis of AtAtg13a	101
3.3.4	AtAtg1a and AtAtg13a interact with each other in the yeast two-hybrid system	101
4.	DISCUSSION	104
4.1	Two novel small heat shock proteins located in the peroxisome matrix	104
4.1.1	Experimental validation of the postulated targeting of two small Hsps to plant peroxisomes	104
4.1.2	Is EYFP-AtAcd31.2 targeted to peroxisomes in a "piggyback" fashion?	108
4.1.3	Why do plants require sHsps in the peroxisome matrix?	111
4.1.4	Towards an elucidation of the function of peroxisomal sHsps	113
4.1.4.1	The two peroxisomal sHsps have a complementary expression profile	113
4.1.4.2	AtHsp15.7 and AtAcd31.2 are indeed small Hsps	115
4.1.4.3	Towards elucidation of the function of peroxisomal sHsps <i>in planta</i>	116

4.1.5	Peroxisomal Hsps acting in concert with AtHsp15.7 and AtAc31.2	117
4.2	Towards an identification of peroxisomal matrix-targeted protein kinases	119
4.2.1	Identification of <i>Arabidopsis</i> putative peroxisomal protein kinases (PPPKs) by a bioinformatics approach	119
4.2.2	Multiple factors are responsible for alternate subcellular targeting of PPPKs in yeast and plant expression systems	122
4.2.3	PPPKs with a functional PTS domain	125
4.2.4	New insights into the nature of auxiliary targeting enhancing and inhibitory elements of PTS1 domains	127
4.2.5	The PTS1 AKI> of PPPK7 is non-functional	129
4.2.6	Do AtAtg1a and AtAtg13a play a role in the pexophagy?	130
5.	SUMMARY	133
6.	REFERENCE	135
7.	APPENDICES	147
7.1	Primers used for gene cloning and subcloning	147
7.2	Abbreviations	150

ACKNOWLEDGEMENT

1. INTRODUCTION

1.1 Peroxisome functions

Peroxisomes are globular organelles that are surrounded by a single lipid bilayer membrane. They are found ubiquitously in eukaryotic cells and, depending on the organism, tissue type, and developmental stage, can differentiate into several metabolically specialized variants (Beevers, 1979; Purdue and Lazarow, 2001). According to the developmental stage and the enzyme content specific for the physiological role of the organelles, plant peroxisomes are categorized into three classes, namely glyoxysomes, leaf peroxisomes, and unspecialized peroxisomes (Beevers, 1979). In addition, in cells of uninfected leguminous root nodules or senescing plant tissue, specific variants of peroxisomes also exist (Webb and Newcomb, 1987; Vicentini and Matile, 1993). A fundamental process of peroxisomes is the production of hydrogen peroxide (H_2O_2) and its subsequent degradation by catalase (Purdue and Lazarow, 2001), although the metabolic function of peroxisomes is often specialized by tissue types and developmental stages. In higher plants, peroxisomes play a pivotal role in three metabolic pathways: fatty acid β -oxidation, photorespiration, and H_2O_2 degradation. However, recent studies of *Arabidopsis* mutants and post-genomic approaches are also shedding new light on important functions of peroxisomes in plant development, (photo-) morphogenesis, and hormone biosynthesis (Hayashi and Nishimura, 2003; Baker and Sparkes, 2005).

1.1.1 Metabolism of reactive oxygen species

Reactive oxygen species (ROS), including the superoxide anion radical ($O_2^{\cdot-}$), hydrogen peroxide (H_2O_2), and hydroxyl radicals ($\cdot OH$), are by-products of normal physiological reactions of peroxisomes (Fig. 1.1). In plants, at least three major metabolic processes contribute to the generation of H_2O_2 : the glycolate oxidase reaction during photorespiration, β -oxidation of fatty acids, and the dismutation of $O_2^{\cdot-}$ (del Rio et al., 2002). The abundant H_2O_2 production is mainly counteracted by peroxisomal catalase that catalyses the degradation of H_2O_2 to water and oxygen. However, catalase is a light-sensitive enzyme and has a rather low turnover rate (Hertwig et al., 1992; Grotjohann et al., 1997).

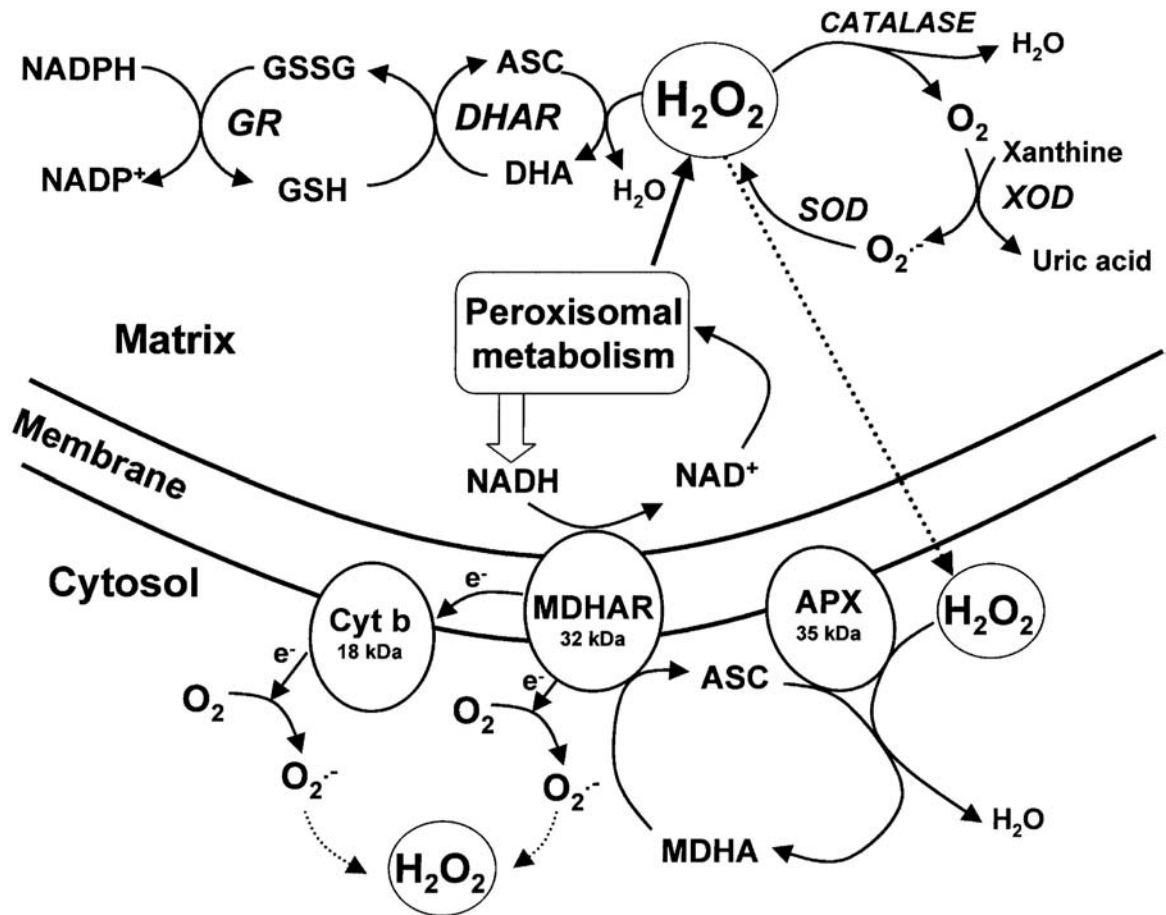


Figure 1.1: Model proposed for the production of ROS in plant peroxisomes and their subsequent detoxification by multiple scavenging systems (according to del Rio et al., 2002).

The oxidation of xanthine by xanthine oxidase (XOD) in the matrix and of NADH in the peroxisomal membrane by monodehydroascorbate reductase (MDHAR) are responsible for the generation of superoxide anion radicals ($O_2^{\cdot-}$). Three major metabolic pathways contribute to the generation of H_2O_2 , namely, photorespiration, fatty acid β -oxidation, and the dismutation of $O_2^{\cdot-}$. These ROS are scavenged by the cooperation of superoxide dismutase (SOD), catalase (CAT), and the ascorbate-glutathione cycle in leaf peroxisomes. ASC, ascorbate peroxidase; APX, ascorbate peroxidase; DHA, dehydroascorbate; GSH, reduced glutathione; GSSG, oxidized glutathione; GR, glutathione reductase; MDHA, monodehydroascorbate.

Reduced peroxisomal catalase activity in catalase-deficient plants has previously been reported to result in increased sensitivity of the plant to a variety of environmental stresses, including ozone and salt stress, confirming an important role of catalase in ROS scavenging (Kendall et al., 1983; Willekens et al., 1997; Vandenabeele et al., 2004). A small portion of H_2O_2 can additionally be removed by cooperative enzymatic reactions of the ascorbate-glutathione cycle that has been demonstrated to partly localize to the peroxisomal membrane. The ascorbate-glutathione cycle is composed of two non-enzymatic antioxidants, ascorbate and glutathione, and four antioxidative enzymes, namely ascorbate peroxidase,

monodehydroascorbate reductase, dehydroascorbate reductase, and glutathione reductase (Jimenez et al., 1997; del Rio et al., 2002; Chew, 2003; Fig. 1.1). This cycle was first identified in chloroplasts, but it is also thought to exist in peroxisomes because the four antioxidative enzymes were identified in microbodies purified from pea leaves (Jimenez et al., 1997). Genes encoding peroxisomal ascorbate peroxidase and monodehydroascorbate reductase have been identified in several plant species (Zhang et al., 1997; Ishikawa et al., 1998; Lisenbee et al., 2005; Leterrier et al., 2005). An advantage of the presence of ascorbate peroxidase and monodehydroascorbate reductase in the peroxisomal membrane could be a more efficient protection against H_2O_2 leaking from peroxisomes when catalase activity is reduced, resulting in an accumulation of H_2O_2 . These enzyme activities could thus ensure *in situ* degradation of ROS (del Rio et al., 2002).

In peroxisomes from pea leaves and watermelon cotyledons, at least two pathways have been demonstrated by biochemical methods to be involved in the generation of $O_2^{\cdot-}$: the oxidation of xanthine and hypoxanthine to uric acid catalysed by xanthine oxidase in the peroxisome matrix and the oxidation of NAD(P)H in the peroxisomal membrane (del Rio et al., 2002). $O_2^{\cdot-}$ is quickly converted to H_2O_2 and O_2 by superoxide dismutase (SOD, Beyer et al., 1991). The enzyme SOD belongs to a family of metalloenzymes, the members of which are distributed over several subcellular compartments, including the cytosol, chloroplasts, mitochondria, and peroxisomes (del Rio et al., 2002, 2003; Chu et al., 2005).

1.1.2 Photorespiration and fatty acid β -oxidation

Photorespiration is a light-dependent metabolic salvage pathway that converts phosphoglycolate, the oxygenation product of ribulose-1,5-bisphosphate, into phosphoglycerate, with concomitant release of CO_2 and NH_3 . Photorespiration is coordinated between three cellular compartments: chloroplasts, peroxisomes, and mitochondria (Douce and Heldt, 2000; Reumann, 2002). At least sixteen enzymes and six membrane translocators are involved in the photorespiratory pathway (Douce and Heldt, 2000). The recycling of phosphoglycolate is one of the main functions of leaf peroxisomes, which house several enzymes involved in photorespiration, including the flavin-dependent glycolate oxidase, serine-glyoxylate aminotransferase, glutamate-glyoxylate aminotransferase, aspartate-glyoxylate aminotransferase, hydroxypyruvate reductase, and malate dehydrogenase. Despite their important role in photorespiration, genes encoding serine (alanine)-glyoxylate

aminotransferase and glutamate-glyoxylate aminotransferase have only recently been cloned (Liepman and Olsen, 2001, 2003; Igarashi et al., 2003).

Fatty acid β -oxidation is the pathway by which germinating seeds mobilize their lipid stores to supply the establishing seedling with carbon skeletons and, ultimately, via succinate oxidation with energy. In plants, β -oxidation occurs exclusively in peroxisomes (Hooks, 2002). For their degradation, free fatty acids first need to be imported into peroxisomes, presumably via an ATP-binding cassette transporter (Zolman et al., 2001). Next, the free fatty acids are activated to acyl-CoA thioesters by peroxisomal acyl-CoA synthases. The CoA-bound acyl chains are repeatedly cleaved to release acetate units by the cooperation of four enzymes, including acyl-CoA oxidase (catalyzing the first step of β -oxidation), enoyl-CoA hydratase, β -hydroxy-acyl-CoA dehydrogenase (catalyzing the hydration and dehydration steps by the activities of multifunctional proteins), and 3-ketoacyl-CoA thiolase (catalyzing the thiolytic cleavage step) (Graham and Eastmond, 2002). The β -oxidation product, acetyl-CoA, is mainly converted to succinate, by the glyoxylate cycle through the coordination of peroxisomal citrate synthase, cytosolic aconitase, and the peroxisomal enzymes isocitrate lyase, malate synthase, and malate dehydrogenase. Succinate is then metabolized either via the tricarboxylic acid (TCA) cycle to oxaloacetate, or via mitochondrial respiration, yielding reducing equivalents or ATP, respectively. In gluconeogenesis, oxaloacetate is converted to phosphoenolpyruvate and ultimately to sucrose. Most genes encoding enzymes involved in β -oxidation and the glyoxylate cycle have previously been characterized (Hayashi and Nishimura, 2003).

Peroxisomal fatty acid β -oxidation is not only important during seedling establishment, but also involved in the production of plant hormones, including jasmonic acid, auxin, and possibly salicylic acid (Sanders et al., 2000; Stinzi and Browse, 2000; Zolman et al., 2001; Reumann et al., 2004; Adham et al., 2005). The biosynthesis of jasmonic acid, auxin, and salicylic acid is thought to take place in peroxisomes by shortening of the side chain of the corresponding precursors by β -oxidation cycles. Peroxisomal proteins, such as 12-oxo-phytodienoic acid 10, 11-reductase isoform 3, β -hydroxyisobutyryl-CoA hydrolase 1, and acyl-CoA oxidase, all of which are critical for the biosynthesis of jasmonic and indole acetic acid, have been identified by reverse or forward genetic approaches (Sanders et al., 2000; Stinzi and Browse, 2000; Zolman et al., 2001; Adham et al., 2005).

1.1.3 Peroxisomes and embryogenesis

In addition to their well-established metabolic functions, peroxisomes also play an essential role in development. Peroxins (Pex) are proteins that are required for peroxisome biogenesis. The peroxins Pex2, Pex10, and Pex12 are integral peroxisomal membrane proteins. They possess RING finger domains that are characteristic elements of E3 ubiquitin ligases, which play a crucial role in defining substrate specificity and subsequent protein degradation by the 26S proteasome (Hershko and Ciechanover, 1998). These three peroxins are hypothesized to function in close proximity to facilitate the import of cargo proteins and the recycling of receptors in yeast and mammals, and possibly in other eukaryotes (Erdman and Schliebs, 2005)

PEX2, *PEX10* and *PEX12* encode essential peroxins in plants because null mutations of either gene caused embryonic lethality (Hu et al., 2002; Schumann et al., 2003; Sparkes et al., 2003; Fan et al., 2005). The *PEX2* gene was first identified as a dominant suppressor of the *det1* mutant, which showed an aberrant photomorphogenesis. Antisense transgenic plants with reduced *PEX2* transcripts are dwarfs, are reduced in chlorophyll content, and are sterile, whereas the *pex2* null mutant is embryonic lethal (Hu et al., 2002). The phenotype of the *pex10* null mutant is similar to that of *pex2*. The T-DNA knock-out mutant was embryo lethal at the heart stage of embryogenesis. Electron microscopy of the embryos of this mutant revealed defects in the formation of lipid bodies, protein bodies, and an accumulation of ER-derived membrane stacks instead of peroxisomes (Schumann et al., 2003). The embryos of the *pex12* null mutant are aborted at an early stage of embryogenesis. RNA interference (RNAi) plants with reduced *PEX12* mRNA levels showed an inhibition of reproductive growth, as indicated by smaller gynoecia and shorter stamens, contained a reduced number of peroxisomes, and showed a significantly weaker fluorescence of peroxisome-targeted enhanced yellow fluorescent protein (EYFP-PTS1) in peroxisomes (Fan et al., 2005).

Several mechanisms have been proposed for the role of peroxisomes in embryo development: (1) peroxisomes may play an essential nutritional role in embryogenesis, which requires fatty acid β -oxidation to provide carbon skeletons and ultimately energy; (2) loss of peroxisome function may result in the accumulation of toxic levels of ROS; (3) peroxisomes may be a source of yet-to-be identified signalling molecules that are necessary for embryo development (Sparkes et al., 2003; Fan et al., 2005).

1.2. Peroxisome biogenesis and degradation

Unlike mitochondria and chloroplasts, peroxisomes do not contain a separate genome or DNA. Therefore, all peroxisomal proteins are encoded by the nuclear genome. Soluble peroxisomal proteins are synthesized on free ribosomes in the cytosol and post-translationally targeted to peroxisomes (Purdue and Lazarow, 2001). Typically, the import of peroxisomal matrix proteins occurs via one of two pathways, which are characterized by specific targeting signals. The peroxisomal targeting signal type 1 (PTS1) is a unique tripeptide sequence (SKL> and related variants) found in the C-terminal end of the proteins (Gould et al., 1989). The PTS2 is a nonapeptide (typically RLX₅HL and related variants) which is located within the first 30 to 40 amino acids at the amino-terminal end (Swinkels et al., 1991). The import of PTS1 and PTS2 proteins requires more than 20 peroxins encoded by PEX genes (Titorenko and Rachubinski, 2001).

1.2.1 Known signals for targeting of matrix proteins to peroxisomes

1.2.1.1 The peroxisome targeting signal type 1 (PTS1)

Most peroxisomal matrix proteins are targeted to peroxisomes by a PTS1, a C-terminal tripeptide that interacts directly with a specific cytosolic receptor, Pex5 (Johnson and Olsen, 2001). The first PTS1 to be characterized was that of the firefly luciferase, which contains the PTS1 serine-lysine-leucine (SKL>). Site-directed mutagenesis experiments revealed that only a limited number of conservative changes were allowed in the PTS1 SKL>, leading to deduce of the PTS1 consensus sequence [SAC][KRH]L> (Gould et al., 1989). However, this consensus sequence became increasingly degenerated as different organisms were discovered to have related but specialized PTS1 sequences. In *Saccharomyces cerevisiae*, a large variety of PTS1 tripeptides were deduced from complementation studies on yeast mutants of peroxisomal malate dehydrogenase (MDH3) using *MDH3* constructs, whose native PTS1 tripeptide was replaced by PTS1-related variants. Some of the tripeptides found to work as PTS1 in yeast, including SEL>, SSL>, and EKL>, do not fit the consensus sequence determined for mammals and plants (Elgersma et al., 1996).

Studies comparing the peroxisomal targeting efficiency of β -glucuronidase constructs, to which various C-terminal tripeptides were fused, revealed the first plant-specific PTS1 consensus sequence [SACP][KR][LMV]>, the so-called Hayashi motif (Hayashi et al., 1996).

In a follow-up study, a more permissive consensus motif ([SACGT][KRHLN][LMIY]>) was deduced by using a slightly different experimental system consisting of the reporter protein chloramphenicol acetyltransferase and transient expression in BY-2 suspension-cultured cells of tobacco (*Nicotiana tabacum*, Mullen et al., 1997). Kragler et al. (1998) deduced the most permissive PTS1 motif based on the interaction of PTS1 tripeptides with tobacco Pex5 in the yeast two-hybrid system, which also allowed a proline residue at position -3 ([SACGTP][KRHLN][LMIY]>).

With the availability of large numbers of DNA sequences in the public databases, bioinformatics approaches can be applied to specify plant PTS1 signals. Reumann (2004) specified the C-terminal tripeptides by retrieving plant cDNAs and expressed sequence tags (ESTs) that are homologous to PTS1-targeted proteins from the public protein sequence and EST databases. According to this study, nine PTS1 tripeptides ([SA][RK][LM] without AKM> plus SRI> and PRL>) were identified in at least 10 sequences and three different orthologous groups are defined as major PTS1. Furthermore, eleven additional PTS1 tripeptides, including some previously unknown plant PTS peptides, were defined as minor PTS1. These analyses strongly suggested that not all 24 tripeptides of the Hayashi motif [SACP][KR][LVM]> and in particular not those 100 to 120 PTS1 peptides of the more permissive PTS consensus motifs are functional PTS1 tripeptides *in vivo*. Instead, a pronounced preference seems to exist in plants for a small set of specific PTS1 tripeptides.

In addition to the tripeptide at the very C-terminal end, accessory elements upstream of the PTS1 have been hypothesized to be important for peroxisomal targeting, in particular for some weak or non-canonical PTS1 peptides (Reumann, 2004). For instance, a basic residue at position -4 can act as an accessory element in some proteins. As demonstrated for the PTS1s of human catalase (ANL>) and rat and human 2-methylacyl-CoA racemase (ANL> and ASL>, respectively), a lysine residue located at the position immediately upstream of the PTS1 tripeptide was found to be essential for peroxisomal targeting (Purdue et al., 1996; Amery et al., 2000; Kotti et al., 2000). Furthermore, residues about 20 upstream of the PTS1 tripeptide can act as accessory elements. In peptides interacting with human Pex5, hydrophobic residues were found with high frequency especially at positions -2 and -5, whereas peptides interacting with *S. cerevisiae* Pex5 were more hydrophilic and frequently contained arginine at position -2 (Lametschwandtner, et al., 1998). The PTS1 domain of plant PTS1-targeted proteins is characterized by a high probability of proline and a second

basic residue in front of the PTS1, as revealed by bioinformatics analyses (Reumann, 2004). Finally, some PTS1 tripeptides have been shown to require sequences located even further upstream of the PTS1 for successful targeting to peroxisomes. For instance, the tripeptide KKL> of human alanine-glyoxylate aminotransferase must cooperate with an ancillary targeting element located between amino acid residues Val³²⁴ to Ile³⁴⁵, i.e. about 50 residues upstream of the PTS1 tripeptide (Huber et al., 2005).

1.2.1.2 The peroxisome targeting signal type 2 (PTS2)

Compared to the large number of proteins that carry a PTS1 peptide, only few proteins that contain a PTS are known. The first PTS2 peptide identified was RLx₅HL, which was located in the N-terminal end of rat thiolase (Swinkles et al., 1991). Subsequent analyses revealed that PTS2 nonapeptides are conserved in yeast, plants, and mammals but that species-related differences also exist. Intriguingly, *Caenorhabditis elegans* lacks any gene encoding the PTS2 receptor Pex7 as well as any PTS2-targeted proteins. In this phylogenetic lineage, the PTS2 targeting pathway seems to have been lost during evolution (Motley et al., 2000). In contrast to yeast, the N-terminal domain including the PTS2 peptide is cleaved off upon arrival of the proteins in the peroxisome matrix in plants and mammals (Johnson and Olsen, 2001).

The PTS2 consensus motif of yeast and mammals has been defined as [RK][LVI]x₅[HQ][LA] by site-directed mutagenesis (Tsukamoto et al., 1994; Glover et al., 1994). The first plant-specific PTS2 consensus motif has been determined by mutational analysis of the PTS2 of citrate synthase and malate dehydrogenase in combination with sequence comparison of known plant PTS2 proteins (R[ILQ]x₅HL, Kato et al., 1996, 1998). A very broad PTS2 motif ([RK]x₆[HQ][ALF]), which is similar to that specified for yeast and mammals, was deduced based on targeting experiments with the mutagenized presequence of rat thiolase (Flynn et al., 1998). In contrast to these experimental studies and similar to the bioinformatics-based definition of the PTS1, a relatively small number of two major (R[LI]x₅HL) and nine minor PTS2 nonapeptides (R[QTMAV]x₅HL and RLx₅H[IF]) have been defined for higher plants (Reumann, 2004).

1.2.2 The mechanism of protein import into the peroxisome matrix

The import of peroxisomal matrix proteins into peroxisomes follows at least four defined stages: (i) receptor and cargo recognition, (ii) docking of the receptor-cargo complex at the peroxisomal membrane, (iii) translocation of the receptor-cargo complex, and (iv) recycling of receptors (Eckert and Erdmann, 2003; Baker and Sparkes, 2005; Fig. 1.2).

After translation on free ribosomes in the cytosol, the PTS1 and PTS2 of peroxisomal matrix proteins are recognized by the cytosolic receptor Pex5 and Pex7, respectively (Purdue and Lazarow, 2001). The first ortholog of the PTS1 receptor was identified in *Pichia pastoris*. The receptor Pex5 binds directly to the PTS1 peptide and is essential for the import of PTS1 proteins (McCollum et al., 1993). All homologs of Pex5 contain a conserved C-terminal domain that comprises up to 7-9 tetratricopeptide repeat (TPR) motifs which interact with the PTS1 signal. As revealed by the three-dimensional structure of the TPR domain of human Pex5 co-crystallized with a PTS1 peptide, the TPRs 1-3 and 5-7 form two clusters that are linked by TPR4. The structure reveals that three highly conserved asparagine residues located within TPR5-7 and the negatively charged patch of strictly conserved glutamic acid residues in TPR1-3 contribute to the recognition of PTS1 tripeptides (Gatto et al., 2001). Single amino acid substitutions in the conserved residues of the TPR domain dramatically reduced or even abolished the affinity between Pex5 and PTS1 proteins, which can lead to severe peroxisomal diseases in mammals (Dodt et al., 1995).

The PTS2 receptor Pex7 consists of seven WD repeats, which are characterized by the presence of a 43-amino acid repeat domain, each containing a central Trp-Asp motif (Purdue et al., 1997). The delivery of PTS2 proteins to peroxisomes can not be fulfilled by Pex7 alone, but requires the co-operation with Pex18 and Pex21 in *S. cerevisiae* or Pex20 in *Yarrowia lipolytica* for correct and sufficient PTS2 import. Mammals and plants appear to lack orthologs of Pex18, Pex20 and Pex21. However, the long isoform Pex5L of mammals and *Arabidopsis* Pex5 can bind to Pex7 and substitute for ScPex18 and ScPex20 in the PTS2 targeting pathway (Matsuzono et al., 1999; Einwachter et al., 2001; Sparkes and Baker, 2002; Hayashi et al., 2005; Woodward and Bartel, 2005). The dependence of Pex7 on Pex5 interaction and PTS2 pathway deficiencies in *pex5* mutants provides direct evidence that the PTS1 and PTS2 pathways is similarly coupled in the receptor-cargo recognition step in mammals and plants (Matsumura et al., 2000; Sparkes and Baker, 2002; Woodward and Bartel, 2005; Hayashi et al., 2005).

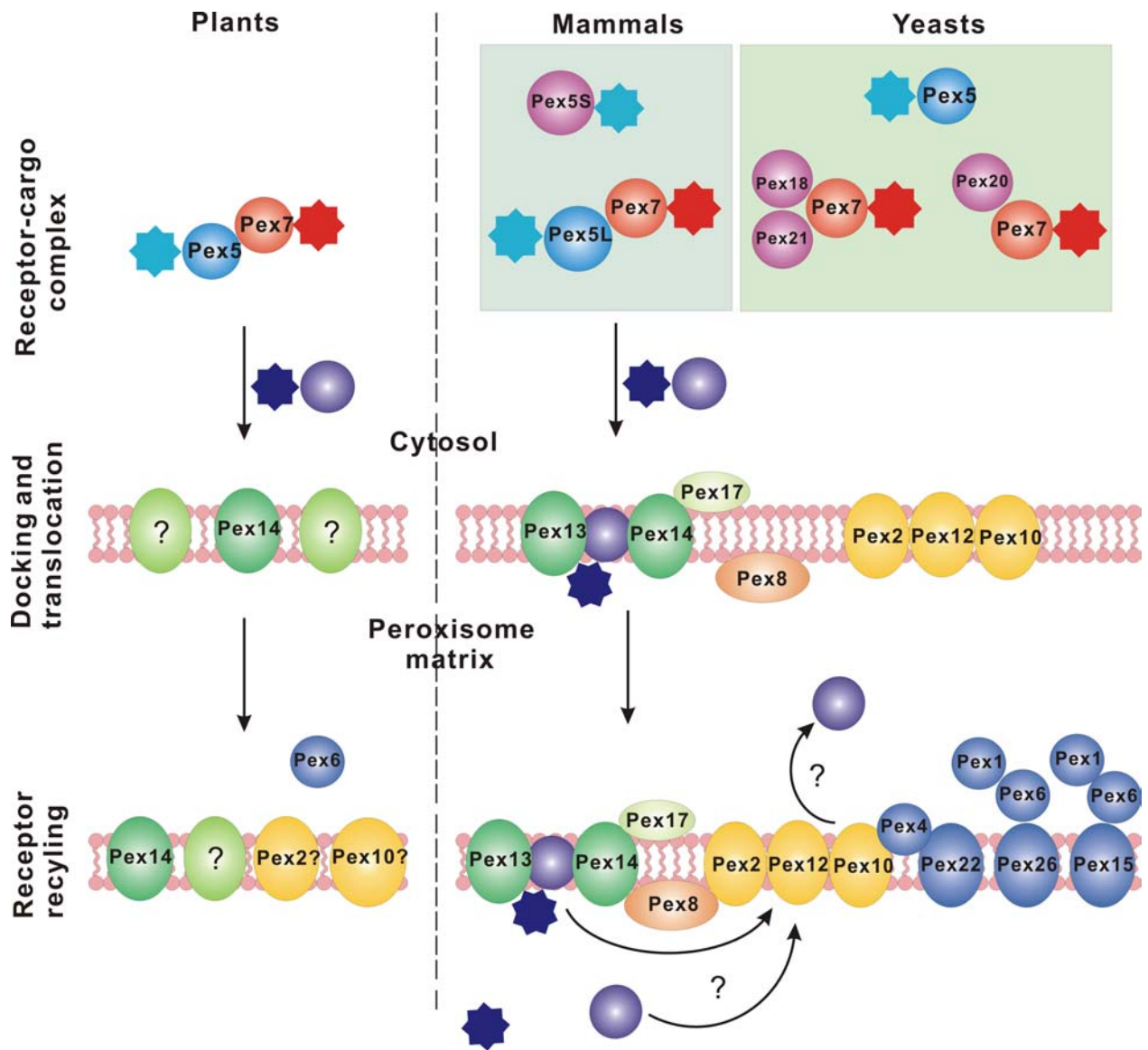


Figure 1.2: Import of peroxisomal matrix protein (according to Baker and Sparkes, 2005).

Receptor–cargo complexes composed of cargo proteins containing PTS1 (blue star) or PTS2 (red star) bind to receptors Pex5 or Pex7, respectively. The Pex7–cargo complex requires accessory factors for import; in plants and mammals it binds Pex5, in *S. cerevisiae* Pex18 and Pex21, and in *Neurospora crassa* Pex20. Pex18 is able to functionally replace the amino terminus of Pex5 for receptor docking. The receptor–cargo complex in yeast and mammals docks at the membrane. The protein components that are involved in docking, Pex13, Pex14 Pex17, are coloured green. It is unclear whether the receptor translocates fully into the matrix or remains associated with the translocation complex. In *S. cerevisiae*, Pex8 has been shown to bridge two complexes involved in cargo-docking (green; Pex13, Pex14 and Pex17) or translocation (yellow; Pex2, Pex10 and Pex12) in yeast and mammals. Additional protein components that are involved in steps downstream of receptor–cargo translocation are shown in blue (Pex4, Pex22, Pex26, Pex15, Pex1 and Pex6) Pex6 binds Pex15 or Pex26 in *S. cerevisiae* or in humans, respectively. It is unclear how receptors are recycled back to the cytosol for further rounds of import.

The cargo-receptor complex docks at the peroxisomal membrane mediated by interactions between receptors and peroxins embedded in the peroxisomal membrane. Pex13, Pex14, and Pex17 have been proposed to serve as the docking complex in *S. cerevisiae* (Purdue and Lazarow, 2001). Pex13 is an integral membrane protein that contains a Src-homology-3 domain and exposes both polypeptide ends to the cytosol. The Src-homolog-3 domain of Pex13 mediates docking of Pex5 and the binding to Pex14, while the N-terminal domain of Pex13 binds Pex7 (Albertini et al., 1997; Pires et al., 2003). The peroxin Pex14 is a peripheral membrane protein facing the cytosol and does not only interact with Pex5 and Pex7, but also binds to Pex13 and Pex17. In mutants deficient in either Pex13, Pex14, or Pex17 matrix proteins can no longer be imported into peroxisomes (Subramani et al., 2000).

Although much is known about targeting of matrix proteins to the peroxisome surface, our knowledge on the translocation of PTS proteins across the peroxisomal membrane is rather limited. A main feature unique to peroxisomes is their ability to import folded, even oligomeric proteins, which distinguishes this import pathway from those of the ER, mitochondria, and plastids, where unfolded polypeptides are the substrates for membrane translocation (Gould and Collins, 2001). Strikingly, a channel-forming protein of peroxisomes, similar in function to Toc75 of plastids or Tom40 of mitochondria, has not been characterized to date in any organism. Instead, a transient pore model has only recently been proposed by Erdmann and Schliebs (2005). This model combines the functions of known peroxins, in particular that of Pex5, into a united, elaborate machinery for the import of folded proteins. Accordingly, the cytosolic Pex5-cargo complex inserts into the peroxisomal membrane in a similar manner as reported for pore-forming toxins, so that Pex5 becomes an integral part of the translocation pore (Gouaux, 1997; Dalla Serra and Menestrina, 2003). Cargo release and receptor recycling is accomplished by a cascade of protein-protein interactions at the peroxisomal membrane that involves Pex1 and Pex6, both of which belong to the ATPase associated with a variety of cellular activity (AAA) protein family, Pex4 (an E2 family member of ubiquitin-conjugating enzymes), Pex2 (an E3 ubiquitin ligase), as well as Pex10 and Pex12.

The PTS receptors Pex5 and Pex7 are predominately cytosolic in many organisms, with a smaller proportion associated with peroxisomes (Purdue and Lazarow, 2001). The dual subcellular localization of Pex5 and Pex7 in the cytosol and in peroxisomes stimulated

the proposal of a receptor recycling mechanism (Marzioch et al., 1994; Dodt and Gould, 1996; Chang et al., 1999). Using complex chimeric proteins, Dammai and Subramani (2001) provided direct evidence in support of the hypothesis that the receptor-cargo complex translocates freely into the peroxisome matrix, where the complex dissociates, and the receptor re-emerges in the cytosol to carry out further rounds of import. The chimeric proteins consisted of the PTS2 domain of thiolase, followed by the minimal processing site of the thiolase precursor protein, the FLAG epitope, and either Pex5S or enhanced fluorescence protein (EGFP). In stably transfected Hela cells, processed Pex5 fusion proteins were detected in the cytosol, whereas the corresponding EGFP fusion protein was confined to the peroxisomal matrix. Thus, it was demonstrated that Pex5 entered peroxisomes and returned to the cytosol after cleavage of the PTS2 nonapeptide (Dammai and Subramani, 2001). Similarly, Nair et al. (2004) demonstrated cycling of Pex7 between the cytosol and the peroxisomal lumen in yeast.

1.2.3 Peroxisome degradation

The number, volume, and enzymatic content of peroxisomes undergo stringent regulation in response to environmental and developmental changes (Leao and Kiel, 2003; Farre and Subramani, 2004). Yeast cells quickly induce peroxisome proliferation when the carbon source is shifted from glucose to fatty acids or methanol (Tuttle and Dunn, 1995; Sakai et al., 1998). When the growth medium is re-supplemented with glucose or ethanol, peroxisome proliferation discontinues, and most peroxisomes are degraded in order to reduce the energetic costs. The process of specific turnover of redundant, damaged, or non-functional peroxisomes by autophagy-related (ATG) pathways has been termed pexophagy.

Two morphologically distinct but mechanistically similar pathways of pexophagy have been described in *P. pastoris*, namely micropexophagy and macropexophagy, referring to their similarities with macroautophagy and microautophagy, respectively (Tuttle and Dunn, 1995; Fig. 1.3). When methanol-grown cells of *P. pastoris* are shifted to ethanol as sole carbon source, the superfluous peroxisomes are degraded by macropexophagy. During this process, a single peroxisome is selectively sequestered out of a cluster of organelles by a newly formed membranous layer, which wraps around the peroxisomes to form a double membrane structure designated the macropexophagosome. Subsequently, this phagosome

fuses with the vacuolar membrane and delivers the peroxisome to the vacuole or lysosome

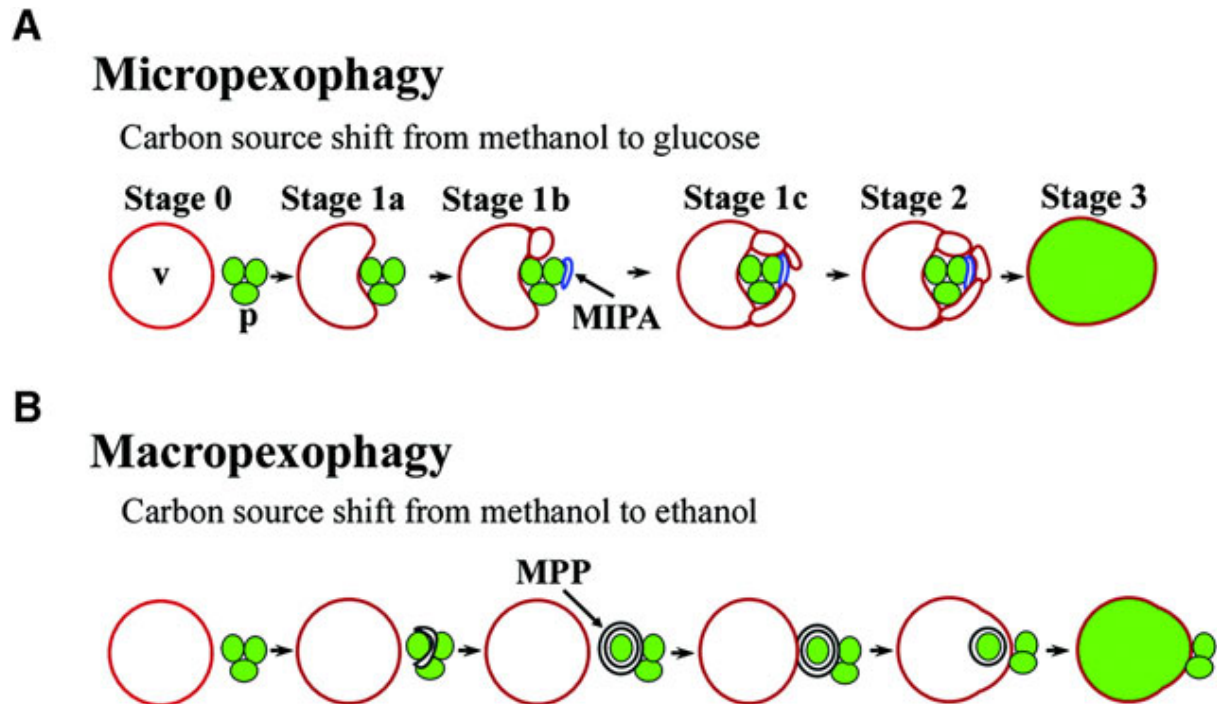


Figure 1.3: Overview of peroxisome sequestration via two distinct modes of pexophagy (according to Oku et al., 2003).

(A) Micropexophagy. The vacuole itself engulfs a peroxisome cluster. At the initial stage (stage 0), spherical vacuoles and peroxisome clusters are observed. Subsequently, the organelles initiate contact (stage 1a), and the vacuolar membrane elongates to form lobes around the peroxisomes (stage 1b). Meanwhile, the MIPA is formed and attaches to the peroxisome cluster. After the vacuolar lobes envelop the MIPA (stage 1c), the vacuole sequesters the peroxisomes (stage 2). Finally, the peroxisomes are lysed within the vacuole (stage 3). (B) Macropexophagy. A newly synthesized macropexophagosome first envelops a single peroxisome within the cluster and subsequently fuses with the vacuolar membrane, resulting in the release of the peroxisome surrounded by the inner membrane of the macropexophagosome into the vacuole. V, vacuole; p, peroxisome cluster; MIPA, micropexophagic apparatus; MPP, macropexophagosome.

for degradation (Tuttle and Dunn, 1995). Micropexophagy is activated when cells of *P. pastoris* adapt from growth on methanol to glucose. During micropexophagy, the vacuole undergoes septation and forms a new compartment proximal to the peroxisomal cluster. In addition, a novel membrane structure called the micropexophagic apparatus (MIPA) is formed and attaches to the peroxisome clusters. The sequestration of peroxisomes from the cytosol is completed when the MIPA seals the membrane tips of the invaginating vacuole. Finally, the sequestered peroxisomes are degraded in the vacuolar lumen to recycle amino acids and lipids (Tuttle, 1993; Sakai et al., 1998).

Both mammals and yeast use macropexophagy as the primary pathway for specific degradation of peroxisomes, whereas *Aspergillus nidulans* performs micropexophagy. *P. pastoris* is the only organism known to employ both macropexophagy and micropexophagy (Farre and Subramani, 2004). To our knowledge, studies on pexophagy in plants have not been reported yet.

Some proteins involved in the autophagy pathway, such as components of the Atg1 complex (Atg1, Atg11 and Atg24), ubiquitin like conjugation systems (Atg4, Atg5, Atg7, Atg8, Atg16), and the Atg9 complex (Atg2, Atg9), do not only have essential roles in autophagy but also in pexophagy because mutants deficient in the corresponding genes were blocked at different sequestration stages (Sakai et al., 1998; Guan et al., 2001; Kim et al., 2002; Stromhaug et al., 2001; Mukaiyama et al., 2002; Komduur et al., 2003; Farre and Subramani, 2004; Ano et al., 2005).

Autophagic systems are remarkably conserved among eukaryotes, and orthologs of most yeast Atg proteins have been found in *Arabidopsis* (Thompson and Vierstra, 2005). *Arabidopsis* null mutants of *atg5*, *atg7*, *atg9*, and *atg4a/atg4b* showed accelerated leaf senescence, even when grown under nutrient-rich conditions (Doelling et al., 2002; Hanaoka et al., 2002; Yoshimoto et al., 2004; Thompson et al., 2005). An even more severe phenotype with increased chlorosis, accelerated bolting, and reduced seed yield, was observed under either carbon or nitrogen starvation.

1.3 Peroxisome research in the post-genomic era

By combining the information provided by the *Arabidopsis* genome sequence, improved mass accuracy and resolution with proteomic approaches have been successfully applied in characterizing the protein content of *Arabidopsis* chloroplasts and mitochondria (Peltier et al., 2002; Schubert et al., 2002; Heazlewood et al., 2004; Kleffmann et al., 2004). These studies demonstrated that a substantial proportion of the proteins identified (more than 30% for chloroplasts and 20% for mitochondria) are of yet unknown function (Heazlewood et al., 2004; Kleffmann et al., 2004). Initial attempts in identifying the proteome of plant peroxisomes have also been published (Fukao et al., 2002, 2003; Babujee, 2004). Proteome analyses of plant peroxisomes, are however made difficult by the facts that (i) *Arabidopsis* is hardly suitable for the isolation of plant peroxisomes, (ii) plant peroxisomes can only be isolated from mature leaves and germinating seeds, thus genes expressing

peroxisomal proteins specifically in other plant tissues (e.g. roots, flowers, siliques) are not detectable, and (iii) catalase and the enzymes of the photorespiratory C_2 cycle and fatty acid β -oxidation dominate in leaf peroxisomes and glyoxysomes, respectively, to such an extent that other peroxisomal proteins are difficult to visualize on 2-D gels. As a result, to date, only a limited number of novel peroxisomal proteins have been detected in leaf peroxisomes from *Spinacia oleracea* L. and *Arabidopsis thaliana* L. (Babujee, 2004).

Fully sequenced genomes allow the prediction of all polypeptides encoded in a genome, including alternative splice variants and translational variants using different start methionines. The large majority of these polypeptides are yet unknown with respect to subcellular localization and physiological function. To predict the subcellular localization of unknown proteins, several programs have been designed that either deduce conserved sequence patterns from large sets of known targeting signals (MitoprotII, PSORT, iPSORT) or apply machine-learning techniques (TargetP; Predotar, DBSubLoc, PTS1 predictor). These programs can be applied to categorize the proteins of an entire genome according to prediction of their subcellular localization, and to set up organelle-specific databases, such as AMPDB for *Arabidopsis* mitochondrial proteins (Heazlewood and Millar, 2005).

By our group, plant PTS peptides were defined in a specific manner using a bioinformatics-based strategy (Reumann, 2004), and these peptides applied to screen the *Arabidopsis* genome for proteins that are targeted to the peroxisome matrix by the PTS1 or PTS2 pathway with moderate to high probability (Reumann et al., 2004). Overall, about 280 *Arabidopsis* proteins were identified that carried a putative PTS peptide. Interestingly, more than 85% of these proteins are of yet unknown function, indicating that the metabolic complexity of plant peroxisomes is higher than previously expected. Together with *in silico* information on sequence homology, expression pattern, subcellular targeting prediction, and published experimental data, these proteins have been collected in the database "AraPerox" (www.araperox.uni-goettingen.de; Reumann et al., 2004) which is available to the scientific community and allow experimental analyses of these proteins in straight-forward approaches.

1.4 Heat shock proteins associated with peroxisomes

1.4.1 Plant heat shock proteins in general

Heat shock proteins (Hsp) are found in most prokaryotic and eukaryotic organisms and were originally identified as a set of proteins quickly induced in response to elevated temperature (Tissieres et al., 1974). Later, only few heat shock proteins turned out to be strictly heat inducible. Most Hsps are constitutively expressed during normal growth and can be further induced in response to various abiotic stresses (Nover and Miernyk, 2001). Heat shock proteins function as molecular chaperones by assisting in the folding of nascent polypeptides or the refolding of partially denatured proteins and by suppressing protein aggregation. In plants, heat shock proteins can be categorized into several protein families according to the apparent molecular weights of their subunits, including the small Hsp or Hsp20 family proteins and proteins of the Hsp40, Hsp70, and Hsp90 family (Vierling, 1991; de Jong et al., 1998; Pearl and Prodromou, 2000).

Proteins of the Hsp70 and Hsp90 family are among the best-characterized heat shock proteins. Hsp70 proteins play a key role in the proper folding of newly-synthesized proteins, preventing unfolded proteins from undergoing aggregation, and maintaining an extended conformation of proteins during translocation (Boston et al., 1996; Hartl, 1996; Miernyk, 1997). Hsp90 proteins play a vital role in the folding, activation, and possibly trafficking of proteins involved in a wide range of signal transduction pathways, including steroid hormone receptors, protein kinases, and mediating cell cycle control (Todt, 1998; Pearl and Prodromou, 2000). Both Hsp70- and Hsp90-mediated protein folding is coupled to intrinsic adenosine triphosphate (ATP)ase activities (Panaretou et al., 1998; Lin et al., 2001).

Hsp70 and Hsp90 genes have been isolated from several plant species and the encoded proteins been localized to different subcellular compartments, including the cytoplasm, plastids, mitochondria, and the ER. The *Arabidopsis* genome contains at least eighteen genes that encode Hsp70 proteins and seven for Hsp90 proteins (Lin et al., 2001, Krishna and Gloor, 2001). Consistent with experimental work from other plants species, the *Arabidopsis* Hsp70 and Hsp90 proteins have predicted localizations in the cytosol and several organelles including the ER, mitochondria, and chloroplasts. However, homologs of both protein families carrying a putative PTS have thus far not been detected in *Arabidopsis* (Reumann et al., 2004).

Small Hsps (sHsps) are a widely distributed and diverse class of molecular chaperones that range in size from approximately 16 to 42 kDa (Scharf et al., 2001). Members of the sHsp family contain a conserved α -crystallin domain of 80-100 amino acids at the C-

terminus that is generally flanked by a highly-variable N-terminal region and a short C-terminal extension (MacRae, 2000). Another notable feature of sHsp is that they form large oligomeric structures of 9-24 subunits, ranging in size from 200 kDa to 800 kDa (Lee et al., 1995; Ehrnsperger et al., 1999; Kirschner et al., 2000). As determined by X-ray crystallo-

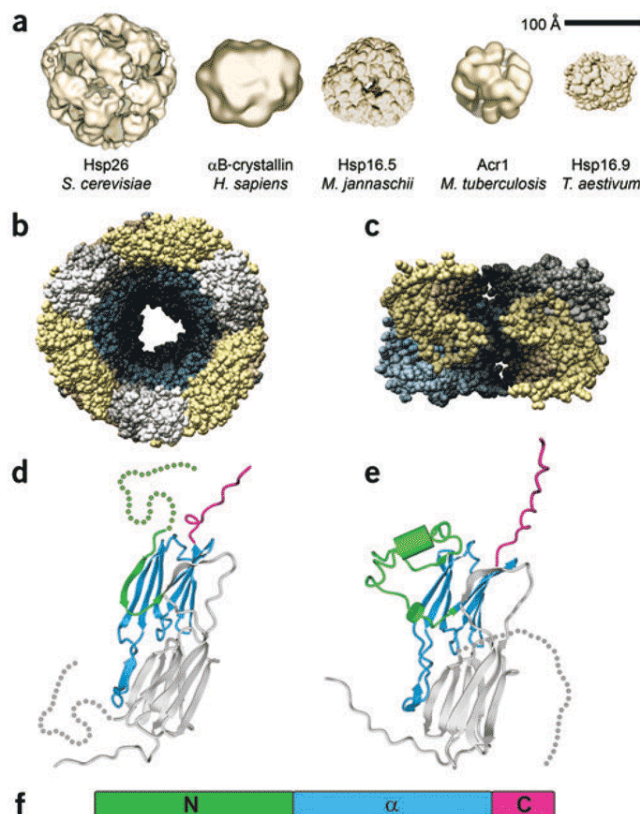


Figure 1.4: Oligomeric structure of sHsps (according to Haslbeck et al., 2005).

(a) Quaternary structures of ScHsp26, α B-crystallin from *Homo sapiens*, Hsp16.5 from *Methanococcus jannaschii*, Hsp16.3/acr1 from *Mycobacterium tuberculosis*, Hsp16.9 from *Triticum aestivum*. (b,c) Hsp16.5 from *M. jannaschii*, whose quaternary structure consists of 24 subunits arranged into a hollow-like structures (b), and Hsp16.9 from *T. aestivum* a barrel-like assembly of 2 subunits (c). (d,e) Crystal structures of two sHsp dimers, from Hsp16.5 and Hsp16.9, highlighting three functionally important regions. Green, N-terminal region; blue, α -crystallin domain; magenta, C-terminal extension; grey, the other sHsp in the dimer; dotted line, N-terminal residues not resolved in the structures. (f) Domain organization of sHsps.

graphy or electron microscopy, sHsps complexes form hollow, ball-like or barrel-shaped structures (Fig. 1.3). Upon heat shock, these sHsp complexes dissociate into distinct homo- or heteromeric protein complexes and trap non-native proteins in a soluble and folding-competent state (Lee et al., 1997; Ehrnsperger et al., 1997; Studer and Narberhaus, 2000). When permissive folding conditions are restored, sHsps bound polypeptides can be trans-

ferred to ATP-dependent chaperones, such as Hsp70 or Hsp100, for refolding (Cashikar et al., 2005; Haslbeck et al., 2005).

In *Arabidopsis*, 19 closely related sHsp homologs and 25 further proteins containing the same α -crystallin domain have been identified (Scharf et al., 2001). In contrast to other organisms, in which sHsps are mainly localized in the cytosol or transiently in the nucleus, plant sHsps are unique because they are targeted to several eukaryotic cell compartments, including mitochondria, plastids, and the ER (Vierling, 1991; Waters et al., 1996; Morrow et al., 2000). However, targeting of a sHsp homolog to the matrix of peroxisomes has not been reported for any organism.

1.4.2 Heat shock proteins involved in peroxisomal protein import

Cell organelles such as mitochondria, plastids, and the ER preferentially import unfolded polypeptides and require intraorganellar Hsps, normally Hsp70s, for pulling the polypeptide chain across the organelle membrane and promoting its correct folding within the organellar lumen (Collin and Gould, 2003; Soll and Schleiff, 2004; Rehling et al., 2004). Although peroxisomes are capable of importing folded proteins, they also seem to require molecular chaperones for the protein import process (Crookes and Olsen, 1998; Johnson and Olsen, 2001). As demonstrated for several organisms, including yeast, plants and mammals, cytosolic, membrane-associated and matrix-targeted Hsps act at various steps of peroxisomal protein import, including receptor-cargo recognition in the cytosol, docking, translocation at the membrane, and probably also protein assembly within the peroxisomal matrix (Lazarow and Fujiki, 1985; Titorenko and Rachubinski, 2001).

Crookes and Olsen (1998) studied the import of radiolabelled isocitrate lyase into pumpkin glyoxysomes in an *in vitro* system in the presence of polyclonal antibodies raised against cytosolic Hsp70 from *T. aestivum* and Hsp90 from *E. coli*. The rate of isocitrate lyase import into isolated peroxisomes was reduced by 80%, when polypeptide synthesis occurred in the presence of antisera against Hsp70 and Hsp90, whereas control levels were obtained when the antisera were added after polypeptide biosynthesis and prior to protein import, indicating that Hsp70 is actively involved in this process mainly before completion of translation. In a similar experiment, Walton et al. (1994) showed that the import of proteins into peroxisomes of human fibroblast cells was inhibited by co-injection of antibodies directed against the constitutive Hsp73. Thus, it was speculated that Hsp70 could bind to the nascent

peroxisomal matrix proteins during synthesis and promote their folding in the cytosol (Crookes and Olsen, 1998).

Intriguingly, a cytosolic DnaJ-like protein (Djp1p, an Hsp40 homolog) is specifically involved in peroxisomal protein import in *S. cerevisiae* (Hettema, et al., 1998). Cells deficient in Djp1 showed a defect unique among peroxisome assembly mutants, including mislocalization of peroxisomal matrix proteins and aberrant peroxisomal structures resembling the early stages of peroxisomal proliferation. Thus, members of this family of Hsps were shown to be required for efficient peroxisomal protein import *in vivo*. In addition, mislocalized peroxisomal enzymes were active in the cytosol of $\Delta djp1$ cells, suggesting that Djp1 might maintain the import-competent conformation of matrix proteins, expose their PTSs, and promote their binding to cytosolic receptors (Hettema et al., 1998). Similar post-translational functions were proposed for other molecular chaperones, such as plant Hsp90 and mammalian constitutive Hsp73 (Walton et al., 1994; Crookes and Olsen, 1998).

With respect to plants, a DnaJ/Hsp40 homolog of cucumber has been localized to cucumber glyoxysomes. In this case, however, the protein was detected at the external surface of glyoxysomal membrane and shown to interact with cytosolic Hsp70. It was proposed that the chaperone might be involved in docking of the cargo-receptor complex to the peroxisomal membrane by promoting conformational changes or translocating matrix proteins into peroxisomes (Diefenbach and Kindl, 2000).

Heat shock proteins have been found to reside in the matrix of plant peroxisomes. An Hsp70 homolog of watermelon has been localized to both chloroplast and peroxisomes, and dual subcellular targeting has been shown to be achieved by the use of two alternative start codons (Wimmer et al., 1997). The longer Hsp70 isoform contains a plastidic transit peptide, whereas the shorter Hsp70 isoform, which starts from the second methionine and lacks the transit peptide, is shortened by 20 amino acid residues so that the PTS2 peptide is positioned in the N-terminal domain. This PTS2 peptide is unusual in carrying a threonine residue at position 2 (RTx₅KL) but was able to target a reporter protein into yeast peroxisomes (Wimmer et al., 1997). In support of these data, Diefenbach and Kindl (2000) reported the detection of two Hsp70 homologs in subfractions of purified cucumber glyoxysomes.

1.5 Protein kinases associated with plant peroxisomes

Protein kinases function in a variety of signal transduction pathways and are critical, for cell division, metabolism, and responses to hormonal, developmental, and environmental signals. Protein kinases catalyze the transfer of the γ -phosphate group from ATP to a specific amino acid, i.e. generally serine, threonine, or tyrosine in plants, of the substrate protein. The downstream targets are thereby either stimulated or inhibited, and due to the ubiquitous presence of rather unspecific phosphatases, this post-translational regulatory mechanism is reversible and referred to as reversible phosphorylation (Stone and Walker, 1995; Hardie, 1999). In the *Arabidopsis* genome, 1085 genes encode putative protein kinases, which represent about 4% of the predicted 25,500 genes (Arabidopsis Genome Initiative, 2000; Hrabak, 2002). These protein kinases can be categorized into six classes, including multiple subfamilies such as the calcium-dependent protein kinases (CDPK), SNF1-related kinases, and leucine-rich receptor-like protein kinases (<http://plantsp.-genomics.purdue.edu/plantsp/family/class.html>). Interestingly, protein kinases often show a dual if not multiple subcellular targeting. For instance, a calcium-dependent protein kinase from *Mesembryanthemum crystallinum* was targeted to the plasma membrane, nucleus, ER, and to the cytosol by binding to actin microfilaments of the cytoskeleton (Patharkar and Cushman, 2000; Chehab et al., 2004).

Even though to date the physiological function of only few protein kinases has been thoroughly characterized, protein kinases are reported to regulate important processes of plant metabolism. In chloroplasts, for instance, protein kinases regulate several steps of photosynthesis. It has been demonstrated recently that an *Arabidopsis* thylakoid-associated serine/threonine kinase, referred to as AtStn7, is involved in the phosphorylation of the major light-harvesting protein (LHCII) and the redistributing of light excitation energy between the two photosystems through state transition (Bellafiore et al., 2005). In addition, protein kinases are possibly involved in chloroplast biogenesis and the regulation of chloroplast redox status (Horling et al., 1998; Depege et al., 2003; Fulgosi and Soll, 2003).

Signal transduction through protein kinase cascades allow a rapid transduction of environmental stimuli into intracellular signals and an amplification of signal intensity. Thus, weak environmental stimuli that may be harmful for the organism can induce cellular responses and protect the organism against environmental stresses. Signal transduction through protein phosphorylation is an important mechanism to protect cells against

unfavourable environmental conditions. It is thought that similar signal transduction mechanisms may also exist in peroxisomes for the following reasons: (1) peroxisomes proliferate in response to external signals, such as an alteration of carbon source (yeast) and application of toxic chemicals (plant); (2) peroxisomes play an important role in response to abiotic and biotic stresses; and (3) some peroxisomal proteins are phosphorylated (de Felipe et al., 1988; Palma et al., 1991; Willekens et al., 1997, de Rio et al., 1998; Barroso et al., 1999; Fukao et al., 2002; Farre and Subramani, 2004).

In addition, preliminary data indicate that some matrix enzymes of leaf peroxisomes are phosphorylated (Babujee, 2004, S. Reumann, unpublished results). Some enzymes, including ascorbate peroxidase, hydroxypyruvate reductase, and isocitrate dehydrogenase, which are encoded by single genes in *Arabidopsis*, were detected in multiple spots arranged in a horizontal line of discrete difference in isoelectric point on 2-D gels of leaf peroxisomes isolated from spinach and also partly from *Arabidopsis* (Babujee, 2004). Such spot patterns are typical for phosphorylated proteins. In support of phosphorylation of matrix proteins, some of these proteins could be specifically enriched by affinity chromatography like phosphorylated control proteins (Babujee, 2004).

In the past few years, the first experimental data on the association of protein kinases with plant peroxisomes have been published. In a proteomic study, putative peroxisomal protein kinases were identified in the leaf peroxisomes isolated from greening cotyledons in a proteome study (Fukao et al., 2002). Among the four protein kinases identified, however, only one carried a putative PTS1 signal, namely the minor PTS1 PKL> (Reumann, 2004). The second protein kinase, for instance, carried the C-terminal tripeptide SKD>, even though acidic residues have not been reported to be allowed in PTS1 tripeptides (Mullen et al., 1997; Kragler et al., 1998). It remains to be investigated in more detail whether all four kinases are indeed peroxisome-associated or derive from organellar contaminations.

In the course of their proteomic study of *Arabidopsis* glyoxysomes, Fukao et al. (2003) characterized a serine/threonine protein kinase, referred to as glyoxysomal protein kinase 1 (GPK1), containing the putative PTS1 peptide AKI> in more detail. As demonstrated by biochemical evidence, subcellular localization experiments and a protease digestion assay, GPK1 was described as a peripheral membrane protein with the putative kinase domain facing the glyoxysomal matrix. A 40-kDa protein was suggested to be the candidate substrate of GPK1, but its identity and function remain to be elucidated.

In an investigation of the subcellular targeting of nine calcium-dependent protein kinase (CDPK) isoforms from *Arabidopsis*, AtCDPK1 was shown to be exclusively attached to the peroxisomal membrane of *Arabidopsis* roots expressing AtCDPK1-GFP (Dammann et al., 2003). This protein kinase is, thus, the first that has convincingly been shown to be associated with peroxisomes *in vivo*. Even though AtCDPK1 was attached to the peroxisomal membrane, no membrane targeting signal was confirmed in the polypeptide. Instead, membrane association of AtCDPK1 was apparently mediated by an acyl anchor attached to the N-terminal domain (Dammann et al., 2003). The peripheral localization of AtCDPK1 at the external side of the peroxisomal membrane makes it a likely candidate for the transduction of Ca^{2+} -mediated signals across the peroxisomal membrane.

1.6 Objectives of the present investigation

For a long time, the function of molecular chaperones in the peroxisome matrix and post-translational regulatory mechanisms of peroxisomal metabolism have been difficult to study because chaperones and protein kinases are generally expressed at low level under standard conditions and can hardly be identified in isolated peroxisomes by traditional biochemical methods. As a result, targeting of small heat-shock proteins (sHsps) to the peroxisome matrix has not been reported for any organism, and matrix-targeted protein kinases of plants have not been cloned and characterized at the molecular level.

Thanks to the availability of (i) the *Arabidopsis* genome sequence, (ii) a bioinformatics-based definition of plant-specific PTS peptides, and (iii) a variety of subcellular localization prediction programs, we were able to identify in the *Arabidopsis* genome ORFs that encoded two sHsps, namely AtHsp15.7 (At5g37670) and AtAc31.2 (At1g06460), and seven putative peroxisomal protein kinases (PPPK1 to PPPK7), all of which possessed putative signals for targeting to peroxisomes and were localized in the peroxisome matrix with moderate to high probability.

The goals of this work were formulated as follows:

1. Molecular analyses of two small heat shock proteins from plant peroxisomes:

The cDNAs of *AtHSP15.7* and *AtACD31.2* should be cloned by RT-PCR and subcellular targeting of these sHsps to peroxisomes be investigated in the transient expression

system of onion epidermal cells as fusion proteins with enhanced yellow fluorescent protein (EYFP) by microscopy. The morphological phenotype of a yeast mutant deficient in cytosolic sHsps was attempted to be complemented by expression of the plant peroxisomal sHsps as cytosol-targeted proteins. To gain insights into the function of these sHsps in plant peroxisomal metabolism, the expression pattern should be investigated and homozygous single and double T-DNA insertion lines for *AtHSP15.7* and *AtACD31.2* be identified and be analyzed phenotypically.

2. Identification of matrix-targeted protein kinases:

The cDNAs of a maximum number of cDNAs encoding PPPKs should be cloned by RT-PCR and subcellular targeting of these proteins be investigated in both a yeast and a plant expression system as fusion proteins with spectral variant of green fluorescent protein by microscopy. To gain insights into the function of one kinase, the gene of a putative regulatory subunit should be cloned as well and complex formation between the two proteins be investigated by yeast two-hybrid assays.

2. Materials and methods

2.1. Materials

2.1.1. Biochemicals

Most chemicals were purchased from Carl Roth (Karlsruhe, Germany), Sigma (Sigma-Aldrich, Taufkirchen, Germany), and Merck (Darmstadt, Germany) if not otherwise indicated. For chemicals and products from other companies, the sources are listed below:

dNTPs	MBI Fermentas, Vilnius, Lithuania
Digoxigenine-dUTP	Roche Molecular Biochemicals, Mannheim, Germany
DNA size marker (bacteriophage λ DNA)	MBI Fermentas, Vilnius, Lithuania
$[\alpha\text{-}^{32}\text{P}]\text{dCTP}$	Hartmann Analytik, Braunschweig, Germany
IPTG (isopropyl- β -D-thiogalactopyranoside)	AppliChem, Darmstadt, Germany
oligonucleotides	MWG Biotech, Ebersberg, Germany
X-Gal (5-brom-4-chlor-3-indoyl- β -D-galactopyranoside)	Roche Molecular Biochemicals, Mannheim, Germany
Hybond N and Hybond N ⁺	Amersham Pharmacia Biotech, Freiburg, Germany
3MM Whatman paper	Biometra Whatman, Germany
2.1.2. Enzymes	
Restriction enzymes	MBI Fermentas, Vilnius, Lithuania
Klenow fragment, exonuclease ⁻	MBI Fermentas, Vilnius, Lithuania
M-MuLV Reverse transcriptase	MBI Fermentas, Vilnius, Lithuania
Thermoscript TM RT-PCR system	Invitrogen, USA
T4 DNA ligase	Promega, Madison, USA
<i>Taq</i> polymerase	Promega, Madison, USA
RNase A	Sigma-Aldrich, Taufkirchen, Germany
Expand High Fidelity PCR System	Roche Molecular Biochemicals, Mannheim, Germany
ThermoZyme	Invitrogen, USA
PfuUltra TM High-Fidelity DNA Polymerase	stratagene, USA
DNaseI	MBI Fermentas, Vilnius, Lithuania

2.1.3. Kits

ABI PRISM dRhodamine Terminator PE Applied Biosystems, Weiterstadt, Germany
Cycle Sequencing Ready Reaction Kit

E.Z.N.A.Peq Lab mini Prep Kit Peq Lab Biotechnologie GmbH, Erlangen,
Germany

HexaLabel Kit MBI Fermentas, Vilnius, Lithuania

Invisorb Spin-Plant RNA mini Kit Invitex, Berlin, Germany

Qiaquick Gel Extraction Kit Qiagen, Hilden, Germany

DNA and Gel Band Purification Kit Amersham Bioscience, Freiburg, Germany

pYES2.1 TOPO® TA Expression Kit Invitrogen, USA

pGEM®-T Easy Vector System I Promega, Mannheim, Germany

2.1.4 *E. coli* and yeast strains

The following *E. coli* strains were used:

Stock	Genotype	Resource
DH5α	<i>F⁻ (Φ80d/lacZΔM15) recA1 end A1 gyrA96 thi-1 hsdR17(r_k⁻m_k⁺) supE44 rel A1 deoR Δ(lacZYA-argF) U169</i>	Invitrogen, USA
XL1-Blue	<i>recA1 endA1 gyrA96 thi-1 hsdR17 supE44 relA1 lac [F proAB lacI.q. ZΔM15 Tn10 (Tet. r.)].</i>	Stratagene, USA

The following yeast strains were used:

BJ1991	<i>MATα, leu2, trp1, ura3-251, prb1-1122, pep4-3, gal2</i>	R. Erdman
SEY6211	<i>MATα ura3-52 leu2-3, 112 his3-Δ200 trp1- Δ901 ade2-101 suc2- Δ9 GAL</i>	M. Haslbeck
SEY6211 <i>hsp26</i>	<i>MATα ura3-52 leu2-3, 112 Δ200 trp1- Δ901 ade2-101 suc2- Δ9 GAL</i>	M. Haslbeck
SEY6211 <i>hsp42</i>	<i>MATα ura3-52 his3-Δ200 trp1- Δ901 ade2-101 suc2- Δ9 GAL</i>	M. Haslbeck
SEY6211 <i>hsp26/42</i>	<i>MATα ura3-52 trp1- Δ901 ade2-101 suc2- Δ9 GAL</i>	M. Haslbeck

2.2 Plant growth conditions

2.2.1. Standard growth

Seeds of *Arabidopsis thaliana* ecotype Col-0 were obtained from The *Arabidopsis* Stock Resource Centre (Nottingham, England). The seeds were sown on a mixture of commercial soil (Balster Einheitserdewerk GmbH, Froendenberg, Germany) and vermiculite (4:1) and grown at 22°C with a light intensity of 100~150 $\mu\text{mol m}^{-2} \text{s}^{-1}$ in a 16/8 h dark cycle (long-day). Between five and seven plants were maintained per pot (9 x 9 x 9 cm: 15 pots/tray). The soil was supplemented with the commercial fertilizer Wuxan (2-3%) every week.

2.2.2. Stress treatment

To investigate the expression of *AtHSP15.7* and *AtACD31.2* under abiotic stress by semi-quantity RT-PCR, 4-weeks old plant of *Arabidopsis* ecotype Col-0 plants were subjected to different stress conditions. All the stress treatments were initiated after three hours of light. For heat and cold stress experiments, plants were incubated in the dark at 37°C and 5°C, respectively, whereas the control plants were incubated at 22°C in the dark. For high light stress, the light intensity was raised to 450 $\mu\text{mol m}^{-2} \text{s}^{-1}$ while keeping the temperature constant at about 23-24°C. Control plants grown at the same temperature but under normal light were analyzed in parallel. For the oxidative stress experiments, soil-grown plants were either watered with 5 mM 3-AT or 100 μM paraquat (about 50 ml per 9 cm pot per day), or rosette leaves were infiltrated with 100 μM 3-AT or 10 μM paraquat (in water) using a syringe and floated on inhibitor solution. Rosette leaves infiltrated with water were used as a mock control.

2.2.3. Growth of *Arabidopsis* seedlings on agar plates

Seeds of *Arabidopsis* Col-0 or T-DNA insertion mutant seeds were briefly washed by 1 ml of 70% ethanol. After discard the ethanol, the seeds were sterilized for 20 min in 1% Na-hypochlorite (Riedel de Haen, 6-14% active chloride, on average 10%) plus 0.1% SDS. After removal of the Na-hypochlorite solution, the seeds were washed 4 times, each with 1 ml of sterile water. The seeds were resuspended in 0.1% agar after the final washing. Sterilized seeds were incubated at 4°C for 2-4 days and grown on $\frac{1}{2}$ MS agar plates with or without sucrose. The plates were incubated at 23°C under continuous light.

For germination experiment under heat stress, surface-sterilized seeds were transferred into a 50°C incubator for 5.5 hours immediately after stratification. And germination rate was counted after growth for 7 days at 22 °C.

½ MS (Murashige-Skoog) medium according to Murashige and Skoog (1962):

2.3 g/l Murashige and Skoog medium, micro- and macroelements including vitamins (Duchefa, Haarlem, Netherlands)

1% (w/v) sucrose

The pH was adjusted to 5.8 with KOH, and 0.8% (w/v) Select Agar (Duchefa) was added before autoclaving.

2.3 Molecular cloning

2.3.1 RNA isolation

Total RNA was isolated from different tissues of *Arabidopsis thaliana* cv. Columbia using the Invisorb Spin Plant mini Kit (Invitek GmbH, Berlin, Germany). Plant materials were harvested and stored at -80°C until use. *Arabidopsis* tissue was ground in liquid nitrogen using a pre-cooled mortar and pestle. The fine powder was transferred into a 2-ml Eppendorf tube that contained 900 µl of the lysis solution provided by the kit. After vigorous vortexing, the suspension was incubated for 30 min with gently shaking at room temperature (RT). All following procedures were also performed at RT. After centrifugation at full speed for 1 min, the supernatant was applied to a spin column with a DNA binding filter and incubated for 1 min. Passage of the lysate through the filter during the following centrifugation (1 min, 10,000 rpm) resulted in the removal of most genomic DNA. The addition of 0.5 vol. of 99.8% ethanol to the RNA-containing lysate provided the conditions for precipitation of RNA from the solution during the following centrifugation. The solution was applied to a spin column with an RNA binding filter, incubated for a minute and centrifuged (30 sec, 10,000 rpm). The filter-bound RNA was washed three times with two washing buffers (30 sec, 10,000 rpm), and residual ethanol were removed by an additional centrifugation step (2 min, 13,000 rpm). The RNA was eluted from the filter with DEPC-water. 20 – 50 µl of DEPC-H₂O were used for elution depending on the desired RNA concentration. The eluted RNA was immediately placed on ice and stored at -80°C.

2.3.2 Plant genomic DNA isolation

2 g of fresh *Arabidopsis* leaf tissue was ground to a fine powder in liquid nitrogen with a chilled mortar and pestle and then transferred to a chilled 50 ml tube. 3~5 ml of preheated (60°C) CTAB buffer was immediately added to the ground tissue powder and incubated at 60°C for 30 min with occasional swirling. The same volume of chloroform was then added to the samples and briefly vortexed for mixing. The sample was centrifuged at 4,000 rpm at RT for 10 min. The aqueous phase was transferred to a new 50 ml tube with a wild-bore pipette. To remove proteins, the same volume of phenol: chloroform: isoamyl alcohol (25:24:1) was added to the sample and the mixture was centrifuged at 4,000 rpm for 10 min at RT. Afterwards, the aqueous phase was transferred into a new 50 ml tube and mixed with two-thirds volume of cold 100% isopropanol, to precipitate the nucleic acids. The mixture was incubated at room temperature for 5 min and centrifuged at full speed for 10 min at room temperature. The pellet was washed with 10 ml of 75% ethanol and incubated for a minimum of 20 min at RT. After centrifugation at 4,000 rpm for 10 min, the pellet was air dried and resuspended in 2-3 ml of TE buffer additioned with 10 µg/ml RNase A, and incubated at 37°C for 30 min to digest away the RNA contaminants. When the pellet was completely dissolved in TE buffer, the DNA solution was extracted again by phenolization (add an equal volume of phenol: chloroform to the samples) and centrifuged at 13,000 rpm for 10 min at RT. The aqueous phase was transferred to a fresh tube and mixed with 1/10 volume of 3 M sodium acetate (pH 5.2) and 2.5 volume of ice cold 99.8% ethanol, and incubated at -80°C for 30 min for DNA precipitation. Afterwards, the reaction was centrifuged at 14,000 rpm for 10 min at 4°C to pellet the DNA. The DNA pellet was washed with 70% ethanol and pelleted by centrifugation at 14,000 rpm for 10 min. The pellet was then air-dried at room temperature for 10 min and resuspend in 100 µl TE buffer.

CTAB buffer :

NaCl	1.4 M
Tris-HCl, pH8.0	100 mM
EDTA	20 mM
CTAB	2% (v/v)
2-mercaptoethanol	0.2% (v/v)

2.3.3 Estimation of the concentration of nucleic acids

2.3.3.1 Photometric method

Nucleic acids were diluted with dd H₂O (1: 50) in a total volume of 100 µl and the extinction was measured at 260 nm and 280 nm against a water blank using a spectrophotometer (Ultrospec 1100 pro, Amersham Bioscience, Freiburg, Germany). The concentration of the nucleic acids were automatically calculated using the following formula:

$$\text{RNA } [\mu\text{g/ ml}] = E_{260} * 42 * V_{\text{cuvette}} * V_{\text{aliquot}}^{-1}$$

$$\text{DNA } [\mu\text{g/ ml}] = E_{260} * 50 * V_{\text{cuvette}} * V_{\text{aliquot}}^{-1}$$

The extinction ratio (E_{260} / E_{280} nm) reflects the contamination by proteins. A typical value is 1.8 to 2.0. For the concentration of isolated plasmids, genomic DNA, and RNA, the photometric method was used.

2.3.3.2 Gel-electrophoretic method

Alternatively, the quality and concentration of nucleic acid was estimated by agarose gel electrophoresis (2.15.3). The nucleic acid samples were separated on a 1% agarose gel and detected under UV light, as described (see sections below). Good RNA quality was indicated by a ratio of band intensities between 28 S rRNA and 18 S rRNA of > 1.5: 1. The concentration of DNA was estimated by comparison against a size standard of known concentration (Gene Ruler DNA Ladder Mix, MBI Fermentas, Vilnius, Lithuania). The concentration of purified DNA fragments, which were used in ligation reactions, was mainly calculated by this gel-electrophoretic method.

2.3.4 Agarose gel electrophoresis, gel staining and documentation

For most analytical purposes, 1% agarose gels prepared in 1 x TEA buffer were used. 1/6 volume of 6x loading dye was added to DNA samples before loading. Electrophoresis proceeded at 5 V/cm using 1x TEA as running buffer. The gel-resolved nucleic acids were stained protected from light for 20 min in an aqueous solution containing 0.25 µg/ ml of the intercalating dye ethidium bromide. The gel was briefly rinsed with water to remove excess dye. The dye-molecules bound to nucleic acids were made visible by UV-light. When DNA fragments or PCR products were purified from an agarose gel, only low UV light intensity was used. The gels were photographed under UV light using a transilluminator (raytest IDA; Herolab, Wiesloch, Germany) connected to a printer.

50 x TEA buffer:

Tris-acetate pH 8.3	2 M
EDTA	100 mM

6x Loading dye:

Glycerol	50% (v/v)
Tris-acetate pH 8.3	40 mM
EDTA	2 mM
Orange G	0.2% (v/v)

5x Tracking dye:

Xylene cyanol	0.1% (w/v)
sucrose	20% (w/v)
EDTA	250 mM
bromphenol blue	50% (w/v)

2.3.5 Synthesis of cDNA by reverse transcription (RT)

The SuperScript III RT-PCR System (Invitrogen, USA) was used for initial gene cloning according to specifications by the manufacturer. 5 µg of total RNA was mixed with 1 µl of oligo (dT)₂₀ (50 µM) and 1 µl of 10 mM dNTP mix in a total volume of 13 µl. The mixture was incubated at 65°C for 5 min and cooled down immediately on ice for 1 min for denaturation of RNA and RNA-primer annealing. Afterwards, 4 µl of 5x First-Strand Buffer, 1 µl of 0.1 M DTT, 1 µl of RNaseOUT™ Recombinant Ribonuclease Inhibitor (40 units/ µl, Invitrogen, USA), and 1 µl of SuperScript III RT (200 units/ µl) were added to the mixture to a total volume of 20 µl. The mixture was then incubated at 50°C for 60 min and inactivated by heating at 70°C for 15 min. The cDNA can now be used as a template for PCR. In case of DNA targets (>1 kb), RNA complementary to the cDNA has to be removed. In such a case, 1 µl (2 units) of *E. coli* RNase H was added to the reverse transcription reaction and incubated at 37°C for 20 min.

The transcriptase M-MuLV (*Moloney Murine Leukemia Virus*) Reverse Transcriptase (MBI Fermentas, Vilnius, Lithuania) was used for semi-quantitative RT-PCR according to specifications by the manufacturer. Each reaction contained 1-5 µg of total RNA with 500 ng of oligo (dT)₁₈-primer and was incubated at 70°C for 5 min for denaturation of RNA and primer annealing. After addition of dNTPs (final concentration: 1.0 mM), 5×

reaction buffer and 40 units of ribonuclease inhibitor were added and incubated for 5 min at 37°C, then 20 units of M-MuLV RT (Fermentas) in a total reaction volume of 20 µl were applied to the reaction for cDNA synthesis. The reaction was then incubated at 37°C for 60 min, and inactivated at 70°C for 10 min.

2.3.6 Polymerase chain reaction (PCR)

Genes were amplified by polymerase chain reaction (PCR, Mullis und Faloona, 1987). A proofreading enzyme (*Pwo*, Peqlab; High Fidelity, Roche; *Pfu*, MBI) was used for gene cloning and plasmid construction. Taq DNA polymerase (Invitex, Berlin, Germany), which derives from *Thermophilus aquaticus*, was used for colony PCR. The annealing temperature was 5°C lower than the melting temperature of the DNA, which was specific for each primer pair. Of each pair of primers, the lowest temperature was chosen. The amplified products were analysed by TEA- agarose gel electrophoresis (2.3.3).

Standard PCR reactions contained the following components:

	<u>Taq</u> <u>polymerase</u>	<u>proofreading</u> <u>polymerase</u>
10x reaction buffer (matching the enzyme)	5 µl	5 µl
50 mM MgCl ₂ (2 mM final conc.)	1 µl	-
10 mM dNTP (0.2 µM final conc.)	1 µl	1 µl
10 µM 5'-primer (0.2 µM final conc.)	1 µl	1 µl
10 µM 3'-primer (0.2 µM final conc.)	0,5 µl	1 µl
DNA template (20-100 ng)	1 µl	1 µl
DNA polymerase	0.3 µl (1.5 U)	1 µl (1 U)
dd H ₂ O	to 25 µl	to 50 µl

A standard PCR program was as follows:

Number of cycles	temperature	duration
1	95 °C	2 min
35	95 °C	30 sec
	annealing temperature	30 sec
	72 °C	1.30 min
1	72 °C	10 min

2.3.7 Semi-quantity RT-PCR

Semi-quantitative RT-PCR was performed using a First Strand cDNA Synthesis Kit (MBI, Fermentas, St. Leon-Rot, Germany) according to the manufacturer's instruction. cDNA first strand was synthesized in a 20 µl reverse transcription reaction containing 2 µg of DNase I-treated total RNA, an oligo (dT) primer, and M-MuLV reverse transcriptase. The reverse transcription reactions were carried out at 37°C for 1 h, then 72 °C, 10 min, and chilled on ice. A 2 µl aliquot of the reverse transcription reaction was used for PCR reaction as template. As a control for DNA contamination of the RNA isolateion, total RNA was subjected to the same RT reaction, with DEPC-water replacing reverse transcriptase. Nucleotide sequences of gene-specific primers used in the experiments were listed in Appendices 7.1.

For the expression analysis of *AtHSP15.7*, the following PCR parameter were used: 5 min at 94 °C; 30 sec at 94 °C, 30 sec at 60°C, 1 min at 72° for 30 cycles; then 10 min at 72°C. For *AtACD31.2* (26 cycles), ubiquitin (UBQ10, 30 cycles) and *AtpMDH1* (24 cycles), similar PCR parameters were used with an adjustment of the annealing temperature to 5°C below the lowest estimated melting temperature.

2.3.8. PCR-based site-directed mutagenesis

The QuikChange II XL kit (Stratagene, USA) was used to introduce point mutations. The basic procedure utilizes a supercoiled double-stranded DNA (dsDNA) vector with an insert of interest and two synthetic oligonucleotide primers, both containing the desired mutation. The oligonucleotide primers, each complementary to opposite strands of the vector, are extended during temperature cycling by PfuUltra HF DNA polymerase, without primer displacement. Extension of the oligonucleotide primers generates a mutated plasmid containing staggered nicks. Following temperature cycling, DpnI was added to the PCR reactions to digest the parental DNA and to select for the containing mutation. DNA isolated from almost all *E. coli* strains is dam methylated and therefore susceptible to DpnI digestion. The nicked vector DNA with the desired mutations is then transformed into DH5α competent cells.

PCR-based site directed mutagenesis was used to introduce point mutation in the PTS signal of *AtHSP15.7* and *AtACD31.2* and in the protein kinase domain of PPPK4. PCR reactions were carried out as described. 50 ng DNA was used as template.

Cycling parameters for the QuickChange II Site-Directed Mutagenesis method

Number of cycles	temperature	duration
1	95 °C	2 min
18	95 °C	30 sec
	55 °C	1 min
	68 °C	1 min per kb of plasmid length
1	72°C	10 min

2.3.9. Elution of resolved nucleic acid fragments from an agarose gel

DNA fragments deriving from PCRs or restriction enzyme-digestions were separated on 1% agarose gels. This step allowed the purification of larger DNA from proteins and primers and the isolation of a DNA fragment of the desired size. The DNA bands were cut from the gel under long-waved UV light. The agarose was removed using the Qiaquick® Gel Extraction Kit (Qiagen) or the DNA and Gel Band Purification Kit (Amersham Biosciences) according to the manufacturer's instructions. After dissolving the agarose at 50°C (Qiagen) or 60°C (Amersham Biosciences) in a chaotropic reagent, the DNA was bound to a silica gel filter in a spin column in the presence of high salt concentrations, washed, and eluted from the filter with dd H₂O.

2.3.10 Phenolization and ethanol precipitation of DNA or RNA fragments

To extract DNA or RNA fragments from a mixture, the nucleic acids are normally subjected to phenolization and ethanol precipitation. For phenolization, the DNA or RNA fragments were first adjusted to a final volume of 300 µl with water in a 1.5 ml eppendorf tube and mixed with equal volume of phenol-chloroform solution. After vortexing for 30 sec, the solution was centrifuged for 10 min at 10,000 rpm at RT. The water phase was transferred to a new tube, then 1/10 volume of 3 M NaAc and 2.5 volume of 100% ethanol were added, and the nucleic acids precipitated at -80°C for 30 min. Then, the reaction was centrifuged at 14,000 rpm for 30 min at 4°C. Afterwards, the supernatant was discarded and the pellet was washed once with cold 70% ethanol. After air drying, the pellet was dissolved in the desired volume of TE buffer.

2.3.11. Ligation of cDNA fragments into destination vectors

DNA fragments were amplified by PCR with the desired restriction enzyme sites introduced to the 5' end, and cloned into the destination vectors using two different strategies: First, the PCR products were subcloned into the TA cloning vector pGEMT (Promega, Madison, USA) and then the correct insert was transferred into different target vectors, such as pCATyfp, pGADT7, pGBKT7. Alternatively, PCR products were purified from agarose gel, digested with appropriate restriction enzymes to get the desired cohesive ends and ligated into target vectors (see chapter 2.3.9 and 2.3.10).

For non-directional cloning, vector dephosphorylation was performed by adding 1 μ l of Shrimp alkaline phosphatase and incubation at 37°C for 30 min. The dephosphorylated vector was purified by the DNA and Gel band Purification Kit (Amersham Biosciences) as described.

The ligation reaction (10 μ l) contained 1 μ l (3 U/ μ l) of T4 DNA ligase (Promega, Madison, USA), 1 μ l of 10x ligase buffer, 25 ng of vector with cohesive ends and the insert in an amount suited to provide a molar vector: insert ratio in the range of 1:3 to 1:10.

$$ng\ insert = \frac{ng\ vector * size\ of\ insert\ (kb)}{size\ of\ vector\ (kb)} * molar\ ratio\ \frac{insert}{vector}$$

The reaction was performed at 16 °C overnight. The 10x ligase buffer contained 300 mM Tris-HCl (pH 7.8 at 25 °C), 100 mM MgCl₂, 100 mM DTT and 10 mM ATP. 2 μ l of ligation products were used for transformation.

2.3.12. Preparation of competent cells

2.3.12.1 Preparation of DH5 α or XL1-Blue competent cells

For the preparation of competent cells, the method of Inoue et al. (1990) was used with some modifications. To obtain optimal competent cells, the glassware used in the protocol had to be free of any detergents. For this purpose, glassware was first autoclaved filled with dd H₂O to remove all the traces of detergents, and then autoclaved again empty. 5 ml of SOB medium were inoculated with a single colony DH5 α or XL1-Blue and grow overnight (37°C, shaking). The overnight culture was then diluted with 250 ml of SOC

medium and grown (18°C, shaking) until the cell density reached an OD₆₀₀ of 0.4. It takes normally 10~18 hours. The cells with the desired density were collected in four 50 ml conical centrifugation tubes and spun at 4,000 rpm for 10 min at 4 °C (Eppendorf 5417R, Germany). The following steps were performed on ice under a laminar flow hood (PRETTTL-TELSTAR, Bio-II-A, Germany). The cell pellets were washed in 15 ml of ice-cold transformation TB buffer per tube, and followed by incubation on ice for 15 min. The suspensions were combined pair-wise into two centrifugation tubes and centrifuged again at 4,300 rpm for 10 min at 4°C. The pellets were again resuspended per tube with 10 ml (total 20 ml) of transformation buffer and 350 µl of DMSO were carefully added to each tube under gentle vortexing to avoid a high local DMSO concentration. After 5 min incubation on ice, this step was repeated resulting in a final concentration of DMSO 7% (v/v). 200 µl aliquots of the competent cells were pipetted into pre-cooled 1.5 ml Eppendorf tubes and shock-frozen in liquid nitrogen. The cells were stored at -80°C.

SOB medium :

Peptone	20 g/l
Yeast extract	0.5 g/l
NaCl	50 mg
KCl	25 mM

The mixture was adjusted to pH 7.0 and autoclaved for 10 min followed by the addition of filter-sterilized solutions of MgCl₂ (1 M), MgSO₄ (1 M) and glucose (2 M) under a cleaning bench to a final concentration of 10 mM, 10 mM and 20 mM, respectively.

Transformation buffer (TB buffer) :

PIPES-KOH, pH6.7	10 mM
CaCl ₂	15 mM
KCl	250 mM
MnCl ₂	55 mM

The transformation buffer without MnCl₂ was adjusted to pH 6.7 with KOH. Then add MnCl₂ was added and the solution and filter-sterilized the mixture using a 0.22-µm filter.

2.3.12.2 Preparation of competent *Agrobacterium tumefaciens* DHA105 cells

5 ml of liquid YEB medium without any antibiotics were inoculated with an *A. tumefaciens* DHA105 colony and grown at 28°C overnight with shaking. 2 ml of the overnight culture were diluted with 50 ml of YEB and grown at 28°C for another 4 h until the

cell density reached an OD₆₀₀ of 0.5. The cells were spin down at 4,000 rpm (10 min, 4°C) and resuspended with 10 ml of ice cold 150 mM NaCl. After incubated on ice for 15 min, the cells were spun down again by centrifugation and another wash with 10 ml of 150 mM NaCl (ice cold). After centrifugation, the cell pellets were resuspended in a total volume of 1 ml of ice cold 75 mM CaCl₂, and 200 µl of aliquots were pipetted into sterile 1.5 ml Eppendorf tubes and stored at -80 °C.

YEB medium :

Gibco beef extract	5 g/l
Bacto yeast extract	1 g/l
Bacto peptone	5 g/l
	pH adjusted to 7.4 with KOH
MgSO ₄ (added to medium after autoclaving)	50 mM

2.3.13 Transformation of competent cells

2.3.13.1 Transformation of *E.coli*

The competent cells were thawed on ice. 2 µl of ligation reaction or 50 – 200 ng of plasmid DNA were added to the suspension of competent cells and mixed by gently pipetting. After incubation on ice for 30 min, the cells were incubated at 42°C for exactly 90 sec and immediately cooled down on ice for two minutes. Then 800 µl of SOC medium were added to the cells under a laminar flow hood, and the cells were incubated on a shaker at 37°C for an hour to allow the expression of antibiotic resistance genes. The transformation reactions were centrifuged at 10,000 rpm for a minute and resuspended in 150 µl of SOC medium. The cells were pipetted under a clean bench onto LB agar plates supplemented with the appropriate antibiotic(s). If the cells were transformed with a ligation product in pGEM[®]-T Easy, the plates were supplemented with IPTG (40 µl, 100 mM) and X-Gal (40 µl, 2% (w/v) in DMF) that allowed for a blue-white selection. The plates were incubated at 37°C overnight.

2.3.13.2 Transformation of yeast cells

5 ml of YNB medium supplemented with appropriate amino acids and bases were inoculated with a single colony (BJ1991) and grown overnight until the cells reached to the early stationary phase. The cells were spin down at 10,000 rpm for 1 min, and then the cell pellets were resuspended in 1 ml of 100 mM LiAc and incubated at 30°C for 5 min. The cells

were collected again and resuspended in the following PEG/LiCl solution (351 μ l in total): 240 μ l of PEG (50% w/v), 36 μ l of 1.0 M LiAc, 50 μ l of SS-DNA (2.0 mg/ml), plasmid DNA and dd H₂O. The transformation reactions were incubated at 42°C for 20 min. The cells were pelleted at 10,000 rpm for 1 min and resuspended in 100 μ l of ddH₂O. The cells were pipetted under a clean bench onto YNB agar plates. The plates were incubated at 30°C for 2-4 days.

YNB medium :

YNB	1.7 g/l
Bacto yeast extract	1 g/l
Ammonium sulfate	1 g/l
10 x amino acids mixture	10 ml
	pH adjust to 5.9 with KOH

2.3.13.3 Transformation of *Agrobacterium tumefaciens* cells

1 μ g of plasmid DNA was mixed with 200 μ l of *Agrobacterium* DHA105 competent cells and incubated at RT for 30 min. The transformation reactions were frozen at -80°C for 5 min and thawed for 5 min at 37°C. 800 μ l of YEB medium was added to the transformation reactions and incubated for about 4 hours at 28°C. The cells were spun down at 4,000 rpm for 5 min and resuspended in 100 μ l of YEB medium, then plated on Kanamycin plates and grow for two days at 28°C. Transformed colonies became visible on the second day of incubation.

2.3.14. Colony PCR

To identify positive clones of transformed bacteria, PCR screening was performed. A PCR master mix with gene-specific primers was prepared, containing all components except the DNA-template (section 2.15.8), and was distributed into PCR-tubes. Each colony was picked with a sterile toothpick. The toothpick was first dipped into a PCR tube containing the master mix and then streaked out on a correspondingly labelled patch of an LB plate. The plate was incubated at 37°C. The PCR was performed using an appropriate program as described in 2.3.6. 10 μ l of each PCR were analyzed on a 1% agarose gel to identify positive clones. These clones were used for the following isolation of plasmid DNA.

2.3.15. Isolation of plasmid DNA

LB medium (10 ml) supplemented with the appropriate antibiotic was inoculated with a single bacterial colony that was transformed with the gene of interest (verified by colony PCR, section 2.3.14). Cells were cultured overnight by incubating at 37°C in a shaker. The cultures were centrifuged at 4,000 x g for 10 min to obtain the cell pellets from which plasmid DNA was isolated using E.Z.N.A.[®] Plasmid miniprep Kit II (Pierce), according to the manufacturer's instructions. The plasmid-DNA was eluted with 50 µl of ddH₂O.

LB medium (Luria-Bertani-Medium) :

Bacto-trptone	10 g/l
Bacto yeast extract	5 g/l
NaCl	10 g/l
	pH adjusted to 7.0 with NaOH

LB-Amp + X-Gal/ IPTG plates:

Solution	Stock solution	Final conc.	Dilution
100 mg/ ml	ampicillin (light and heat sensitive; cool down the agar prior to the addition of ampicillin, store plates no longer than 2 weeks)	100 µg/ ml	1: 1, 000
20 mg/ ml (2% w/v)	X-Gal (dissolved in di-methylformamide, stored in the dark at -20 °C)	40 µg/ ml	1: 500
100 mM	IPTG (dissolve 0.119 g in 5 ml of H ₂ O, filter sterilize, store at -20 °C)	200 µM	1: 500

2.3.16. Restriction digestion

Restriction digestion was performed for further analysis of positive colonies or subcloning. For a restriction digest, 1 µg of plasmid-DNA was mixed with 0.5 µl of restriction enzyme and 1 µl of the appropriate 10x reaction buffer and made up to 10 µl with sterile ddH₂O. The mixture was incubated for 4 h or overnight at 37°C followed by an electrophoretic analysis of the restricted fragments. For double digests, (1) plasmids DNA or PCR fragment was digested with two restriction enzymes at the same time if they required a compatible reaction buffer available to reach the maximum activity; (2) if there was no appropriate reaction buffer for both restriction enzymes, plasmids DNA or PCR fragment was

first digested by one restriction enzyme, phenolized and ethanol precipitated (see chapter 2.3.10) and then further digested by the second restriction enzyme.

2.3.17. Sequencing

The method of Sanger et al. (1977) was followed for DNA-sequencing based on differential labelling of dideoxynucleotides using dRhodamine (ABI PRISM dRhodamine Terminator Cycle Sequencing Ready Reaction Kit, Perkin Elmer Applied Biosystems, Weiterstadt, Germany). The differentially labelled ddNTPs have absorption and emission spectra at 450~650 nm. The PCR mix comprised the following:

Terminator Ready Reaction Mix	2 µl
plasmid DNA	150-300 ng
sequencing primer	10 pmol
H ₂ O	fill to 10 µl

Chain elongation proceeded under the following conditions in a Personal Mastercycler (Eppendorf, Hamburg, Germany):

Cycle	Temperature	Duration
25	96°C	10 sec
	50°C	5 sec
	60°C	4 min

The DNA was precipitated using EDTA-sodium acetate in order to remove dRhodamine-ddNTPs that interfere with the sequencing. To 10 µl PCR-mixture 3 M sodium acetate containing 125 mM EDTA were added to obtain a final concentration of 0.3 mM and 12.5 mM, respectively and mixed by vortexing. Then 25 µl of 99.6% (v/v) ethanol were added and mixed by inverting. The samples were incubated for 15 min at room temperature, followed by centrifugation for 15 min at 13,000 rpm at 4°C. After removal of the supernatant, the pellet was washed twice in 35 µl of 70% (v/v) ethanol. The pellet was dried for 10 min at 37°C and finally dissolved in 30 µl sterile ddH₂O. The sample was then ready to be sequenced using ABI Prism 3100 Genetic Analyzer (Perkin Elmer Applied Biosystems, Weiterstadt, Germany) in Prof. Pieler's lab (Institut für Biochemie und Molekulare Zellbiologie, Göttingen).

2.4. Subcellular localization studies in *S. cerevisiae* and *Allium cepa* L.

For characterization of the subcellular localization of putative peroxisomal proteins, both yeast and plant expression system were used. Targeting prediction was performed as described earlier (Reumann et al., 2004). Fusion proteins with N- or C- terminally located yellow fluorescent protein (YFP) were generated to investigate the function of C- terminal and N- terminal targeting signals, respectively. For labelling of peroxisomes in double transformants of onion epidermal cells, a fusion protein of the N- terminal 50 residues of glyoxysomal malate dehydrogenase (gMDH) from *Cucumis sativus* L. comprising the PTS2 targeting domain (Gietl, 1990) and enhanced cyan fluorescent protein (ECFP) was used (gMDH-ECFP, Fulda et al., 2002). For labelling of mitochondria in onion epidermal cells, a fusion protein of the mitochondrial presequence of the cytochrome C oxidase subunit IV from *S. cerevisiae* and ECFP was used (CoxIV-ECFP, Fulda et al., 2002). The gMDH-ECFP and CoxIV-ECFP plasmids were kindly provided by Dr. M. Fulda (University of Göttingen, Göttingen, Germany). For double labelling of peroxisomes in yeast, the DsRed protein of the reef coral *Discosoma* sp. supplemented by a C- terminal SKL tripeptide was used (kindly provided by Dr. Schmitt, University of Saarland, Saarbrücken, Germany).

2.4.1 cDNA constructs of peroxisomal small heat shock proteins

The full-length cDNAs of *AtHSP15.7* (At5g37670) and *AtACD31.2* (At1g06460) were amplified from pGEMT with primers containing appropriate restrictions sites (see Appendices 7.1.) and subcloned in frame into the plant expression vector pCAT-YFP-N-fus (Fulda et al., 2002) under control of a double 35S CaMV promoter. The full-length fusion protein and deletion construct lacking the C- terminal 14 residues were subcloned in frame into the pCAT-YFP-N-fus yielding EYFP-AtHsp15.7 and EYFP-AtHsp15.7 Δ C, respectively. To investigate the targeting function of the predicted mitochondrial presequence of AtHsp15.7, the same cDNA fragment was attached via *Nco*I to the 5' end of EYFP in the vector pCAT-YFP-C-fus. For analysis of the targeting function of the putative PTS2 of AtAcd31.2, the full-length cDNA was cloned likewise into pCAT-YFP-C-fus (Fulda et al., 2002). To investigate if AtAcd31.2 contains a functional PTS2, a deletion construct (residues 30-285) lacking the N-terminal 29 residues and the putative PTS2 (RHx₅HF, residues 11 to 19) was subcloned in frame into pCAT-YFP-C-fus. Site-directed mutagenesis was performed using PfuUltra™ high-fidelity (HF) DNA polymerase for mutagenic primer-directed replication

of both plasmid strands (AtAc31.2-EYFP and EYFP-AtAc31.2) according to the Quick-Change II Site-Directed Mutagenesis Kit (Stratagene, USA). The mutagenic primers are listed in Appendices 7.1. The PTS2 of AtAc31.2 was changed from RLx₅HF to RLx₅DF and the PTS1 from PKL> to PEL> as confirmed by sequencing. The full-length fusion protein and deletion construct lacking the C-terminal three residues were subcloned in frame into the pCAT-YFP-N-fus yielding EYFP-AtAc31.2 and EYFP-AtAc31.2ΔPTS1, respectively. To investigate whether the AtAc31.2 was targeted to peroxisomes by piggybacking, the putative dimerization loop was deleted in both cDNAs (yielding EYFP-AtAc31.2Δ226-252 and EYFP-AtAc31.2Δ226-252ΔPTS1) by two successive of PCR. In the first reaction, the N-terminal fragment (residues 1-225) and C-terminal fragment (residues 253-285 or 253-282) were amplified and used as templates for the second PCR. To amplify the entire PCR fragment, the forward primer of the N-terminal fragment and the reverse primer of the C-terminal fragment were used.

2.4.2. cDNA constructs of putative peroxisomal protein kinases (PPPKs)

To study the subcellular localization of PPPK1-4 in *S. cerevisiae*, all of which contained a putative C-terminal PTS1 tripeptide, the proteins were fused at their N-terminal end to green fluorescent protein (GFP). The full-length genes of interest were amplified from pGEMT constructs with primers containing appropriate restriction sites (mostly *Xba*I at the 5'-end and *Sma*I at the 3'-end, see Appendices 7.1.) and subcloned in-frame into the yeast expression vector pGFP-N-fus under the control of the *MET25* promoter and containing the *Ura-3* gene encoding a protein involved in uracil biosynthesis for selection of transformants.

To study the subcellular targeting of putative PTS1-containing PPPKs in plant cells, fusion proteins with N-terminally located yellow fluorescent protein (YFP) were generated. The full-length cDNAs of *PPPK1-4* or fragments thereof were amplified from pGEMT constructs with primers containing appropriate restriction sites (mostly *Not*I at the 5'-end and *Xba*I at the 3'-end, see Appendices 7.1.) and subcloned in frame into the plant expression vector pCAT-YFP (Fulda et al., 2002) under the control of a double 35S promoter. For analysis of the peroxisome targeting efficiency of putative PTS domains, the C-terminal ten residues of PPPK2-7 and HPR (Fig.1) were fused to the C-terminal of the EYFP by PCR using an appropriate reverse primer and subcloned in-frame into the plant expression vector pCAT. Due to its unusual stretch of eight acidic residues at position -5 to -

12, the C-terminal domain fused to YFP was extended for PPPK1 to 13 residues (Fig. 1). To define targeting enhancing and inhibitory elements of putative PTS1 domains, the stretch of eight acidic residues was removed from the putative targeting domain (PTD) of PPPK1 and 6 upstream residues of the endogenous protein added to yield the construct EYFP-PTD Δ _{EPPPK1}. Analogously, four neutral residues of the PTS1 targeting domain of HPR were changed to acidic residues and subcellular targeting of the corresponding YFP fusion protein investigated. Likewise, the two arginine residues were removed from the PTD of PPPK4 and exchanged to neutral residues to yield the construct EYFP-PTD Δ R_{PPPK4}.

2.4.3 Subcellular localization studies in *S. cerevisiae*

The *S. cerevisiae* strain BJ 1991 (*MAT α* , *leu2*, *trp1*, *ura3-251*, *prb1-1122*, *pep4-3*, *gal2*; Jones, 1977) was transformed as described above (see chapter 2.3.13.2), and transformants were maintained on synthetic complete plates (2 % (w/v) glucose and 0.17 % (w/v) yeast nitrogen base, 0.5 % (w/v) ammonium sulfate, 0.5 % (w/v) yeast extract, 3 % (w/v) agar) supplemented with appropriate amino acids and bases. For growth of single transformants, the cells were cultured overnight in 2 % glucose and 0.17 % yeast nitrogen base, 0.5 % ammonium sulfate, and 0.5 % yeast extract. For growth of transformants expressing both GFP and DsRedSKL, the cells were first cultured overnight in a slightly different selective synthetic complete liquid medium of reduced glucose concentration (0.3 %) to an OD₆₀₀ of about 2~3. To induce peroxisome proliferation, cells were transferred to selective 0.1 % oleic acid medium (0.1 % (v/v) oleic acid, 0.2 % (v/v) Tween 40 and 0.67 % yeast nitrogen base) at a starting OD₆₀₀ of 0.05 and cultured for about 24 h to an OD of about 2-3. The cells were then boosted by the addition of 2 % glucose and cultured for another 10-16 h. The cells were concentrated by centrifugation (10,000x g) and observed within 60 min without fixation.

2.4.4. Subcellular localization analysis in *Allium cepa* L.

The transformed onion slices were placed on wet paper in Petri dishes and stored on a bench top for 16-24 h. For analysis by fluorescence microscopy the onion skin epidermal cell layer was peeled and transferred to a glass slide.

2.4.5. Fluorescence microscopy

Analysis of yeast and onion epidermal cells was performed using a fluorescence microscope (Olympus BX51) with the following filter sets: GFP (U-MW IB A2; excitation filter BP 460-490, barrier BA 510-550, Olympus); DsRed (excitation filter HQ545/30, barrier HQ610/75); EYFP (F41-028; excitation filter HQ500/20, barrier HQ535/30), and ECFP (F31-044; excitation filter D436/20, barrier D480/40). Digital images were captured using a CCD camera (ColorViewII) with analySIS3.1 Imaging software (Soft imagine system GMDH).

2.5 Yeast two-hybrid analyses

The Matchmaker Two-Hybrid System 3 (Clontech, Palo Alto, USA) was used in this study. Two vectors, pGADT7 and pGBKT7, and two yeast strains AH109 and Y187 were provided in this system. The genotypes of the yeast strains are shown in chapter 2.14. AH109 utilizes two nutritional markers, *HIS3* and *ADE2*, to control the stringency of selection: the *ADE2* gene, under the control of the *GAL2* promoter, reduces the number of false positives, while the *HIS3* gene, under the control of the *GAL1* promoter, provides sensitive growth selection that helps to identify weak positive signals. β -galactosidase activities encoded by *lacZ* can be detected by the so-called colony lift assay. The yeast co-transformation method is described in chapter 2.5.2.

2.5.1 cDNA constructs for protein-protein interactions studies using yeast two-hybrid system

To investigate whether PPPK7 interacts with the PTS1 receptor, AtPex5, the full-length cDNA of *PPPK7* was transferred to the vector pGBKT7 and the cDNA fragment corresponding to TPR domain (amino acid residues 457 to 728) of *AtPex5* was transferred to the vector pGADT7. The full-length of the cDNA of *AtHSP15.7* was transferred to the vector pGBKT7 as a positive control. To investigate if AtAtg1a interacts with AtAtg13a, several cDNA fragments of *AtAtg1a* (amino acid residues 1-300, 300-623, and 415-623) were transferred to the vector pGBKT7 and the cDNA fragment of *AtATG13a* (amino acid residues between 340 and 500) was transferred to the vector pGADT7.

2.5.2 Protein-protein interaction studies by yeast two-hybrid analyses

All cDNAs encoding full-length or truncated proteins were cloned into pGBKT7 (a Gal4 DNA-binding domain “bait” vector) or pGADT7 (a Gal4 activation domain “prey” vector). Two-hybrid assays were carried out according to the procedures described in the manufacturer’s manual. To determine protein-protein interactions, the bait and prey plasmids were co-transformed into the yeast strain AH109 by using the lithium acetate method (section 2.5.3). The co-transformed yeast cells were plated onto minimal synthetic dropout (SD) medium lacking leucine and tryptophan and incubated at 30 °C for 3-5 days. Co-transformants were then replicated on two different selective media: SD/-His for selection of activation of the *GAL1-HIS3* reporter gene and SD/-Ade-His-Leu-Trp for selection of the activation of both the *GAL1-HIS3* and the *GAL2-ADE2* reporter gene. In each assay, empty vectors pGADT7 and pGBKT7 were used as negative controls, and BD-AtHsp15.7/AD-AtPex5-TPR as a positive control. At least two independent co-transformants were tested for each experiment.

2.5.3 LiAc-mediated yeast co-transformation

Yeast colonies were grown in 15 ml of YPDA medium overnight at 30°C until they had reached the stationary phase ($OD_{600} > 1.5$) and were used to inoculate 150 ml of YPD medium containing 0.003 % (v/v) adenine sulphate to produce an OD_{600} of 0.2~0.3. The flask was incubated at 30 °C for 3-5 hours while shaking (230~270 rpm) to reach the mid-log phase (OD_{600} 0.4~0.6). This culture was sufficient for 30 transformations. The yeast culture was transferred into sterile 50 ml centrifugation tubes and centrifuged at 2,000 rpm for 5 min at RT. The medium was poured off and washed with 15 ml of sterile distilled water. The cells were combined into one tube and collected. 3.0 ml of PEG/LiAc solution was added to the pellets and vortexed to resuspend the cells. This treatment leads to permeabilization of the yeast cells, resulting in competent cells.

100 µl of yeast competent cells were added to a 1.5- ml sterile microcentrifuge tubes containing 5 µl of salmon sperm DNA (10 mg/ ml) and ~ 1.0 µg DNA plasmids from bait and prey and were mixed well by pipetting. The tubes were incubated at 42 °C for 20-30 minutes. Then the cells were chilled on ice immediately for 1-2 minutes, and centrifuged at 7, 000 rpm for 10 seconds to remove the supernatant. 50-100 µl of sterile dd H₂O was added to the

tubes and the pellets were resuspended by pipetting gently. The transformation mix was spread on an SD/ -Leu-Trp. The plates were incubated at 30 °C until colonies appeared.

1 ml PEG :

50% PEG 3300	800 µl
1 M LiCl, pH 7.5	100 µl
10x TE buffer, pH 7.5	100 µl

2.5.4 Colony-lift filter assay

The colony-lift filter assay was used to detect β -galactosidase activity. It is used to investigate interactions between two known proteins in the GAL4 yeast two-hybrid system. Plates were incubated at 30°C until colonies appeared and grew to a size of 1-2 mm. This usually took 4-5 days. For each plate of transformants, a piece of sterile Whatman #5 paper was pre-soaked in 2.5-5.0 ml of Z buffer/X-gal solution in a clean 150 mm plate. Using clean forceps, a clean dry filter was placed on the surface of the plate with colonies and gently rubbed with the side of the forceps, which helped the colonies to cling to the filter. After the filter was evenly wetted, it was carefully lifted and transferred to liquid nitrogen (colonies facing up). Liquid nitrogen lyses the yeast cells, thus allowing detection of the reporter gene. The filters were submerged for 10 seconds and subsequently thawed at RT. The filter colony side facing up was then cautiously placed on the pre-soaked filter, with care not to trap any bubbles between the two filters. Filters were incubated at 37°C and checked periodically (up to 8 hours) for the appearance of blue colonies.

2.6 Plant transformation

2.6.1. Transformation of *Arabidopsis thaliana* with *Agrobacterium tumefaciens*

A. thaliana ecotype Columbia plants were grown as described in 2.2.1. Secondary bolts were encouraged to proliferate by clipping the first bolts. Plants were ready 4-6 days after clipping. Clipping can be repeated to delay plant flowering. Optimal plants have many immature flower clusters and not many fertilized siliques, although a range of plant stages can be successfully transformed. Flowering plants were used for transformation with *Agrobacterium* (Clough and Bent, 1998). 500 ml of YEB with kanamycin (50 µg/ml) were inoculated with several colonies of *A. tumefaciens* DHA105 transformed with desired plasmids and grown at 28 °C overnight until the cells reached early stationary phase. The cells were spun down and resuspended in about 200 ml of 5 % (w/v) sucrose solution to a

final OD₆₀₀ of 0.8. Before dipping, Silwet L-77 (General Electric Sarl, Antwerpen, Belgium) was added to the cell suspensions to a final concentration of 0.02 % and mixed by vortexing. The inflorescences of *A. thaliana* plants were then dipped into the *Agrobacterium* suspension for 2~3 sec under gentle agitation. The dipped plants were left in open air for several hours and then placed under a transparent plastic foil to provide a high humidity for two days. For high rates of transformation, plants were dipped two or three times at seven day intervals. Plants were then watered and grown as normally until seed production.

2.6.2. Transformation of onion epidermal cells

2.6.2.1 DNA precipitation onto gold particles

50 mg of gold particles was resuspended in 1 ml of 99.8 % ethanol and vortexed thoroughly for 1~2 min. The gold particles were then sedimented at 10,000 rpm for 10 sec and washed again with 1 ml of pure ethanol. The washing step was repeated twice. After the last washing step, the gold particles were washed with 1 ml of dd H₂O instead of ethanol and mixed thoroughly as described above. After being spun down, the gold particles were resuspended again in 1 ml water, and 50 µl of gold particles was equally aliquoted into 1.5 ml eppendorf tubes. The following steps were carried out on ice. For DNA precipitation, the following components were added in the given order and vortexed thoroughly for 10 sec to 2 min: 5~7 µl of plasmid DNA (1 µg/ µl) (final concentration about 40 ng/ µl); 50 µl of 2.5 M CaCl₂ (final concentration about 1 M); and 20 µl of 0.1 M spermidine (final concentration about 10 mM). The DNA was precipitated onto the gold particles by centrifugation at 10,000 rpm for 10 sec. The gold particles were further washed twice using 250 µl of 99.8 % ethanol and finally resuspended in 60 µl of 99.8 % ethanol for bombardment.

2.6.2.2. Transformation of onion epidermal cells by bombardment

The biolistic system uses high pressure helium, released by a rupture disk that bursts at a defined pressure, and partial vacuum to propel a macrocarrier sheet loaded with millions of microscopic gold microcarriers toward target cells at high velocity. The macrocarrier is halted after a short distance by a stopping screen. The DNA-coated microcarriers continue travelling toward the target to penetrate and transform the cells.

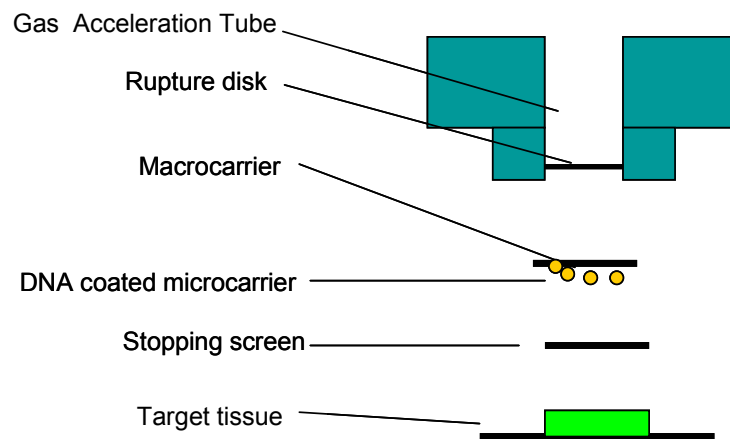


Figure 2.1: Biolistic PDS-1000/He Particle Delivery system

The gun chamber was washed with 70% ethanol including macro-carrier, rupture disk, retaining cap before operation of the particle delivery system. The helium pressure was adjusted to 2000 PSI. The gold particles coated with desired plasmids were vortexed thoroughly and loaded onto the macro-carrier holder in the shooting device. The gold particles were spread over an area of about 1 cm² in the middle. A sterilized rupture disk was loaded into the sterile retaining cap and tightly secured to the end of the gas acceleration tube. The micro-carrier, macro-carrier, and stopping screening were assembled into the micro-carrier launch device. The micro-carrier launch device and targeted onion epidermal cells was inserted into the top shelf and the third shelf, respectively. The bombardment was carried out using 1100 PSI rupture disks and a vacuum of 0.1 bar. The helium bottle was closed, when all the experimental steps were finished. The helium pressure was released by applying a vacuum and “shooting” a couple of times.

2.7 Southern blotting

The principle of Southern blots (Southern, 1975) is the electrophoretical separation of DNA fragments of various sizes on an agarose gel, followed by transfer and immobilization of the DNA fragments onto a nylon membrane. The membrane-bound DNA can be then hybridized with labelled DNA probes to identify complementary sequences among the immobilized DNA.

2.7.1 Digestion of genomic DNA with restriction enzymes

10-15 µg of genomic DNA from *Arabidopsis* Col-0 and T-DNA knock-out mutants were digested overnight with different restriction enzymes (150 µg): *EcoRI*, *EcoRV*, and *HindIII*. The sample was incubated at 37 °C overnight and additional 150 units of restriction enzyme were added and digested for another 6 to 8 hours. The completeness of the digestion was checked by electrophoresis on a 0.7 % agarose gel. The restricted DNA samples were purified by phenol: chloroform extraction (see 2.3.9), precipitated with 99.8 % ethanol at -20 °C and re-dissolved in 25 µl of dd H₂O. After supplementation with blue loading dye, the DNA samples were loaded on a 0.7 % agarose gel next to 1 µg of GeneRuler DNA ladder Mix (MBI) as size marker. The electrophoresis was run at 1 V/ cm overnight.

2.7.2 Transfer of digested genomic DNA to nylon membrane

Blotting was performed by alkaline transfer to a Hybond N⁺ nylon membrane (Amersham-Pharmacia, Freiberg, Germany). First, the gel was photographed and shortly washed in water. The upper part of the gel that contained DNA fragments > 10 kb was washed with depurination solution for 15 min. The gel was placed in denaturation (alkaline) buffer and incubated for 20 min under gentle shaking. The incubation was repeated with a fresh portion of the buffer. In the meantime, a piece of Hybond N⁺ membrane of the size of the gel was wetted with water and incubated for 20 min in denaturation buffer. Then, a capillary blot was set up as following: A plastic tray was half filled with denaturation buffer; a wick of the breadth of the gel was cut from Whatman 3 MM paper, equilibrated with denaturation buffer and placed on a platform on top of the plastic tray with its ends hanging into the buffer. The gel was placed on the wick with the DNA-side upwards, and the membrane was placed on top of the gel. The membrane was overlayed with three sheets of 3 MM paper of membrane size pre-wetted in denaturation buffer, and a stack of absorbent towels was placed on top of the 3 MM paper. The parts of the wick that were not in contact with the gel were covered with pieces of parafilm to ensure that the suction of the buffer proceeded only through the gel. Finally, a plastic plate and a weight of ca.1 kg were placed on the stack, and the transfer proceeded overnight. The membrane was washed in 2 x SSC

for 20 min for neutralization and dried at room temperature on a piece of 3 MM paper. The membrane could be stored in a plastic bag at 4 °C.

Depurination solution :

HCl 0.125 mM

Denaturation buffer :

NaCl 1.5 M

NaOH 0.4 M

20 x SSC :

NaCl 3 M

Na₃ citrate 0.3 M

adjust pH7.0

2.7.3 Hybridization of DNA gel blots

2.7.3.1 Labelling of probes

For hybridization of DNA (Southern blot) immobilized on a nylon membrane, DNA probes were labelled radioactively using α -³²P-dCTP. The probes were prepared using the HexaLabel Kit from MBI Fermentas (Vilnius, Lithuania). 100 ng of DNA template (DNA fragment isolated from an agarose gel) and 10 μ l of a hexanucleotide mixture provided in the kit were denatured in buffer at 100 °C for 10 min in a total volume of 40 μ l. Then, 3 μ l of Klenow nucleotide mixture (minus dATP), 3 μ l of α -³²P-dCTP (10 μ Ci/ μ l; Hartmann Analytik, Braunschweig, Germany) and 1 μ l of Klenow exo-polymerase were added. The reaction was incubated at 37 °C for 30 min. Unincorporated α -³²P-dCTP was removed from the probes using a ProbeQuant™ G-50 Micro Columns (Amersham Pharmacia Biotech, Freiburg, Germany). The eluted probes were denatured by heating at 95 °C for 5 min and immediate chilling in ice water. The synthesized probes were ready to use.

2.7.3.2. Hybridization and washing of blots

DNA blots were placed in hybridization tubes containing ca. 15 ml of hybridization buffer and incubated at 65 °C for at least 3 hour in the hybridization oven under rotation. The labelled probes (section 2.7.3.1) were added to the hybridization tube with 15 ml fresh hybridization buffer. The hybridization proceeded at 65 °C in the hybridization oven for 16~20 hours. Afterwards, to remove non-hybridized label, the membrane was washed first twice with 200 ml of low stringent wash buffer at RT for 15 min. Then the DNA blots were washed

in 200 ml of high stringent buffer at 65 °C for 30 min twice. The membrane was then dried on 3MM paper, sealed into plastic bags, and the hybridization signal was detected by X-ray film at -80 °C for several days.

Hybridization buffer:

Na ₂ HPO ₄ pH 7.2	250 mM
SDS	7 % (w/v)
EDTA	1 mM

Low stringent buffer :

Na ₂ HPO ₄ pH 7.2	40 mM
SDS	5 % (w/v)
EDTA	1 mM

High stringent buffer :

Na ₂ HPO ₄ pH 7.2	40 mM
SDS	1 % (w/v)
EDTA	1 mM

2.8 Yeast complementation studies (in collaboration with Dr. Haslbeck, University Munich, Germany)

Deletion constructs of AtHsp15.7 or AtAcd31.2 lacking the C-terminal three residues and/ or the N-terminal PTS2 (residues 1 to 29), namely AtHsp15.7 Δ PTS1, AtAcd31.2 Δ PTS1 and AtAcd31.2 Δ PTS1+2, were generated to target the proteins to the yeast cytosol and subcloned without any terminal tags into the pYES2.1-topo cloning vector under the control of a *GAL1* promoter and containing the *ura-3* gene for selection of transformants. (pYES2.1 TOPO TA expression kit, Invitrogen, Karlsruhe, Germany). For all *in vivo* studies *S. cerevisiae* single or double deletion strains deficient in ScHsp42 and/or ScHsp26 were used (Haslbeck et al., 2004). After transformation yeast deletion strains expressing *Arabidopsis* sHsps were first selected on URA-CSM media containing glucose. Prior to induction of the expression of the peroxisomal sHsps, mid logarithmic phase cells cultivated at 30 °C were transferred to URA-CSM media containing raffinose for 2 hours. Next, the cells were transferred to URA-CSM media containing galactose for induction. After 4 hours of induction the cultures were heat shocked for 1 hour at 43 °C and subsequently analysed by scanning electron microscopy. As negative control, equally treated but uninduced cells, which were

incubated in URA-CSM containing glucose instead of galactose for 4 hours before heat shock, were used.

2.9 Characterization of *Arabidopsis* T-DNA knock-out mutants

Arabidopsis T-DNA insertion mutants were ordered from NASC. The following T-DNA insertion lines were used: *hsp15.7-1* (salk_038951), *hsp15.7-2* (salk_038954), *hsp15.7-3* (salk_107711), *acd31.2-1* (salk-114949), and *atg1-1* (salk-54351). Two primers, LP (left primer) and RP (right primer) were designed in order to confirm the T-DNA insertion in the ordered mutants. The RP is always on the side of the flanking sequence, that is, RP is always on the 3' end of the insertion. Therefore, LP is always on the 5' end of the insertion. So, in homozygote populations, the PCR reactions always set up as BP (left border primer of the T-DNA insertion)+RP to confirm the presence of T-DNA insertion allele, LP+RP to confirm the absence of wild-type allele of the interested gene locus.

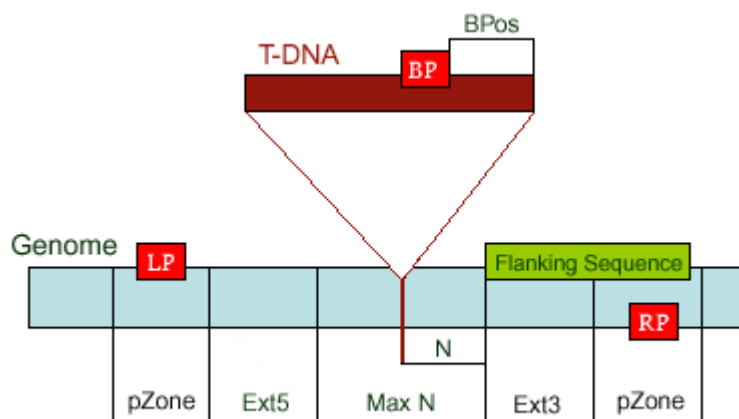


Figure 2.2 Diagram of the location of LP, RP and BP used for genomic PCR

2.10 Protein analysis in *Arabidopsis* peroxisomes

2.10.1 Isolation of leaf peroxisomes from *Arabidopsis*

All steps were performed at 4°C. About 200 g of fresh leaf material from 4 weeks old plants grown under long day light condition were ground thoroughly in 350 ml grinding buffer in the presence of protease inhibitors (final concentration: PMSF, 0.1 mM; Benzamidin, 0.2 mM; α-amino caproic acid; 0.2 mM) using a mortar and pestle. The homogenate was filtered through one layer of Mira cloth. Cell debris and chloroplasts were

removed by differential centrifugation of the homogenate at 5,000 x g for 1 min in a Sorvall SS34 rotor (Sorvall RC5B). The supernatant was collected in a new tube over a 2 ml of 50 % (w/w) sucrose cushion (in TE buffer, with 0.5 % BSA). Peroxisomes were sedimented by centrifugation at 25,000 x g for 5 min. The pellets were gently resuspended using a soft paint brush and homogenized for 5 strokes in a tight fitting Potter-Elvehjem homogenizer. The suspension was equally layered over 6 preformed discontinuous sucrose density gradients. The gradients were spun for 2 h at 83,000 xg in a Beckman Coulter Ultracentrifuge using an SW28 rotor.

The peroxisome band at the 52-60% interface was pooled from the six gradients and homogenized as described before. The peroxisome suspension (about 52% (w/w) sucrose) was gradually diluted with 40% (w/w) sucrose to make a gradient from 50 % to about 43% in two SW28 centrifugation tubes and underlaid with 2 ml 60% (w/w) sucrose. The gradients were centrifuged for 10 h at 83,000 xg. After centrifugation, the gradients were fractionated in 2 ml aliquots. Protease inhibitors were added into the peroxisomal aliquots (final concentration: PMSF, 1 mM; benzamidin, 2 mM; α -amino caproic acid, 2 mM; leupeptin, 2 μ M; aprotinin, 1 μ g/ml; pepstatin, 1 μ g/ml).

Grinding buffer:

tricine -KOH pH 7.5	170 mM
sucrose	1.0 M
EDTA (Na ²⁺)	2 mM
KCl	10 mM
MgCl ₂	1 mM
BSA	1.0 % (w/v)
DTT (freshly added)	5 mM

Sucrose density gradient medium:

Tricine KOH pH 7.5	10 mM
EDTA (Na ²⁺)	1 mM
Sucrose	18, 25, 35, 41, 52, 60 % (w/v)

2.10.2 Protein determination (Lowry et al., 1951)

A sample volume containing between 1 and 20 μ g protein was mixed with 800 μ l of the ABC mixture by vortexing and incubated for 15 min. Afterwards, 32 μ l of Folin-Ciocalteu's phenol reagent were added, mixed rapidly by vortexing and the samples were incubated for 10 min and the extinction was measured at 578 nm. From each sample, two aliquots were

analyzed. For each analysis, a calibration curve was made using bovine serum albumin (BSA). The calibration curve points corresponded usually to 2.5, 5, 7.5, 10, 15, 20, and 25 μg protein in the sample. Typically, a calibration curve with an equation of $y = 0.115x + 0.0274$ was obtained.

Stock solutions:

Solution A	2 % (w/v) Na_2CO_3 in 0.1 M NaOH
Solution B	1 % (w/v) $\text{CuSO}_4 \cdot 5\text{H}_2\text{O}$
Solution C	2 % (w/v) Na-K-tartrate

Prior to use, the stock solutions A, B and C were mixed in the ratio of 20:1:1

2.10.3 Protein precipitation (Wessel and Fluegge, 1984)

The entire procedure was performed at 4°C. The diluted protein sample was mixed successively first with a four-fold volume of methanol, an equal volume of chloroform and three volumes of water and briefly spun at 12, 000 x g for a minute for phase separation. The upper phase was carefully removed using a finely drawn capillary followed by precipitation of the proteins with three volumes of methanol. The protein pellet was air-dried at room temperature or was dried at 37°C.

2.10.4 Sodium dodecyl sulphate polyacrylamide gel electrophoresis (SDS-PAGE)

Standard procedures according to Laemmli (1970) were followed for the electrophoretic resolution of proteins by denaturing SDS-PAGE.

Stacking gel:

Tris-HCl pH 6.8	0.13 M
SDS	0.1% (w/v)
Acrylamide	4.6% (w/v)
N,N-Methylenebisacrylamide	0.12% (w/v)
APS	0.06% (w/v)

Resolving gel:

Tris-HCl pH 8.8	0.13 M
SDS	0.1% (w/v)
Acrylamide	4.6% (w/v)
N,N-Methylenebisacrylamide	0.12% (w/v)
APS	0.06% (w/v)

The gel was run first at constant current (30 mA/ gel) for 20 min to stack the proteins. Resolution of proteins was carried out at a constant current of 32 mA/ gel until the bromophenol blue had migrated nearly to the end of the gel.

2.11 Western blotting

Proteins separated by SDS-PAGE were transferred to nitrocellulose membrane (Amersham, Freiberg, Germany) using a tank electroblotting system. The gel was first equilibrated in transfer buffer for 15 min, and then it was put between two sheets of whatman paper together with pre-equilibrated nitrocellulose membrane, with the gel facing the cathodic side of the cassette. The cassette was inserted into the tank that had been filled with transfer buffer. For a midi-gel, the transfer was performed at 15 V for overnight. The membrane was briefly washed by TBS buffer and blocked in blocking buffer for 1 h at RT. After blocking, the membrane was washed by TBS buffer and incubated with primary antibody against proteins of interest for one hour at RT (anti-GFP serum) or 24 hours at 4°C (anti-AtHsp15.7 serum) on a rocking platform. The membrane was washed three times for 10 min each and then incubated with a second antibody (anti-rabbit IgG-AP for anti-AtHsp15.7 serum GFP and anti-guinea pig IgG-AP for anti-AtHsp15.7 serum) for 1 h at RT. After washing the membrane for three times with TBS, the ECL detection reagents was applied on the membrane and exposed to X-ray film for 5 min to several hours until strong signals were obtained.

Blotting buffer

Tris pH around 8.2	25 mM
Glycin	192 mM
Methanol	20%

TBS buffer

Tris-HCl, pH 7.5	20 mM
NaCl	500 mM

Blocking buffer: in TBS buffer

Dry milk powder	5%
Tween 20	0,02%

RESULTS

3.1. Identification and characterization of two small heat shock proteins (sHsps) targeted to the matrix of plant peroxisomes

Thanks to the availability of the *Arabidopsis* genome sequence, defined plant-specific PTS peptides, and a variety of subcellular localization prediction programs, we were able to screen the *Arabidopsis* genome by bioinformatics tools for proteins that are targeted to the peroxisomal matrix by one of the two PTS targeting pathways with moderate to high probability (Reumann, 2004, Reumann et al., 2004). In total, 280 largely unknown proteins with putative PTSs were detected. In the course of this study, two small heat shock proteins (sHsps) and several putative protein kinases were analyzed experimentally.

3.1.1 Protein identification, polypeptide structure, and peroxisome targeting prediction

Small heat shock proteins (sHsps) form a ubiquitous family of molecular chaperones with a size range of approximately 16-42 kDa. The members of the sHsp family are generally characterized by a conserved C-terminal domain, referred to as the α -crystallin domain (Ac), a highly variable N-terminal sequence, and, in most cases, a short C-terminal extension. As determined by X-ray crystallography or electron microscopy, sHsps form oligomers that resemble either hollow ball-like or barrel-shaped structures (Fig. 1.4). In both cases, dimers serve as the basic building block of the oligomers (Kim et al., 1998; Van Montfort et al., 2001; Kennaway et al., 2005). Small Hsps are most prevalent in plants and known to reside in several cell organelles like mitochondria, chloroplasts, and the ER (Scharf et al., 2001). For no organism, however, sHsps have been characterized to date in the peroxisomal matrix. In *Arabidopsis*, 19 closely related sHsp homologs and 25 further proteins containing the same Ac domain have been identified based on sequence homology (Scharf et al., 2001).

In a screen of the *Arabidopsis* genome for putative peroxisomal proteins, two of these 44 sHsps-related proteins from *Arabidopsis* were identified, which were designated AtHsp15.7 and AtAc31.2 according to their relative molecular mass, following the nomenclature introduced by Scharf et al. (2001). Both proteins contain an Ac domain and a putative PTS (Reumann et al., 2004, Fig. 3.1). The protein AtHsp15.7 (At5g37670) carries the

putative major PTS1 SKL> at its C-terminus (Reumann, 2004) and was predicted to be targeted to peroxisomes with high probability by three different programs (PTS1 predictor: score=11.8, PSORTI: score=0.800 and PSORTII: score=77.8%). In addition, a mitochondrial presequence was predicted by TargetP (score=0.82) and DBSubLoc (score=91%) in the N-terminus of AtHsp15.7.

The protein AtAcid31.2 (At1g06460) belongs to a new family of Ac domain containing proteins and possesses a predicted C-terminal PTS1 tripeptide (PKL>) as well as a putative PTS2 nonapeptide (RLX₅HF), both of which have been defined as minor PTS peptides (Reumann, 2004), indicating protein targeting to peroxisomes with moderate probability. Compared to other sHsps, the members of the new Ac protein family including AtAcid31.2 contain a pronounced N-terminal extension, but lack the last β -strand of the Ac domain and the following short C-terminal extension.

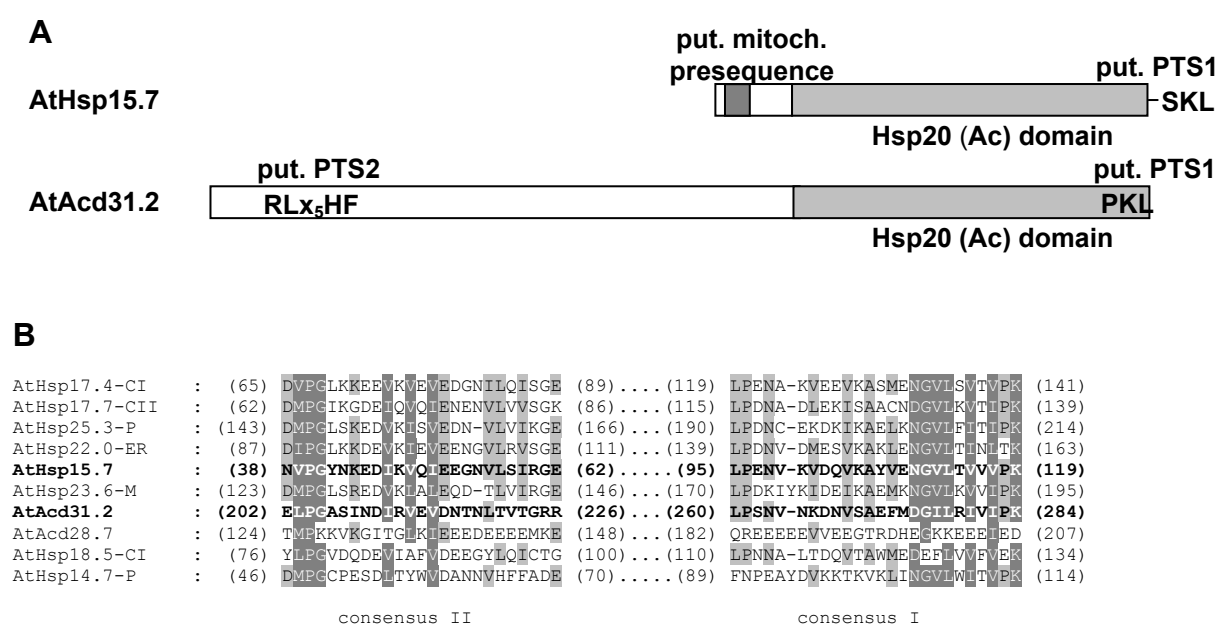


Figure 3.1: Domain structure and predicted targeting signals of AtHsp15.7 and AtAcid31.2.

For both putative sHsps from plant peroxisomes, several subcellular targeting signals (A) and the presence of a conserved Hsp20/ α -crystallin (Ac) domain (B) were predicted. For AtHsp15.7 a mitochondrial presequence and a putative PTS1 were predicted. AtAcid31.2 contains both a putative PTS2 and PTS1 (Reumann et al., 2004, AraPerox: www.araperox.uni-goettingen.de). Light and dark grey shading indicate the localization of the Ac domain and the putative mitochondrial presequence, respectively. For representative members of the *Arabidopsis* family of sHsps and Ac proteins a multiple sequence alignment of the most conserved regions of the Ac domain, consensus I and II, are presented (B).

A

```

At_Hsp15.7 : MADRGILFLYPPFR-----RFQEWRSSTALIDWMESEN (30) ... (108) VENGVLTVVVPKDTSSKSSKVRNVNITSKL*: 137
Bg_Hsp16.0 : MGES-IPGHPPRRFLFWG-PP-IFREWSGSTALMDWFESE (36) ... (112) VESGVLTIIVPKDTSKSSKVRNINVASRL*: 141
Bp_Hsp15.6 : MADG-VEGYPPRRFLFLT-PS-IFREWSGSTALMDWLESP (36) ... (112) VENGVLTIIVPKDATQKSSKVRNINISSKL*: 141
Cs_Hsp14.6 : -----MS-PP-VFREWSGSTALMDWLESP (22) ... (101) VDNGLVTVVVPKDNHKKSSVRNINITSKL*: 130
Gm_Hsp16.2 : MAGT-IPGYPPRRFIWGHPP-IFREWSGSTALLDWLESP (37) ... (115) VENGVLTIIVPKDATEPKTPKVRNINITSRL*: 144
In_Hsp16.1 : --MAAFGDPFRFLWSPTF-YHRAPPGSAALLDWLESP (36) ... (116) VDNGLVTVTVPKDTSKPKSKIRNINITSKL*: 145
Le_Hsp16.1 : ---MAIFGDPFRRLLSPT--IHRSFSGSPALLDWLESP (34) ... (116) CENGVLTIIVPKDAPKPKTSKVTNINITSKL*: 145
Lj_Hsp15.9 : MAES-IFGYPPGRFLWGHPP-IYREWSGSTPLLDWLESP (37) ... (115) VENGVLTVLVPKEAAPKSPKVRNVNITSRL*: 144
Ls_Hsp15.6 : ---MALLGDPFRRFEN-PP-IYRTGVSATGLMDWLETP (34) ... (112) VENGVLTVVLPKDLSPKSKVRNINISSKL*: 141
Mt_Hsp16.0 : MAET-ILGYPPKRFELDHTP-IFRGYSGSTALDWLESP (37) ... (113) VENGVLTVVVPKDAKPKSHKVRNINITSKL*: 142
Os_Hsp16.0 : MADLFFGG-PFRRLYGRPPPDWASASATAAMDWVETP (38) ... (117) VDNGLVTVVVPKEPAPARPRTRPTAVSKL*: 146
Pv_Hsp16.2 : MADT-IFGYPPRRFVFNHPP-VFREWSGSTALDWLESP (37) ... (115) VENGVLTIILPKDITPKSPKVRNINITSRL*: 144

```

B

```

                                RLxxxxxHF
At_Acd31.2 : MEHESITARRRRLAFAAFPA----TSYDASTA (30) ... (256) VSWPLPSNVNKNVSAEFMDGILRVIPKL* : 285
Gm_Acd28.7 : --MESESVKRRRIHMTAAHFAP---NDDIST----T (26) ... (232) VVWPLPAGVKNDRISAFLDGGFLQIIVPKV* : 261
Mt_Acd28.6 : --MNEFVKRRRLDTIAAHFAS---NEDISS----T (26) ... (230) VCVWPLPHGVNKNVSAEFLDGGFLQI*----- : 254
Vv_Acd28.6 : --MEKQAARRRINLIAGHFAP---TDDLSAS---T (26) ... (230) VAWTLPEFNANKDRVSAQFVDGFLQITPKL* : 259
Le_Acd26.5 : --MESQIVRRRVNMTAHLTA---HDDISASA--T (28) ... (209) VFWPLPSNANKNRVSAEFVDGGLQITPKL* : 238
Mc_Acd30.7 : --MESQAARRRITITSGHFGTGIVTEVDVTAAN--P (31) ... (247) VVWPLPAGANKDAVYAEFVEGILHITPKL* : 276
Ah_N-EST : --MESELVRRRVNLIASHFAS---TDDISA---T (26) ..... :
Amar_N-EST : --MESQVRRRVNVIAAHFAS---REDISAT--AT (28) ..... :
Bv_N-EST : --MESQVRRRINTISGHLAARIVTEVDVNAFN--T (31) ..... :
Hp_N-EST : --VASELARRRVEMIGAHFSA---VDHISATAVAP (30) ..... :
Ls_N-EST : --METETAIRRVEMIAAHFSA---ADNISSTGVAT (30) ..... :
PtxPt_N-EST : --MDEAVRRRMNIVAHFAPTI--ADDISSP---A (29) ..... :
Br_C-EST : ..... VSWPLPSNVNKNVSAEFMDGILRVIPKI*- :
Mp_C-EST : ..... VVWPLPANVNRDSISAFLDGGFLRVIPKL*- :

```

Figure 3.2: Conservation of putative PTSs in plant homologs of AtHsp15.7 and AtAcd31.2.

Plant EST sequences from different organisms that shared high sequence similarity with AtHsp15.7 (A) and AtAcd31.2 (B) and are presumably orthologous were retrieved from organism-specific plant EST databases by TblastN and reverse translated from the putative start methionine that aligned with the start methionine of AtHsp15.7 and AtAcd31.2 to the stop codon that aligned with the C-terminal end of the query proteins (www.expasy.ch). Full-length protein sequences were assembled by alignment of overlapping ESTs and supplemented by the genomic full-length ORF from *Oryza sativa* (Os_Hsp16.0). The molecular mass of the proteins was calculated (www.expasy.ch) and the protein names abbreviated following the nomenclature introduced by Scharf et al. (2001) (e.g. Bv_Acd14.5). For AtAcd31.2 full-length homologs (e.g. Am_Acd30.7) assembled by overlapping ESTs were supplemented by partial N-terminal (e.g. Ah_N-EST) or C-terminal ESTs (e.g. Br_C-EST). The alignment presented comprises the N- and C-terminal 30 residues of AtHsp15.7 and AtAcd31.2. Abbreviations and accession numbers are as follows: (A) AtHsp15.7-CI (At5g37670, *Arabidopsis thaliana*), Bg_Hsp16.0, BP943597, *Bruguiera gymnorrhiza*; Bp_Hsp15.6, CD278503, *Betula pendula*; Cs_Hsp14.6, CK932957, *Citrus sinensis*; Gm_Hsp16.2, BF066236, *Glycine max*; In_Hsp16.1, BJ568951, *Ipomoea nil*; Le_Hsp16.1, AW929113, *Lycopersicon esculentum*; Lj_Hsp15.9, BI418471, *Lotus japonicus*; Ls_Hsp15.6, BQ989674, *Lactuca sativa*; Mt_Hsp16.0, AJ500975, *Medicago truncatula*; Os_Hsp16.0, BAD46159, *Oryza sativa*; Pv_Hsp16.2, CV532726, *Phaseolus vulgaris*; (B) Ah_N-EST, CD038232, *Arachis hypogaea*; Amar_N-EST, BM173239, *Avicennia marina*; Br_C-EST, CO749426, *Brassica rapa*; Bv_N-EST, BQ585004, *Beta vulgaris*; Gm_Acd28.7, BI427588 and BM178755, *Glycine max*; Hp_N-EST, CF086378, *Helianthus paradoxus*; Ls_N-EST, BQ993055, *Lactuca sativa*; Le_Acd26.5, AW037627, AI780912, and AI782263, *Lycopersicon esculentum*; Mc_Acd30.7, BF479323 and CA834824, *Mesembryanthemum crystallinum*; Mp_C-EST, CN446454, *Malva pusilla*; Mt_Acd28.6, CX518484, and CF068210, *Medicago truncatula*; Vv_Acd28.6, CA808634 and CB003599, *Vitis vinifera*.

In order to investigate if the putative PTSs of AtHsp15.7 and AtAcd31.2 are conserved among plant species and to provide further bioinformatics evidence for peroxisome targeting of orthologs, plant EST sequences that displayed high sequence similarity with AtHsp15.7 and AtAcd31.2 were retrieved from plant EST databases by TblastN and were reverse translated into protein sequences. All plant homologs of AtHsp15.7 contained a major PTS1 tripeptide, namely either SKL> or SRL> (Fig. 3.2). For AtAcd31.2 homologs, a variety of PTS2 nonapeptides (RLx₅HF, Rlx₅H[LVF], RTx₅HL, or R[MV]x₅HF) were found, most of which lie within the range of defined PTS2 peptides (Reumann, 2004). Two conserved arginine residues generally precede the putative PTS2 and were suspected to serve as auxiliary elements for enhanced peroxisome targeting. In summary, the putative PTS1 of AtHsp15.7 and PTS2 of AtAcd31.2 were largely conserved as PTS peptides among closely related plant homologs, indicating targeting of orthologous proteins to peroxisomes in several plant species with high probability. By contrast, the PTS1 of AtAcd31.2 was less conserved, because homologous ESTs also encoded tripeptide deviations of PTS1 peptides (e.g. PKI> or PKV>) that had neither been defined as major or minor PTS peptides yet nor experimentally been verified as functional PTS1 tripeptides (Mullen et al., 1997; Kragler et al., 1998; Reumann, 2004), suggesting that the PTS1 of AtAcd31.2 was non-functional.

The cDNA sequences of *AtHSP15.7* and *AtACD31.2* were cloned by RT-PCR from flowers and cold-stressed rosette leaves, respectively. Sequence analysis confirmed their identity with the corresponding annotated cDNA sequences (*Arabidopsis* Genome Initiative, 2000). The open reading frame (ORF) of *AtHSP15.7* comprised 411 bp, encoding a protein of a single exon and 137 amino acid residues in length, while *AtACD31.2* was 855 bp in length and composed of seven exons, encoding a protein of 285 amino acid residues.

3.1.2 Localization of AtHsp15.7 to the peroxisome matrix

3.1.2.1 Subcellular targeting analysis of EYFP fusion proteins

To elucidate the subcellular localization of AtHsp15.7, the full-length cDNA of *AtHSP15.7* or truncated or mutagenized versions were fused in-frame to either end of the cDNA of enhanced yellow fluorescent protein (EYFP) in the vector pCAT-YFP under the control of a two-fold 35S promoter of the cauliflower mosaic virus (CaMV, Fulda et al., 2002). To study peroxisomal targeting by the putative PTS1 tripeptide SKL>, *AtHSP15.7* was fused

in-frame with the 3' end of EYFP (EYFP-AtHsp15.7) to guarantee PTS1 accessibility at the C-terminal end of the fusion protein. To test the targeting properties of the predicted N-terminal mitochondrial presequence, the C-terminal 14 amino acid residues of AtHsp15.7 including the putative PTS1 tripeptide were deleted and the truncated cDNA was fused inversely with the 5' end of EYFP (Fig. 3.3).

As reporter genes for specific labelling of mitochondria or peroxisomes, two constructs of enhanced cyan fluorescent protein (ECFP) fused with peptides harbouring organelle-specific targeting information were used (Fulda et al., 2002). For mitochondria, the presequence of the cytochrome c oxidase subunit IV (CoxIV) from yeast was fused C-terminally with ECFP, whereas the control construct for peroxisomes had been generated by fusing the PTS2 domain of glyoxysomal malate dehydrogenase (gMDH) from cucumber to the N-terminal region of ECFP (Fulda et al., 2002). Both plasmids were kindly provided by Dr. M. Fulda (University of Göttingen, Göttingen, Germany). Onion epidermal cells were transformed by bombardment with gold particles coated with plasmid DNA, and subcellular targeting of the fusion proteins was analyzed upon transient gene expression by fluorescence microscopy. Independent control experiments demonstrated that the fluorescence emitted by EYFP and ECFP could be specifically detected and did not interfere with each other (data not shown).

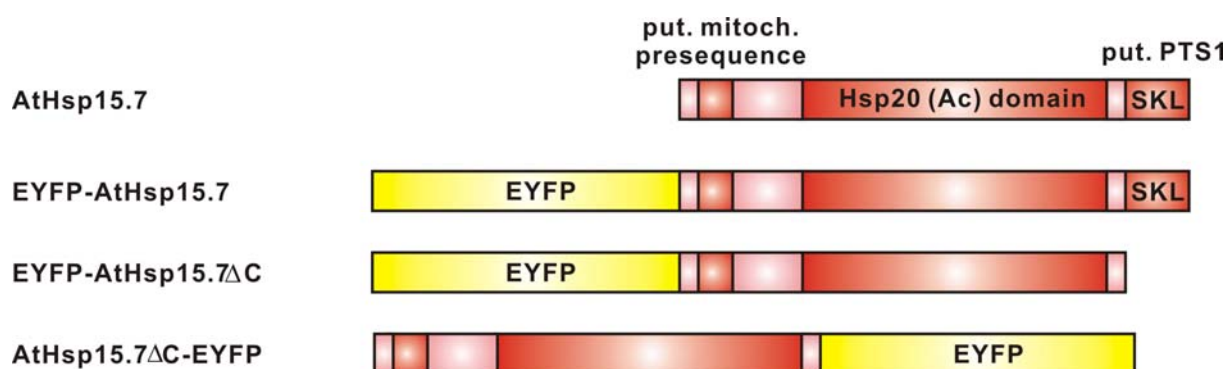


Figure 3.3: Diagram of constructed fusion proteins between AtHsp15.7 and EYFP.

In order to verify the predicted PTS1 SKL> and the mitochondrial presequence, the cDNA of *AtHSP15.7* was fused at the 5'- or the 3'-terminal end, respectively, to *EYFP* and expressed under the control of a double 35S CaMV promoter. The truncated fusion proteins lack the C-terminal 14 amino acid residues of AtHsp15.7 including the predicted PTS1 SKL>:

The fusion protein EYFP-AtHsp15.7 was targeted to small punctate structures that moved quickly along cytoplasmic strands in living cells of single transformants (Fig. 3.4A). These punctate structures were identical with peroxisomes labelled by gMDH-ECFP (Fig. 3.4B, C), but did not overlap with mitochondria labelled by CoxIV-ECFP (Fig. 3.4D, E). These results demonstrated that EYFP-AtHsp15.7 was targeted to peroxisomes in onion epidermal cells. To determine whether the targeting signal of EYFP-AtHsp15.7 was indeed the putative PTS1 tripeptide SKL> of AtHsp15.7, a truncated construct of AtHsp15.7, lacking the C-terminal 14 amino acid residues including the putative PTS1 tripeptide (EYFP-AtHsp15.7 Δ C), was used for transformation of onion epidermal cells. This C-terminal deletion construct was no longer targeted to peroxisomes but dispersed in the cytosol and the nucleus (Fig. 3.4F).

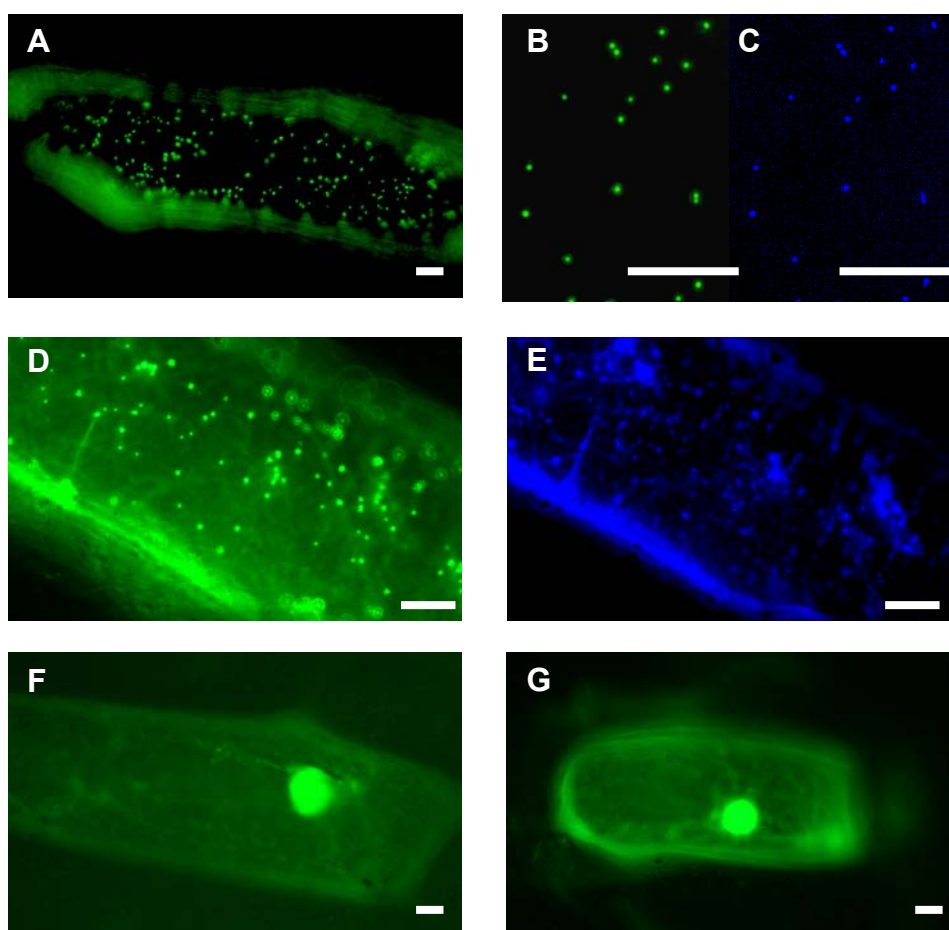


Figure 3.4: Subcellular targeting analysis of AtHsp15.7 in onion epidermal cells (*Allium cepa* L.).

For subcellular localization of AtHsp15.7, onion epidermal cells were transformed biolistically with EYFP and/or ECFP constructs, and subcellular protein targeting was analyzed by fluorescence microscopy. In single transformants the fusion protein EYFP-AtHsp15.7 was targeted to punctate cell structures (A) that were identified as peroxisomes by double labeling with the peroxisomal ECFP

fusion protein gMDH-ECFP in double transformants using appropriate filter sets (B, C), whereas the punctate structures did not overlap with mitochondria labelled by CoxIV-ECFP (D, E). The deletion construct EYFP-AtHsp15.7 Δ PTS1 (F), which was shortened by the C-terminal 14 residues including SKL>, and the inverse fusion protein AtHsp15.7 Δ C-EYFP (G) with accessible predicted mitochondrial presequence were detected in the cytosol and the nucleus. For imaging either EYFP- (A, B, D, F, G) or ECFP-specific filters were used (C, E). The bar represents 20 μ m.

These data demonstrated that the C-terminal tripeptide SKL> of AtHsp15.7 is a functional PTS1 and necessary for directing AtHsp15.7 to peroxisomes *in vivo*.

As mentioned above, AtHsp15.7 also contained a predicted N-terminal mitochondrial presequence. However, possible mitochondrial targeting of AtHsp25.7 was abolished in the fusion proteins EYFP-AtHsp15.7 and EYFP-AtHsp15.7 Δ C, in which the putative mitochondrial targeting signal was placed in the back of EYFP. Therefore, an inversely arranged fusion protein was constructed. The C-terminal fusion protein AtHsp15.7 Δ C-EYFP with accessible N-terminal end was scattered in the cytosol (Fig. 3.4G), strongly suggesting that the predicted mitochondrial presequence in AtHsp15.7 was not functional *in vivo* and that the PTS1 was not overruled *in vivo* by any N-terminal targeting signal.

In conclusion, the subcellular targeting studies based on EYFP fusion proteins demonstrated that AtHsp15.7 is a peroxisomal protein targeted to the organelle by the C-terminal PTS1 SKL>.

3.1.2.2 Biochemical identification of AtHsp15.7 in leaf peroxisomes isolated from *Arabidopsis*

To provide a second independent line of evidence for peroxisomal targeting of AtHsp15.7 to plant peroxisomes, leaf peroxisomes were isolated from *Arabidopsis* by applying a new method established recently (Babujee 2004, Ma et al., submitted). By this method, a significant quantity of relatively pure leaf peroxisomes can be obtained by the use of two successive sucrose density gradients. An efficient separation of peroxisomes from chloroplasts, thylakoid membranes, and mitochondria was obtained in the first sucrose gradient and further improved by a second gradient to remove residual contaminating plastids and mitochondria and to enrich leaf peroxisomes near the bottom of the gradient.

However, as revealed by RT-PCR, *Arabidopsis* plants grown under standard conditions were unsuitable for the identification of AtHsp15.7, because the gene was hardly expressed (see chapter 3.1.5). Instead, *AtHSP15.7* was highly expressed under heat stress

conditions (see chapter 3.1.5.2). An induced band of about 16 kDa could indeed be resolved by SDS-PAGE of leaf peroxisomal proteins isolated from *Arabidopsis* plants that had been subjected to heat stress conditions as compared to control plants; yet, identification of this protein as AtHsp15.7 turned out to be difficult by both mass spectrometry and immunochemical means (Reumann, unpublished). To overcome this problem, transgenic *Arabidopsis* lines overexpressing *AtHSP15.7* under the constitutive 35S CaMV promoter were generated by *Agrobacterium*-mediated transformation to achieve stable and high expression of *AtHSP15.7*. Transgenic plants with high *AtHSP15.7* expression levels were selected by RT-PCR in the T1 generation, and plants of the corresponding T2 generation

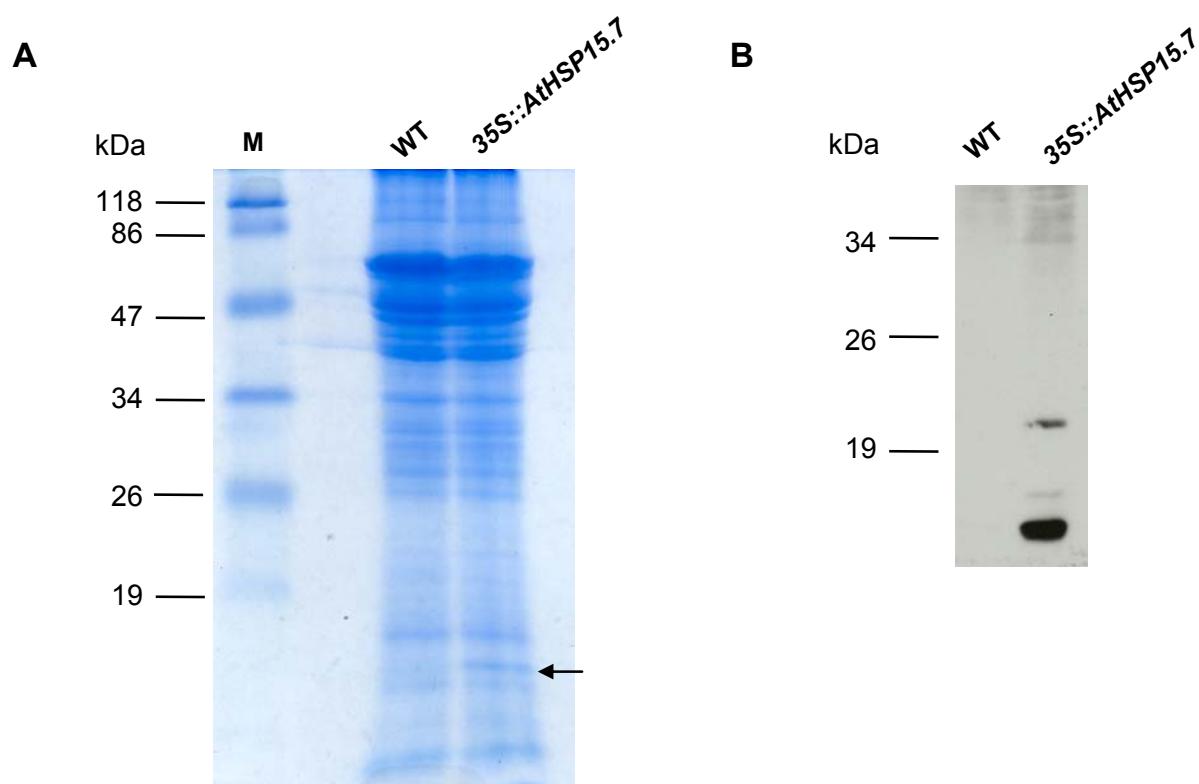


Figure 3.5: Identification of AtHsp15.7 in isolated leaf peroxisomes.

Leaf peroxisomes were isolated from an AtHsp15.7 overexpression line by two successive sucrose density gradients. The proteins were separated by SDS-PAGE (A) and analyzed by immunoblotting (B). In comparison with the proteins from wild-type plants, an additional band of about 16 kDa appeared in the overexpression line. In an immunoblot with polyclonal antibodies raised against AtHsp15.7 (B), a band with an apparent size of about 16 kDa was detected, suggesting that AtHsp15.7 was targeted to leaf peroxisomes in the *AtHSP15.7* overexpression line. M: molecular mass standard. The AtHsp15.7 antiserum was kindly provided by Dr. Scharf (University Frankfurt, Germany).

were grown on a large scale to allow the isolation of leaf peroxisomes. Leaf peroxisomal proteins isolated from an *AtHSP15.7* overexpression line were separated by one dimensional gel electrophoresis. In comparison to the wild-type, an additional Coomassie-stained band of about 16 kDa was specifically detected in the overexpression line (Fig. 3.5A). Moreover, a band of similar size was identified by immunoblotting using a polyclonal antiserum raised against *AtHsp15.7* (kindly provided by Dr. Scharf, University Frankfurt, Germany; Fig. 3.5B). These biochemical data provided additional evidence that *AtHsp15.7* was targeted to leaf peroxisomes in *Arabidopsis*.

3.1.3 Localization of *AtAcid31.2* to the peroxisome matrix

To investigate if the two putative PTSs of *AtAcid31.2* are functional *in vivo*, several constructs were generated as depicted in Fig. 3.6. The fusion protein *AtAcid31.2*-EYFP with

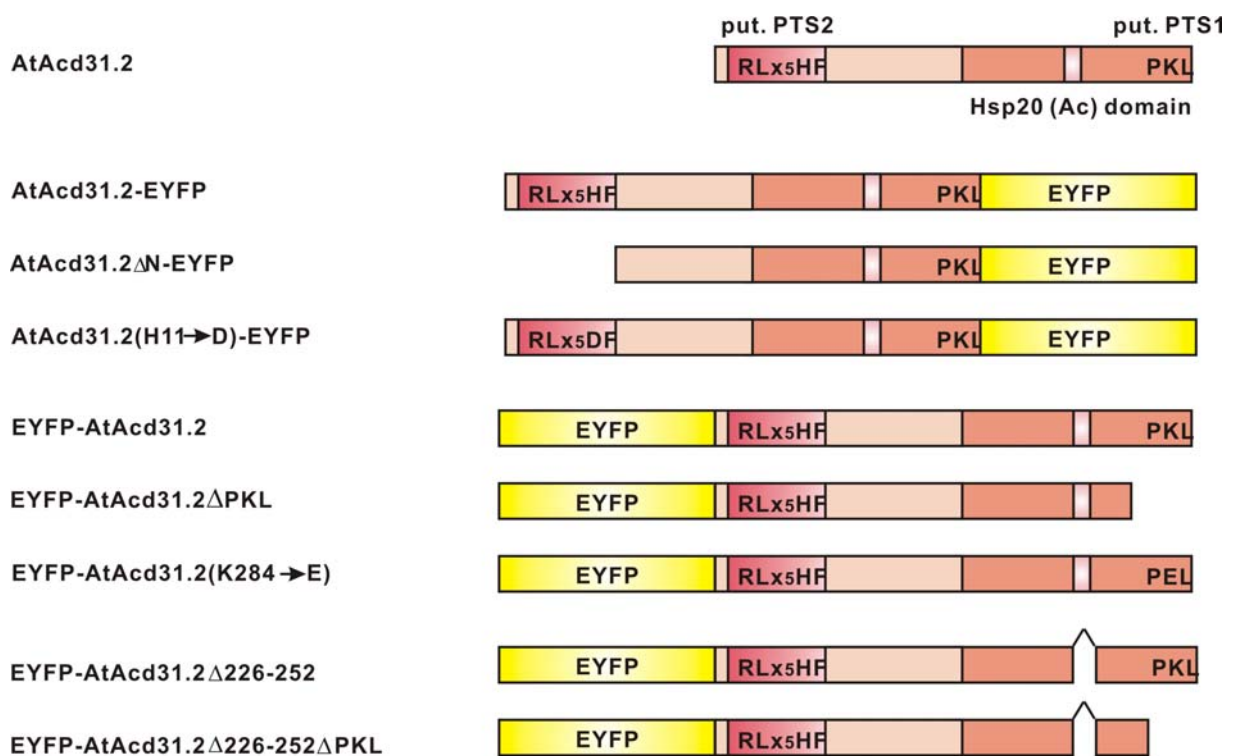


Figure 3.6: Diagram of constructed fusion proteins between *AtAcid31.2* and EYFP.

In order to verify the predicted PTS1 and PTS2 peptides, the cDNA of *AtACD31.2* was fused at the 5'- or the 3'-terminal end, respectively, to *EYFP* and expressed under the control of a double 35S CaMV promoter. Deletion of the putative dimerization loop, which was presumably located between amino acid residues 226 to 252, is indicated by a gap in the protein sequence. In addition, the predicted PTSs (PTS2: RLx₅HF \rightarrow RLx₅DF; PTS1: PKL \rightarrow PEL) were mutagenized by site-directed mutagenesis.

accessible putative N-terminal PTS2 nonapeptide RLx₅HF was directed to small punctate structures that were identified as peroxisomes in double labelling experiments using gMDH-CFP (Fig. 3.7A-C). To demonstrate that the N-terminal domain was necessary for directing AtAc31.2 to peroxisomes and that RLx₅HF was the PTS2 nonapeptide of this chaperone, a deletion construct AtAc31.2ΔN-EYFP was generated by removing the N-terminal most 29 residues including the putative PTS2 (position 11 to 19). The fusion protein AtAc31.2ΔN-EYFP was no longer targeted to peroxisomes, but directed to plastids, as indicated by the larger size of the organelles and their characteristic stromuli extensions (Fig. 3.7D). This result was consistent with a moderate prediction of a plastidic transit peptide in the N-terminal end of this deletion construct (e.g. TargetP: score=0.70). Conclusive evidence that AtAc31.2 possesses a functional PTS2 derived from site-directed mutagenesis of the PTS2, in which the absolutely conserved histidine residue at position 8 of the putative PTS2 nonapeptide was replaced by aspartic acid (RLx₅HF→RLx₅DF). As shown in Fig. 3.7E, the fusion protein with mutagenized PTS2 peptide indeed remained in the cytosol.

Interestingly, the inversely arranged fusion protein EYFP-AtAc31.2 with accessible C-terminal tripeptide PKL> was also targeted to peroxisomes (Fig. 3.7F, G). In order to investigate whether PKL> is a second PTS of AtAc31.2 and necessary for peroxisomal targeting, two altered fusion proteins were generated: (i) a deletion construct lacking the tripeptide PKL>, and (ii) a construct with a mutagenized PTS1, in which the conserved lysine residue at position -2 was changed to glutamic acid. However, the deletion construct EYFP-AtAc31.2ΔPTS1 and the construct EYFP-AtAc31.2(K284E) with mutagenized C-terminal tripeptide (PKL→PEL) still entered peroxisomes (Fig. 3.7 H-K). These data strongly suggested that the putative PTS1 was not necessary for targeting of AtAc31.2 to peroxisomes.

In summary, these results demonstrated that AtAc31.2 is a peroxisomal protein that is targeted to the matrix by a functional PTS2, and that the putative PTS1 of AtAc31.2 is not required for peroxisome targeting.

Because EYFP-AtAc31.2 ΔPTS1 was targeted to peroxisomes but apparently did neither follow the PTS1 nor the PTS2 pathway, an alternative targeting pathway had to be postulated. It has been demonstrated that subunits of oligomeric enzymes that lack a PTS still enter peroxisomes when co-expressed in cells together with PTS-containing subunits,

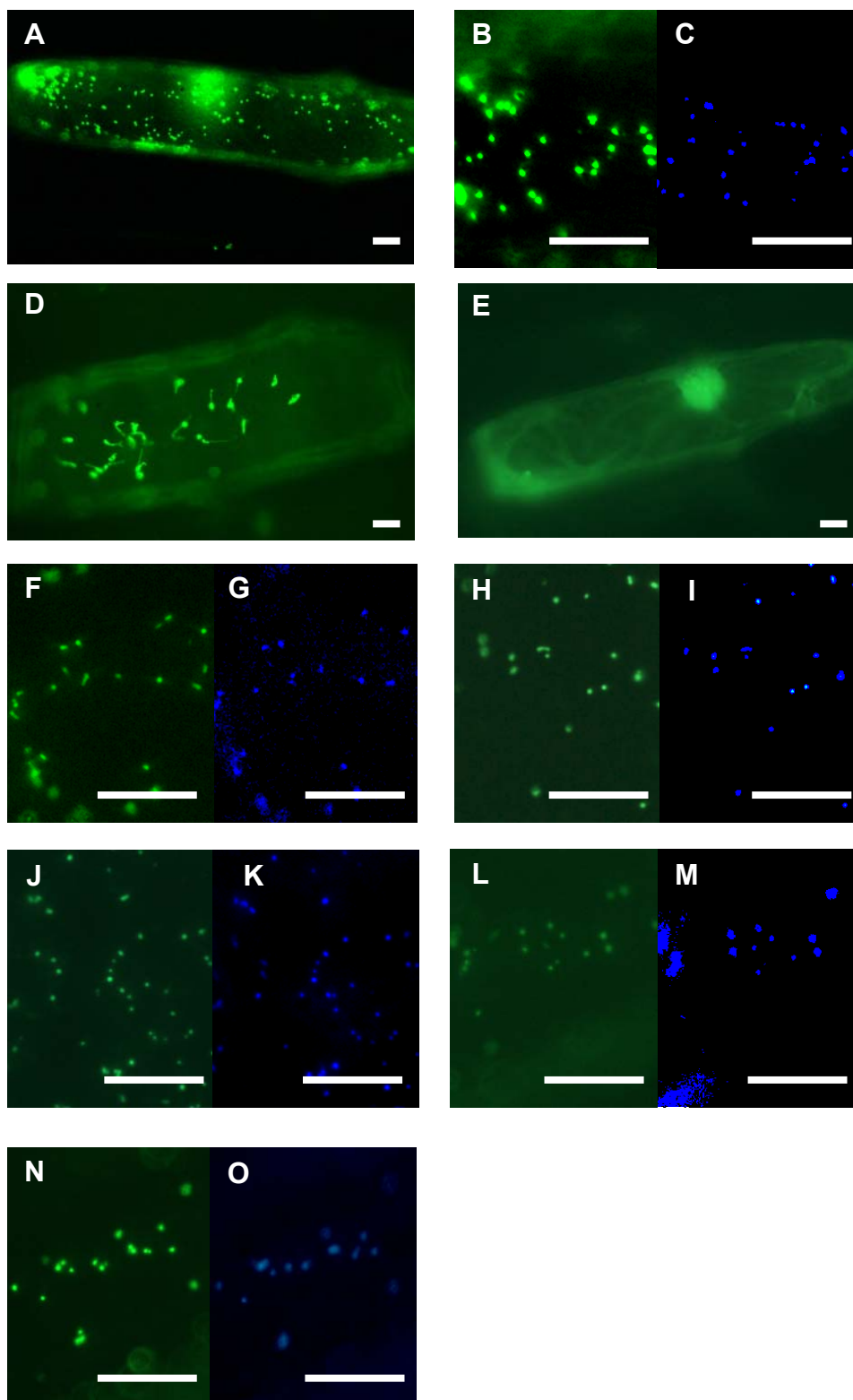


Figure 3.7: Subcellular targeting analysis of AtAcd31.2 in onion epidermal cells (*Allium cepa*).

For subcellular localization of AtAcd31.2, onion epidermal cells were transformed biolistically with EYFP and/or ECFP constructs, and subcellular protein targeting was analyzed by fluorescence microscopy. The fusion protein AtAcd31.2-EYFP (A to C) with accessible PTS2 (RLx₅HF) was targeted to punctate cell structures (A) that were identified as peroxisomes by double labeling (B, C). The shortened construct lacking the most 29 amino acid residues of the N-terminus was targeted to chloroplasts in line with a moderate prediction of a plastidic transit peptide in the N-terminus (D), (cont. next page)

either by oligomerization with native enzyme subunits or subunits of closely related homologs. The protein import mechanism is referred to as peroxisome piggyback import (Purdue and Lazarow, 2001).

The import of specific peroxisomal matrix proteins into peroxisomes in a piggyback fashion has profound consequences of physiological relevance for (i) subunit hetero-oligomerization and (ii) the import of homologous subunits, belonging to the same protein superfamily but lacking putative PTS peptides, into peroxisomes. Therefore, as a side aspect of this thesis, we intended to clarify the targeting mechanism of EYFP-AtAc31.2 into peroxisomes.

To import EYFP-AtAc31.2 into peroxisomes of onion epidermal cells in a piggybacked fashion, a gene orthologous to AtAc31.2 had to be encoded and expressed in onion epidermal cells, and the protein had to form dimers or oligomers with EYFP-AtAc31.2 (see also chapter 4.2). In fact, homologs of AtAc31.2 from diverse plant species, which were retrieved by translating EST sequences from publicly available databases, also contained a conserved PTS2 nonapeptide (chapter 3.1.1), suggesting that these proteins were probably orthologous to AtAc31.2 and targeted to peroxisomes as well. Thus, *Allium cepa* was likely to possess a gene for a peroxisome-targeted ortholog of AtAc31.2 as well. In addition and unlike most sHsps, *AtACD31.2* was constitutively expressed in leaves under physiological conditions (chapter 3.1.5). This atypical expression pattern of *AtACD31.2* led to the reasonable prediction that the gene was probably also expressed under standard conditions in non-green tissue such as storage organs like onions. Thus, it was hypothesized that the fusion proteins EYFP-AtAc31.2(K284E) and EYFP-AtAc31.2 Δ PTS1 may be targeted to peroxisomes via piggybacking by the formation of mixed oligomers with the onion ortholog of AtAc31.2 or another peroxisome-targeted sHsp homolog.

(Figure 3.7 length continued),

whereas site-directed mutagenesis of the PTS2 from RLx₅HF to RLx₅DF abolished peroxisome targeting (E). The inverse fusion protein EYFP-AtAc31.2 was targeted to peroxisomes as well (F, G). In this case, however, deletion (EYFP-AtAc31.2 Δ PKL, H, I) or mutagenesis of the C-terminal tripeptide (PKL \rightarrow PEL, J, K) did not abolish peroxisome targeting. Deletion of the dimerization loop of AtAc31.2 also failed to abolish peroxisome targeting (EYFP-AtAc31.2 Δ 226-252, L, M; EYFP-AtAc31.2 Δ 226-252 Δ PKL, N, O). For imaging either EYFP- (A, B, D, E, F, H, J, L, N) or ECFP-specific filters were used (C, G, I, K, M, O). The bar represents 20 μ m.

According to two reported crystal structures of sHsps, namely that of Hsp16.5 from *Methanococcus jannaschii* and that of Hsp16.9 from *Triticum aestivum*, the β -strand β 6 of the Ac domain is exchanged between two subunits and thus stabilizes the formation of a dimer, which is the building block of larger sHsp oligomers (Kim et al., 1998; van Montfort et al., 2001). Based on a multiple sequence alignment of Hsp16.5 of *M. jannaschii*, the homolog of *Triticum aestivum*, and AtAc31.2, the putative dimerization loop of AtAc31.2 was deduced to be located between amino acid residue 226 and 252 (data not shown). To dissect whether the fusion proteins EYFP-AtAc31.2(K284E) and EYFP-AtAc31.2 Δ PTS1 were targeted to peroxisomes by piggybacking, the dimerization loop was deleted in both cDNAs (yielding EYFP-AtAc31.2 Δ 226-252 and EYFP-AtAc31.2 Δ 226-252 Δ PTS1) by two successive PCR reactions. The fusion protein EYFP-AtAc31.2 Δ 226-252, however, still entered peroxisomes (Fig. 3.7L, M). The peroxisome targeting of this fusion protein was clearly not mediated by the retained C-terminal PKL> since the fusion protein lacking both the dimerization loop and the putative PTS1 PKL> was likewise targeted to peroxisomes (Fig. 3.7N, O). Deletion of the putative dimerization loop of AtAc31.2 thus did not affect peroxisome targeting.

3.1.4 Complementation of a yeast mutant deficient in cytosolic sHsps

S. cerevisiae contains two small heat shock proteins (ScHsp26 and ScHsp42) both of which are localized in the cytosol. Haslbeck et al. (2004) recently reported that cells of single or double *S. cerevisiae* knock-out mutants of these genes, referred to as *hsp26* or *hsp42*, show a shrunken phenotype at early stationary phase or at early exponential phase after heat shock when observed by scanning electron microscopy (SEM). The dehydrated phenotype resembled cells undergoing dehydration or aging and probably reflects a general disturbance in proteome homeostasis (Haslbeck et al., 2004). In addition to the morphological phenotype, the *hsp42* strain showed a slight increase in protein aggregation at early stationary phase, and in the double mutant an even two-fold increase of insoluble protein compared to the wild-type (Haslbeck et al., 2004).

The availability of yeast heat shock mutants allowed functional complementation assays to investigate if plant peroxisomal sHsps have a conserved chaperone function *in vivo* similar to their yeast counterparts. Since ScHsp26 and ScHsp42 are located in the cytosol, it was predicted that AtHsp15.7 and AtAc31.2 could not complement the phenotype of *hsp42* and *hsp26* if they were targeted to peroxisomes in yeast. Therefore, the PTS

peptides were deleted from AtHsp15.7 and AtAcd31.2. The deletion constructs (*AtHSP15.7 Δ PTS1*, *AtACD31.2 Δ PTS1*, and *AtACD31.2 Δ PTS2 Δ PTS1*) were then transferred to the vector pYES2.1 and expressed as presumably cytosolic proteins from a galactose-inducible promoter. After transformation of the single or double deletion mutants with the constructs described above, the changes in cell morphology were analyzed by SEM. Except for *AtAcd31.2 Δ PTS1* expressed in *hsp26*, both plant peroxisomal sHsps were able to complement the morphological defects of the single mutants *hsp42* and *hsp26* and the double mutant *hsp26/hsp42* (Fig. 3.8). In about 30% of the complementation experiments with *AtAcd31.2*, however, the normal cell morphology of the wild-type was not restored (data

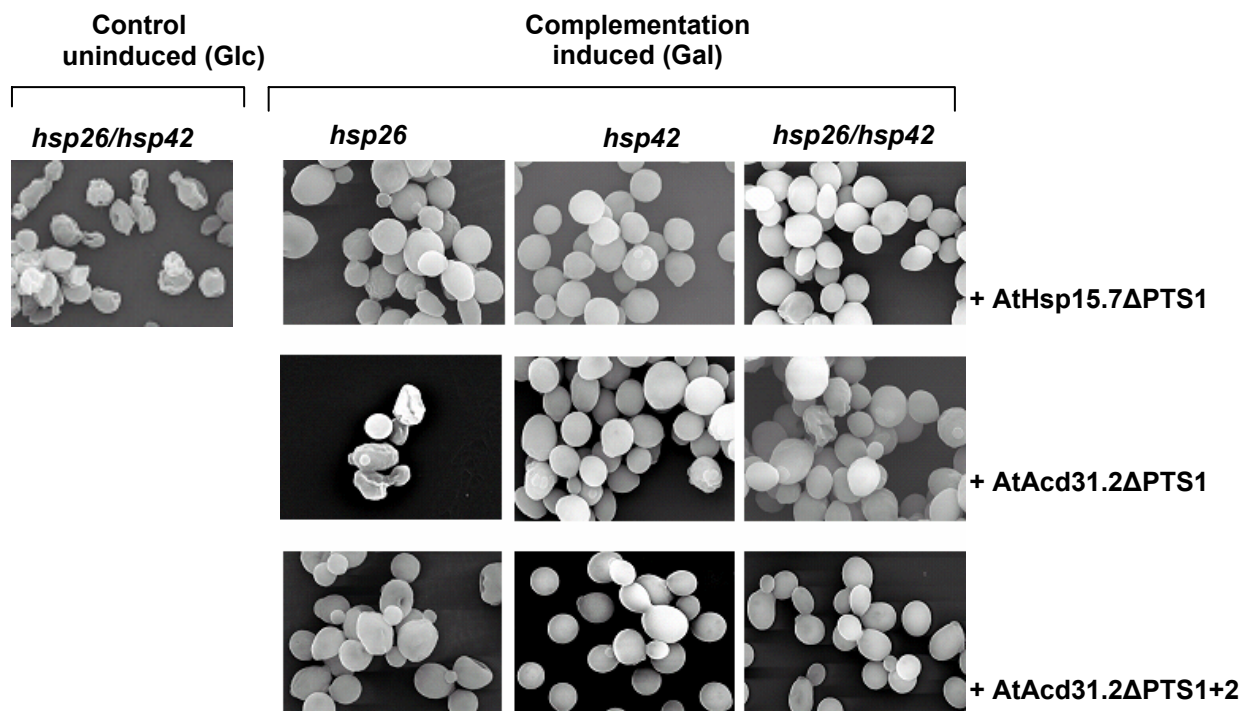


Figure 3.8 Complementation studies of single and double deletion strains of *S. cerevisiae* deficient in ScHsp42 and ScHsp26 with plant peroxisomal sHsps.

The mutants of *S. cerevisiae* *hsp26*, *hsp42*, and *hsp26/hsp42* were transformed with *AtHSP15.7* or *AtACD31.2* under the control of a galactose inducible promoter, and yeast cells were imaged by SEM. After induction (Gal) for the expression of the *Arabidopsis* sHsps, the yeast cells were heat shocked for 1 hour at 43°C prior to SEM analysis. As a negative control, yeast cells of an equally treated but uninduced (Glc) deletion strain (*hsp26/hsp42*) are shown, which exhibited the wrinkly phenotype typical of the mutant. Yeast deletion strains and complementing AtHsps are indicated. The bar represents 10 μ m. The pictures were kindly provided by Dr. Haslbeck (Technical University München, Germany).

not shown). These negative results were possibly caused by an insufficient expression level of the transgene and/or low targeting efficiency of the fusion protein to the cytosol.

Overexpression of AtHsp15.7 Δ PTS1 and AtAcd31.2 Δ PTS1 Δ PTS2 also led to a reduction of unspecific protein aggregation in the cell lysate of the yeast deletion mutants after heat shock (Fig. 3.9). These results demonstrated that both plant sHsps were able to suppress the aggregation of a broad variety of cytosolic proteins under heat stress conditions in *S. cerevisiae*. In summary, the microscopic and biochemical data indicated that not only AtHsp15.7, which is a close homolog of some well-studied plant sHsps, but also AtAcd31.2, which belongs to a largely unknown novel family of Acd proteins (Scharf et al., 2001), plays a role as molecular chaperones in the peroxisome matrix, similar to that of the well-defined

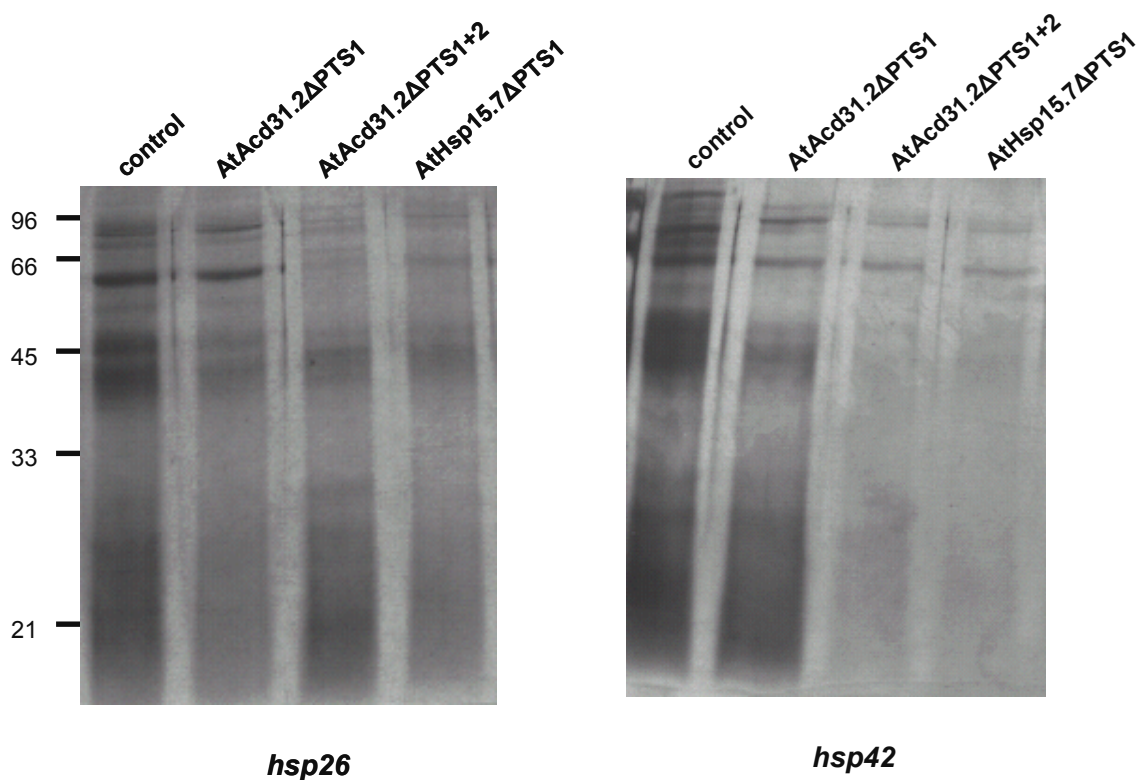


Figure 3.9: Reduction of protein aggregation in *S. cerevisiae* ScHsp42 and ScHsp26 deletion strains by plant peroxisomal sHsps.

Insoluble protein aggregates in lysates of *S. cerevisiae* *hsp26* and *hsp42* mutants, upon induction of AtAcd31.2 Δ PTS1, AtAcd31.2 Δ PTS1+2, or AtHsp15.7 Δ PTS1 (lanes 2 to 4), were analyzed by Coomassie-stained SDS-PAGE. The *hsp26/hsp42* double mutant was used as a control. Yeast cells were grown and heat-stressed as for SEM analysis. An equal number of cells were lysed and insoluble proteins enriched by centrifugation (Haslbeck et al., 2004). The pictures were kindly provided by Dr. Haslbeck (Technical University München, Germany).

physiological function of cytosolic sHsps in *S. cerevisiae* (Haslbeck et al., 2004, 2005; Cashikar et al., 2005).

3.1.5 Expression analysis of peroxisomal sHsps

3.1.5.1 Tissue and developmental specific expression of *Arabidopsis* sHsps

Small Hsps play an important role under abiotic stress conditions including heat, drought, salt, and high light stress by forming distinct homo- or heteromeric protein complexes and trapping non-native proteins in a soluble and folding-competent state. In addition, some sHsps are expressed under standard conditions at various developmental stages such as embryogenesis, germination, and fruit development (Wehmeyer et al., 1996; Sun et al., 2002). To investigate if *AtHSP15.7* and *AtACD31.2* show a tissue- or development-specific expression pattern and to obtain first indications for their function in plant stress tolerance, publicly available expression data provided by a microarray gene expression database were retrieved using GENEVESTIGATOR (www.geneinvestigator.ethz.ch, Zimmermann et al., 2004). Accordingly, expression of *AtHSP15.7* was hardly detectable at most stages of plant development and in different plant organs, and showed the highest mRNA levels in roots, seeds, at the latest leaf age of more than 45 days, and in suspension cultured cells (Fig. 3.10). By contrast, *AtACD31.2* was overall highly expressed at a level that exceeded that of *AtHSP15.7* in seedlings, leaves, flowers, and siliques about five to 20-fold (Fig. 3.10), suggesting a constitutive expression of *AtACD31.2* under physiological conditions.

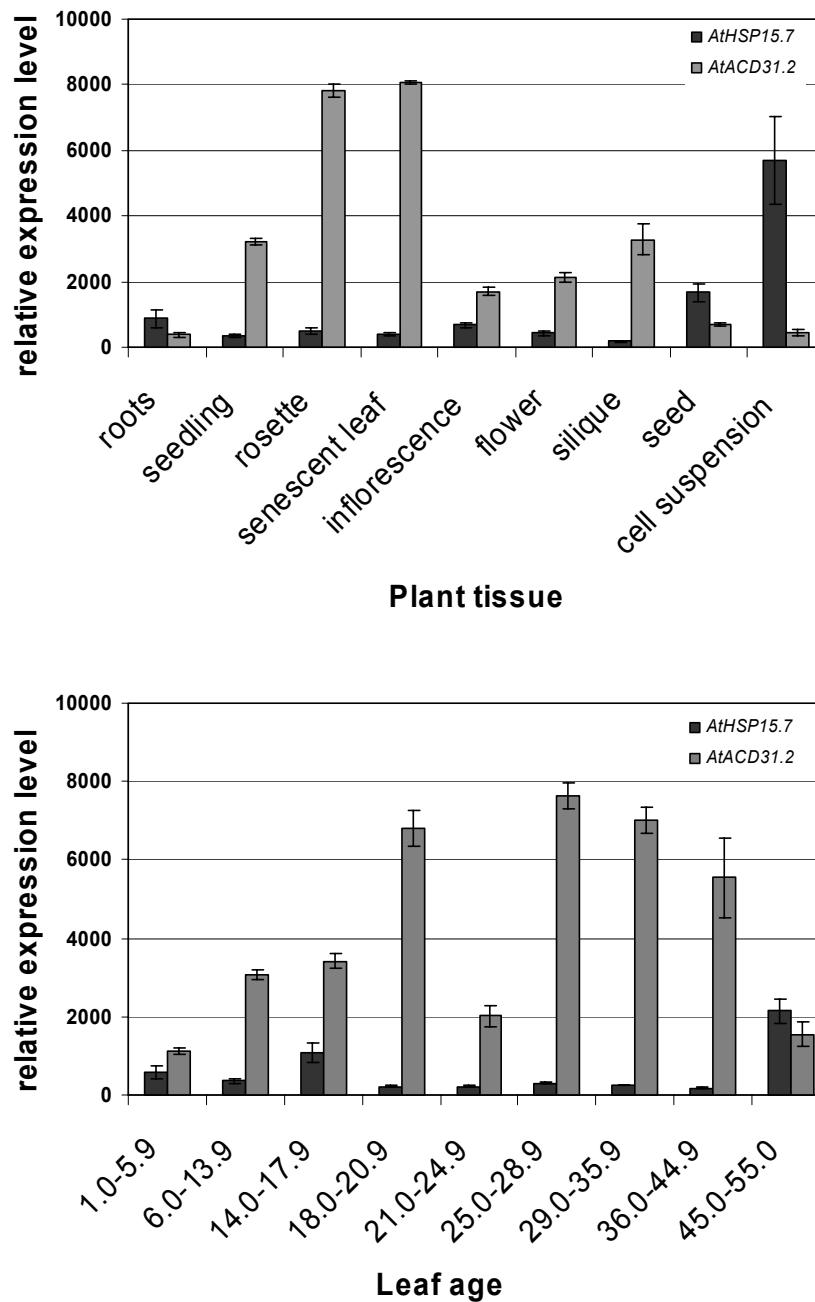


Figure 3.10: Relative tissue-specific and developmental expression levels of *AtHSP15.7* and *AtACD31.2*.

A, Expression in various plant organs. B, Expression at successive developmental stages, shown in days starting from seed germination to senescence. The publicly available microarray expression data used for analysis were retrieved by GENEVESTIGATOR (<https://www.genevestigator.ethz.ch>; Zimmermann et al., 2004).

3.1.5.2 Differential expression of *AtHSP15.7* and *AtACD31.2* under temperature stress conditions

To examine the effect of temperature stress on *AtHSP15.7* and *AtACD31.2* mRNA levels, 4-week-old soil grown *Arabidopsis* plants were shifted to high (37°C) or low (5°C) temperature under dark conditions for different times of incubation. Leaves were then harvested, and the level of gene expression was analyzed by reverse transcription-PCR (RT-PCR).

Complete removal of residual genomic DNA from total RNA preparation by DNaseI digestion was verified for the intron-less gene of *AtHSP15.7* by PCR analysis of control samples lacking reverse transcriptase (data not shown). The specificity of *AtHSP15.7* amplification by PCR was confirmed by restriction endonuclease digestion of the PCR product, and yielded fragment sizes that corresponded specifically to the prediction from the cDNA sequence of *AtHSP15.7* (data not shown). To increase the specificity and facilitate the amplification of *AtACD31.2*, its expression was studied by amplifying the highly variable N-terminal fragment (470 bp) rather than the conserved Ac domain (see Fig. 3.1). The ubiquitously expressed ubiquitin gene (*UBQ10*) was used as a control for equal concentrations of cDNA in different samples. The amplification product of *UBQ10* was 483 bp long, and the amplification rate of the cDNA is reported to be constant up to 32 PCR cycles (Weigel and Glazebrook, 2002). To investigate peroxisome proliferation, the peroxisomal house-keeping gene *AtpMDH1* (peroxisomal malate dehydrogenase, At5g09660) was amplified in parallel. To analyze gene expression semi-quantitatively in the linear range, *AtHSP15.7* and *UBQ10* were amplified by 30 PCR cycles to obtain a visible band on an ethidium bromide-stained gel. For *AtACD31.2* and *AtpMDH1*, 26 and 24 PCR cycles, respectively, were chosen to guarantee amplification in the linear range.

The expression level of *AtHSP15.7* and *AtACD31.2* in rosette leaves responded differently to temperature. As shown in Fig. 3.11, transcripts of *AtHSP15.7* were barely detectable at standard temperature of 23°C or chilling temperature (5°C), but quickly and strongly accumulated after 30 min of heat stress at a temperature of 37°C. The high expression level of *AtHSP15.7* was maintained for 6 hours of heat shock with no obvious decline. Control studies showed that the induction of *AtHSP15.7* was gene-specific and not due to overall peroxisome proliferation under heat stress, because the expression level of a house-keeping gene like *AtpMDH1* was not altered by increased temperature (Fig. 3.11).

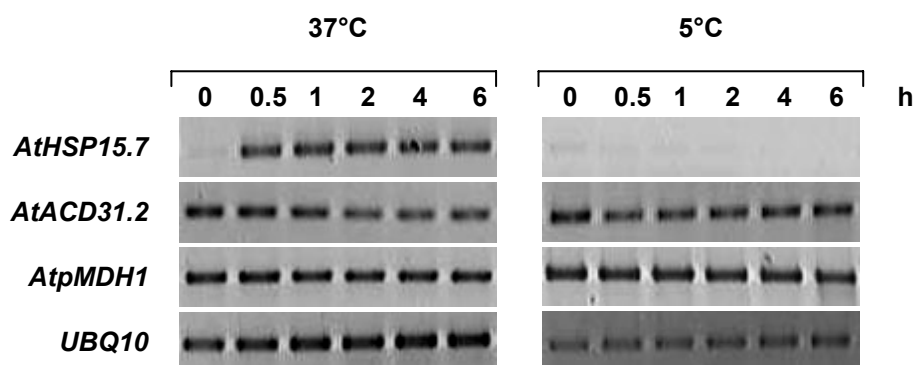


Figure 3.11: The effects of temperature stress on *AtHSP15.7* and *AtACD31.2* mRNA levels.

Plants were grown for about four weeks under standard growth conditions ($100 \mu\text{mol m}^{-2} \text{sec}^{-1}$, $T=23^\circ\text{C}$). The temperature stress conditions were initiated three hours after the beginning of the light period. The plants were transferred to elevated (37°C) or cold temperature (5°C) and incubated in the dark for the time indicated, whereas control plants were kept in the dark at 23°C (data not shown). Gene expression was analyzed in leaves by RT-PCR using appropriate oligonucleotide primers and ubiquitin (*UBQ10*) as a control for equal cDNA concentrations. The gene of *AtpMDH1* was used to monitor peroxisome proliferation. For analysis of DNA contamination, total RNA was treated similarly but reverse transcriptase replaced by water. All experiments were performed three times and showed similar changes in transcript levels in each case.

Unusual for an sHsp, *AtACD31.2* was constitutively expressed at standard temperature and both heat and chilling stress conditions, indicating a complementary expression pattern as compared to *AtHSP15.7* and a role in protecting peroxisomal enzymes under physiological conditions.

3.1.5.3 Differential expression of *AtHSP15.7* and *AtACD31.2* under oxidative stress

Several sHsps including tomato Hsp21 and AtHsp17.6 have been shown to play an important role under oxidative stress conditions (Sun et al., 2001; Neta-Sharir et al., 2005). Chloroplast Hsp21 presumably acts as an antioxidant, prevents protein aggregation, and facilitates refolding of photosystem II under oxidative stress conditions (Neta-Sharir et al., 2005). Overexpression of cytosolic AtHsp17.6 in *Arabidopsis* slightly increased plant tolerance to oxidative stress induced by salt and drought (Sun et al., 2001). To investigate if AtHsp15.7 and AtAcd31.2 play an important role in response to oxidative stress, two ROS inducing agents were applied to soil grown *Arabidopsis* plants by watering, i.e. paraquat (100

μM) and the catalase inhibitor 3-amino-1,2,4-triazole (3-AT, 5 mM). In the presence of paraquat and under leaf illumination the D1 protein of photosystem II is inhibited and leads to

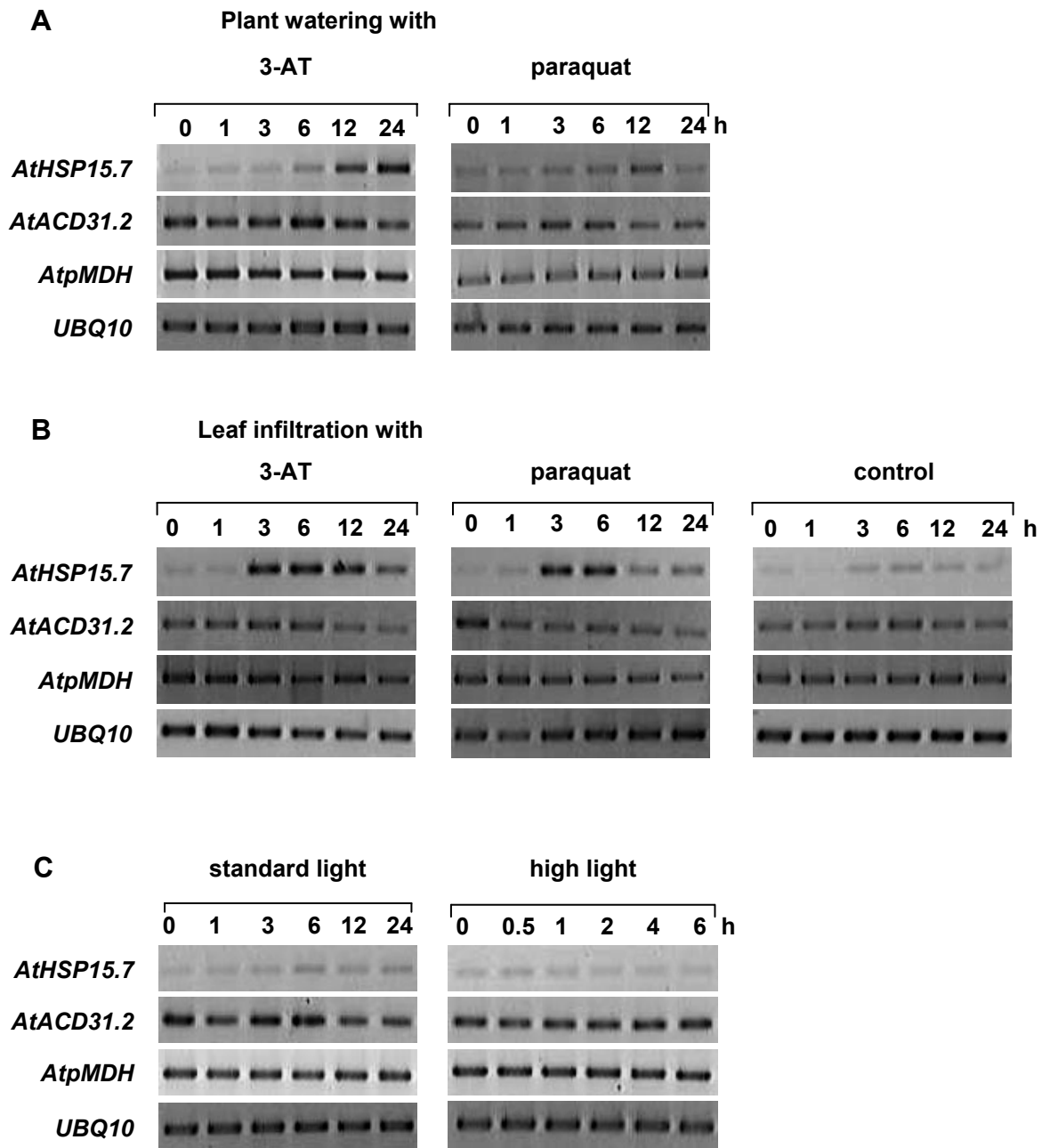


Figure 3.12: Expression of *AtHSP15.7* and *AtACD31.2* under oxidative stress conditions

Expression analysis of *AtHSP15.7* and *AtACD31.2* by oxidative stress with inhibitor application by watering (A) or infiltration (B), and under standard light conditions and high light stress (C). Plants were grown for about four weeks under normal growth conditions ($100 \mu\text{mol m}^{-2} \text{sec}^{-1}$, $T=23 \text{ }^\circ\text{C}$). The abiotic stress conditions were initiated three hours after the beginning of the light period. For oxidative stress analysis, soil-grown plants were either watered with 5 mM 3-AT or 100 μM paraquat (A), or rosette leaves were infiltrated with 100 μM 3-AT or 10 μM paraquat (B), and further incubated under a light intensity of $100 \mu\text{mol m}^{-2} \text{sec}^{-1}$. For high light stress analysis (C), plants were transferred to $450 \mu\text{mol m}^{-2} \text{sec}^{-1}$, whereas control plants were kept at normal light intensity. All experiments were performed three times and showed similar changes in transcript levels in each case.

the generation of $O_2^{\cdot-}$ in chloroplasts (Miyagawa et al., 2000), whereas 3-AT application results in an accumulation of H_2O_2 in peroxisomes by suppressing the activity of catalase (Bi et al., 1995). When plants were treated with paraquat in the light, mRNA of *AtHSP15.7* accumulated after 12 hours of treatment and increased further for up to 24 hours (Fig. 3.12A). As for the temperature-dependence of gene expression, the drastic increase of *AtHSP15.7* expression was specific and not observed for *AtpMDH1* (Fig. 3.12). In comparison with *AtHSP15.7*, *AtACD31.2* remained expressed at rather constant levels (Fig. 3.12) with a slight decline that coincided with the accumulation of *AtHSP15.7* transcripts.

Because uptake of ROS-producing chemicals from the soil by the plants cannot be thoroughly controlled, leaf infiltration was performed as an alternative system for analysis of *AtHSP15.7* expression under oxidative stress conditions. Rosette plants of *Arabidopsis* were cut above the roots, infiltrated with paraquat (10 μ M) or 3-AT (100 μ M), and floated on inhibition solution under standard growth conditions (100 μ mol m^{-2} sec^{-1} light intensity, $T=23^\circ C$) to ensure fast and homogenous inhibitor application. Mock controls were performed in parallel by infiltrating water into leaves instead of inhibitors. The expression of *AtHSP15.7* was induced after 3 hours of leaf infiltration with 100 μ M 3-AT, stayed roughly at this level during the entire light period (12-hour time point), and increased again on the second day from a lower level (24 h, Fig. 3.12B). Control plants infiltrated with water showed a minor induction of *AtHSP15.7* expression during the light period similar to standard plants (Fig. 3.12B, C), suggesting that leaf wounding itself did not alter *AtHSP15.7* expression to a considerable extent. Likewise, expression of *AtHSP15.7* was induced within about 3 h after infiltration with 10 μ M paraquat and declined after 6 h (Fig. 3.12B). Expression of *AtACD31.2* was hardly affected by either inhibitor and only seemed to decline slightly upon *AtHSP15.7* induction.

High light irradiation enhances photorespiration and leads to elevated H_2O_2 production in chloroplasts (mainly $O_2^{\cdot-}$ and H_2O_2) and peroxisomes (mainly H_2O_2). To investigate more physiological oxidative stress conditions, we assessed the response of *Arabidopsis* plants to high light irradiation. To avoid any side effect by temperature increase, the temperature was strictly controlled at around $23^\circ C$ and a maximum light intensity of 450 μ mol m^{-2} sec^{-1} was chosen. However, similar to the expression at standard light intensity (around 100 μ mol m^{-2} sec^{-1} , $23^\circ C$), no obvious induction was observed for *AtHSP15.7* or *AtACD31.2*,

suggesting that the rise in ROS production and concentration was quickly and efficiently scavenged by the plant antioxidative system.

It was concluded that the two peroxisomal sHsps showed a complementary expression pattern with *AtHSP15.7* being induced by high temperature and ROS-generating chemicals, whereas *AtACD31.2* was constitutively expressed, indicating a house-keeping function in protection of peroxisomal matrix enzymes under normal physiological conditions.

3.1.6 *Arabidopsis* T-DNA insertion mutants deficient in one or both peroxisomal sHsps

3.1.6.1 Isolation of *hsp15.7* T-DNA insertion mutants

Insertional mutagenesis provides a direct approach to investigate a causal relationship between protein identity and biological function. With the establishment of *Agrobacterium*-mediated transformation of *Arabidopsis* and the knowledge of the entire *Arabidopsis* genome sequence, it is possible to identify a mutation in most genes (Krysan et al., 1999). In a screen of the SALK T-DNA insertion population (Sequence-indexed T-DNA Lines, The Salk Institute Genomic Analysis Laboratory, La Jolla, USA) generated in the wild type Col-0 background of *Arabidopsis thaliana*, three T-DNA mutant alleles of *AtHSP15.7* were identified, which were designated *hsp15.7-1* (salk_038951), *hsp15.7-2* (salk_038954), and *hsp15.7-3* (salk_107711) (Fig.3.13A). In the mutants *hsp15.7-1* and *hsp15.7-2*, the T-DNA was inserted into the promoter region, i.e. 248 bp and 215 bp upstream of the translational initiation codon, respectively. In *hsp15.7-3*, the T-DNA was located in the sole exon, 270 bp downstream of the translational start codon.

In order to obtain homozygous plants of *hsp15.7-1*, *hsp15.7-2*, and *hsp15.7-3*, two series of genomic PCRs were carried out (Fig. 3.13B). The amplification with a gene-specific left primer (LP, upstream of the T-DNA insertion, SR57f or SR93f) and right primer (RP, downstream of the T-DNA insertion, SR71r) were used to confirm the absence of an uninterrupted wild-type allele, whereas the amplification with LB (T-DNA left border primer) and RP were used to verify the presence of the T-DNA insertion in the *AtHSP15.7* gene. As shown in Fig. 3.13, homozygous plants were identified for *hsp15.7-1*, *hsp15.7-2* and *hsp15.7-3* by this method.

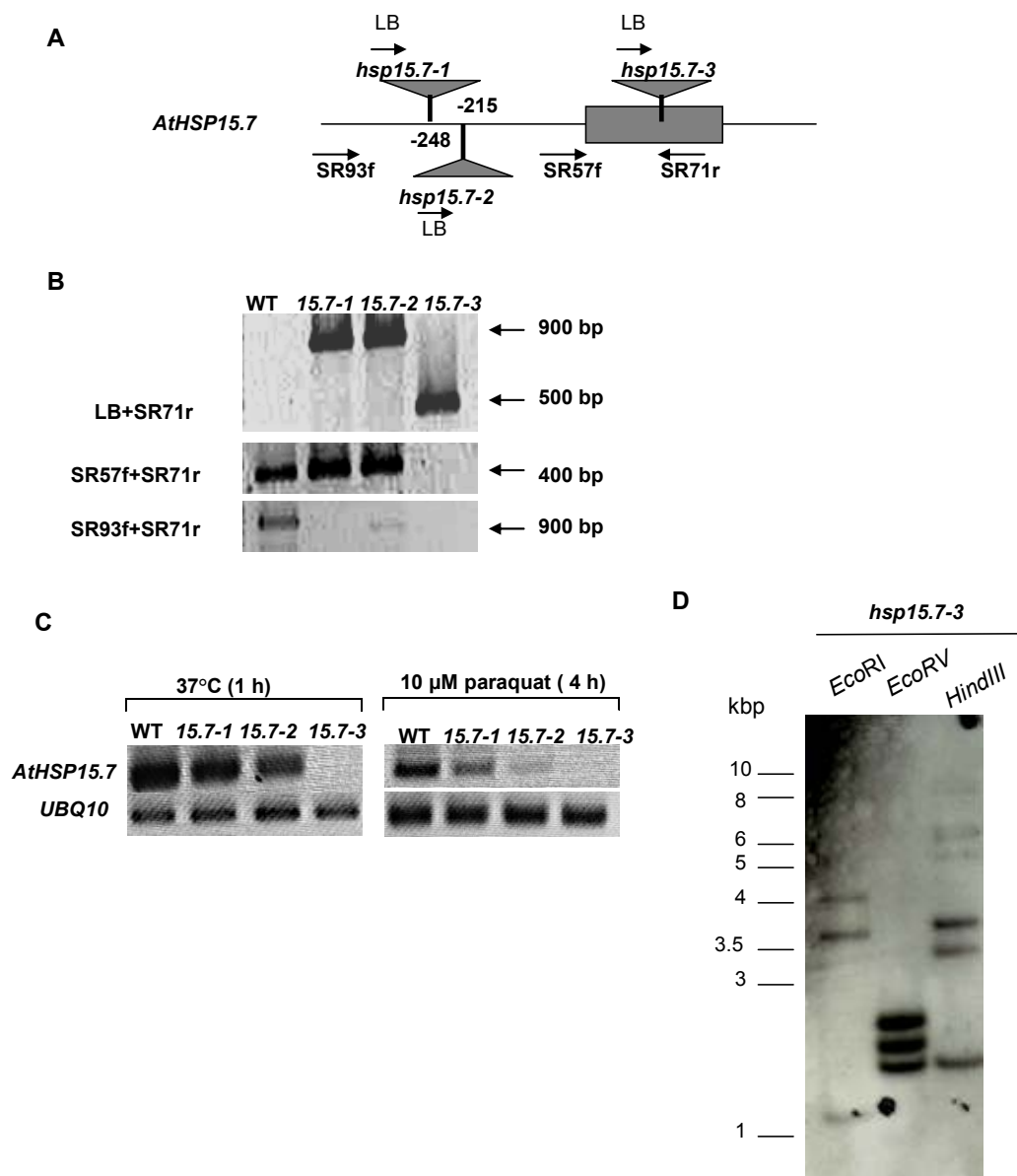


Figure 3.13: Characterization of three mutant alleles of *AtHSP15.7*

Three T-DNA knock-out mutant lines of *hsp15.7* (A) were ordered from NASC (The Nottingham *Arabidopsis* Stock Centre, Nottingham, UK); the T-DNA insertions were verified by genomic PCR (B); the mRNA level of *AtHSP15.7* was analyzed by RT-PCR under heat and oxidative stress (C); the number of T-DNA inserts in *hsp15.7-3* was analyzed by Southern hybridization (D). A. Diagram of the *Arabidopsis HSP15.7* gene. The box indicates the exon. The location of the T-DNA in *hsp15.7-1*, *hsp15.7-2*, and *hsp15.7-3* is indicated by a triangle. B. Genomic PCR analysis of *hsp15.7-1*, *hsp15.7-2*, and *hsp15.7-3*. Genomic DNA was isolated from wild-type Col-0, *hsp15.7-1*, *hsp15.7-2*, and *hsp15.7-3* mutants and subjected to PCR using either two gene-specific primers (SR93f and SR71r) to confirm the absence of the wild-type allele or SR71r with the left primer of the T-DNA (LB) to confirm the presence of T-DNA insertion alleles. C. RT-PCR analysis of the expression of *AtHSP15.7* gene in wild-type and T-DNA insertion mutants under heat stress and oxidative stress induced by paraquat infiltration. Total RNA was isolated from wild-type, *hsp15.7-1*, *hsp15.7-2*, and *hsp15.7-3* mutants and subjected to RT-PCR. RT-PCR was performed for 30 cycles using gene-specific primers to amplify a 335-bp fragment of *AtHSP15.7*. D. Analysis of the numbers of T-DNA insertion numbers in *hsp15.7-3* by Southern blotting. Genomic DNA was isolated from *Arabidopsis* leaves and 10- μ g aliquots were digested completely with different restriction enzymes. The blot was hybridized with a 0.5-kb 32 P-labeled T-DNA fragment. Three T-DNA inserts were detected in the *hsp15.7-3* mutant.

To investigate the absence of full-length *AtHSP15.7* mRNA in the three homozygous mutants, RT-PCR analyses using cDNA-specific primers that spanned the T-DNA insertion site of *hsp15.7-3* were performed (Fig. 3.13C). Accordingly, the full-length mRNA of *AtHSP15.7* was absent in leaves of *hsp15.7-3* under conditions at which *AtHSP15.7* was expressed in wild-type plants, i.e. temperature stress (37°C for 1 h) or infiltration with paraquat (10 µM, for 4 h; Fig. 3.13C). These data characterized homozygous *hsp15.7-3* as a complete knock-out mutant. In contrast, expression of *AtHSP15.7* was reduced but still detectable in the promoter insertion lines *hsp15.7-1* and *hsp15.7-2* (Fig. 3.13C). These results indicated that the T-DNA insertion into the promoter region in these two mutants did not completely prevent expression of full-length *AtHSP15.7*. Therefore, only the *hsp15.7-3* was selected for the following analyses since it was likely that the strongest phenotype would be observed for this mutant line.

To deduce a causal relationship between a mutant phenotype and mutation in a particular gene, it is important that a single T-DNA insertion is present in the genome. Prior to functional analyses of *AtHSP15.7*, the number of T-DNA insertions in genome of *hsp15.7-3* was intended to be determined by testing the segregation pattern of kanamycin resistance, conferred to the mutants by a plant selection marker, namely neomycin phosphotransferase type II, inserted into the T-DNA. However, the drug resistance phenotype seemed to be lost in the *hsp15.7-3* line because *hsp15.7-3* plants did not survive on MS medium containing kanamycin (data not shown). Such a loss of kanamycin resistance is not unusual for Salk lines after several generations of growth. Nevertheless, this method was thus not suitable for determining the number of T-DNA copies in the mutant.

Next, Southern hybridization analysis was performed as an alternative approach to investigate the number of T-DNA copies in *hsp15.7-3*. The T-DNA fragment (1229 bp) was amplified by PCR from the vector pBI 101.3, transferred to the pGEMT vector, and the entire plasmid was digested by *EcoRI*. The smaller *EcoRI* fragment (572 bp) was labelled with ³²P-dCTP and used as a probe for hybridization. Genomic DNA was purified from *hsp15.7-3* and digested by *EcoRI*, *EcoRV* and *HindIII*, and fractionated on a 0.7% agarose gel. Since there were no internal *EcoRI*, *EcoRV*, or *HindIII* restriction sites in the ³²P-labeled *EcoRI* fragment of the T-DNA, a single genomic fragment was expected to be detected if only one T-DNA insertion was present in the genomic DNA. The theoretical sizes of these fragments were 1.6 kb (*EcoRI*), 1.2 kb (*EcoRV*) and 3.4 kb (*HindIII*), respectively, according to the genomic

sequence surrounding *AtHSP15.7*. However, three genomic fragments hybridized with the T-DNA probe in different restriction digests (Fig. 3.13D), indicating that at least three T-DNAs had inserted into the genome of *hsp15.7-3*.

To eliminate the two additional T-DNAs in *hsp15.7-3*, the mutant line was back-crossed twice with wild-type *Arabidopsis* Col-0, and progenies containing the *hsp15.7-3* knock-out allele again identified by genomic PCR analysis (data not shown). These heterozygous progenies were finally self-crossed to obtain homozygous plants.

3.1.6.2 Isolation of an *acd31.2* T-DNA insertion mutant

Likewise, to elucidate the function of *AtAcd31.2* in plants, a T-DNA insertion mutant, which was designated *acd31.2-1* (salk_114949), was identified in the SALK collection and ordered from NASC (The Nottingham Arabidopsis Stock Centre, Nottingham, UK). The T-DNA of *acd31.2-1* was inserted into the sixth intron, (Fig. 3.14A). Using gene-specific primers in combination with the T-DNA left border primer (LB), several homozygous plants were identified by genomic PCR (Fig. 3.14B).

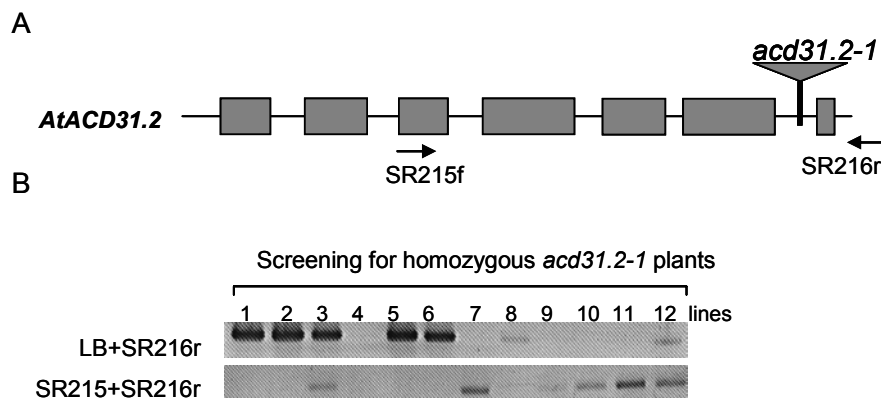


Figure 3.14: Identification and characterization of the *acd31.2-1* knock-out mutant by genomic PCR

A. Diagram of the *Arabidopsis* gene *ACD31.2*. Boxes indicate exons and lines between the boxes introns. The location of the T-DNA in *acd31.2-1* is shown by a triangle. B. Genomic PCR was performed to screen for homozygous *acd31.2-1* mutants. Genomic DNA was subjected to PCR using either two gene-specific primers (SR215f and SR216r, for the wild-type allele of *AtACD31.2*) to confirm the absence of any wild type allele or SR216r with left primer (located in the T-DNA) to confirm the presence of the T-DNA insertion into *AtACD31*. Plants 1, 2, 5 and 6 were identified as homozygous *acd31.2-1* mutants.

3.1.6.3 Isolation of a sHsp double mutant

The previous results showed that both AtHsp15.7 and AtAcd31.2 were localized in plant peroxisomes and expressed under heat and oxidative stress (Fig. 3.11, 3.12). Based on the results of the yeast complementation studies (Fig. 3.8), it was speculated that AtHsp15.7 and AtAcd31.2 played similar roles in protecting leaf peroxisomal enzymes from polypeptide denaturation and were functionally redundant. Therefore, a double mutant deficient in both peroxisomal sHsps (*hsp15.7/acd31.2*) was expected to show the strongest phenotype as compared to the single mutants.

To create a double mutant, the twice back-crossed *hsp15.7-3* mutant was crossed first with homozygous plants of *acd31.2-1*. Then, the heterozygous progeny containing both *AtHSP15.7* and *AtACD31.2* mutant alleles was self-crossed to finally identify homozygous double mutants, referred to as *hsp15.7/acd31.2*. As shown in Fig. 3.15, homozygous double mutants were indeed identified in a genomic PCR screen comprising four PCR reactions for each plant (in total identification of 6 positive plants among 72 plants screened).

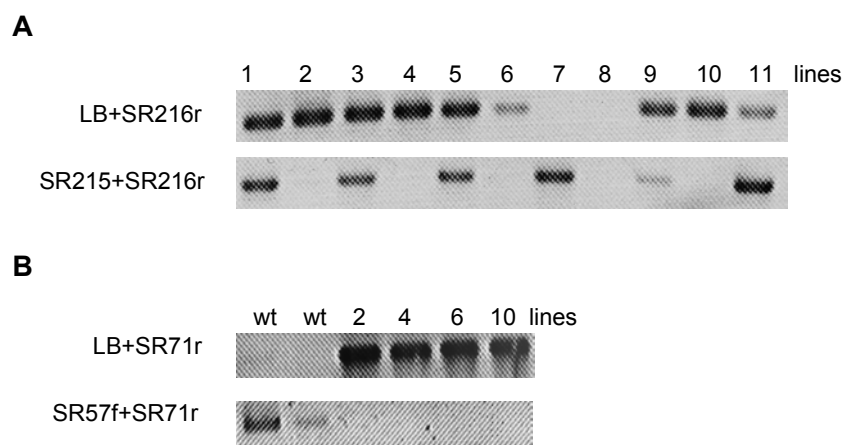


Figure 3.15: Identification of an *hsp15.7/acd31.2* homozygous knock-out mutant by genomic PCR

Genomic PCR used to screen of homozygous *hsp15.7/acd31.2* mutants. Genomic DNA was isolated from progenies of heterozygous plants (*hsp15.7/acd31.2*) and analyzed by PCR for plants both homozygous to *acd31.2* allele (SR215f and SR216r, for the wild-type allele of *AtACD31.2*; LB and SR216r, for the T-DNA insertion allele) and *hsp15.7-3* allele (SR57f and SR71r for the wild type allele of *AtHSP15.7*; LB and SR71r for the *hsp15.7-3* T-DNA insertion allele). Plants 2, 4, 6, and 10 were identified as homozygous *hsp15.7/acd31.2* double mutants. In total, 6 lines out of 72 screened plants were homozygous (data not shown).

3.1.7 *hsp15.7-3* mutant shows a germination defect under heat stress

The homozygous progeny of *hsp15.7-3*, *acd31.2-1* and the double mutant *hsp15.7/acd31.2* were not obviously distinguishable from the wild-type plants if grown under normal growth conditions. Further detailed analyses of the mutants including the timing and speed of germination and seedling establishment in the presence or absence of sucrose did not reveal any substantial difference as compared to wild-type plants (data not shown). According to microarray analyses and our own expression data (chapter 3.1.5), *AtHSP15.7* showed the highest mRNA level in seeds and at the stage of seed maturation, and was upregulated in response to heat stress and oxidative stress. This expression pattern inspired the hypothesis that *AtHsp15.7* deficiency may disturb plant peroxisomal metabolism most if seeds were subjected to heat stress.

To investigate whether *AtHsp15.7* plays an important role in seed germination by preventing heat-induced denaturation of peroxisomal proteins, seeds of *hsp15.7-3* were planted, along with seeds of the wild-type, *acd31.2-1*, and *hsp15.7/acd31.2* on the agar plates containing sucrose and subjected to heat stress (50°C for 5.5 hours) immediately after 3 days of stratification at 4°C (Larkindale et al., 2005). To ensure identical heat-stress conditions (e.g. the same height of agar), seeds of all four *Arabidopsis* lines were planted on the same agar plate. After heat stress application, the seeds were allowed to grow in a growth chamber for seven days (23°C), and the rate of seed germination was calculated (Fig. 3.16). In contrast to a germination rate of about 85% for wild-type seeds, those of the mutant *hsp15.7-3* germinated at a reduced rate of about 40%. Likewise, the *hsp15.7/acd31.2* double mutant showed a similar germination rate as *hsp15.7-3*. No obvious defect of germination was observed for seeds of *acd31.2-1*.

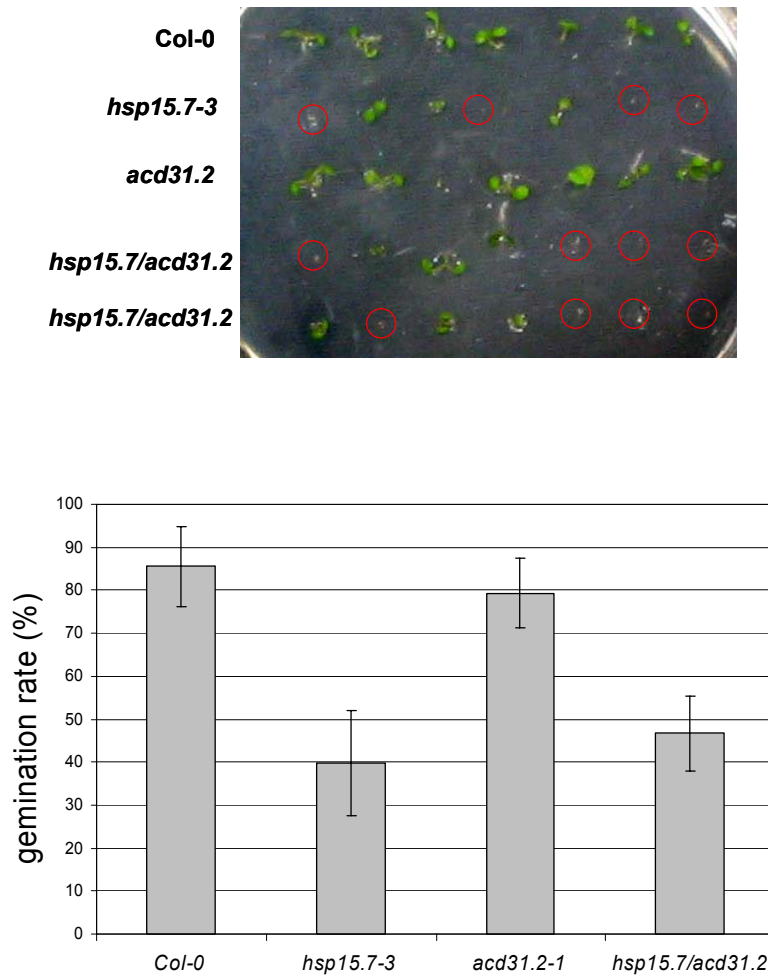


Figure 3.16: Heat stress phenotype of *hsp15.7-3* during germination.

Surface-sterilized seeds were heated to 50°C for 5.5 hours immediately after stratification at 4°C for 3 days. The rate of germination was analyzed after one week of growth at 22°C. A. A representative plate with seedlings of wild-type, *hsp15.7-3*, *acd31.2-1* and *hsp15.7-3/acd31.2-1*. B. Germination rate of wild-type plants and mutants. Error bars represent the SD over five replicate experiments, each comprising 20 to 200 plants for each line.

3.2. Identification and characterization of putative peroxisomal protein kinases (PPPKs) in *Arabidopsis*

In the previous chapter, we demonstrated that two sHsp reside in the peroxisome matrix, play a role as molecular chaperones, and probably are involved in the protection of protein aggregation under oxidative stress conditions. Similar to molecular chaperones, only limited data are available about protein kinases that regulate peroxisomal metabolism by reversible phosphorylation. Among 280 proteins with a putative PTS, several putative protein kinases were found in the database “AraPerox” (www.araperox.uni-goettingen.de). In the following part of this thesis, the subcellular localization of these putative peroxisomal protein kinases (PPPKs) was investigated.

3.2.1 Identification of PPPKs in the *Arabidopsis* genome by bioinformatics tools

Signal transduction through protein phosphorylation is an important mechanism to protect plants against unfavourable environmental conditions. Similar signal transduction mechanisms may also exist in peroxisomes because of the following indications: (1) peroxisomes proliferate in response to external signals (Palma et al., 1991; Farre and Subramani, 2004), (2) peroxisomes play an important role against abiotic and biotic stresses (de Felipe et al., 1988; Willekens et al., 1997; de Rio et al., 1998; Barroso et al., 1999), and (3) some peroxisomal proteins are phosphorylated (Fukao et al., 2003). In addition, proteome data obtained by our own research group indicated phosphorylation of selected matrix proteins of leaf peroxisomes (Babujee, 2004; see also chapter 1.4).

In order to fill the large gap of knowledge about posttranslational regulation of peroxisomal metabolism, the *Arabidopsis* genome was screened for PPPKs with specific PTSs defined for higher plants (Reumann, 2004). In total, six unknown PPPKs with complete kinase domain were identified in the *Arabidopsis* genome (Fig. 3.17). The protein kinase PPPK1 (At3g20530) carries the major PTS1 SKL> and overall moderate peroxisomal targeting probability; additionally, a mitochondrial presequence was predicted in the N-terminal end with high probability by two independent programs. The protein kinase PPPK2 (At4g31230) contains the minor PTS1 tripeptide PKL>. In support of the peroxisomal localization of PPPK2, a protein of about 30 kDa representing the kinase domain of PPPK2 was identified in leaf peroxisomes of *Arabidopsis* greening cotyledons in a proteome study

(Fukao et al., 2002). However, with the recent update of the *Arabidopsis* genome annotation, it turned out that the upstream gene At4g31220 encoding a USPA (universal stress protein A) domain protein represented the N-terminal domain of PPPK2. In the beginning of the project, the C-terminal fragment comprising the kinase domain and the putative PTS1 PKL> was cloned by RT-PCR from flowers and subcloned for the subcellular targeting analyses. Both kinases PPPK3 and PPPK4 (At4g18950 and At3g61960, respectively) carry the C-terminal tripeptide SHL>, which has not only been shown to represent an efficient targeting

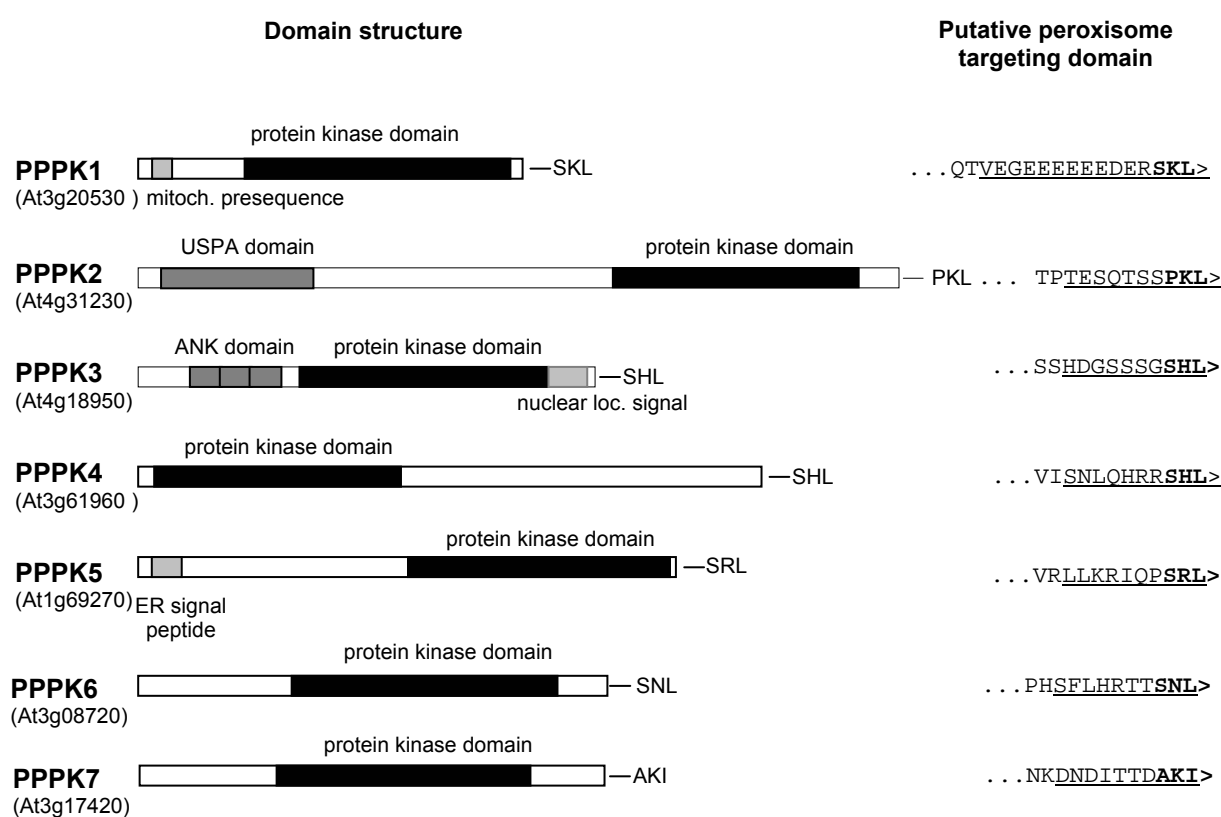


Figure 3.17: Domain structure and predicted targeting signals for PPPKs from *Arabidopsis*.

Seven putative protein kinases with putative PTS1s were identified in *Arabidopsis*, and the subcellular localization of six and one additional protein kinase (GPK1, PPPK7, Fukao et al., 2003) was investigated experimentally. Size and localization of functional domains and targeting signals are drawn schematically to scale. The C-terminal residues of the putative peroxisome targeting domains that were fused to YFP are underlined. The protein kinase domain pfam00069 and other annotated domains (e.g. USPA and ANK) are indicated by black and dark grey boxes, respectively. Targeting signals that were predicted with high probability by two independent programs, are indicated by light grey shading. USPA: universal stress protein A domain; ANK: ankyrin repeat domain.

peptide for yeast peroxisomes but also to be functional in plants as demonstrated by its interaction with tobacco Pex5p in yeast two-hybrid assays (Elgersma et al., 1996; Mullen et al., 1997; Kragler et al., 1998; Lametschwandtner et al., 1998). In PPPK3 two predicted nuclear localization signals (NLS) resided in the C-terminus as well and an ankyrin repeat, possibly mediating protein-protein interaction. The protein kinase PPPK4 belongs to a small gene family, comprising three members, which are homologous to the cytosolic protein kinase ATG1 from yeast (autophagy-related gene). The protein kinase PPPK5 contains the major PTS1 tripeptide SRL> and an ER signal peptide in the N-terminal end predicted by targetP and iPSORT with high probability. The kinase PPPK6 carries the minor non-canonical PTS1 peptide SNL>. The kinase PPPK7 was added to the set of kinases of interest and analyzed experimentally as well because the protein had been identified in *Arabidopsis* glyoxysomes and carries the PTS1-like tripeptide AKI> (Fukao et al., 2003).

3.2.2 Subcellular targeting analysis of PPPKs in *Saccharomyces cerevisiae*

Since the targeting pathways of peroxisomal matrix proteins as well as the PTS consensus motifs are largely conserved in diverse eukaryotes (Gould et al., 1989), most plant peroxisomal proteins were expected to be targeted to yeast peroxisomes. Thus, peroxisome targeting of PPPKs was first investigated by expression of GFP (green fluorescence protein) fusion proteins in yeast cells. The proteins PPPK1-4 were available for this approach because the cDNAs of these genes could be cloned by RT-PCR in the beginning of this project. Because all four protein kinases carry a putative PTS1 peptide, the cDNAs were N-terminally fused with GFP in the plasmid pGFP-N-fus and expressed in yeast under the control of the methionine-repressible promoter *MET25* (Niedenthal et al., 1996). Yeast cells were either transformed only with the GFP plasmid or co-transformed with the plasmid pDsRedSKL, which harbours the cDNA of the red fluorescence protein (DsRed) supplemented by the peroxisome targeting signal SKL> (kindly provided by Dr. Schmitt, University of Saarland, Saarbrücken, Germany).

To verify that the yeast expression system was suitable for analyzing the subcellular localization of plant peroxisomal proteins including PPPKs, we first evaluated whether *Arabidopsis* hydroxypyruvate reductase (HPR) with the PTS1 SKL>, a marker enzyme of peroxisomes, was correctly targeted to yeast peroxisomes. The fusion protein GFP-HPR was

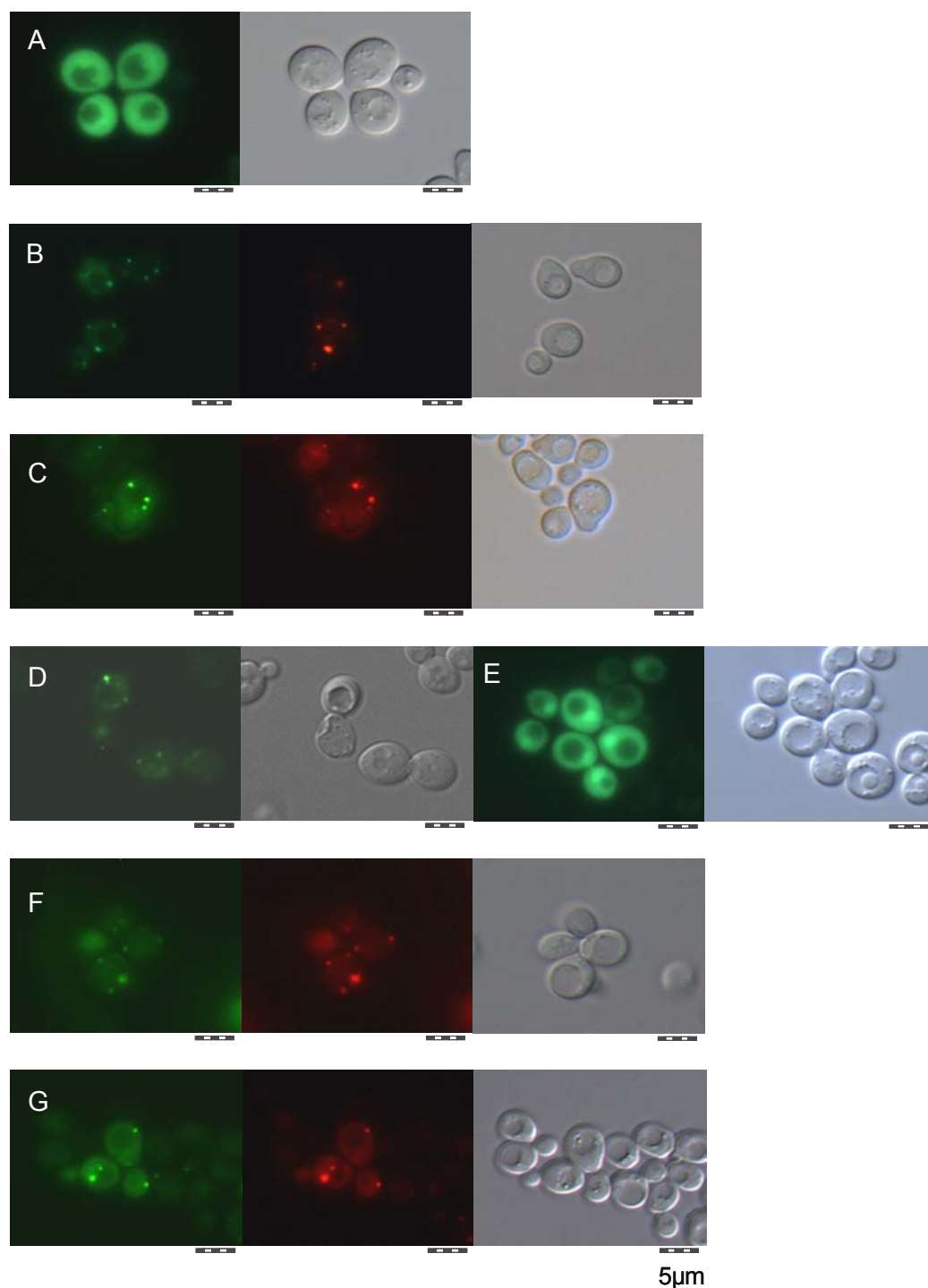


Figure 3.18: Subcellular targeting analysis of PPPK1 to PPPK4 in *S. cerevisiae*

Cells of *S. cerevisiae* were transformed with the plasmid pGFP-N-FUS, in which the genes encoding putative peroxisomal proteins with a C-terminal PTS1 were fused at the N-terminal end to GFP and expressed under control of the *MET25* promoter. The subcellular localization of the GFP fusion proteins was examined by fluorescence microscopy. Peroxisomes were labelled by the red fluorescence protein (DsRed) targeted to peroxisomes by the addition of the C-terminal tripeptide SKL> (kindly provided by Dr. Schmitt, University of Saarland, Saarbrücken, Germany). The gene of plant peroxisomal matrix enzyme HPR (SKL>) was used as a control for targeting analysis of known plant peroxisomal proteins. Yeast cells were analyzed using an appropriate filter set for the

expressed by growing yeast cells in YNB medium supplied with glucose but omitting methionine. In contrast to GFP alone, which was dispersed in the entire cytoplasm (Fig. 3.18A), when observed by fluorescence microscopy, GFP-HPR was concentrated in punctate structures and co-localized with DsRedSKL labelled peroxisomes (Fig. 3.18B). The green fluorescence emitted by GFP was not visible by the filter that was used to detect the red fluorescence of DsRed, when the light intensity was adjusted by use of specific grey filters, and *vice versa*. Therefore, signals detected by both filters were specific for the corresponding fluorescent proteins. These data indicated that the plant protein HPR was correctly targeted to yeast peroxisomes by the PTS1 pathway. To confirm peroxisome targeting of HPR in yeast biochemically, immunoblotting was performed first with total protein extracts from yeast cells expressing GFP-HPR using a commercial anti-GFP serum. A band of expected size of about 70 kDa was detected (data not shown), indicating expression of the full-length chimeric protein. Despite various attempts to stimulate gene expression, however, the concentration of the chimeric protein remained insufficient to proceed to peroxisome isolation (data not shown).

The subcellular localization of the protein kinases was analyzed by studying peroxisome targeting by fluorescence microscopy in the same yeast expression system. The GFP fusion protein of PPPK1 with accessible C-terminal prototypical PTS1 tripeptide SKL> was detected in peroxisomes as shown by co-localization with DsRedSKL (Fig. 3.18C). The fusion protein GFP-PPPK2 also localized to some punctate structures (Fig. 3.18D), suggestive of peroxisomes, but it was not possible to perform double labeling experiments due to the low expression level of the construct. The GFP fusion protein of PPPK3 was targeted to both the cytosol and the nucleus (Fig. 3.18E), in line with the prediction of an

(Figure 3.18 length continued),

corresponding fluorescent protein. In contrast to GFP alone, which was distributed in the cytoplasm and the nucleus (A), the fusion proteins GFP-HPR (B) and GFP-PPPK1 (C) were targeted to punctate structures that were identical with peroxisomes as indicated by their co-localization with DsRed-SKL in double transformants. The fusion protein GFP-PPPK2 was targeted to punctate structures as well (D), whereas GFP-PPPK3 was mainly detected in the nucleus (E). Upon deletion of two predicted nuclear localization signals (NLS) from PPPK3 while conserving the putative PTS1, the fusion protein (GFP-PPPK3 Δ NLS) was targeted to peroxisomes labelled by DsRed-SKL (F). The fusion protein GFP-PPPK4 was targeted to peroxisomes as well (G). For PPPK1, 3, and 4 the full-length genes were fused with GFP, whereas for PPPK2 the C-terminal kinase domain (residues 521 to 764, previously At4g31220) was used.

NLS. Since punctate structures were observed in a few yeast cells, the possible dual targeting of GFP-PPPK3 to the nucleus and peroxisomes was investigated by removing the predicted NLS (between amino acid residues 410-442) while conserving the last 10 amino acid residues of the C-terminus including the putative PTS1 SHL> (GFP-PPPK3 Δ NLS). Upon heterologous expression in yeast, the chimeric protein was indeed targeted to peroxisomes as shown by double labeling with DsRed (Fig. 3.18F), indicating that PPPK3 may have a dual subcellular localization *in vivo* in the nucleus and peroxisomes. The fusion protein GFP-PPPK4 with the C-terminal SHL> was also targeted to peroxisomes (Fig. 3.18G). Interestingly, punctate structures were scattered in the vacuole in some yeast cells as well when the carbon source was changed from oleic acid to glucose (data not shown).

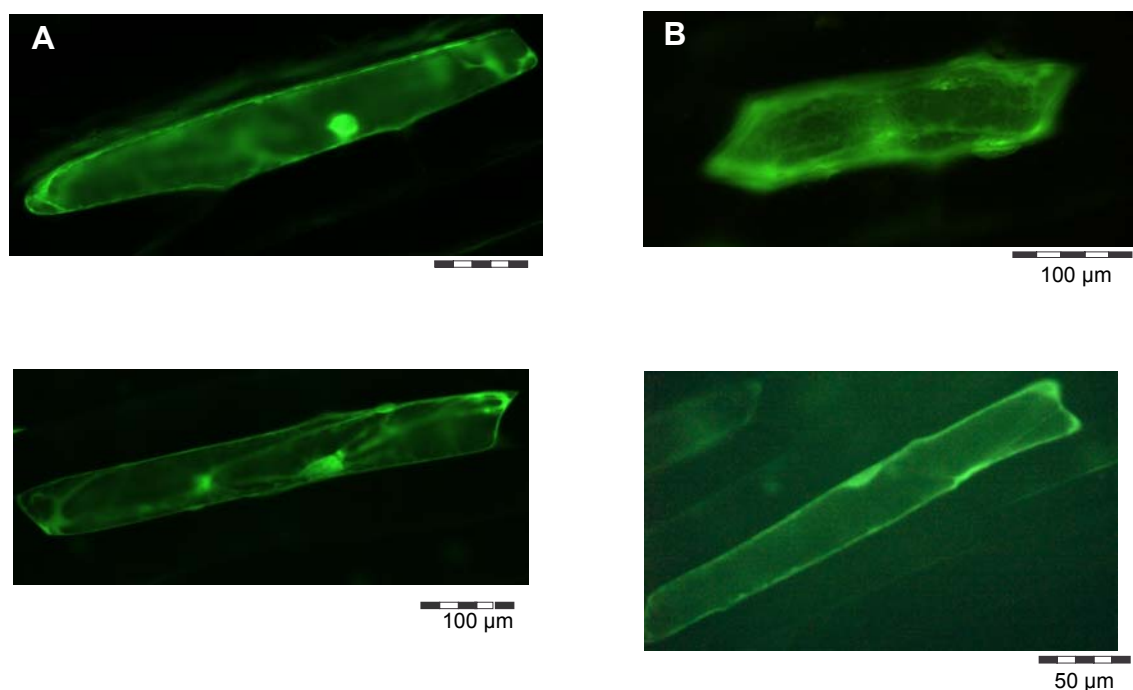


Figure 3.19: Subcellular targeting analysis of PPPK1 to PPPK4 in onion epidermal cells (*Allium cepa* L.).

The genes of PPPK1 to PPPK4 were fused at the 5' end of *EYFP* under the control of double 35S CaMV promoter. Onion epidermal cells were transformed by cell bombardment with gold particles covered with plasmid DNA, and protein targeting was analyzed by fluorescence microscopy. The fusion proteins EYFP-PPPK1 (294-386) (A) and EYFP-PPPK2 (B) remained in the cytoplasm with a tendency of EYFP-PPPK1 to accumulate in the nucleus. The fusion proteins EYFP-PPPK3 (C) and EYFP-PPPK4 (D) remained cytosolic as well. For PPPK3 and PPPK4 the full-length genes were fused with EYFP, whereas for PPPK1 and PPPK2 the C-terminal domains were used (PPPK1: residues 294 to 386; PPPK2: residues 521 to 764). For PPPK1, the full-length construct showed the same subcellular distribution (data not shown).

3.2.3 Subcellular targeting analysis of PPPKs in *Allium cepa* L. (onion) epidermal cells

Although the peroxisomal protein import pathways are largely conserved in diverse eukaryotes, minor differences do also exist between plant, mammals, and fungi. Related but in some aspects specialized PTS consensus motifs have been deduced for the organisms of the three major eukaryotic kingdoms. Thus, some cytosolic plant proteins with PTS1-like peptides may be incorrectly targeted to yeast peroxisomes. To ascertain whether GFP-PPPK fusion proteins were also targeted to peroxisomes of plant cells, we transferred the cDNAs of PPPKs to the plant expression vector pCAT-YFP. The bombardment and visualization of onion epidermal cells were performed as described in chapter 3.1.1.

In onion epidermal cells that transiently expressed a truncated version of PPPK1 (residues from 294 to 386) attached at the 5' end to EYFP, yellow fluorescence was observed in the cytosol and nucleus despite the presence of the prototypical PTS1 SKL> (Fig. 3.19A). An identical result was obtained for full-length PPPK1, suggesting that the putative targeting domain of PPPK1 was not recognized by Pex5 in *Allium cepa*. Similarly, the chimeric protein EYFP-PPPK2 with the putative PTS1 PKL> was scattered in the cytosol (Fig. 3.19B). The fusion protein EYFP-PPPK3 with the C-terminal SHL> was predominantly transported into the nucleus with weak cytoplasmic staining (Fig. 3.19C), further supporting the presence of a functional NLS. The fusion protein YFP-PPPK4 with the C-terminal tripeptide SHL> remained cytosolic in plant cells as well with indications for an accumulation at the plasma membrane (Fig. 3.19D).

In summary, whereas four fusion proteins of PPPKs were targeted to peroxisomes or small cell organelles in *S. cerevisiae*, they remained in the cytosol when transiently expressed in onion epidermal cells. The major possible reasons that accounted for these results were considered to be (1) a fundamentally different PTS1-binding specificity of Pex5 between plants and fungi, and (2) a major difference in polypeptide folding and conformation in both expression systems affecting PTS1 exposure.

3.2.4 Analysis of the peroxisome targeting ability of putative peroxisome targeting domains (PTD) of PPPKs *in planta*

To dissect independent of polypeptide folding if specific PPPKs possessed a functional PTS domain that was capable of directing a reporter protein to plant peroxisomes, a fragment encoding the C-terminal last ten amino acids of the PPPKs including the putative PTS1 was engineered in-frame behind *EYFP* by PCR amplification and transferred back to the pCAT-*YFP* vector to replace the original *EYFP*. The PTS1 targeting domain has recently been shown to comprise about 10 residues (Neuberger et al., 2003, 2004; Reumann, 2004). Upon transient expression in onion epidermal cells, the chimeric proteins comprising the putative targeting domains (PTDs) of three out of seven PPPKs, namely EYFP-PTD_{PPPK1}, EYFP-PTD_{PPPK3}, and EYFP-PTD_{PPPK7} (Fig. 3.20A, D, K) were dispersed in the cytosol, demonstrating that these proteins did not possess a functional PTS1 targeting domain that could direct the PPPKs to peroxisomes *in vivo*. By contrast, punctate structures were observed for the corresponding chimeric proteins of PPPK2, PPPK4, PPPK5, and PPPK6 (EYFP-PTD_{PPPK2}, EYFP-PTD_{PPPK4}, EYFP-PTD_{PPPK5}, and EYFP-PTD_{PPPK6}; Fig. 3.20 B, C, E-J). Even though the yellow fluorescent organelles moved quickly along cytoplasmic strands, they could be shown, by quick filter exchange and image documentation, to be identical to peroxisomes labelled by gMDH-CFP. It was concluded that the C-terminal domains of PPPK2, PPPK4, PPPK5 and PPPK6 can serve as functional peroxisomal targeting domains and target the protein kinases to peroxisomes in *Arabidopsis* if the PTS1 targeting domain was transiently exposed on the polypeptide surface.

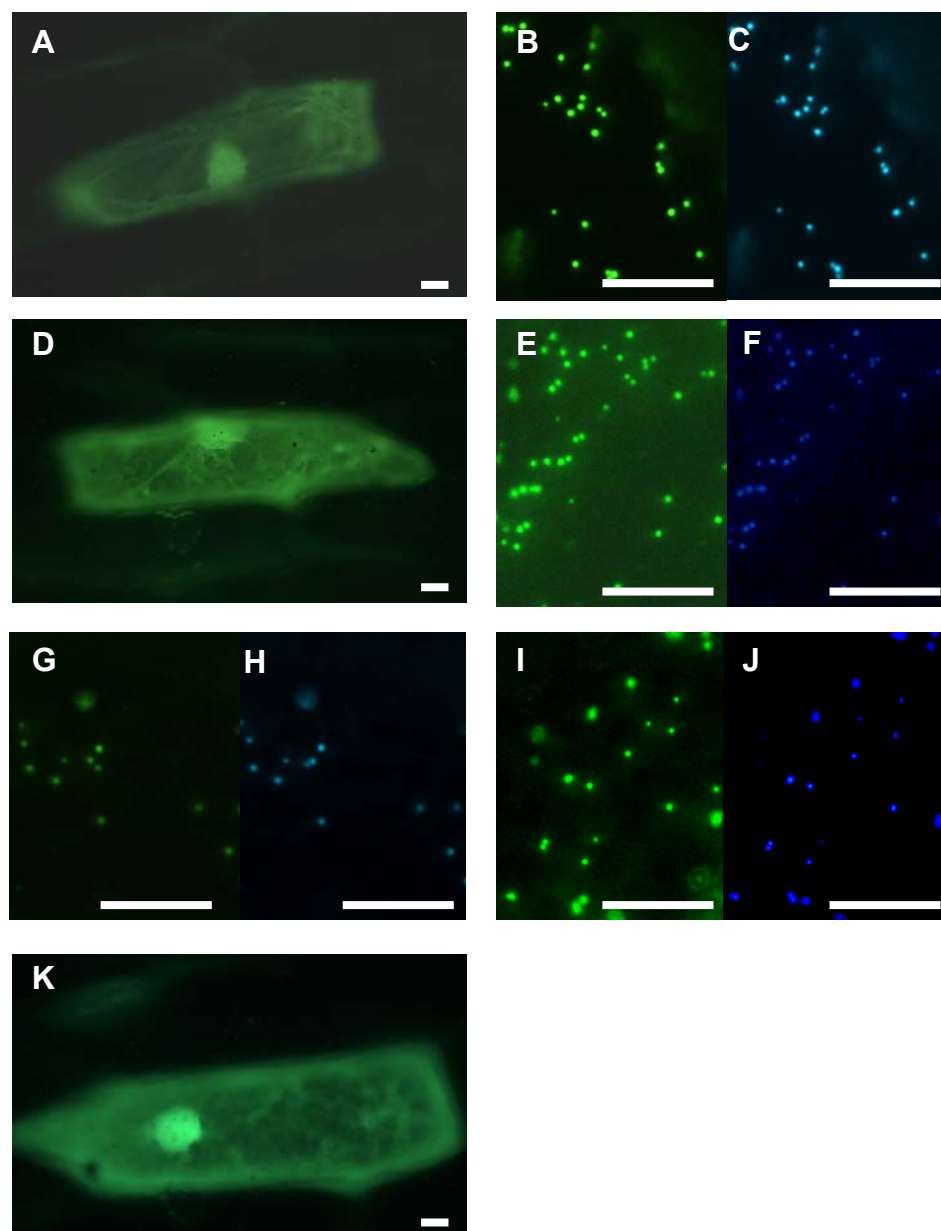


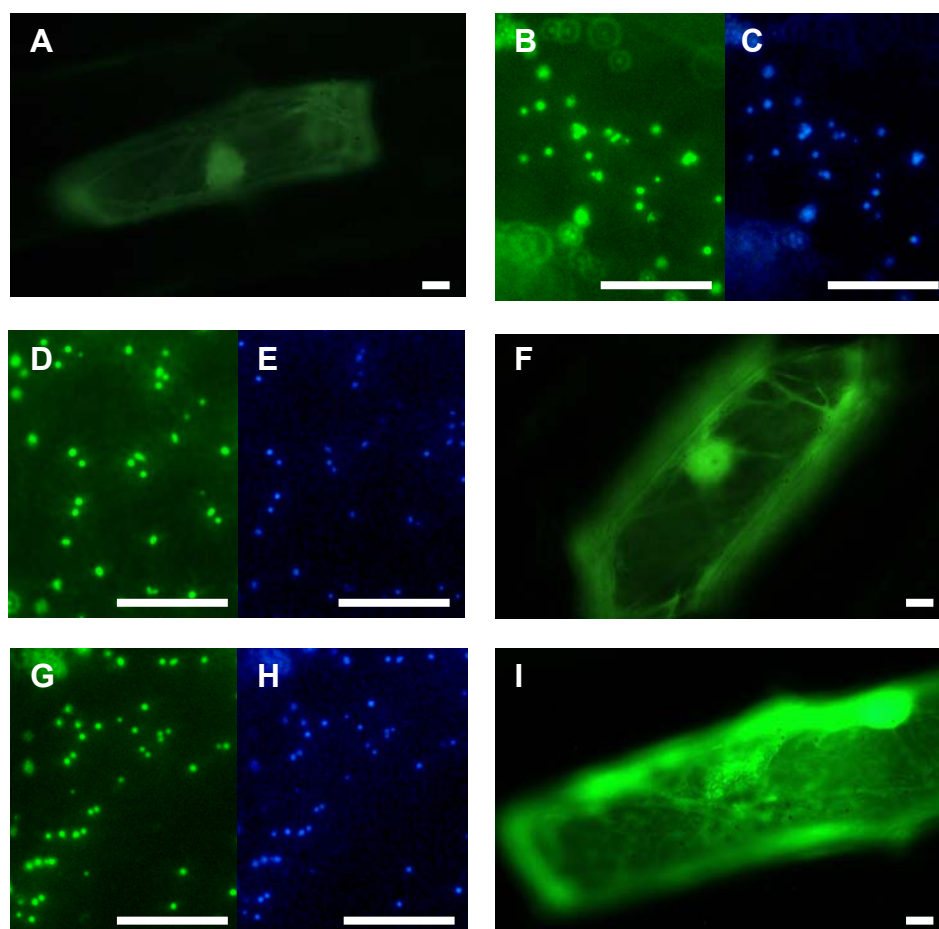
Figure 3.20: Subcellular targeting analysis of putative PTS1 targeting domains of PPPKs in onion epidermal cells.

The putative PTS targeting domains of PPPK1 to PPPK7 comprising generally the C-terminal 10 residues were fused to the C-terminus of EYFP under the control of a double 35S CaMV promoter, and subcellular targeting of the fusion proteins was examined by fluorescence microscopy. The fusion proteins comprising the putative peroxisome targeting domains (PTD) of PPPK1 (A), which notably comprised the C-terminal tripeptide SKL>, of PPPK3 (D), and of PPPK7 (K) remained in the cytosol and nucleus, indicating that these kinases are not targeted to peroxisomes by the PTS1 pathway and probably are not peroxisomal in *Arabidopsis*. The targeting domains of PPPK2 (B, C), PPPK4 (E, F), PPPK5 (G, H), and PPPK6 (I, J), however, targeted EYFP to punctate structures that were identified as peroxisomes by double labelling with the peroxisomal fusion protein gMDH-ECFP and using appropriate filter sets. For imaging either EYFP- (A, B, D, E, G, I, K) or ECFP-specific filters were used (C, F, H, J). The bar represents 20 μm.

3.2.5 Definition of auxiliary and inhibitory elements for peroxisome targeting

Despite the presence of the PTS1 peptides SKL> and SHL>, the fusion proteins EYFP-PTD_{PPPK1} and EYFP-PTD_{PPPK3} remained in the cytosol (Fig. 3.20), suggesting that the residues upstream of the PTS1 tripeptide prevented successful protein-protein interaction with Pex5. Cytosolic targeting of EYFP-PTD_{PPPK1} was particularly surprising because SKL> is a major PTS1 in plants and reported to be sufficient to target reporter proteins to peroxisomes (Gould et al., 1989; Hayashi et al., 1997; Reumann et al., 2004). In addition, the targeting domain of PPPK1 contained a basic residue at position -4, which functions as a targeting enhancing element in front of minor PTS1 peptides (Purdue et al., 1996; Amery et al., 2000; Kotti et al., 2000). Apart from this basic residue, C-terminal domain of PPPK1 was rather unique in containing a high content of eight acidic residues closely upstream of the SKL> peptide. Thus, this C-terminal domain showed a pronounced negative net charge at physiological pH and a positive pI, both of which are properties that are opposite to those that are conserved features of PTS1-targeted proteins, i.e. a preference for basic and proline residues as well as a positive net charge and a basic pI (Reumann, 2004).

To investigate if an accumulation of acidic residues located closely upstream of major PTS1 peptides reduces or even prevents their interaction with Pex5 and the targeting efficiency of a reporter protein to plant peroxisomes, the stretch of acidic residues was eliminated from the targeting domain of PPPK1. As predicted, this modified peptide indeed directed EYFP to peroxisomes (Fig. 3.21B,C). To provide further support for the hypothesis that an accumulation of acidic residues closely upstream of well-known PTS1 peptides prevents protein import by the PTS pathway and presumably interaction of the peptide with Pex5, four neutral residues of the targeting domain of HPR were replaced by acidic residues (A378D, G380E, P382D and V383E). In contrast to peroxisomal targeting of EYFP-PTD_{HPR} (Fig. 3.21D,E), EYFP fused to the mutagenized C-terminal peptide of HPR enriched in acidic residues was no longer targeted to peroxisomes in onion epidermal cells (Fig. 4F). It was concluded from these results that an accumulation of acidic residues in putative PTS targeting domains can prevent protein targeting to peroxisomes even in case of strong prototypical PTS1 tripeptides like SKL>.



Protein	PTD	EYFP targeting	Picture
PPPK1	(...GQT)VEGEEEEEDERSKL>	cytosolic	A
PPPK2	GQTVEGRSKL>	peroxisomal	B, C
HPR	KALGLPVSKL>	peroxisomal	D, E
HPR (G→E)	KDLELDESKL>	cytosolic	F
PPPK4	...(VI)SNLQHRRSHL>	peroxisomal	G, H
PPPK4ΔR	...(VI)SNLGASHL>	cytosolic	I

Figure 3.21: Functional analysis of amino acid residues located upstream of PTS1 tripeptides.

The fusion proteins comprising the putative targeting domain (PTD) of PPPK1 remained in the cytosol (A). Upon deletion of eight acidic residues from the putative PTS domain of PPPK1, the fusion protein was targeted to peroxisomes (B, C). Vice versa, the fusion protein comprising the PTD of HPR was targeted to peroxisomes (D, E), whereas exchange of four neutral into acidic residues in the PTD prevented peroxisome targeting of the fusion protein (F), indicating that a pronounced accumulation of acidic residues in front of a putative PTS1 prevents targeting to plant peroxisomes. Two arginine residues in front of SHL> in the peroxisome targeting domain of PPPK4 were found to be required for peroxisome targeting (G, H, native PTD of PPPK4; I, PTD lacking two arginine residues). The PTDs fused to EYFP for definition of the peroxisomal auxiliary elements and the corresponding subcellular localization in onion epidermal cells are listed below the pictures. Residues in brackets indicate residues that preceded the PTD. For imaging either EYFP- (A, B, D, F, G, I) or ECFP-specific filters were used (C, E, H). The bar represents 20 μm.

Both PPPK3 and PPPK4 contained the PTS1 tripeptide SHL>, but only the targeting domain of PPPK4 was able to direct the reporter protein EYFP to plant peroxisomes (Fig. 3.20D-F). These data suggested that residues upstream of the PTS1 of PPPK4 were critical for peroxisome targeting. In contrast to the mostly neutral amino acid residues of the C-terminal domain of PPPK3, that of PPPK4 was characterized by two arginine residues located in front of SHL>. To investigate whether these basic residues acted as targeting enhancing elements and were necessary for peroxisome targeting of EYFP-PTD_{PPPK4}, both arginine residues were replaced by neutral residues. As predicted, the fusion protein EYFP:PTDΔR_{PPPK4} remained in the nucleus and the cytosol. However, around 30% of the transformed cells still have tiny punctate structures, suggesting the fusion protein still able to target to peroxisomes at a very low level (Fig. 3.21I and data not shown).

3.2.6 PPPK7 does not interact with the PTS1 receptor Pex5 in the yeast two-hybrid system

The protein kinase PPPK7 (GPK1) did not possess one of the PTS1 peptides defined bioinformatically for plants (Reumann, 2004) but had been identified in *Arabidopsis* glyoxysomes in a proteome study and was suspected to be targeted to the organelle via the PTS1 pathway by its C-terminal tripeptide AKI> (Fukao et al., 2003). Our data, however, showed that the C-terminal domain of PPPK7 did not direct EYFP to peroxisomes in onion epidermal cells (Fig. 3.20K), providing strong evidence against the idea that PPPK7 was targeted to peroxisomes by the PTS1 pathway. To investigate by independent tools whether the PPPK7 passes the PTS1 targeting pathway, we analyzed the full-length polypeptide of PPPK7 and the PTS1 receptor AtPex5 for protein-protein interactions in the yeast two-hybrid system. The TPR (tetratricopeptide repeat) domain of Pex5, which mediates interaction with the PTS1 peptide (McCollum, et al., 1993) was fused to the GAL4-transactivation domain (AD) of the yeast expression vector pGADT7. The full-length cDNA of PPPK7 was fused to the GAL4-binding domain (BD) of the vector pGBKT7.

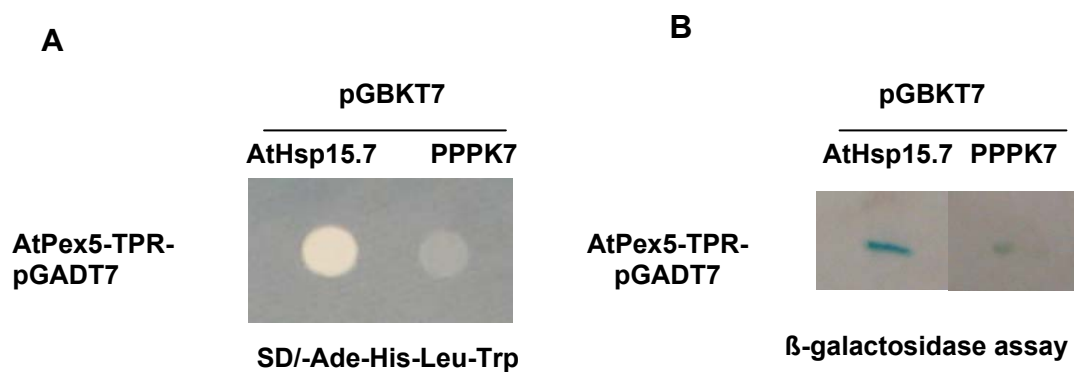


Figure 3.22: Protein-protein interaction between PPPK7 and the PTS1 receptor, AtPex5 as detected by the yeast two-hybrid system.

Yeast cells transformed with the plasmids indicated were spotted on minimal synthetic medium in the absence of adenine, histidine, leucine, and tryptophane (SD/-Ade-His-Leu-Trp) for growth tests (A) or immobilized on Whatman paper for analysis of β -galactosidase activity (B). The full-length cDNAs of *PPPK7* and *AtHSP15.7* were transferred to the vector pGBKT7 (containing a tryptophane nutritional maker, *TRP1*). The TPR domain of AtPex5 was transferred to the vector pGADT7 (containing a leucine nutritional maker, *LEU2*). The PTS1 protein AtHsp15.7 is able to interact with AtPex5-TPR and used as a positive control. In contrast to the positive control, yeast cells transformed with PPPK7 and AtPex5-TPR could not grow on SD/-Ade-His-Leu-Trp medium (30°C, for 3-5 days, A) and did not express β -galactosidase (37°C, 8 hours, B). These results strongly suggested that the PPPK7 cannot interact with AtPex5-TPR in the yeast two-hybrid system.

As a positive control for protein interaction with AtPex5, AtHsp15.7, which had been shown to possess the functional PTS1 SKL> (see chapter 3.1.2), was cloned into pGBKT7 as well. One of the two pGBKT7 plasmids was co-transformed with AtPex5-pGADT7 into the yeast strain AH109 to investigate protein-protein interactions between the two proteins. The yeast strain AH109 is prototrophic for adenine and histidine but possesses three kinds of reporter genes, namely the auxotrophic marker genes *ade2* and *his3*, which encode enzymes of adenine and histidine biosynthesis, respectively, and *lacZ* which encodes the enzyme β -galactosidase that cleaves the colourless substrate X-gal (5-bromo-4-chloro-3-indolyl-beta-D-galactopyranoside) into a product of intense blue colour. All three yeast genes are placed under the control of distinct GAL4 upstream activating sequences and TATA boxes that can be activated and the selection marker genes thereby be transcribed, if the GAL4-transactivation domain (AD) and the GAL4-binding domain (BD) are brought in close proximity to each other mediated by protein-protein interactions between the two proteins of

interest fused to these domains. In case of successful protein-protein interaction, the transformed yeast cells are able to grow prototrophically in the absence of adenine and histidine and show β -galactosidase activity. In control experiments, yeast cells were transformed with one empty vector (pGADT7 or pGBKT7) to investigate if one protein alone was able to activate transcription of the reporter genes.

Transformed yeast cells were spotted on a plate lacking adenine and histidine for prototrophic growth analysis (Fig. 3.22A) or immobilized on Whatman paper for analysis of the β -galactosidase activity (Fig. 3.22B). Regarding the control protein AtHsp15.7, the yeast cells expressing both fusion proteins BD-AtHsp15.7 and AD-AtPex5-TPR could grow prototrophically in the absence of histidine and adenine (Fig. 3.22A) and expressed β -galactosidase, indicating that the yeast two-hybrid system was indeed suitable to determine protein-protein interaction between plant PTS1 proteins and AtPex5. By contrast, yeast cells expressing AD-AtPex5-TPR and BD-PPPK7 remained auxotrophic and were not able to convert X-gal to the blue-coloured reaction product by the expression of β -galactosidase (Fig. 3.22). These data suggested that PPPK7 did not interact with AtPex5 in the yeast two-hybrid system. Considering the subcellular localization data of PPPK7 in onions, the most likely explanation of these protein-protein interaction studies was that PPPK7 did not possess a functional PTS1. However, other factors like a low rate of expression of *BD-PPPK7* or a prevention of targeting of the fusion protein to the yeast nucleus to allow reporter gene activation cannot be fully excluded.

3.3. Characterization of two ATG proteins that may be involved in peroxisome degradation

Among the four PPPKs that possessed a functional PTS1 domain directing a reporter protein to plant peroxisomes, PPPK4 represents one of three *Arabidopsis* homologs of yeast Atg1. In *S. cerevisiae*, Atg1 has been characterized as a protein kinase that is involved in the initiation stage of pexophagy in *Hansenula polymorpha*. The homology with yeast Atg1 prompted us to investigate PPPK4 (=AtAtg1a) more detail.

3.3.1 Identification of a potential regulatory subunit of PPPK4 (AtAtg1a)

Peroxisomes are dynamic organelles that can be induced or degraded in yeasts and animals by a strictly regulated mechanism. The turnover of redundant, damaged, or non-functional peroxisomes by an autophagy-related pathway is referred to as pexophagy (see chapter 1.2.3). Pexophagy and autophagy pathways share many proteins although these processes also use unique components. The protein kinase Atg1 is a central regulatory unit of autophagy and plays, for instance in yeast, an important role not only in the cytoplasm-to-vacuole targeting pathway and autophagy but also in pexophagy (Klionsky, 2005). In yeast, this kinase forms a complex with Atg13 (ScAtg1-ScAtg13) that might act as a molecular trigger for switching between the cytoplasm-to-vacuole targeting pathway and the autophagy pathway (Kamada et al., 2000). Under standard conditions, ScAtg13 is hyperphosphorylated and had a low affinity for ScAtg1, whereas under nutrient deficient conditions, ScAtg13 becomes dephosphorylated and forms a complex with ScAtg1. The kinase Atg1 is essential for selective peroxisome degradation in yeast because the *atg1* mutant from *Hansenula polymorpha* was blocked at the initiation stage of pexophagy (Hutchins et al., 1999; Komduur et al., 2003).

Three homologs of Atg1 have been identified in *Arabidopsis* by sequence similarity, namely AtAtg1a, which is identical with PPPK4 investigated in our study (see chapter 3.2), AtAtg1b, and AtAtg1c (Hanaoka et al., 2002). Sequence analysis revealed that all three homologs contain a conserved kinase domain (about 30% identity with ScAtg1) in their N-terminus and a less conserved domain in the C-terminal half. Two *Arabidopsis* Atg1 homologs are more closely related to each other (70% sequence identity between AtAtg1b and AtAtg1c), whereas AtATG1a shares about 40% sequence identity with AtAtg1b and AtAtg1c over the entire length of the protein.

Our results according to which AtAtg1a possesses a functional PTS1 domain for targeting to peroxisomes and reports on the regulation of Atg1 kinase activity by Atg13 in *S. cerevisiae* raised the question of whether AtAtg1a interacts *in vivo*, either in the cytosol or the peroxisome matrix, with an *Arabidopsis* homolog of yeast Atg13. Two genes encoding homologs of ScAtg13 have indeed been found in *Arabidopsis*, referred to as AtAtg13a and AtAtg13b (Hanaoka et al., 2002, sequence ID: *AtATG13a*, AL132964; *AtATG13b*, AB026654, Fig. 3.23). Interestingly, thorough sequence analysis revealed that AtAtg13a carried a putative minor PTS2 signal (RLX₅HF), similar to AtAcd31.2 (see chapter 3.1.1), and was

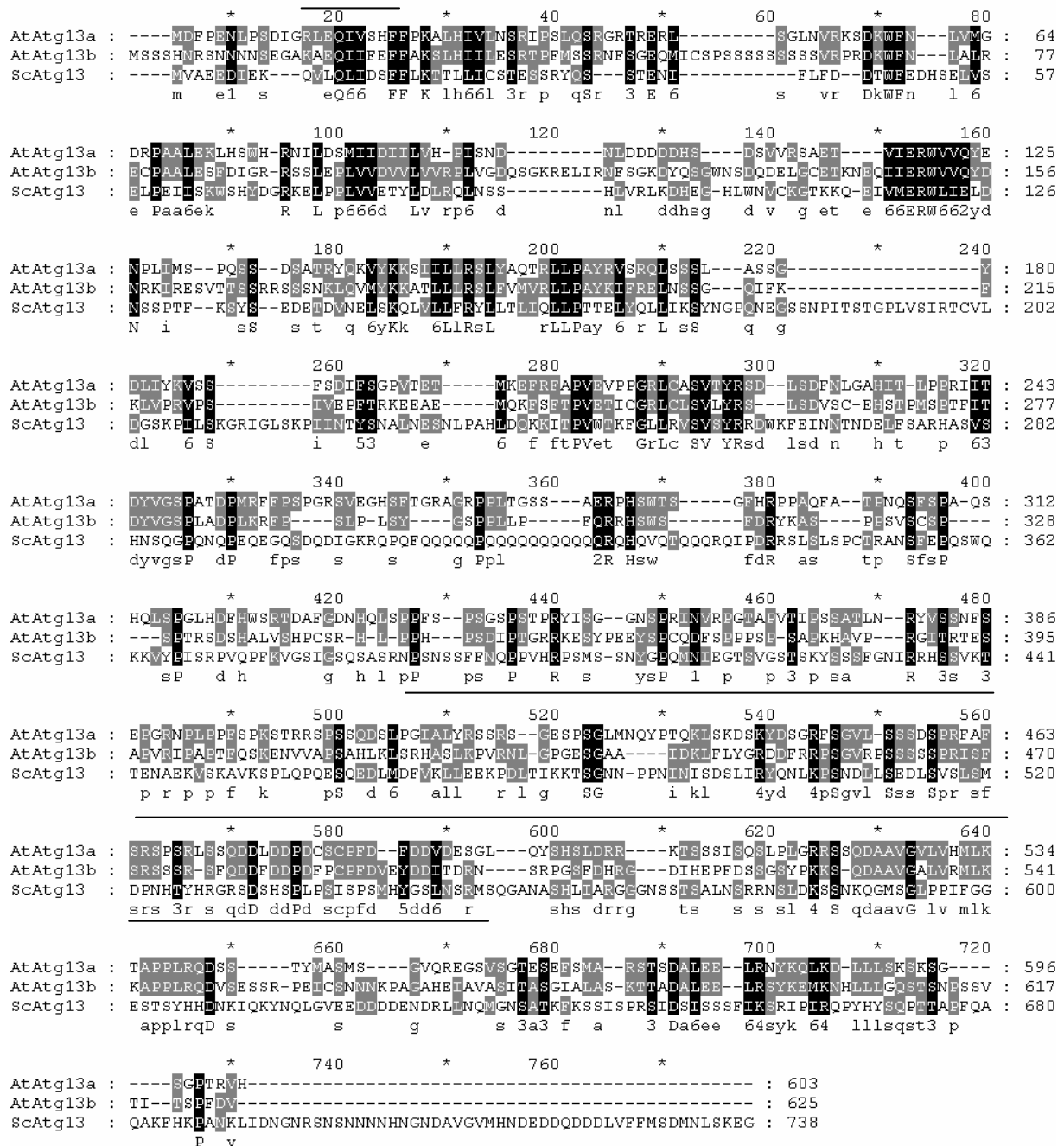


Figure 3.23: Sequence comparison of the *Arabidopsis* Atg13 homologs with *S. cerevisiae* Atg13 protein.

Accession numbers are as follows: ScAtg13, Q06628; AtAtg13a, At3g49590; AtAtg13b, At3g18770. Identical residues are shaded black, and similar residues are shaded grey. The solid lines indicate the putative PTS2 of AtAtg13a and the fragment that shown relatively high similarity to the domain of ScAtg13 that had been shown to mediate protein-protein interaction with ScAtg1, respectively (Kamada et al., 2000).

identical with an unknown protein of our database “AraPerox” that lacked any functional annotation. The sequence surrounding the putative PTS2 of AtAtg13a showed additional properties that are conserved in PTS2-targeted plant proteins, e.g. the presence of one additional basic and one to two proline residues and slightly basic pI, which provided additional support for predicted protein targeting to peroxisomes. The detection of a putative PTS2 in AtAtg13a led to the hypothesis that AtAtg13a was targeted to peroxisomes as well and regulated the activity of AtAtg1a (PPP4K) in the peroxisome matrix. The cDNA of *AtATG13a* was cloned by RT-PCR from *Arabidopsis* flowers. Even though the cDNA contained an unspliced intron between exon two and three, appropriate fragments were subcloned for subcellular targeting analyses and yeast two-hybrid studies.

3.3.2 Expression profile of *Arabidopsis* homologs of *AtATG1* and *AtATG13*

AtATG1 and *AtATG13* are encoded by small gene families in *Arabidopsis*, which indicates that different Atg1-Atg13 complexes may form *in vivo* to play different tissue- or cell-specific roles or to respond to various environmental stresses. A specifically correlated expression pattern of two genes of interest possibly indicates a function of both proteins in the same pathway. To investigate the expression of the unknown genes *ATG1* and *ATG13* from *Arabidopsis*, the *Arabidopsis* microarray gene expression database was queried (<https://www.geneinvestigator.ethz.ch/>) and searched for gene expression in various plant organs, at several developmental stages, and in response to abiotic stress. Except for *AtATG13b*, significant transcript levels were detected for *AtATG1* and *AtATG13* homologs in all tissues examined (Fig. 3.24A), possibly indicating that the autophagic pathway is maintained under normal physiological conditions in *Arabidopsis*. The highest level of expression was observed in senescent leaves and in particular for *AtATG1a* and *ATG13a* (Fig. 3.24A), implying that autophagy plays an important role in recycling of carbon and nitrogen during senescence. The mRNA level of *AtATG1a* accounted for about half of the total *AtATG1* transcripts in all tissues. The expression level of *AtATG13a* was similar to that of *AtATG1a* and much higher than that of the second Atg13 homolog. Interestingly, the expression of *AtATG1a*, *AtATG1b*, and *AtATG13a* was slightly induced by osmotic and salt stress (Fig. 3.24B), pointing to a possible but as yet not established role of autophagy under these stress conditions. In summary, the roughly correlated expression pattern of *AtATG1a*

and *AtATG13a* suggested that *AtAtg1a* may associate with *AtAtg13a* and form a functional complex *in vivo*.

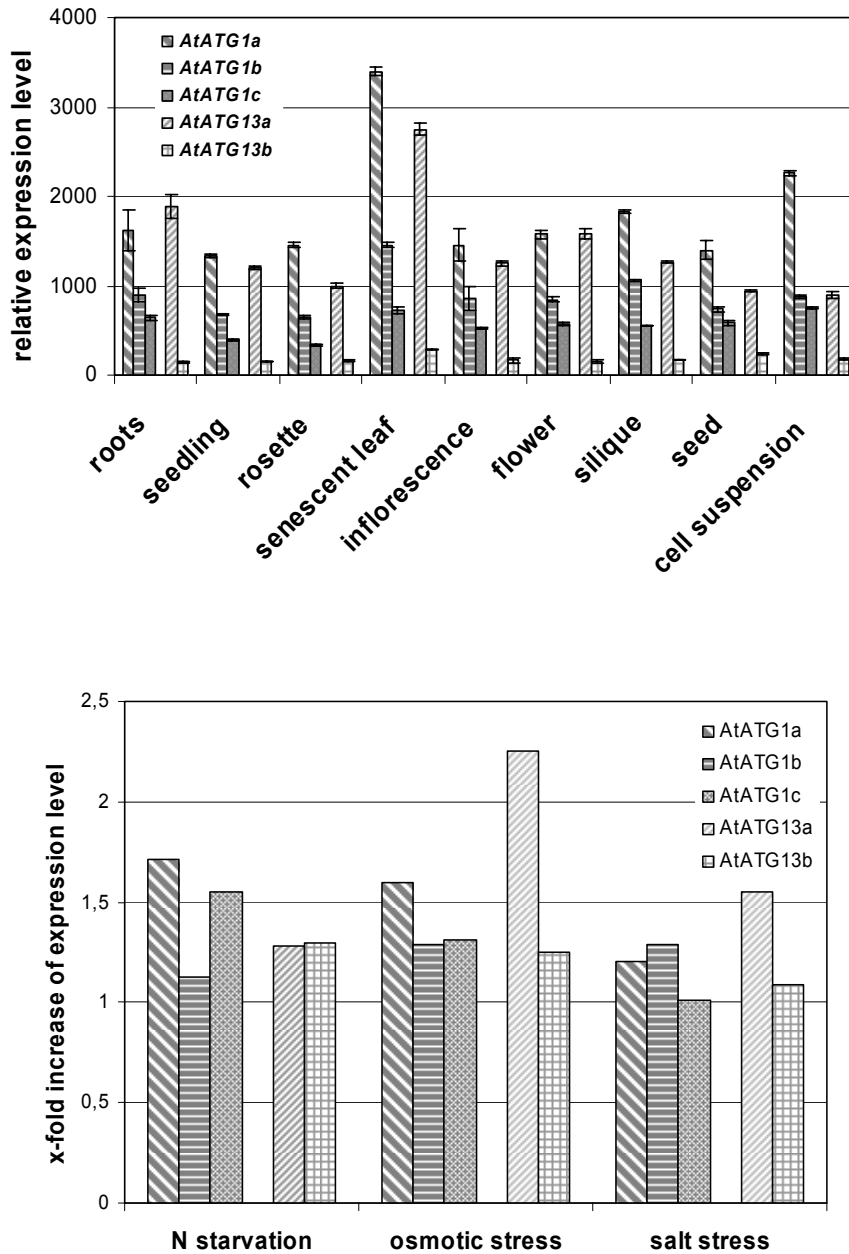


Figure 3.24: Relative expression of *Arabidopsis* *ATG1* and *ATG13* homologs.

A, Expression in various plant organs. B, Expression under different stress conditions, e.g., nitrogen starvation, mannitol-induced osmotic stress, and salt stress, shown in relative expression level (fold) compared with the stress control. The publicly available microarray expression data used for analysis were retrieved from GENEVESTIGATOR (<https://www.genevestigator.ethz.ch>; Zimmermann et al., 2004).

3.3.3 Peroxisome targeting analysis of AtAtg13a

To elucidate the subcellular localization of AtAtg13a and circumvent an interference between PTS2 recognition and polypeptide folding, two peptides comprising either the first 61 or 120 amino acid residues of the N-terminal domain were placed in-frame in front of EYFP to allow interaction of the putative PTS2 (RLX₅HF) with the cytosolic PTS2 receptor Pex7 from *Allium cepa*. Upon gene expression in onion epidermal cells, the longer fusion protein (AtAtg13a₁₋₁₂₀-EYFP) was detected in the cytosol (Fig. 3.25A). The shorter fusion protein (AtAtg13a₁₋₆₁-EYFP) was indeed targeted to some punctate structures (Fig. 3.25B). However, these punctate structures did not overlap with gMDH-CFP labelled peroxisomes (Fig. 3.25C), questioning the peroxisome targeting function of the putative PTS2 of AtAtg13a. Whether AtAtg13 is piggybacked into the peroxisome matrix by complex formation with Atg1a in the cytosol remains to be investigated in more detail.

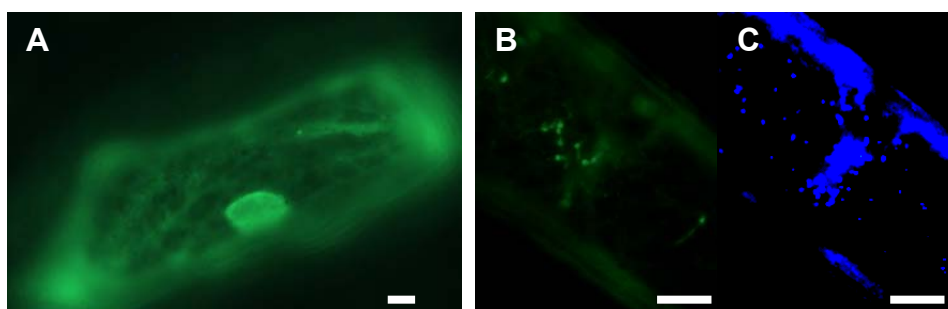


Figure 3.25: Subcellular localization analysis of AtAtg13a in onion epidermal cells.

The fusion protein AtAtg13a (1-120)-EYFP (A) remained in the cytoplasm, whereas AtAtg13a(1-62)-EYFP was targeted to some punctate structures that did not overlap with gMDH-CFP labelled peroxisomes (B, C). The bar represents 20 μ m.

3.3.4 AtAtg1a and AtAtg13a interact with each other in the yeast two-hybrid system

If AtAtg13a regulates the activity of the protein kinase AtAtg1a and both proteins form a stable functional complex *in vivo*, protein-protein interaction between both proteins can possibly be demonstrated by yeast two-hybrid assays. In case of positive results, this system further allows a definition of the corresponding binding sites by successively shortening the cDNAs. For *S. cerevisiae*, it had previously been shown that an internal fragment of Atg13 (residues 343-520) was essential for interaction with Atg1 (Kamada et al., 2000). The domain

in AtAtg13a that was homologous to this yeast fragment was identified by sequence comparison (residues 340 and 500 of AtAtg13a, Fig. 3.23).

This internal fragment of AtAtg13a was transferred into the vector pGADT7 and used to test its interaction with AtAtg1a. However, it was not possible to subclone the full-length cDNA or the kinase domain of AtAtg1a (residues 1 to 300) in-frame into the yeast two-hybrid vector pGBKT7. The few plasmids that could be isolated from *E. coli* after transformation

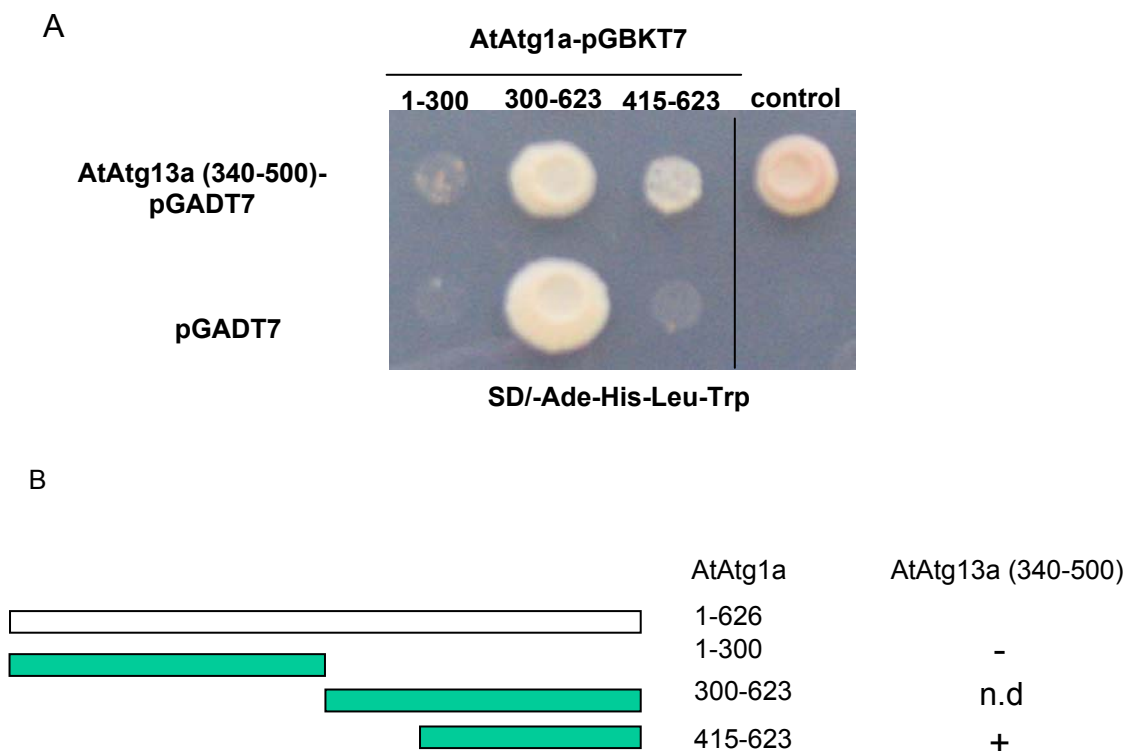


Figure 3.26: Protein-protein interaction between AtAtg1a and AtAtg13a as detected by yeast two-hybrid assays.

Yeast cells transformed with the plasmids indicated were spotted on minimal medium for prototrophic growth analysis (A). Truncated cDNA fragments of *AtATG1a* were transferred to the vector pGBKT7. The cDNA fragment of *AtATG13a(340-500)* was transferred to the vector pGADT7. As a positive control, *AtPex5-TPR-pGADT7* and *AtHsp15.7-pGBKT7* were used (see Fig. 3.22). The yeast cells expressing *AtATG1a(415-623)* and *AtATG13a(340-500)* could grow on minimal medium (37°C, 3-5 days) but not those expressing *AtATG1a(1-300)*. The C-terminal fragment *AtAtg1a(300-623)* exhibited an autocatalytic activation of reporter gene transcription since yeast cells still could grow when transformed with the empty vector pGADT7. These results strongly suggested that the C-terminal fragment (amino acid residues 415-623) of *AtAtg1a* interacted with *AtAtg13a(340-500)*. Regions of *Atg1a* fused to the binding domain (BD) are depicted in green (B). The ability of the deletion constructs of *AtAtg1a* to interact with *Atg13a(340-500)* is indicated on the right. n.d.: not detected.

contained the kinase domain of AtAtg1a with a frame shift. In line with these subcloning problems, previous attempts to transfer *AtATG1a* from the pENTR vector to the prokaryotic overexpression vector pDEST17 by homologous recombination only generated inversely oriented insertions (data not shown). It was concluded that a minimum expression level of AtAtg1 was toxic for *E. coli* and prevented subcloning of *AtATG1a* in-frame and in correct orientation.

A point mutation of an essential active site lysine residue (K→R) in the protein kinase domain leads to an essentially "kinase dead" protein (Hanks and Hunter, 1995). This conserved lysine residue was identified in AtAtg1a by sequence comparison (data not shown) and exchanged likewise to arginine (K36→R) by site-directed mutagenesis. Indeed, the mutagenized kinase domain of AtAtg1a could be subcloned into pGBKT7 and applied to yeast two-hybrid assays. Yeast cells expressing *AD-ATG13a*₃₄₀₋₅₀₀ and *BD-ATG1a*₁₋₃₀₀ remained auxotrophic, indicating that interaction between Atg13a₃₄₀₋₅₀₀ and Atg1 was not mediated by the kinase domain of Atg1. The C-terminal half of AtAtg1a (300-623) exhibited an autocatalytic activation of reporter genes, because yeast cells expressing BD-AtATG1a₃₀₀₋₆₂₃ and which had been transformed with the empty vector pGADT7 grew prototrophically on SD medium lacking adenine and histidine (Fig. 3.26A). The autocatalytic activation of BD-AtATG1a₃₀₀₋₆₂₃ could be eliminated by N-terminal shortening of this fragment (AtAtg1a₄₁₅₋₆₂₃, Fig. 3.26A). The fusion proteins BD-AtAtg1a₄₁₅₋₆₂₃ and AD-AtAtg13a₃₄₀₋₅₀₀ conferred prototrophy to the yeast transformants and supported their growth on minimal medium (Fig. 3.26), indicating that AtAtg1a and AtAtg13a form a functional kinase complex *in vivo* and that the binding domains are located in the C-terminal (residues 415-623) and the middle domain (residues 340-500), respectively.

4. Discussion

4.1 Two novel small heat shock proteins located in the peroxisome matrix

4.1.1 Experimental validation of the postulated targeting of two small Hsps to plant peroxisomes

The availability of the *Arabidopsis* genome sequence (*Arabidopsis* Genome Initiative, 2000) and diverse bioinformatics tools for genome analysis bear the potential to identify low-abundance and inducible proteins of plant peroxisomes (Reumann et al., 2004). In the past, this goal could not be accomplished by traditional biochemical methods. Small heat-shock proteins (sHsps) have been localized to several subcellular compartments but not to the matrix of peroxisomes in any organism (Scharf et al., 2001). In a screen of the *Arabidopsis* genome sequence for putative peroxisomal proteins, we identified two small Hsps (AtHsp15.7 and AtAcd31.2) both of which carried a putative PTS peptide for targeting to plant peroxisomes (Reumann, 2004; Reumann et al., 2004).

While the presence of a PTS peptide is a strong indication, it is not a sufficient criterion to conclude import of unknown proteins into the peroxisome matrix. First, there are indications that subcellular protein targeting is hierarchically organized. If the same polypeptide contains a second targeting signal, in particular an N-terminal signal for targeting to plastids, mitochondria, or the ER, PTS1s can be overruled, because N-terminal targeting signals are translated first (Neuberger et al., 2004). In some cases, dual targeting of one polypeptide to different subcellular compartments is regulated by alternative translation by either including or excluding N-terminal targeting signals. For instance, two mammalian alanine-glyoxylate aminotransferase isoforms are synthesized from a single gene and, by the use of alternative translation, either contain or lack an N-terminal mitochondrial targeting sequence. The former isoform enters mitochondria and the latter peroxisomes (Oatey et al., 1996). Likewise, the distribution of an Hsp70 homolog from *Citrullus vulgaris* L. between chloroplasts and peroxisomes is regulated by alternative translation and results in two polypeptides differing by the presence of an N-terminal chloroplast targeting sequence (Wimmer et al., 1997).

Second, some eukaryotic PTS1 proteins are non-peroxisomal because the PTS tripeptide is not accessible for protein-protein interaction with the cytosolic receptor Pex5.

This is, for instance, exemplified by cytosolic targeting of human dihydrofolate reductase supplemented by the tripeptide SKL> to its C-terminal end. According to the crystal structure of dihydrofolate reductase, the C-terminal domain forms a β -sheet that is buried in the folded protein (Oefner et al., 1988). Therefore, this tertiary structure seems to prevent surface-exposure of SKL> in the fusion protein and binding of the PTS to Pex5 (Oefner et al., 1988; Neuberger et al., 2003). Polypeptide folding and surface accessibility, however, can currently hardly be considered by any subcellular prediction program.

Third, accessory elements located upstream of the PTS1 tripeptide have been proposed to play an important role in peroxisome targeting in case of less abundant 'weak' signals (Neuberger et al., 2003; Reumann et al., 2004). However, these accessory elements are poorly defined and only considered in a single subcellular prediction program, namely the PTS1 predictor (Neuberger et al., 2003). Because these data suggested for the first time that sHsps resided in the matrix of plant peroxisomes, the localization needed to be demonstrated and verified experimentally.

In this study, we used the transient expression system of onion epidermal cells to analyze subcellular targeting of both sHsps *in vivo*. The single cell layer of onion epidermal cells is well suitable for subcellular localization studies by fluorescence microscopy, and its successful application to analyze protein targeting to peroxisomes has been reported (Fulda et al., 2002; Goepfert et al., 2005). A significant advantage of the transient expression system of onion epidermal cells is the easy cell transformation by bombardment with plasmid-coated gold particles and rapid gene expression within 12 to 24 hours. By contrast, stable gene expression in transgenic plants is time-consuming and requires at least four to five weeks from plant transformation to preliminary expression analyses. However, studies on transient gene expression and subcellular localization in onion epidermal cells have the disadvantage that subcellular targeting of proteins with tissue-dependent expression or of those affected by specific environmental stress conditions cannot be analyzed. Moreover, in some cases the high expression activity of the widely used 35S CaMV promoter may overwhelm the peroxisomal targeting pathway and lead to a pronounced cytosolic fluorescence that prevents the simultaneous visualization of weakly fluorescent peroxisomes. This may be problematic in particular for regulatory peroxisomal proteins that are expressed from the native promoter at low levels and possess PTS peptides of low peroxisome targeting efficiency.

As shown by double-labelling experiments using full-length and deletion constructs (Fig. 3.4B, C, F), AtHsp15.7 was targeted to peroxisomes in onion epidermal cells by the C-terminal PTS1 tripeptide SKL>. Non-peroxisomal targeting of EYFP-AtHsp15.7(K136→E, data not shown) with a single amino acid exchange in the PTS1 excluded also the possibility that EYFP-AtHsp15.7 was imported into peroxisomes presumably in a piggyback fashion by dimerization with sHsp homolog from *Allium cepa*.

PTS1-containing proteins are recognised in the cytosol by the receptor Pex5 through its conserved C-terminal domain (about 260 amino acid residues) which comprises about 7-9 tetratricopeptide repeat (TPR) motifs (Gatto et al., 2000). To provide a second line of evidence for targeting of AtHsp15.7 to peroxisomes, the full-length cDNA of AtHsp15.7 and that of the *Arabidopsis* Pex5 ortholog comprising the C-terminal TPR domain were cloned into the corresponding yeast expression vectors and protein-protein-interaction of these two proteins investigated in a yeast two-hybrid approach. Both proteins were found to strongly interact with each other (Fig. 3.22) but did not activate expression of the reporter gene when expressed alone (Fig. 3.26A). These data provided further solid support for targeting of AtHsp15.7 to peroxisomes via the PTS1 targeting pathway.

In addition to the PTS a mitochondrial sequence was predicted in AtHsp15.7 by two independent programs with high probability (TargetP: score=0.82, DBSubLoc: score=91%). However, the cytosolic localization of the inverse fusion protein AtHsp15.7ΔC-EYFP with accessible putative mitochondrial presequence (Fig 3.4G) excluded the possibility that the peroxisomal signal was overruled *in vivo* by the mitochondrial presequence and that AtHsp15.7 was only targeted to peroxisomes under very specific conditions. In summary, these results demonstrated that AtHsp15.7 is exclusively localized in plant peroxisomes *in vivo*.

The second sHsp homolog AtAc31.2 was unique in containing both a putative PTS1 tripeptide (PKL>) and a PTS2 nonapeptide (RLx₅HF). Until now only *Arabidopsis* long chain acyl-CoA synthetase isoform 7 has been demonstrated to possess a functional PTS1 as well as a PTS2 (Fulda et al., 2002). Both fusion proteins, namely AtAc31.2-EYFP (Fig. 3.7B, C) and EYFP-AtAc31.2 (Fig. 3.7F, G), were targeted to peroxisomes. Cytosolic targeting of the mutagenized fusion protein AtAc31.2 (H11D)-EYFP (Fig. 3.7E), in which the absolutely conserved histidine residue of the PTS2 nonapeptide was changed to aspartic acid, confirmed that AtAc31.2 was targeted to peroxisomes via the PTS2 pathway. Because

mutagenesis affected only a single amino acid residue in AtAc31.2, cytosolic targeting of this fusion protein strongly suggested furthermore the absence of an additional yet unknown internal PTS in AtAc31.2. Therefore, peroxisome targeting of EYFP-AtAc31.2 was initially thought to be mediated by the putative PTS1 PKL>. It needs to be stressed that the location of PTS2 nonapeptides has been defined in native PTS2 proteins to the N-terminal 40 residues (Reumann, 2004) and that PTS peptides are generally thought not to be functional if placed at the C-terminus of a reporter protein like EYFP. Since the N-terminal fusion proteins of AtAc31.2 with deleted PTS1 (EYFP-AtAc31.2 Δ PTS1) or with mutagenized PTS1 (EYFP-AtAc31.2(K284E)) were still directed into peroxisomes (Fig. 3.7H-K), we concluded that the putative PTS1 tripeptide PKL> is not necessary for peroxisomal targeting. Whether these fusion proteins were imported into peroxisomes by a specific targeting mechanism, for instance in a "piggyback" fashion mediated by endogenous sHsp homologs of the onion expression system, was investigated and is discussed in more detail in chapter 4.2.

Independent experimental support for the localization of both sHsps in plant peroxisomes was provided by the identification of AtHsp15.7 and AtAc31.2 in isolated *Arabidopsis* leaf peroxisomes. An isolation protocol to enrich peroxisomes from mature leaves of *Arabidopsis* had recently been described (Babujee, 2004; Reumann, unpublished; Ma et al., submitted). Although leaf peroxisomes from *Arabidopsis* are extremely fragile for unknown reasons, an enrichment of these organelles in relatively high purity and in sufficient quantity has been realized by combining published methods (Yu and Huang et al., 1986; Lopez-Huertas et al., 1995) and the addition of further steps, for instance by gentle sedimentation of leaf peroxisomes onto a sucrose cushion during differential centrifugation and by addition of a second sucrose density gradient to increase their purity (Babujee, 2004; Reumann, unpublished). The leaf peroxisomes isolated by this method were suitable for downstream biochemical analyses since contaminating organelles were hardly detectable in the final peroxisome fraction as indicated by the low activity of various marker enzymes, which was close to the detection limit (Babujee, 2004; Ma et al., submitted).

Since AtACD31.2 was constitutively expressed (Fig. 3.11 and chapter 3.15), its polypeptide could indeed be identified in several independent leaf peroxisomal protein preparations from *Arabidopsis* by using one- and two-dimensional gels in combination with different mass spectrometric techniques (Babujee, 2004; Ma et al., submitted). Even though the purity of *Arabidopsis* leaf peroxisomes had remained lower as compared to, for instance,

that of spinach, and even though dominant chloroplastic and mitochondrial proteins could still be detected in this fraction, the identification of AtAc31.2 in isolated leaf peroxisomes provided further support for targeting of this chaperone to *Arabidopsis* peroxisomes *in vivo* because neither a mitochondrial presequence nor a plastidic transit peptide had been predicted for AtAc31.2.

Since the expression of *AtHSP15.7* was hardly detectable under physiological conditions (Fig. 3.11 and chapter 3.15.) and initial efforts in identifying AtHsp15.7 in leaf peroxisomes from *Arabidopsis* plants subjected to *AtHSP15.7*-inducing conditions, including heat stress, were not successful (see chapter 3.1.5), we generated *Arabidopsis* lines stably overexpressing *AtHSP15.7*. After selection for transgenic plants with high expression level of *AtHSP15.7* by RT-PCR (data not shown) and growth of these plants on a large-scale, peroxisomes were isolated from mature leaves and their polypeptide composition analyzed in comparison to that of wild-type plants. An obvious overexpression band about 16 kDa was identified in the leaf peroxisomes from *AtHSP15.7* overexpression lines. A band of similar size strongly cross-reacted with a polyclonal anti-serum raised against AtHsp15.7 (Fig. 3.5). Conclusive evidence that the 16-kDa protein overexpressed in the transgenic lines and the protein that cross-reacted with anti-AtHsp15.7 serum are identical with AtHsp15.7 will be provided by identification of this protein by mass spectrometry. In summary, the biochemical data presented demonstrate that AtAc31.2 and AtHsp15.7 are targeted to *Arabidopsis* peroxisomes *in vivo*. *Arabidopsis* is thus the first organism shown to bear small Hsps in the peroxisome matrix.

4.1.2 Is EYFP-AtAc31.2 targeted to peroxisomes in a "piggyback" fashion?

Cytosolic targeting of the C-terminal fusion protein of AtAc31.2 with mutagenized PTS2 nonapeptide (AtAc31.2(H11D)-EYFP) suggested the absence of an additional internal PTS in AtAc31.2 (Fig. 3.7E). However, inversely arranged N-terminal fusion proteins of AtAc31.2 with deleted or mutagenized C-terminal tripeptide PKL> still entered peroxisomes (Fig. 3.7H-K). These results led to the hypothesis that EYFP-AtAc31.2 might be targeted to peroxisomes by hetero-oligomerization with a peroxisomal sHsp homolog from onion or even the onion ortholog of AtAc31.2 itself, which still contained its functional PTS.

A unique property of peroxisomes as compared to other cell organelles is that protein subunits lacking a targeting signal have been reported to gain access to the peroxisomal

matrix in a "piggyback" fashion by forming homodimers during the import process with subunits possessing a PTS signal. For example, McNew and Goodman (1994) demonstrated that the non-peroxisomal enzyme chloramphenicol acetyltransferase could be directed from the cytosol to peroxisomes in *S. cerevisiae* and mammalian CV-1 cells by trimerization with modified enzyme polypeptides that were supplemented with the C-terminal tripeptide SKL>. This import mechanism is also referred to as "piggybacking". Likewise, it was shown that thiolase subunits lacking a PTS2 were piggybacked from the cytosol into yeast peroxisomes by dimerization with thiolase subunits possessing a PTS2 (Glover et al., 1994). For plants, Lee et al. (1997) reported that isocitrate lyase subunits lacking a PTS1 were piggybacked as multimers into glyoxysomes by association with the wild-type orthologs possessing a PTS1. Interestingly, not only endogenous and artificially modified polypeptides of the same organism can form oligomers and be imported into peroxisomes by piggybacking. Homologous enzymes that share relatively low similarity can be piggybacked into peroxisome as hetero-oligomers as well. As demonstrated in *S. cerevisiae*, $\Delta 3$, $\Delta 2$ -enoyl-CoA isomerase could be piggybacked into peroxisomes in yeast as hetero-oligomers with $\Delta 3,5$, $\Delta 2,4$ -dienoyl-CoA isomerase, a homolog of the former, both of which share only about 50% sequence identity at the amino acid level (Yang et al., 2001).

If EYFP-AtAcd31.2 was piggybacked into onion peroxisomes, we hypothesized that a number of prerequisites had to be fulfilled. First, a peroxisomal sHsp homolog must exist in onions. Second, a peroxisomal sHsp homolog or the onion ortholog of AtAcd31.2 must be constitutively expressed in onion epidermal cells. Third, AtAcd31.2 must be able to form heterooligomers with these sHsp homologs from *Allium cepa* L.

For both AtHsp15.7 and AtAcd31.2, several ESTs from different plant species were detected (Fig. 3.2) that shared high sequence similarity with the *Arabidopsis* homologs and were presumably orthologous. In addition, the PTS1 and the PTS2 were highly conserved in these homologs. Thus, it was reasonable to propose that orthologs of AtHsp15.7 and AtAcd31.2 are ubiquitous in higher plants including *Allium cepa* L. and targeted to peroxisomes as well. Regarding constitutive expression of a peroxisomal sHsp homolog from onion, AtACD31.2 was indeed constitutively expressed under physiological conditions, and its expression level was not significantly altered in response to heat, cold, and oxidative stress (see chapter 3.1.5). Therefore, it was reasonable to assume that the onion ortholog of AtAcd31.2 was also constitutively expressed under normal conditions and that the

polypeptide was synthesized and available for subunit piggybacking during heterologous expression of *AtACD31.2*.

Finally, sHsps are characterized by a tendency for oligomerization because the formation of oligomeric complexes is a prerequisite for chaperone activity (Haslbeck et al., 2005). In addition, even though sHsps normally build homomeric complexes, comprising between two to 40 subunits, the formation of hetero-oligomers has also been reported (Studer and Narberhaus, 2000). For instance, two closely related mammalian sHsps, α A- and α B-crystallin, were identified as hetero-oligomers in a subunit ratio of approximately 3:1 in mammalian eye lenses (Horwitz, 1992). Human α B-crystallin can even form heteromeric complexes with the more distantly related human Hsp27, when co-expressed in the same tissue (Zantema et al., 1992). In bacteria expressing heterologous genes, hetero-oligomers were observed between members of the same sHsp class, even when these proteins originated from different species such as *E. coli* and *Bradyrhizobium japonicum* (Studer and Narberhaus, 2000). Although oligomeric complex formation between members of the same class of sHsps has not been addressed in plants to date (Sun et al., 2002; Wang et al., 2004), sHsps localized in the same organelle should have the opportunity to interact with each other and form hetero-oligomers.

In order to abolish piggybacking, it was attempted to abolish oligomerization of *AtAcD31.2*. According to the solved crystal structures of Hsp16.5 of *Methanococcus jannaschii* and Hsp16.9 of *Triticum aestivum*, a specific β -strand, the so-called dimerization loop, is exchanged between the subunits and critical for the formation of dimers, which are the building blocks of sHsp oligomers (Kim et al., 1998; van Montfort et al., 2001). Based on a multiple sequence alignment of these two sHsps and *AtAcD31.2* (data not shown), the region homologous to the dimerization loop was identified in *AtAcD31.2* (residues 226-252) and the effect of deletion of this domain on targeting of EYFP fusion proteins investigated. However, both fusion proteins lacking the dimerization loop and containing or lacking in addition the C-terminal tripeptide PKL> (EYFP-*AtAcD31.2* $_{\Delta 226-252}$ and EYFP-*AtAcD31.2* $_{\Delta 226-252}\Delta$ PTS1) still entered peroxisomes (Fig. 3.7L-O). These data suggested that the dimerization loop of *AtAcD31.2* is not essential for dimerization. Possibly, one dimerization loop provided by the onion ortholog is sufficient for hetero-dimerization. Alternatively, the affinity between two sHsp subunits both lacking the dimerization loop may be strong enough

for stable complex formation. More deletion constructs need to be generated to disrupt the postulated hetero-dimerization in order to further test the proposed piggybacking pathway.

As an alternative approach, expression of a fusion protein between EYFP and two AtAcd31.2 subunits is underway to stimulate homo-oligomerization and reduce the rate of hetero-oligomerization with onion homologs. In this regard, the availability of *acd31.2-1* knock-out mutant lines (see chapter 3.1.6.2 and 4.4.3) provides an important tool to test the piggybacking hypothesis. Upon expression of *EYFP-AtACD31.2* in either protoplasts generated from *acd31.2-1* or wild-type plants, the fusion proteins should remain in the cytosol in the mutants, since native AtAcd31.2 polypeptides with functional PTS2 are absent for oligomerization and piggybacking is prevented, but not in the wild-type.

Whether EYFP-AtAcd31.2 is imported into peroxisomes by piggybacking is not only relevant to fully understand the peroxisome targeting pathway of AtAcd31.2 *in vivo*, but also has profound consequences for targeting of sHsp to peroxisomes in general. If EYFP-AtAcd31.2 lacking a PTS is imported into plant peroxisomes via hetero-dimerization in a piggyback fashion, further sHsp and Acd protein homologs from *Arabidopsis* lacking a PTS may be imported into the peroxisome matrix by the same mechanism. Considering the large number of more than 19 sHsp and 25 Acd protein homologs in *Arabidopsis* (Scharf et al., 2001) and the fact that AtAcd31.2 and AtHsp15.7 reveal a complementary expression pattern so that at least one of the two isoforms is expressed under all conditions investigated to date (Fig. 3.11 and Fig. 3.12), targeting of further sHsp subunits into the peroxisome matrix by piggybacking with AtAcd31.2 and AtHsp15.7 under specific stress conditions may indeed occur. In the near future, these questions will be addressed by immunoprecipitation and proteome studies of leaf peroxisomes from stressed plants.

Although the PTS2 nonapeptide was hidden in the middle of the N-terminal fusion protein EYFP-AtAcd31.2, it cannot fully be excluded that the PTS2 was still functional in this construct and targeted the fusion protein to peroxisomes via the PTS2 pathway. Mutagenesis and deletion of the PTS2 in this construct are appropriate strategies to address this question and need to be put into practice in the near future.

4.1.3 Why do plants require sHsps in the peroxisome matrix?

With this study *Arabidopsis* is the first organism shown to bear small Hsps in the peroxisome matrix. To investigate if AtHsp15.7 and AtAcd31.2 are specific to *Arabidopsis* or

their orthologs wide-spread in higher plants, various EST databases from higher plants, including monocotyledonous species like *Oryza* and *Triticum*, were screened and AtHsp15.7 homologs were assembled from overlapping ESTs. Sequences of high sequence similarity were detected in many plant species, and all full-length sequences carried a major PTS1 peptide as well (SKL> or SRL>, Fig. 3.2). Furthermore, some full-length ESTs were detected along with several N- or C-terminal ESTs of high sequence similarity to AtAc31.2. Most homologs of AtAc31.2 contained a conserved PTS2 as well (Fig. 3.2). These data suggested that orthologs of AtHsp15.7 and AtAc31.2 are wide-spread in higher plants and most likely also targeted to plant peroxisomes.

Small Hsps comprise multigene families of different sizes in the known eukaryotic genomes. The sizes range from four in *Drosophila melanogaster* to ten in *Homo sapiens* and 16 in *Caenorhabditis elegans* (Morrow et al., 2000; Candido, 2002; Kappe et al., 2003). Interestingly, sHsps are by far most prevalent in plants. In total, 19 sHsps and 25 further genes encoding proteins with one or more α -crystallin domains were found in *Arabidopsis* (Scharf et al., 2001). The unusual complexity of plant sHsps appears to have evolved independently after the divergence of plants from other kingdoms (Waters 1995; de Jong et al., 1998). Plants are also unique in expressing a large number of organelle-specific isoforms that are targeted, for instance, to mitochondria, chloroplasts, and the ER. Our studies show that another organelle-specific class needs now to be defined for peroxisomes. In contrast to plants, sHsps of other organisms are generally restricted to the cytoplasm and only transiently targeted to the nucleus. The only exception is Hsp22 of *Drosophila* which was recently reported to be located in mitochondria (Morrow et al., 2000). No homologs of AtHsp15.7 and AtAc31.2 with putative PTSs have been found in other organisms except for plants. Therefore, organelle- and peroxisome-specific sHsps may be specific to plants.

During their entire life cycle, plants may experience a variety of environmental stress conditions, including heat stress due to rapid and drastic changes in temperature and oxidative stress. Unlike animals, plants are sessile and cannot run away from potentially damaging stresses. Thus, plants might have evolved a larger number and more sophisticated mechanisms for stress-resistance to cope with environmental stresses. The organellar-specific sHsp isoforms may be one part of important defence mechanisms that help to avoid severe protein aggregation under unfavourable stress conditions.

4.1.4 Towards an elucidation of the function of peroxisomal sHsps

4.1.4.1 The two peroxisomal sHsps have a complementary expression profile

Most known sHsps are hardly detectable under standard physiological conditions and only accumulate in plants in response to high temperature stress. Some sHsps can also be induced by other environmental stress conditions, including cold, drought, salinity, or by chemically induced oxidative stress. Developmental stages, under which sHsps are predominantly expressed include embryogenesis, germination, and fruit development (Wehmeyer et al., 1996; Sun et al., 2002).

Because expression analysis of several *Arabidopsis* tissues like pollen tubes is technically challenging, we first investigated the tissue expression specificity of *AtHSP15.7* and *AtACD31.2* based on publicly available microarray data (Zimmermann et al., 2004; Fig. 3.10). Regarding gene expression during plant development, the expression of *AtHSP15.7* was maximum in dry seeds, but declined during seedling establishment, possibly indicating a role of *AtHsp15.7* in desiccation tolerance, dormancy, or germination. By contrast, *AtACD31.2* was rather constitutively expressed in most tissues with a significant increase in rosette and senescing leaves, indicating an important role of this chaperone even under normal physiological conditions.

Our expression analyses at the mRNA level by RT-PCR were consistent with reported microarray data. *AtACD31.2* was indeed constitutively expressed at significant levels, whereas the expression of *AtHSP15.7* was hardly detectable under standard conditions but strongly induced by heat and oxidative stress (Fig. 3.11 and Fig. 3.12). The heat-inducibility of *AtHSP15.7* was further supported by an extended cluster of heat shock element motifs in the gene's promoter region (Scharf et al., 2001). In two slightly different experimental systems, i.e. inhibitor application by watering or infiltration, and using two alternative ROS-producing inhibitors (3-AT and paraquat), an induction of *AtHSP15.7* expression by ROS was observed. Under elevated light conditions, the ROS production is enhanced both in chloroplasts (mainly $O_2^{\cdot -}$ and H_2O_2) and peroxisomes (mainly H_2O_2 ; Sharkey et al., 1988). However, in contrast to our expectation, we did not detect an induction of *AtHSP15.7* under an elevated light intensity of $450 \mu\text{mol m}^{-2} \text{sec}^{-1}$. This result may be explained by the fact that under these conditions, the transient rise in H_2O_2 production in peroxisomes was efficiently scavenged by the peroxisomal antioxidative systems. The light intensity of $450 \mu\text{mol m}^{-2} \text{sec}^{-1}$ was the highest that could be applied without significantly

increasing the ambient temperature. A constant temperature was considered necessary to distinguish between an induction of *AtHSP15.7* by high light and elevated temperature. A transient induction of *AtHSP15.7* was reported in a recent study by microarray analysis but a much higher light intensity of 1,600 to 1,800 $\mu\text{mol m}^{-2} \text{sec}^{-1}$ was applied in this case (Vanderauwera et al., 2005).

Overexpression of cytosolic *AtHsp17.6A* in *Arabidopsis* and *Quercus ruber* *Hsp10.4* in *E. coli* has been reported to increase tolerance to oxidative stress. The proteins that are actually protected by these sHsps have not been identified and details regarding the protection mechanism not been elucidated yet (Sun et al., 2001; Jofre et al., 2003). An intriguing hypothesis explaining the protective mechanism of sHsps has recently been published for plastidic sHsps, which might play a role as antioxidants. A unique feature of chloroplast sHsps is an amphipathic, methionine-rich domain at their N-terminus. Hamilton and Heckathorn (2001) provided evidence that methionine residues of plastidic sHsp are involved in scavenging of ROS by a kind of reversible oxidation process. However, this hypothesis is still under debate since substitution of the conserved methionine residues in plastid *Hsp21* by oxidation-resistant leucine residues did not abolish its protective activity (Gustavsson et al., 2001).

Under oxidative stress conditions or when the main scavenger of H_2O_2 , catalase is inactivated, the intraperoxisomal concentration of ROS may reach such a high level that matrix proteins are oxidized, hydrophobic polypeptide patches exposed, and the enzymes are inactivated. The induction of *AtHsp15.7* may thus indicate that *AtHsp15.7* plays an important role in minimizing oxidative damage on leaf metabolism.

Another intriguing property of the plant peroxisomal sHsps is that one of them is constitutively expressed. Large amounts of ROS are produced in peroxisomes under normal physiological conditions in metabolic processes including the photorespiratory C_2 cycle and the activity of glycolate oxidase, fatty acid β -oxidation and the dismutation of O_2^- (del Rio et al., 2002). Moreover, ROS production in peroxisomes can be further enhanced by oxidative stress (Noctor and Foyer, 1998). Although most intraperoxisomal ROS are thought to be scavenged by the cooperation of peroxisomal antioxidants (ascorbate and glutathione) and antioxidative enzymatic systems, including catalase, ascorbate peroxidase, and SOD, peroxisomal matrix proteins may still be threatened by oxidation under physiological conditions and require the protection by sHsps. The constitutive and high expression level of

AtACD31.2 suggests that this chaperone plays an important physiological role even under standard physiological conditions. To the best of our knowledge, so far constitutive expression as determined for *AtACD31.2* has not been described for a plant sHsp. According to publicly available microarray data, several *Arabidopsis ACD* genes without functional annotation were constitutively expressed at significant levels and not induced by heat, possibly indicating a similar physiological role of these proteins under standard conditions in subcellular compartments other than peroxisomes.

4.1.4.2 AtHsp15.7 and AtAc31.2 are indeed small Hsps

We investigated the molecular chaperone activity of AtHsp15.7 and AtAc31.2 by functional complementation of a yeast mutant that was deficient in sHsp function (Haslbeck et al., 2004). Previously, the molecular chaperone activity of sHsp was defined by performing *in vitro* refolding assays, which relied on the reactivation of citrate synthase in the presence of purified recombinant sHsps expressed in prokaryotic expression systems (Jacob et al., 1993). The results of these assays, however, are compromised by the fact that the *in vivo* polypeptide refolding requires the ATPase activity of co-chaperones.

Knock-out mutants of *S. cerevisiae* deficient in one of two cytosolic sHsps exhibited upon heat-stress at the early stationary phase a morphological phenotype with a dehydrated cell appearance in scanning electron micrographs (SEM) and an increased level of aggregated proteins (Haslbeck et al., 2004). Since the peroxisomal targeting pathway is conserved among yeast, plants, and mammals (Gould et al., 1989), we assumed that a sHsp targeted to the peroxisome matrix could not complement yeast mutants deficient in cytosolic sHsps. To target the plant peroxisomal sHsps to the cytosol in yeast, their PTS peptides were deleted prior to expression of AtHsp15.7 and AtAc31.2 in the yeast mutants. Upon expression, both proteins were able to complement the shrunken phenotype both in single mutants of *hsp26* and *hsp42* as well as in the double mutant *hsp26/42* and to reduce the extent of unspecific protein aggregation in single and the double mutants (Fig. 3.8 and Fig. 3.9). Functional complementation of these mutants by AtAc31.2, however, was less effective and only observed in about 70% of the experiments. A lower expression level of AtAc31.2 is more likely responsible for this result, rather than slight differences in primary structure and higher sequence divergence of its Ac domain from the consensus pattern. The expression level was not analyzed at the protein level because any terminal tags for

immunodetection were omitted to prevent possible interference with subunit oligomerization, which is thought to be mediated by both the C-terminal α -crystallin and the N-terminal domain (Giese and Vierling, 2002; Stromer et al., 2004; Haslbeck et al., 2004). From the complementation experiments, it can be concluded that AtHsp15.7 and AtAcd31.2 exhibit sHsp function *in vivo*. Because both plant sHsps could replace the yeast homologs, which have been shown to accept a rather broad range of substrates (Haslbeck et al., 2004), we further propose that AtHsp15.7 and AtAcd31.2 have an unspecific and probably largely overlapping substrate specificity regarding the peroxisomal proteins that they can protect and keep in a folding competent state.

4.1.4.3 Towards elucidation of the function of peroxisomal sHsps *in planta*

In order to investigate the function of AtHsp15.7 and AtAcd31.2 in more detail, we identified and characterized single T-DNA insertion mutants of both sHsps (*hsp15.7-3* and *acd31.2*) as well as a double mutant (*hsp15.7/acd31.2*). Consistent with the high expression level of AtHSP15.7 in seeds (Fig. 3.10), germinating *hsp15.7-3* single mutant plants showed an increased sensitivity to heat stress, suggesting a role of AtHsp15.7 in desiccation tolerance, dormancy, or germination. In contrast, the germination rate after heat stress was not reduced for *acd31.2-1*. In line with this result, the germination rate of the single *hsp15.7-3* mutant and the *hsp15.7/acd31.2* double mutant did not differ significantly, indicating that AtHsp15.7 and AtAcd31.2 do not display an overlapping or redundant expression and/or function in peroxisomes.

Germinating seeds consume their lipid stores to supply the establishing seedling with carbon skeletons and, ultimately, energy. Mutants deficient in metabolism of fatty acids frequently show defects in germination and post-germinative growth. For instance, the peroxisomal ATP-binding cassette transporter presumably is involved in the import of fatty acids into peroxisomes (Zolman et al., 2001; Footitt et al., 2002; Hayashi et al., 2002). Mutants deficient in this transporter display a phenotype ranging from arrested development when germinated in the absence of sucrose to a so-called 'forever' seed dormancy (Zolman et al., 2001; Footitt et al., 2002; Hayashi et al., 2002). Seed dormancy with germination rates < 0.1% was also found in *aim1* homozygous mutants that are defective in the multifunctional protein, catalyzing the hydration and dehydrogenation steps of fatty acid β -oxidation (Richmond and Bleecker, 1999). While mutants deficient in other components of fatty acid β -

oxidation, including long-chain acyl-CoA synthetase (*lacs6/lacs7*), acyl-CoA oxidase (*acx3/acx4*), or thiolases, were compromised in their β -oxidation capability, the mutant plants still germinated as defined by radicle emergence (Fulda et al., 2004; Adham et al., 2005; Germain et al., 2001; Hayashi et al., 1998). At this point it is still unknown whether the germination defect of *hsp15.7-3* was due to a failure of protecting enzymes involved in fatty acid β -oxidation under heat stress. The hypothesis that sHsps protect enzymatic activities of β -oxidation enzymes can be tested by measuring the activity of specific peroxisomal enzymes such as HPR and catalase in mutant seeds or seedlings upon heat stress. In this way, total plant extract can be analyzed without requiring the isolation of leaf peroxisomes. Detailed studies are underway to investigate whether sHsp proteins protect HPR and catalase under heat stress.

Since additional T-DNA insertions were detected in *hsp15.7-3*, the germination defect needs to be confirmed by complementation of the mutant with the wild-type *AtHSP15.7* allele. Attempts to eliminate additional T-DNA insertions by backcrossing were not successful, indicating that the insertion sites might be located in close proximity to each other. Also, further experiments need to be performed to investigate whether *hsp15.7* and *acd31.2* show a specific heat stress phenotype by analyzing seedlings at different stages.

4.1.5 Peroxisomal Hsps acting in concert with AtHsp15.7 and AtAcd31.2

The localization of two sHsps to the matrix of plant peroxisomes raises new questions and hypotheses. Small Hsps play important roles in protecting cells from a variety of abiotic stresses, such as heat and oxidative stress, by binding non-native proteins in large quantities per oligomeric sHsp complex and trapping them in a soluble and folding-competent state until restoration of physiological conditions (Jakob and Buchner, 1993; Haslbeck, 2002). It was shown in *in vitro* experiments that release of sHsp-bound substrates absolutely requires the ATP-hydrolyzing activity of Hsp70, whereas spontaneous dissociation of non-native proteins from the complex has not been observed (Ehrnsperger et al., 1997; Lee et al., 1997, 2000). In *E. coli*, sHsp-substrate complexes were transferred to ClpB (the prokaryotic homolog of Hsp100) for disaggregation, followed by refolding by Hsp70 and Hsp40 (Mogk et al., 2003a, b). Using citrate synthase and GFP as substrates, Haslbeck et al. (2005) provided both *in vitro* and *in vivo* evidence that yeast sHsps do cooperate with ATP-dependent Hsp70 and Hsp100 in disaggregating and refolding proteins.

Although sHsps of different organisms are only moderately conserved in primary structure, the basic refolding mechanisms and the cooperation with ATP-dependent chaperones seems similar between bacteria, plants, and mammals (Stege, 1995; Veinger, 1998; Lee and Vierling, 2000; Haslbeck et al., 2005). Most experimental evidence regarding the interaction of sHsps with other chaperones is restricted to cytosolic sHsps, but it is reasonable to speculate that similar folding mechanisms exist in subcellular organelles, and that additional Hsps, mainly an Hsp70 and/or an Hsp100 homolog, probably are required in the peroxisome matrix to act in concert with AtHsp15.7 and AtAc31.2.

Hsp70 homologs have been localized to peroxisomes in two independent studies. A cytosolic and a plastidic Hsp70 homolog have been localized to glyoxysomes in cucumber cotyledons (Diefenbach and Kindl, 2000). An Hsp70 homolog from *Citrullus lanatus* was shown to be targeted both to chloroplasts and the peroxisome matrix via two alternative translation start codons, leading to translation of the protein with either a transit peptide, overruling the PTS2, or a PTS2 at the N-terminal end only (Wimmer et al., 1997). Several lines of evidence, however, point to a role of the *Citrullus* Hsps in peroxisome biogenesis and protein assembly within the peroxisomal matrix, rather than in refolding of stress-damaged matrix proteins (see chapter 1.3.2).

Heat shock proteins such as Hsp70 homologs are frequently required for protein translocation into membrane-sealed compartments such as the ER, mitochondria, and plastids. Intraorganellar molecular chaperones have multiple roles, such as (i) pulling nascent polypeptides across membranes, (ii) promoting the folding of unfolded import substrates within the lumen, or (iii) assisting the folding of polypeptides encoded in organellar genomes (Johnson and Olsen, 2001; Gould and Collin, 2002). Unlike in mitochondria or plastids, all peroxisomal proteins are encoded in the nuclear genome and synthesized on free ribosomes in the cytosol. In addition, peroxisomes can import folded polypeptides and even 9-nm gold particles coated with PTS peptides and thus seem to obviate the need of Hsps in the peroxisomal matrix for polypeptide folding (Purdue and Lazarow, 2001). It is unknown for most matrix proteins to what extent Hsp70 isoforms are required for correct refolding of peroxisomal proteins upon their import into the matrix.

To date, no members of the Hsp70 or Hsp100 family have been detected in any proteomic study of peroxisomes. So far, Hsp70 or Hsp100 homologs with putative PTSs have also not yet been found in the *Arabidopsis* genome (Reumann et al., 2004). When the

Hsp70 homolog from watermelon, which is targeted to peroxisomes by alternative translation via the PTS2 pathway (Wimmer et al., 1997), is used as a template for homology analysis, two related *Arabidopsis* Hsp70 homologs are detected, one of which also contains a conserved methionine residue, potentially serving as an alternative initiation codon for translation. The domain of this homolog aligning with the PTS2 of watermelon Hsp70 (RTx₅KL) deviates considerably from defined PTS2 peptides (At4g24280: RSx₅RT). It will be tested in the near future whether this peptide represents an unusual PTS2 or whether an Hsp70 or Hsp100 homolog from *Arabidopsis* is imported into the peroxisomal matrix in a piggyback fashion or by an internal PTS as is the case for catalase (Kamigaki et al., 2003).

In an alternative approach, the presence of Hsp70 or Hsp100 homologs in *Arabidopsis* peroxisomes was addressed by biochemical means. Cross-reactivity between a Hsp70 antiserum and a polypeptide of about 65 kDa was observed in leaf peroxisomes isolated from standard plants and slightly induced upon heat-stress (Reumann, unpublished). These data suggest that an *Arabidopsis* Hsp70 isoform is targeted to the peroxisomal matrix. In contrast, a faint cross-reacting protein band was observed with antiserum against plastidic Hsp100 and may reflect a minor contamination of leaf peroxisomes by chloroplasts. In the future, the putative peroxisomal Hsp70 homolog may be enriched by immuno-precipitation and identified by mass spectrometry.

4.2 Towards an identification of peroxisomal matrix-targeted protein kinases

4.2.1 Identification of *Arabidopsis* putative peroxisomal protein kinases (PPPKs) by a bioinformatics approach

Plant peroxisomal research so far has focused on peroxisomal metabolism, protein import into the organelle, and peroxisome biogenesis, whereas post-translational regulation of peroxisomal metabolism has not received much attention (Fukao et al., 2003; Reumann et al., 2004). Diverse signals may be transduced across the peroxisomal membrane to regulate processes, including peroxisome proliferation or the activity or turnover of key enzymes involved in photorespiration, fatty acid β -oxidation, and ROS detoxification. One or several of these processes may be regulated by reversible phosphorylation. Thiolase was identified as

a phosphorylated glyoxysomal protein in an *in vitro* phosphorylation assay (Fukao et al., 2003). Recent experimental data have provided evidence that a number of protein kinases may be targeted to plant peroxisomes (Yang and Poovaiah, 2002; Dammann et al., 2003; Fukao et al., 2003). Four putative protein kinases were detected in leaf peroxisomes by mass spectrometry in a proteome study (Fukao et al., 2002). However, only one of them carried a PTS tripeptide, and about 2/3 of the unknown proteins identified in leaf peroxisomes in the same study lacked a PTS as well, raising doubts regarding the purity of the organelle fraction. More recently, a calcium-dependent protein kinase was reported to be anchored in the peroxisomal membrane by an acyl anchor (Dammann et al., 2003). Finally, a protein kinase, referred to as glyoxysomal protein kinase 1 (GPK1), has been found in glyoxysomes from *Arabidopsis* cotyledons (Fukao et al., 2003). This protein kinase is identical with PPPK7 investigated in this study and carries a PTS1-like motif (AKI>). The precise subcellular localization and physiological function of the protein are unknown (Fukao et al., 2003).

The study of post-translational regulatory mechanisms of peroxisomes by biochemical approaches is challenging because regulatory proteins are generally expressed at low levels and under specific environmental conditions and therefore difficult to be caught by traditional biochemical methods. In a bioinformatics approach the *Arabidopsis* genome sequence was screened for PPPKs with putative PTS peptides. This method allowed the identification of protein kinases that reside in the peroxisome matrix, but cannot be expected to identify protein kinases attached to the cytosolic side or inserted into the peroxisomal membrane from the cytosol, because these proteins do not use the PTS1 or PTS2 import pathway. Also, protein kinases may interact with peroxisomal proteins in the cytosol shortly after polypeptide synthesis will be missed. However, matrix-targeted protein kinases were thought to play major roles in regulating the activity and/or the turnover of peroxisomal enzymes. Reversible phosphorylation of pre-existing polypeptides like those located in the peroxisome matrix enables quick adaptation of metabolism to drastically changing environmental and cellular conditions like light or cytosolic ROS concentration and thus is an ideal mechanism to complement enzyme regulation at the transcriptional level.

In total, seven PPPKs with five different putative PTS1s were identified in *Arabidopsis*. The tripeptides SKL> and SRL> had previously been classified together with seven further peptides as major PTS1 peptides, because these tripeptides were identified in a large number of plant EST sequences that were homologous to PTS1-targeted proteins

and in different orthologous groups (Reumann, 2004). These high-abundance PTS1 peptides were thought to indicate peroxisome targeting of unknown proteins with high probability. The remaining PTS1 peptides of the putative protein kinases (PKL>, SHL>, SNL>, and AKI>) have been defined as minor PTS1 peptides and indicated peroxisome targeting with lower accuracy (Reumann, 2004).

At the beginning of this study solid experimental evidence for peroxisomal targeting was lacking for all PPPKs. In addition, peroxisomal orthologs from other organisms have not been reported for any of these seven kinases. Two homologs of PPPK4 from *Colletotrichum lindemuthianum* (AAB61403, SRL>) and *Caenorhabditis briggsae* (CAE56822, SRI>) contained a putative PTS. The presence of these major PTS1 tripeptides in two PPPK4 homologs raised the question as whether homologs of these proteins were targeted to peroxisomes in some organisms.

Two protein kinases, PPPK2 and PPPK7, have been detected in *Arabidopsis* leaf peroxisomes and glyoxysomes, respectively (Fukao et al., 2002, 2003). However, some experimental and bioinformatics data regarding these proteins were discrepant. For instance, the predicted size of PPPK2 (At4g31230) is 84.5 kDa, but the protein spot on the 2-D gels identified as this protein had an apparent molecular mass of about 30 kDa (Fukao et al., 2002) and represented the protein kinase domain, which was at that time predicted to be encoded by an obsolete gene locus (At4g31220). Thus, this protein spot may have represented a degradation product of PPPK2 or falsely been assigned to PPPK2 according to flawed MALDI-TOF-MS data (matrix-assisted laser desorption/ionization-time of flight-mass spectrometry). The protein kinase PPPK7 was detected in glyoxysomes in a proteome study (Fukao et al., 2003). As for PPPK2, so far no *in vivo* data have been reported to support the postulated targeting of this protein to peroxisomes, nor have any downstream targets been identified (Fukao et al., 2003).

As outlined in chapter 4.1, the presence of a putative PTS1 peptide in unknown proteins is a strong yet insufficient indication for peroxisome localization *in vivo*. Therefore, the subcellular localization of the seven PPPKs was verified by experimental analyses. To this end, the cDNAs of PPPK1-4 were cloned. At the beginning of this project, the gene structure of none of these four PPPKs as predicted from the genome sequence had been confirmed by the identification of full-length cDNAs or overlapping ESTs. Therefore, gene prediction regarding the start codon of translation and exon-intron borders was first analyzed

manually by homology analysis and indeed had to be corrected for PPPK1, 3, and 4. Appropriate cloning primers were designed according to the optimized gene structure. The primary structure of the cloned cDNAs was identical with that of our gene prediction and finally consistent with a more recent release of *Arabidopsis* gene structure prediction. cDNA clones for PPPK5 and PPPK7 were obtained from NASC (The Nottingham *Arabidopsis* Stock Centre, Nottingham, UK). For PPPK6, the full-length cDNA could not successfully be cloned in the course of this study.

4.2.2 Multiple factors are responsible for alternate subcellular targeting of PPPKs in yeast and plant expression systems

In line with subcellular targeting of the control protein hydroxypyruvate reductase (HPR) and previous reports of correct import of plant peroxisomal proteins into yeast peroxisomes (van der Klei et al., 1993) it was observed that three out of four PPPKs (PPPK1, PPPK4, and PPPK3 lacking the NLS) were targeted to punctate structures in *S. cerevisiae* that were identified as peroxisomes by double-labelling experiments using GFP-PPPK and DsRed-SKL>. The fusion protein, GFP-PPPK2, was localized in punctate structures most likely identical with peroxisomes. In onion epidermal cells, however, identical and similar fusion proteins of the same three PPPKs and EYFP remained cytosolic. Even though it is tempting to argue that the plant expression system is more likely to yield correct subcellular targeting data of plant peroxisomal proteins and therefore to conclude that the four PPPKs are non-peroxisomal, the interpretation is more complex and several reasons may have accounted for the observations made.

First, the PTS1 receptor Pex5 from plants and yeast may have a slightly different affinity to PTS1 tripeptides of the PPPKs. For instance, watermelon Pex5 only partially restored the import deficiency of the *pex5* mutant from *Hansenula polymorpha* (Wimmer et al., 1998). Upon expression of watermelon *PEX5* in this mutant, the peroxisomal enzyme alcohol oxidase was insufficiently imported into peroxisomes, because enzyme crystalloids accumulated in the cytoplasm (Wimmer et al., 1998). The partial complementation indicated that the primary structure and PTS1 binding affinity of the TPR domain of Pex5 differs between plants and fungi, thereby altering the import efficiency of PTS1 proteins.

Particular the PTS1 tripeptide SHL> appears to mediate protein import into peroxisomes with varying efficiency in different organisms. SHL> is a frequent PTS1 in fungi

and was able to interact with tobacco Pex5 in the yeast two-hybrid system and to direct chloramphenicol acetyltransferase from the cytosol to peroxisomes in tobacco BY2 cells (Mullen et al., 1997; Kragler et al., 1998). However, among about 400 ESTs that were homologous to PTS1-targeted plant peroxisomal proteins, not a single sequence contained SHL> and no PTS1 tripeptide even contained a histidine at position -2 (Reumann, 2004). These data suggest that spontaneous mutation at position -2 in PTS1 tripeptides to histidine residues generally abolish peroxisome targeting in plants (Reumann, 2004).

Upon removal of the nuclear localization signal, the kinase PPPK3 with the C-terminal tripeptide SHL> was targeted to yeast peroxisomes but its C-terminal domain did not direct EYFP to peroxisomes in onion cells, strongly suggesting that the C-terminal domain interacted with yeast Pex5 but not with onion Pex5 to achieve import into peroxisomes. In addition, the results presented demonstrate that targeting of proteins to plant peroxisomes by SHL> strongly depends on auxiliary targeting elements. Removal of both arginine residues from the C-terminal domain of PPPK4 significantly reduces the peroxisome targeting efficiency. In summary, the subcellular targeting results obtained in yeast and onions most likely differed for the SHL> containing kinases PPPK3 and PPPK4, because Pex5 from fungi has a higher affinity to SHL> peptides, whereas successful cargo delivery of SHL> proteins to plant peroxisomes by plant Pex5 relies on the presence of affinity enhancing basic residues upstream of SHL>.

Another explanation for the discrepancies in subcellular targeting of PPPKs in yeast and onion regards the expression level of the fusion proteins. Overexpression of EYFP fusion proteins under a two fold CaMV promoter in a transient expression system may have overwhelmed the transport capacity of the peroxisomal targeting pathway and resulted in aberrant targeting or a pronounced cytosolic fluorescence staining that shadowed the detection of tiny organelles such as peroxisomes. Such an effect may prove particularly important for low-abundance regulatory proteins like protein kinases which may not contain PTSs of high targeting efficiency. A high rate of expression would then lead to an increased ratio of cytosol-to-peroxisome targeting. Attempts to reduce the rate of transcription, for instance by incubation at chilling temperature, did not alter subcellular targeting.

The third and possibly most important factor potentially interfering with peroxisomal targeting of *Arabidopsis* PPPKs in onion epidermal cells is related to the tightness of polypeptide folding and the protein conformation affecting PTS1 exposure. Plant

polypeptides expressed heterologously in yeast may fold slower and less tightly in *S. cerevisiae* due to the absence of plant-specific chaperones. The rate of polypeptide folding in combination with PTS1 exposure, however, is likely to determine whether or not Pex5 can interact with the PTS1 peptide and initiate targeting to peroxisomes. Experimental data are not available to gain insights into this process. For specific plant proteins, in which PTS1 peptides are permanently or transiently buried in the folded proteins, incomplete folding of the polypeptide is likely to facilitate interaction between the PTS1 and Pex5, leading to successful peroxisomal targeting in yeast. Thus, plant PTS1 proteins that remained cytosolic in onion epidermal cells may either be permanent cytosolic proteins, because the putative PTS1 peptide is permanently buried in the folded polypeptide, or transiently targeted to peroxisomes, because the PTS1 is transiently surface-exposed by signal-induced conformational changes.

Targeting analysis of the putative C-terminal domains of the PPPKs provided information as to which PPPKs may represent false positives for peroxisomal targeting, because they are located permanently in the cytosol, and which ones are likely to be transiently targeted to peroxisomes. The C-terminal domain of PPPK3, for instance, did not direct EYFP, and thus most likely neither the kinase itself, to peroxisomes. In contrast, four other kinases possessed functional PTS1 domains, including PPPK2 and PPPK4 (see chapter 4.8). The localization of the C-terminal domain fusion proteins of PPPK2 and PPPK4 to the cytosol of onion epidermal cells indicated that the cytosol was the default location of these kinases under standard conditions, and that PTS1 interaction with Pex5 was apparently hindered by a specific polypeptide conformation. The conformation of protein kinases is well-known to be dynamic and altered by reversible phosphorylation, i.e. either phosphorylation by an upstream kinase or autophosphorylation, or by association with interacting proteins. PPPKs may display dual or even multiple subcellular localizations in response to specific signals. A dual conditional targeting has, for instance, been observed for a calcium-dependent protein kinase in *Mesembryanthemum crystallinum*. This protein kinase was targeted from the plasma membrane to the nucleus in epidermal cells under salt stress (Patharkar and Cushman, 2000). An even more complex subcellular localization between the plasma membrane, the ER, the nucleus, and the cytosol was observed for a fusion protein of the skinase with GFP in response to humidity and was attributed to binding to actin microfilaments (Chehab et al., 2004). Although the mechanism underlying the conditional

targeting of this protein kinase is still not clear, the conformational changes may represent a very important parameter for the diverse subcellular localization.

Due to the presence of functional PTS1 domains in these kinases, we propose that, in the course of signal transduction, the conformation of these PPPKs and thereby PTS1 exposure may be altered. In line with the postulation of conformational changes, the protein kinases PPPK2 and PPPK4 contain N- and C-terminal domains, respectively, next to the kinase domain that may function as regulatory domains and alter PTS1 exposure. Conclusive evidence for transient targeting of these PPPKs to peroxisomes needs to be provided by constitutive gene expression in *Arabidopsis* and a definition of developmental or environmental conditions, under which these kinases are targeted to the peroxisome matrix.

4.2.3 PPPKs with a functional PTS domain

To analyze subcellular targeting of PPPKs independent of potential masking by polypeptide folding, the putative PTS1 targeting domain was fused to the C-terminal end of the EYFP. Co-crystallization of Pex5p with a PTS1 peptide as well as previous bioinformatics analyses have indicated that the PTS1 targeting domain comprises about eight to 12 residues (Gatto et al., 2000; Neuberger et al., 2003, 2004; Reumann, 2004). The C-terminal ten amino acid residues of PPPK2, PPPK4, PPPK5, and PPPK6 with the putative PTS1 tripeptides PKL>, SHL>, SRL>, and SNL>, respectively, all directed the reporter protein EYFP to peroxisomes. These results indicate that the PTS1s of these four PPPKs are recognized by Pex5 and represent functional PTS1 domains. Accordingly, these kinases can be targeted to the peroxisome matrix if the tripeptides are exposed transiently on the protein surface. PPPK4 is thus the first plant protein shown to possess the PTS1 SHL>. Thus, in the course of this study four proteins were identified among about 1085 protein kinases from *Arabidopsis* (*Arabidopsis* Genome Initiative, 2000; Hrabak, 2002) that represent the most likely candidates for protein kinases targeted to the matrix of peroxisomes (see chapter 3.24).

Detection of a functional PTS1 domain in PPPK2 is in line with the identification of this kinase in *Arabidopsis* glyoxysomes (Fukao et al., 2002). It remains to be clarified why microarray data did not indicate PPPK2 expression in cotyledons (data not shown) and whether the protein has an unusual turnover rate. The kinase PPPK2 may have been identified as a 30-kDa protein on 2-D gels as a protein of lower than predicted molecular

mass because of residual proteolytic activity in peroxisomes, which is an effect common in peroxisome isolation.

The protein kinase PPPK2 belongs to a USPA (universal stress protein A) protein family, three subfamilies of which contain a protein kinase domain (Kerk et al., 2003). The USPA domain is termed after UspA (Universal stress protein A) of *E. coli* and widespread in prokaryotic and eukaryotic organisms. In *E. coli*, UspA has been shown to be phosphorylated and to accumulate in the stationary phase of growth. Genetic evidence revealed that UspA plays an essential role under starvation conditions, and with a wide variety of environmental stresses, including osmotic stress, UV light, and toxic chemicals inducing oxidative stress (Nystrom and Neidhardt, 1992, 1993, 1994). To date, no function was attributed to any of the 13 USPA-containing protein kinases in *Arabidopsis*. Based on sequence similarity, it has been postulated that some USPAs may be important for protein ubiquitinylation (Kerk et al., 2003). Several USPA-containing protein kinases including PPPK2 are exclusively expressed in pollen according to microarray data retrieved from PlantsP (<http://plantsp.genomics.purdue.edu/>, data not shown). The possible role of PPPK2 in pollen development is currently under investigation using *Arabidopsis* T-DNA knock-out mutants.

PPPK4 is one of three *Arabidopsis* homologs of yeast ATG1 (Hanaoka et al., 2002), which is an essential cytosolic protein kinase involved in three distinct but partly overlapping protein degradation pathways, namely microautophagy including micropexophagy (in *Pichia pastoris*), macroautophagy including macropexophagy (in *S. cerevisiae* and *P. pastoris*), and in the pathway of cytosol-to-vacuole-targeting (Cvt in *S. cerevisiae*, Klionsky, 2005; see chapter 4.10). Because the sequence homology of PPPK4 allowed us to build detailed hypotheses regarding the function of this protein kinase in plants and peroxisomal metabolism, further experimental analyses regarding protein-protein interaction and the analysis of *Arabidopsis* mutants focused on this protein kinase (see chapter 4.10).

The protein kinase PPPK5 is annotated as a receptor-like protein kinase and carries an N-terminal targeting signal, namely an ER signal peptide, which is predicted with high probability by two programs (TargetP: score=0.769; iPSORT: positive score) in addition to a functional PTS1 targeting domain. In line with protein targeting via the secretory pathway, the constitutively expressed fusion protein PPPK5-GFP has recently been reported to be targeted to the plasma membrane in the roots of transgenic *Arabidopsis* plants (Osakabe et al., 2005). The possible peroxisomal targeting, however, was likely obscured in this reporter

construct because the major PTS1 peptide was masked in the middle of the fusion protein. In fact, dual protein targeting is challenging to investigate *in vivo* if both terminal tags are thought to interfere with the subcellular targeting signals. The actual localization of native PPPK5 may be solved by immunocytochemistry using electron microscopy and antibodies against the native protein kinase. As shown by Hong et al. (1997), *PPPK5* is expressed in various tissues and can be further induced in response to ABA and several environmental stresses, such as dehydration, high salt, and low temperature.

PPPK6 is one of two *Arabidopsis* homologs of human p70 ribosomal S6 kinase (p70s6k) (Mizoguchi et al., 1995), which is a mitogenically activated protein (MAP) kinase that phosphorylates ribosomal protein S6 and activates protein synthesis (Thomas and Hall, 1995). In *Drosophila*, the activity of p70s6k is regulated by the Tor (target of rapamycin) kinase and required for maximal autophagic activity (Scott et al., 2004). The Tor kinase also phosphorylated Atg13, the regulatory subunit of the protein kinase Atg1, reduced its affinity to the kinase, and inhibited autophagy under nutrient rich conditions (Kamada et al., 2000). Possibly, the general autophagic pathway has partially been transferred in evolution into the matrix of plant peroxisomes to regulate enzyme activity or protein turnover.

In the future, further solid evidence for peroxisomal targeting of PPPK2, PPPK4, PPPK5 and PPPK6 needs to be provided by creation of transgenic plants expressing these kinases with a reporter gene or an epitope tag from their endogenous or a constitutive promoter. These plants will be screened under different environmental conditions to reveal conditional protein targeting to the peroxisome matrix. Transgenic *Arabidopsis* plants that constitutively express PPPK4 supplemented by an antigenic N-terminal tag have been generated. The plants will allow us to systematically screen by immunochemical means for *in vivo* conditions, under which PPPK4 is targeted to peroxisomes. Identification of the substrates of PPPK4 can be addressed in a straight-forward approach because the expression profile of PPPK4 indicates its activity in senescent leaves (see chapter 3.3.2). Because the proteins to be phosphorylated by PPPK4 are located in the peroxisome matrix, leaf peroxisomes will be isolated from senescent leaves of the transgenic overexpression lines of c-myc-PPPK4 and directly be subjected to *in-gel* kinase assays.

4.2.4 New insights into the nature of auxiliary targeting enhancing and inhibitory elements of PTS1 domains

It was demonstrated that the C-terminal targeting domains of PPPK1, PPPK3, and PPPK7 failed to direct the reporter protein EYFP from the cytosol to peroxisomes, even though SKL> and SHL> are well-known PTS1 tripeptides (Mullen et al., 1997; Kragler et al., 1998), and AKI> is a single amino acid variant, for instance of the PTS1 peptides SKI> and AKL>. These results demonstrated that the seven to ten amino acid residues located immediately upstream of the PTS1 of these PPPKs determined non-peroxisomal targeting of EYFP and, most likely, of the full-length PPPKs *in vivo*. Non-peroxisomal targeting of EYFP-PTD_{PPPK1} was surprising in particular because SKL> is a major and the prototypical PTS1 peptide *per se* and has been reported to be sufficient to direct various reporter proteins to peroxisomes in diverse organisms (Mullen et al., 1997; Kragler et al., 1998).

The most likely explanation of this result is that native residues located upstream of SKL> in PPPK1 interfered with PTS1 peptide interaction with the onion ortholog of Pex5. A unique feature of PPPK1 was the presence of eight acidic residues closely upstream of SKL>, which contrasted the preference for additional basic residues in the targeting domain of PTS1 targeted plant peroxisomal proteins (Reumann, 2004). Indeed, deletion of these acidic residues from the C-terminal domain of PPPK1 directed EYFP from the cytosol to peroxisomes. In a reciprocal experiment it could be demonstrated that the exchange of four neutral residues against acidic residues in the C-terminal domain of HPR abolished peroxisomal targeting. These results demonstrate that an accumulation of acidic residues closely upstream of PTS1 peptides reduces and can even suppress targeting to peroxisomes not only in case of PTS1 peptides of weak peroxisome targeting efficiency but even for major PTS1 peptides like SKL>. Such an inhibitory function of acidic residues in PTS1 targeting domains had recently also been proposed from bioinformatics data (Reumann, 2004; Neuberger et al., 2003) but not been supported by experimental data for any organism. A more precise determination of the number of acidic residues that are required to suppress peroxisome targeting of different PTS1 peptides would be desirable to predict peroxisome targeting of unknown proteins with increased probability. A gradual distribution of a reporter protein between the cytosol and peroxisomes, however, cannot be quantified in plants.

When compared to the C-terminal domain of PPPK3, PPPK4 contained two additional arginine residues upstream of SHL>. Because the C-terminal domain of PPPK4, but not that of PPPK3, was sufficient to target EYFP to peroxisomes, it was hypothesized that targeting of a reporter protein to peroxisomes by SHL> relied on the presence of

additional basic residues acting as targeting enhancing elements in close proximity of SHL>. The fusion protein lacking both basic residues, namely EYFP-PTD Δ R_{PPPK4}, significantly reduces the peroxisomal targeting efficiency, and it was concluded that the two arginine residues in the C-terminal domain of PPPK4 served as important targeting enhancing elements. The dependence of peroxisome targeting by SHL> on the presence of auxiliary basic residues is consistent with the previous observation that SHL> was not found in any of about 400 plant sequences homologous to plant PTS1 proteins. Peroxisome targeting of a protein containing, for instance the PTS1 SKL>, apparently is only maintained, if two mutations occur at the same time: conversion of SKL> to SHL> by spontaneous point mutation and introduction of additional basic residues in front of SHL>. Such parallel but independent mutations, however, are very unlikely and, therefore, rare. The precise number of basic residues required for peroxisome targeting and their exact location in the C-terminal domain may be determined for SHL> as well as other minor PTS1 peptides in future studies.

4.2.5 The PTS1 AKI> of PPPK7 is non-functional

The protein kinase GPK1, which was identical to PPPK7 in our study, had been detected on 2-D gels of plant peroxisomes from *Arabidopsis* cotyledons, and peroxisomal targeting was further supported by immunochemical subfractionation studies (Fukao et al., 2003). Limited proteolytic digest experiments indicated that the kinase domain was facing the matrix side (Fukao et al., 2003), indicating that the kinase was imported into the matrix via one of the two general import pathways. The PTS1-like tripeptide AKI> of GPK1 further suggested protein targeting via the PTS1 pathway.

However, the tripeptide AKI> has not been reported to target a passenger protein to plant peroxisomes (Hayashi et al., 1997; Mullen et al., 1997; Kragler et al., 1998) nor been detected in a significant number of plant peroxisomal homologs of PTS1-targeted proteins (Reumann, 2004). The presence of three acidic residues and the lack of additional basic and proline residues in front of AKI> indicated the presence of targeting-inhibitory elements and further reduced the probability that this protein was targeted to plant peroxisomes by a PTS1 (Reumann, 2004, see also chapter 4.9).

We demonstrated that the C-terminal targeting domain of PPPK7 (GPK1, Fukao et al., 2003) failed to direct the reporter protein EYFP from the cytosol to peroxisomes (Fig. 3.20K). Consistent with this result, full-length PPPK7 did not interact with the TPR domain of

the cytosolic PTS1 receptor Pex5 (AtPex5-TPR) in yeast two-hybrid assays (Fig. 3.22). These results argued strongly against the idea that GPK1 was targeted to peroxisomes by AKI>. Further experimental studies are required to investigate if peroxisome targeting of GPK1 is mediated by unknown internal signals. Preliminary data according to which the full-length fusion protein EYFP-GPK1 accumulated near the nucleus (data not shown), did not support the presence of a yet unknown internal PTS in GPK1. More detailed studies are necessary to analyse for conformational changes that may alter surface-exposure of this putative internal PTS.

4.2.6 Do AtAtg1a and AtAtg13a play a role in pexophagy?

The protein kinase PPPK4 was shown to contain a functional PTS1 and is identical with Atg1a, which represents one of three plant homologs of the protein kinase Atg1 involved in auto- and pexophagy. In yeast Atg1 interacts with the regulatory subunit Atg13 (Kamada et al., 2000; Nair et al., 2005) and plays a role in switching between the cytosol-to-vacuole targeting pathway and the autophagy pathway (Klionsky, 2000; Nair and Klionsky, 2005). Under nutrient rich conditions, Atg13 is hyperphosphorylated by the so-called target-of-rapamycin (Tor) kinase, exhibits a reduced affinity for Atg1 and dissociates from the Atg1-Atg13 complex, which is thought to block autophagy (Klionsky, 2000). Under starvation conditions, Atg13 is largely dephosphorylated by a yet-to-be-identified phosphatase, and forms a complex with Atg1 (Klionsky, 2000). The association of these two proteins might trigger the switch from the cytosol-to-vacuole pathway to autophagy. Regarding selective peroxisome degradation, Atg1 is essential for pexophagy in yeast. Peroxisomes are dynamic organelles that possess strictly regulated mechanisms for their proliferation and degradation. The turnover of redundant, damaged, or non-functional peroxisomes by an autophagy-related pathway is referred to as pexophagy (Farre and Subramani, 2004). Atg1 was functional at the initiation stage of pexophagy because the sequestration event was blocked in a specific mutant of *Hansenula polymorpha* (Komduur et al., 2003; Fig. 1.3 and chapter 1.2.3).

In this study, we demonstrated that the putative PTS2 of AtAtg13a could not direct a reporter protein to peroxisomes, although the sequence surrounding the putative PTS2 showed additional properties that are conserved in PTS2-targeted plant proteins. In addition, the same PTS2 nonapeptide RLx₅HF was present in AtAcd31.2 and experimentally shown to

target AtAcd31.2 to peroxisomes *in vivo*. Even though the N-terminal domain had already been reduced to 60 and 120 residues, we cannot fully exclude that an unusual and artificial polypeptide folding affected subcellular targeting of these constructs. Also, if Atg13a does not possess a functional PTS, the protein can still be imported into the peroxisome matrix in a piggyback fashion by forming a complex with Atg1a in the cytosol (see below). To characterize the putative piggybacking import mechanism of AtAtg13a into peroxisomes, both *AtATG1a* and *AtATG13a* supplemented by appropriate tags can be co-expressed in a plant expression system.

We further showed by application of yeast two-hybrid assays that the C-terminal fragment of AtAtg1a (residues 415 to 623) interacted with an internal fragment of AtAtg13a (residues 340 to 500). A similar internal domain of the Atg13 homolog from *S. cerevisiae* (residues 343 to 520) had previously been shown to interact with Atg1 in the same experimental system (Kamada et al., 2000). However, in this study only the full-length Atg1 had been analyzed. Binding of AtAtg13a to AtAtg1a not via the kinase but the C-terminal domain appears probable as the kinase domain would still be accessible for interaction with the substrate protein to be phosphorylated. In summary, these data indicate that AtAtg1a and AtAtg13a form a functional complex *in vivo*. Considering the functional studies of the Atg1-Atg13 complex in yeast (Kamada et al., 2000), it is reasonable to hypothesize that AtAtg13a activates AtAtg1a by protein-protein interaction and thereby induces autophagy in plants.

Interestingly, a splice variant of AtAtg1a lacking a C-terminal fragment (amino acid residues 522-565) of the full-length protein has been identified recently in an update of gene annotation of the *Arabidopsis* genome sequence. Likewise, AtAtg1c is also reported to produce two different splice variants. Expression analyses at the protein level using an AtAtg1a-specific antiserum will allow us to investigate, in which tissue and under which stress conditions the splice variants of AtAtg1a are produced. For the production of polyclonal antisera, an internal hydrophilic fragment of AtAtg1a (residues 268-461) has been transferred into the prokaryotic expression vector pQE30. Because the splice variation lies in the C-terminal domain of AtAtg1a, it will be interesting to investigate in more detail whether the presence of this domain affects protein-protein interaction with AtAtg13a.

To selectively degrade peroxisomes, the organelles must be specifically labelled for recognition by the autophagic degradation machinery (Leao and Kiel, 2003). In *pex14* mutants of *H. polymorpha*, glucose-induced selective degradation of peroxisomal remnants

was prohibited (Veenhuis et al., 1996). No other peroxins have been found to be involved in peroxisome degradation. In a follow-up study, it has been demonstrated that the N-terminus of Pex14 was essential for macropexophagy because short deletions (31 and 64 amino acid residues) of the N-terminus of Pex14 abolished peroxisome degradation in *H. polymorpha*. These data show that the peroxisome biogenesis protein Pex14 is not only involved in matrix protein import (see chapter 1.2.2) but also an important player in switching between peroxisome biogenesis and degradation.

Pex14 of *H. polymorpha* is phosphorylated, as demonstrated by *in vivo* labelling with radiolabelled phosphate (Komori et al., 1999, 2000). By overexpression of truncated forms of Pex14 in the *pex14* deletion strain of *H. polymorpha*, Komori and Veenhuis (2000) narrowed down the phosphorylation site to the C-terminal 58 residues. Phosphorylation of Pex14 may alter the conformation of the integral membrane protein and represent a mechanism of signal transduction to label non-functional peroxisomes specifically for degradation (Bellu et al., 2001). Because the membrane topology of Pex14 has not been fully elucidated, the orientation of the phosphorylation site towards the cytosol or the peroxisomal matrix is not known. If the phosphorylation site of Pex14 faces the matrix, Atg1 may be a candidate kinase for the phosphorylation of Pex14.

Autophagy is a ubiquitous degradation mechanism also in plants (Thompson and Vierstra, 2005). Whether non-functional or redundant plant peroxisomes can be removed or recycled by pexophagy is not clear (Thompson and Vierstra, 2004). Studies have been initiated in the course of this thesis to study pexophagy in both tobacco BY-2 suspension-cultured cells and *Arabidopsis* plants by expressing EYFP-SKL> constitutively in these plants in order to monitor peroxisome degradation by fluorescence and electron microscopy. To investigate if AtAtg1a is involved in the pexophagy, we have introduced EYFP-SKL> into *atg1a* T-DNA knock-out and wild-type plants for comparative analysis. These transgenic lines are expected to become important tools in the future to investigate under which conditions pexophagy is induced in plants and how Atg1a is involved in plant autophagy and pexophagy.

5. SUMMARY

This Ph.D. thesis presents molecular analyses of two putative small heat shock proteins (sHsps) from plant peroxisomes and the identification of matrix-targeted protein kinases:

1. The cDNAs of two sHsps, namely *AtHSP15.7* (At5g37670) and *AtACD31.2* (At1g06460), with putative peroxisomal targeting signals type 1 (PTS1) and type 2 (PTS2), were cloned by RT-PCR, and targeting to peroxisomes was demonstrated for fusion proteins with enhanced yellow fluorescent protein (EYFP) in onion (*Allium cepa* L.) epidermal cells in double labelling experiments.
2. Peroxisomal localization of *AtHsp15.7* was confirmed by isolation of leaf peroxisomes from an *Arabidopsis* line overexpressing *35S:AtHSP15.7* and immunodetection. The data obtained by these two independent methods demonstrated for the first time that sHsps are located in the peroxisome matrix in any organism.
3. *AtHsp15.7* and *AtAcd31.2* are targeted to the peroxisome matrix by a functional PTS1 (SKL>) and a functional PTS2 (RLx₅HF), as revealed by targeting studies of fusion proteins with single amino acid exchanges or deletions.
4. *AtHsp15.7* and *AtAcd31.2* acted as molecular chaperones when heterologously expressed in yeast and directed to the cytosol by deletion of the PTSs. Both sHsps complemented the morphological phenotype of yeast mutants deficient in endogenous cytosolic sHsps.
5. Expression studies by RT-PCR demonstrated that *AtACD31.2* is constitutively expressed, whereas *AtHSP15.7* is induced by heat and chemical-induced oxidative stress.
6. *Arabidopsis* T-DNA insertion lines were isolated for both sHsps and a double mutant was created. The T-DNA insertion mutant *hsp15.7-3* exhibited a germination defect under heat stress, indicating a role of *AtHsp15.7* in protecting peroxisomal proteins from aggregation during seed germination.
7. Four cDNAs encoding putative protein kinases of peroxisomes (PPPKs) were cloned by RT-PCR; two cDNAs were obtained from a cDNA stock center.
8. Subcellular targeting studies in yeast and onion cells provided discrepant results. To investigate interaction between the PTS1 domains of PPPKs with plant Pex5 independent of polypeptide folding, the polypeptide of PPPKs in the fusion proteins was shor-

tened to the C-terminal domain comprising ten amino acid residues. Four PPPKs contained a functional PTS1 domain that was sufficient to direct EYFP to plant peroxisomes.

9. Based on the analysis of deletion constructs and mutagenized PTS1 targeting domains, basic residues located upstream of the PTS1 could be defined as targeting enhancing elements for SHL>. By contrast, acidic residues were defined as targeting inhibitory elements that were, for the first time, shown to prevent targeting of a reporter protein to peroxisomes by the strong and prototypical PTS1 tripeptide SKL>.
10. A T-DNA insertion line deficient in the expression of *PPPK4* (*AtATG1a*), an *Arabidopsis* homolog of the protein kinase Atg1 involved in auto- and pexophagy in yeast and mammals, was isolated. *Arabidopsis* lines overexpressing 35S:*EYFP-SKL* were generated in this mutant background as well as in wild-type plants which will allow future studies of plant auto- and pexophagy in plants.
11. The cDNA of a possible regulatory subunit of AtAtg1, namely AtAtg13a, was cloned by RT-PCR and its subcellular targeting investigated in plant cells. In yeast two-hybrid analyses, the proteins were shown to interact with each other. These results suggest that the protein kinase AtAtg1a forms an activation complex with Atg13a *in vivo* and is involved in reversible phosphorylation of peroxisomal matrix proteins and/or plant autophagy, a hypothesis to be tested in the near future.

6. REFERENCE

- Adham AR, Zolman BK, Millius A, Bartel B.** Mutations in *Arabidopsis* acyl-CoA oxidase genes reveal distinct and overlapping roles in beta-oxidation. *Plant J.* 2005 Mar; 41(6):859-74
- Albertini M, Rehling P, Erdmann R, Girzalsky W, Kiel JA, Veenhuis M, Kunau WH.** Pex14p, a peroxisomal membrane protein binding both receptors of the two PTS-dependent import pathways. *Cell.* 1997 Apr 4;89(1):83-92
- Amery L, Franssen M, De Nys K, Mannaerts GP, Van Veldhoven PP.** Mitochondrial and peroxisomal targeting of 2-methylacyl-CoA racemase in humans. *J Lipid Res.* 2000 Nov;41(11):1752-9.
- Ano Y, Hattori T, Oku M, Mukaiyama H, Baba M, Ohsumi Y, Kato N, Sakai Y.** A sorting nexin PpAtg24 regulates vacuolar membrane dynamics during pexophagy via binding to phosphatidylinositol-3-phosphate. *Mol Biol Cell.* 2005 Feb; 16(2):446-57
- Baker A, Sparkes IA.** Peroxisome protein import: some answers, more questions. *Curr Opin Plant Biol.* 2005 Dec; 8(6):640-7
- Barroso, J.B., Corpas, F.J., Carreras, A., Sandalio, L.M., Valderrama, R., Palma, J.M., Lupianez, J.A. and del Río, L.A.** Localization of nitric-oxide synthase in plant peroxisomes. *J. Biol. Chem.* 1999; **274**: 36729–36733
- Beevers H.** Microbodies in higher plants. *Annu Rev Plant Physiol* 1979; 30:159-193
- Bellafiore S, Barneche F, Peltier G, Rochaix JD.** State transitions and light adaptation require chloroplast thylakoid protein kinase STN7. *Nature.* 2005 Feb 24;433(7028):892-5
- Beyer W, Imlay J, Fridovich I.** Superoxide dismutases. *Prog Nucleic Acid Res Mol Biol* 1991, 40: 221–253
- Bi YM, Kenton P, Mur L, Darby R, Draper J.** Hydrogen peroxide does not function downstream of salicylic acid in the induction of PR protein expression. *Plant J.* 1995 Aug;8(2):235-45
- Boston RS, Viitanen PV, Vierling E.** Molecular chaperones and protein folding in plants. *Plant Mol Biol.* 1996 Oct; 32(1-2):191-222. Review.
- Bueno P, Varela J, Gimenez-Gallego G, del Rio LA.** Peroxisomal copper, zinc superoxide dismutase. Characterization of the isoenzyme from watermelon cotyledons. *Plant Physiol.* 1995 Jul; 108(3):1151-60
- Candido EP.** The small heat shock proteins of the nematode *Caenorhabditis elegans*: structure, regulation and biology. *Prog Mol Subcell Biol.* 2002; 28:61-78. Review.
- Cashikar AG, Duennwald M, Lindquist SL.** A chaperone pathway in protein disaggregation. Hsp26 alters the nature of protein aggregates to facilitate reactivation by Hsp104. *J Biol Chem.* 2005 Jun 24; 280(25):23869-75
- Chang CC, Warren DS, Sacksteder KA, Gould SJ.** PEX12 interacts with PEX5 and PEX10 and acts downstream of receptor docking in peroxisomal matrix protein import. *J Cell Biol.* 1999 Nov 15; 147(4):761-74
- Chehab EW, Patharkar OR, Hegeman AD, Taybi T, Cushman JC.** Autophosphorylation and subcellular localization dynamics of a salt- and water deficit-induced calcium-dependent protein kinase from ice plant. *Plant Physiol.* 2004 Jul; 135(3):1430-46
- Chew O, Whelan J, Millar AH.** Molecular definition of the ascorbate-glutathione cycle in *Arabidopsis* mitochondria reveals dual targeting of antioxidant defenses in plants. *J Biol Chem.* 2003 Nov 21; 278(47):46869-77
- Chu CC, Lee WC, Guo WY, Pan SM, Chen LJ, Li HM, Jinn TL.** A copper chaperone for superoxide dismutase that confers three types of copper/zinc superoxide dismutase activity in *Arabidopsis*. *Plant Physiol.* 2005 Sep; 139(1):425-36
- Clough SJ, Bent AF.** Floral dip: a simplified method for *Agrobacterium*-mediated transformation of *Arabidopsis thaliana*. *Plant J.* 1998 Dec; 16(6):735-43
- Crookes WJ, Olsen LJ.** The effects of chaperones and the influence of protein assembly on peroxisomal protein import. *J Biol Chem.* 1998 Jul 3; 273(27):17236-42.

- Dalla Serra M, Menestrina G.** Liposomes in the study of pore-forming toxins. *Methods Enzymol.* 2003;372:99-124
- Dammai V, Subramani S.** The human peroxisomal targeting signal receptor, Pex5p, is translocated into the peroxisomal matrix and recycled to the cytosol. *Cell.* 2001 Apr 20; 105(2):187-96
- Dammann C, Ichida A, Hong B, Romanowsky SM, Hrabak EM, Harmon AC, Pickard BG, Harper JF.** Subcellular targeting of nine calcium-dependent protein kinase isoforms from *Arabidopsis*. *Plant Physiol.* 2003 Aug; 132(4):1840-8
- De Jong, W.W., Caspers, G.J. and Leunissen, J.A.** Genealogy of the alpha-crystallin--small heat-shock protein superfamily. *Int. J. Biol. Macromol.*, 1998 May-Jun; 22: 151-162
- de Felipe, M.R., Lucas, M.M. and Pozuelo, J.M.** Cytochemical study of catalase and peroxidase in the mesophyll of *Lolium rigidum* plants treated with isoproturon. *J. Plant Physiol.* 1988; 132: 67-73
- del Rio LA, Corpas FJ, Sandalio LM, Palma JM, Gomez M, Barroso JB.** Reactive oxygen species, antioxidant systems and nitric oxide in peroxisomes. *J Exp Bot.* 2002 May; 53(372):1255-72
- del Rio LA, Corpas FJ, Sandalio LM, Palma JM, Barroso JB.** Plant peroxisomes, reactive oxygen metabolism and nitric oxide. *IUBMB Life.* 2003 Feb; 55(2):71-81
- del Río, L.A., Pastori, G.M., Palma, J.M., Sandalio, L.M., Sevilla, F., Corpas, F.J., Jimenez, A., Lopez Huertas, E. and Hernandez, J.** The activated oxygen role of peroxisomes in senescence. *Plant Physiol.* 1998; 116: 1195-1200
- Depege N, Bellafiore S, Rochaix JD.** Role of chloroplast protein kinase Stt7 in LHCII phosphorylation and state transition in *Chlamydomonas*. *Science.* 2003 Mar 7; 299(5612):1572-5
- Diefenbach J, Kindl H.** The membrane-bound DnaJ protein located at the cytosolic site of glyoxysomes specifically binds the cytosolic isoform 1 of Hsp70 but not other Hsp70 species. *Eur J Biochem.* 2000 Feb; 267(3):746-54
- Dotd G, Braverman N, Wong C, Moser A, Moser HW, Watkins P, Valle D, Gould SJ.** Mutations in the PTS1 receptor gene, PXR1, define complementation group 2 of the peroxisome biogenesis disorders. *Nat Genet.* 1995 Feb; 9(2):115-25
- Dotd G, Gould SJ.** Multiple PEX genes are required for proper subcellular distribution and stability of Pex5p, the PTS1 receptor: evidence that PTS1 protein import is mediated by a cycling receptor. *J Cell Biol.* 1996 Dec;135(6 Pt 2):1763-74
- Doelling JH, Walker JM, Friedman EM, Thompson AR, Vierstra RD.** The APG8/12-activating enzyme APG7 is required for proper nutrient recycling and senescence in *Arabidopsis thaliana*. *J Biol Chem.* 2002 Sep 6; 277(36):33105-14
- Douce R, Heldt HW** (2000) Photorespiration. In *Photosynthesis: Physiology and metabolism*, pp 115-136. Eds: Leegood RC, Sharkey RD, von Cammerer S. Kluwer Academic Publishers, Dordrecht, The Netherlands
- Eckert JH, Erdmann R.** Peroxisome biogenesis. *Rev Physiol Biochem Pharmacol.* 2003;147:75-121
- Ehrnsperger M, Graber S, Gaestel M, Buchner J.** Binding of non-native protein to Hsp25 during heat shock creates a reservoir of folding intermediates for reactivation. *EMBO J.* 1997 Jan 15;16(2):221-9
- Ehrnsperger M, Lilie H, Gaestel M, Buchner J.** The dynamics of Hsp25 quaternary structure. Structure and function of different oligomeric species. *J Biol Chem.* 1999 May 21; 274(21):14867-74
- Einwachter H, Sowinski S, Kunau WH, Schliebs W.** *Yarrowia lipolytica* Pex20p, *Saccharomyces cerevisiae* Pex18p/Pex21p and mammalian Pex5pL fulfil a common function in the early steps of the peroxisomal PTS2 import pathway. *EMBO Rep.* 2001 Nov; 2(11):1035-9
- Elgersma Y, Vos A, van den Berg M, van Roermund CW, van der Sluijs P, Distel B, Tabak HF.** Analysis of the carboxyl-terminal peroxisomal targeting signal 1 in a homologous context in *Saccharomyces cerevisiae*. *J Biol Chem.* 1996 Oct 18; 271(42):26375-82

- Erdmann R, Schliebs W.** Peroxisomal matrix protein import: the transient pore model. *Nat Rev Mol Cell Biol.* 2005 Sep; 6(9):738-42
- Fan J, Quan S, Orth T, Awai C, Chory J, Hu J.** The *Arabidopsis* PEX12 gene is required for peroxisome biogenesis and is essential for development. *Plant Physiol.* 2005 Sep; 139(1):231-9
- Farre JC, Subramani S.** Peroxisome turnover by micropexophagy: an autophagy-related process. *Trends Cell Biol.* 2004 Sep; 14(9):515-23. Review.
- Flynn CR, Mullen RT, Trelease RN.** Mutational analyses of a type 2 peroxisomal targeting signal that is capable of directing oligomeric protein import into tobacco BY-2 glyoxysomes. *Plant J.* 1998 Dec; 16(6):709-20
- Footitt S, Slo SP, combeLarner V, Kurup S, Wu Y, Larson T, Graham I, Baker A, Holdsworth M.** Control of germination and lipid mobilization by COMATOSE, the *Arabidopsis* homologue of human ALDP. *EMBO J.* 2002 Jun 17; 21(12):2912-22
- Fransen M, Brees C, Baumgart E, Vanhooren JC, Baes M, Mannaerts GP, Van Veldhoven PP.** Identification and characterization of the putative human peroxisomal C-terminal targeting signal import receptor. *J Biol Chem.* 1995 Mar 31; 270(13):7731-6
- Fulda M, Schnurr J, Abbadì A, Heinz E, Browse J.** Peroxisomal Acyl-CoA synthetase activity is essential for seedling development in *Arabidopsis thaliana*. *Plant Cell.* 2004 Feb; 16(2):394-405
- Fulda M, Shockey J, Werber M, Wolter FP, Heinz E.** Two long-chain acyl-CoA synthetases from *Arabidopsis thaliana* involved in peroxisomal fatty acid beta-oxidation. *Plant J.* 2002 Oct; 32(1):93-103
- Fulgosi H, Soll J.** The chloroplast protein import receptors Toc34 and Toc159 are phosphorylated by distinct protein kinases. *J Biol Chem.* 2002 Mar 15; 277(11):8934-40
- Fukao Y, Hayashi M, Hara-Nishimura I, Nishimura M.** Novel glyoxysomal protein kinase, GPK1, identified by proteomic analysis of glyoxysomes in etiolated cotyledons of *Arabidopsis thaliana*. *Plant Cell Physiol.* 2003 Oct; 44(10):1002-12
- Fukao Y, Hayashi M, Nishimura M.** Proteomic analysis of leaf peroxisomal proteins in greening cotyledons of *Arabidopsis thaliana*. *Plant Cell Physiol.* 2002 Jul; 43(7):689-96
- Gatto GJ Jr, Geisbrecht BV, Gould SJ, Berg JM.** Peroxisomal targeting signal-1 recognition by the TPR domains of human PEX5. *Nat Struct Biol.* 2000 Dec; 7(12):1091-5
- Germain V, Rylott EL, Larson TR, Sherson SM, Bechtold N, Carde JP, Bryce JH, Graham IA, Smith SM.** Requirement for 3-ketoacyl-CoA thiolase-2 in peroxisome development, fatty acid beta-oxidation and breakdown of triacylglycerol in lipid bodies of *Arabidopsis* seedlings. *Plant J.* 2001 Oct; 28(1):1-12
- Giese KC, Vierling E.** Changes in oligomerization are essential for the chaperone activity of a small heat shock protein *in vivo* and *in vitro*. *J Biol Chem.* 2002 Nov 29; 277(48):46310-8
- Gietl C.** Glyoxysomal malate dehydrogenase from watermelon is synthesized with an amino-terminal transit peptide. *Proc Natl Acad Sci U S A.* 1990 Aug; 87(15):5773-7
- Glover JR, Andrews DW, Subramani S, Rachubinski RA.** Mutagenesis of the amino targeting signal of *Saccharomyces cerevisiae* 3-ketoacyl-CoA thiolase reveals conserved amino acids required for import into peroxisomes *in vivo*. *J Biol Chem.* 1994 Mar 11; 269(10):7558-63
- Goepfert S, Vidoudez C, Rezzonico E, Hiltunen JK, Poirier Y.** Molecular identification and characterization of the *Arabidopsis* delta(3,5),delta(2,4)-dienoyl-coenzyme A isomerase, a peroxisomal enzyme participating in the beta-oxidation cycle of unsaturated fatty acids. *Plant Physiol.* 2005 Aug; 138(4):1947-56
- Gouaux E.** Channel-forming toxins: tales of transformation. *Curr Opin Struct Biol.* 1997 Aug; 7(4):566-73
- Gould SJ, Collins CS.** Opinion: peroxisomal-protein import: is it really that complex? *Nat Rev Mol Cell Biol.* 2002 May; 3(5):382-9
- Gould SJ, Keller GA, Hosken N, Wilkinson J, Subramani S.** A conserved tripeptide sorts proteins to peroxisomes. *J Cell Biol.* 1989 May; 108(5):1657-64

- Graham IA and Eastmond PJ.** Pathways of straight and branched chain fatty acid catabolism in higher plants. *Prog. Lipid Res.* 2002; 41:156–181
- Grotjohann N, Janning A, Eising R.** *In vitro* photoinactivation of catalase isoforms from cotyledons of sunflower (*Helianthus annuus* L.). *Arch Biochem Biophys.* 1997 Oct 15; 346(2):208-18
- Guan J, Stromhaug PE, George MD, Habibzadegah-Tari P, Bevan A, Dunn WA Jr, Klionsky DJ.** Cvt18/Gsa12 is required for cytoplasm-to-vacuole transport, pexophagy, and autophagy in *Saccharomyces cerevisiae* and *Pichia pastoris*. *Mol Biol Cell.* 2001 Dec;12(12):3821-38
- Gustavsson N, Kokke BP, Anzelius B, Boelens WC, Sundby C.** Substitution of conserved methionines by leucines in chloroplast small heat shock protein results in loss of redox-response but retained chaperone-like activity. *Protein Sci.* 2001 Sep; 10(9):1785-93
- Hamilton EW, Heckathorn SA.** Mitochondrial adaptations to NaCl. Complex I is protected by anti-oxidants and small heat shock proteins, whereas complex II is protected by proline and betaine. *Plant Physiol.* 2001 Jul;126(3):1266-74
- Hanaoka H, Noda T, Shirano Y, Kato T, Hayashi H, Shibata D, Tabata S, Ohsumi Y.** Leaf senescence and starvation-induced chlorosis are accelerated by the disruption of an *Arabidopsis* autophagy gene. *Plant Physiol.* 2002 Jul; 129(3):1181-93
- Hanks SK, Hunter T.** Protein kinases 6. The eukaryotic protein kinase superfamily: kinase (catalytic) domain structure and classification. *FASEB J.* 1995 May;9(8):576-96
- Hardie DG.** Plant protein serine/threonine kinases: Classification and Functions. *Annu Rev Plant Physiol Plant Mol Biol.* 1999 Jun; 50:97-131
- Hartl FU.** Molecular chaperones in cellular protein folding. *Nature.* 1996 Jun 13; 381(6583):571-9. Review.
- Haslbeck M.** sHsps and their role in the chaperone network. *Cell Mol Life Sci.* 2002 Oct; 59(10):1649-57
- Haslbeck M, Braun N, Stromer T, Richter B, Model N, Weinkauff S, Buchner J.** Hsp42 is the general small heat shock protein in the cytosol of *Saccharomyces cerevisiae*. *EMBO J.* 2004 Feb 11;23(3):638-49
- Haslbeck M, Miess A, Stromer T, Walter S, Buchner J.** Disassembling protein aggregates in the yeast cytosol. The cooperation of Hsp26 with Ssa1 and Hsp104. *J Biol Chem.* 2005 Jun 24; 280(25):23861-8
- Haslbeck M, Walke S, Stromer T, Ehrnsperger M, White HE, Chen S, Saibil HR, Buchner J.** Hsp26: a temperature-regulated chaperone. *EMBO J.* 1999 Dec 1; 18(23):6744-51.
- Hayashi M, Aoki M, Kondo M, Nishimura M.** Transport of chimeric proteins that contain a carboxy-terminal targeting signal into plant microbodies. *Plant J.* 1996 Aug; 10(2):225-34
- Hayashi M, Aoki M, Kondo M, Nishimura M.** Changes in targeting efficiencies of proteins to plant microbodies caused by amino acid substitutions in the carboxy-terminal tripeptide. *Plant Cell Physiol.* 1997 Jun; 38(6):759-68
- Hayashi M, Nito K, Takei-Hoshi R, Yagi M, Kondo M, Suenaga A, Yamaya T, Nishimura M.** Ped3p is a peroxisomal ATP-binding cassette transporter that might supply substrates for fatty acid beta-oxidation. *Plant Cell Physiol.* 2002 Jan; 43(1):1-11
- Hayashi M, Nishimura M.** Entering a new era of research on plant peroxisomes. *Curr Opin Plant Biol.* 2003 Dec; 6(6):577-82. Review.
- Hayashi M, Toriyama K, Kondo M, Nishimura M.** 2, 4-Dichlorophenoxybutyric acid-resistant mutants of *Arabidopsis* have defects in glyoxysomal fatty acid beta-oxidation. *Plant Cell.* 1998 Feb; 10(2):183-95
- Hayashi M, Yagai M, Nito K, Kamada T, Nishimura M.** Differential contribution of two peroxisomal protein receptors to the maintenance of peroxisomal functions in *Arabidopsis*. *J Biol Chem.* 2005 Apr 15; 280(15):14829-35
- Heazlewood JL, Millar AH.** AMPDB: the *Arabidopsis* Mitochondrial Protein Database. *Nucleic Acids Res.* 2005 Jan 1; 33(Database issue):D605-10
- Heazlewood JL, Tonti-Filippini JS, Gout AM, Day DA, Whelan J, Millar AH.** Experimental analysis of the *Arabidopsis* mitochondrial proteome highlights signaling and regulatory

- components, provides assessment of targeting prediction programs, and indicates plant-specific mitochondrial proteins. *Plant Cell*. 2004 Jan; 16(1):241-56
- Hershko A, Ciechanover A.** The ubiquitin system. *Annu Rev Biochem*. 1998;67:425-79
- Hettema EH, Ruigrok CC, Koerkamp MG, van den Berg M, Tabak HF, Distel B, Braakman I.** The cytosolic DnaJ-like protein djp1p is involved specifically in peroxisomal protein import. *J Cell Biol*. 1998 Jul 27; 142(2):421-34.
- Hertwig B, Streb P, Feierabend J.** Light dependence of catalase synthesis and degradation in leaves and the influence of interfering stress conditions. *Plant Physiol*. 1992;100: 1547-1553
- Horling, F. Baier, M. and Dietz, K.-J.** Redox-regulation of the expression of the peroxide-detoxifying chloroplast 2-Cys peroxiredoxin in the liverwort *Riccia fluitans*. *Planta* 2001; 214: 304–313
- Hong SW, Jon JH, Kwak JM, Nam HG.** Identification of a receptor-like protein kinase gene rapidly induced by abscisic acid, dehydration, high salt, and cold treatments in *Arabidopsis thaliana*. *Plant Physiol*. 1997 Apr;113(4):1203-12
- Hooks M (2002)** Molecular biology, enzymology, and physiology of beta-oxidation In: *Plant Peroxisomes: Biochemistry, Cell Biology and Biotechnological Applications*, pp 19-55. Eds Baker A, Graham IA. Kluwer Academic Publishers, Dordrecht, The Netherlands
- Horwitz J.** Alpha-crystallin can function as a molecular chaperone. *Proc Natl Acad Sci U S A*. 1992 Nov 1;89(21):10449-53.
- Hrabak EM, Chan CW, Gribskov M, Harper JF, Choi JH, Halford N, Kudla J, Luan S, Nimmo HG, Sussman MR, Thomas M, Walker-Simmons K, Zhu JK, Harmon AC.** The *Arabidopsis* CDPK-SnRK superfamily of protein kinases. *Plant Physiol*. 2003 Jun; 132(2):666-80
- Huber PA, Birdsey GM, Lumb MJ, Prowse DT, Perkins TJ, Knight DR, Danpure CJ.** Peroxisomal import of human alanine: glyoxylate aminotransferase requires ancillary targeting information remote from its C terminus. *J Biol Chem*. 2005 Jul 22; 280(29):27111-20
- Hu J, Aguirre M, Peto C, Alonso J, Ecker J, Chory J.** A role for peroxisomes in photomorphogenesis and development of *Arabidopsis*. *Science*. 2002 Jul 19; 297(5580):405-9
- Hutchins MU, Veenhuis M, Klionsky DJ.** Peroxisome degradation in *Saccharomyces cerevisiae* is dependent on machinery of macroautophagy and the Cvt pathway. *J Cell Sci*. 1999 Nov;112 (Pt 22):4079-87
- Igarashi D, Miwa T, Seki M, Kobayashi M, Kato T, Tabata S, Shinozaki K, Ohsumi C.** Identification of photorespiratory glutamate:glyoxylate aminotransferase (GGAT) gene in *Arabidopsis*. *Plant J*. 2003 Mar; 33(6):975-87
- Inoue H, Nojima H, Okayama H.** High efficiency transformation of *Escherichia coli* with plasmids. *Gene*. 1990 Nov 30;96(1):23-8
- Ishikawa T, Yoshimura K, Sakai K, Tamoi M, Takeda T, Shigeoka S.** Molecular characterization and physiological role of glyoxysome-bound ascorbate peroxidase from spinach. *Plant and Cell Physiology* 1998; 39: 23–34
- Jakob U, Gaestel M, Engel K, Buchner J.** Small heat shock proteins are molecular chaperones. *J Biol Chem*. 1993 Jan 25;268(3):1517-20
- Jimenez A, Hernandez JA, Del Rio LA, Sevilla F.** Evidence for the presence of the ascorbate-glutathione cycle in mitochondria and peroxisomes of pea leaves. *Plant Physiol*. 1997 May; 114(1):275-284
- Jofre A, Molinas M, Pla M.** A 10-kDa class-C1 sHsp protects *E. coli* from oxidative and high-temperature stress. *Planta*. 2003 Sep; 217(5):813-9
- Johnson TL, Olsen LJ.** Building new models for peroxisome biogenesis. *Plant Physiol*. 2001 Nov; 127(3):731-9
- Kamada Y, Funakoshi T, Shintani T, Nagano K, Ohsumi M, Ohsumi Y.** Tor-mediated induction of autophagy via an Apg1 protein kinase complex. *J Cell Biol*. 2000 Sep 18;150(6):1507-13
- Kamigaki A, Mano S, Terauchi K, Nishi Y, Tachibe-Kinoshita Y, Nito K, Kondo M, Hayashi M, Nishimura M, Esaka M.** Identification of peroxisomal targeting signal of

- pumpkin catalase and the binding analysis with PTS1 receptor. *Plant J.* 2003 Jan;33(1):161-75
- Kappe G, Franck E, Verschuure P, Boelens WC, Leunissen JA, de Jong WW.** The human genome encodes 10 alpha-crystallin-related small heat shock proteins: HspB1-10. *Cell Stress Chaperones.* 2003; 8(1):53-61
- Kato A, Hayashi M, Kondo M, Nishimura M.** Targeting and processing of a chimeric protein with the N-terminal presequence of the precursor to glyoxysomal citrate synthase. *Plant Cell.* 1996 Sep;8(9):1601-11
- Kato A, Takeda-Yoshikawa Y, Hayashi M, Kondo M, Hara-Nishimura I, Nishimura M.** Glyoxysomal malate dehydrogenase in pumpkin: cloning of a cDNA and functional analysis of its presequence. *Plant Cell Physiol.* 1998 Feb;39(2):186-95
- Kendall, A.C., Keys, A.J., Turner, J.C., Lea, P.J. and Mifflin, B.J.** (1983) The isolation and characterization of a catalase-deficient mutant of barley (*Hordeum vulgare*). *Planta*, **159**, 505–511
- Kennaway CK, Benesch JL, Gohlke U, Wang L, Robinson CV, Orlova EV, Saibi HR, Keep NH.** Dodecameric structure of the small heat shock protein Acr1 from *Mycobacterium tuberculosis*. *J Biol Chem.* 2005 Sep 30;280(39):33419-25
- Kerk D, Bulgrien J, Smith DW, Gribskov M.** Arabidopsis proteins containing similarity to the universal stress protein domain of bacteria. *Plant Physiol.* 2003 Mar;131(3):1209-19
- Kim J, Huang WP, Stromhaug PE, Klionsky DJ.** Convergence of multiple autophagy and cytoplasm to vacuole targeting components to a perivacuolar membrane compartment prior to *de novo* vesicle formation. *J Biol Chem.* 2002 Jan 4;277(1):763-73
- Kim R, Kim KK, Yokota H, Kim SH.** Small heat shock protein of *Methanococcus jannaschii*, a hyperthermophile. *Proc Natl Acad Sci U S A.* 1998 Aug 4;95(16):9129-33
- Kim J, Klionsky DJ.** Autophagy, cytoplasm-to-vacuole targeting pathway, and pexophagy in yeast and mammalian cells. *Annu Rev Biochem.* 2000; 69:303-42. Review.
- Kirschner M, Winkelhaus S, Thierfelder JM, Nover L.** Transient expression and heat-stress-induced co-aggregation of endogenous and heterologous small heat-stress proteins in tobacco protoplasts. *Plant J.* 2000 Nov;24(3):397-411.
- Kleffmann T, Russenberger D, von Zychlinski A, Christopher W, Sjolander K, Gruissem W, Baginsky S.** The *Arabidopsis thaliana* chloroplast proteome reveals pathway abundance and novel protein functions. *Curr Biol.* 2004 Mar 9; 14(5):354-62
- Kliebenstein DJ, Monde RA, Last RL.** Superoxide dismutase in *Arabidopsis*: an eclectic enzyme family with disparate regulation and protein localization. *Plant Physiol* 1998; 118: 637–650
- Klionsky DJ.** The molecular machinery of autophagy: unanswered questions. *J Cell Sci.* 2005 Jan 1;118(Pt 1):7-18
- Komduur JA, Veenhuis M, Kiel JA.** The *Hansenula polymorpha* PDD7 gene is essential for macropexophagy and microautophagy. *FEMS Yeast Res.* 2003 Mar;3(1):27-34
- Kotti TJ, Savolainen K, Helander HM, Yagi A, Novikov DK, Kalkkinen N, Conzelmann E, Hiltunen JK, Schmitz W.** In mouse alpha -methylacyl-CoA racemase, the same gene product is simultaneously located in mitochondria and peroxisomes. *J Biol Chem.* 2000 Jul 7; 275(27):20887-95
- Kragler F, Lametschwandtner G, Christmann J, Hartig A, Harada JJ.** Identification and analysis of the plant peroxisomal targeting signal 1 receptor NtPEX5. *Proc Natl Acad Sci U S A.* 1998 Oct 27; 95(22):13336-41
- Krishna P, Gloor G.** The Hsp90 family of proteins in *Arabidopsis thaliana*. *Cell Stress Chaperones.* 2001 Jul; 6(3):238-46
- Krysan PJ, Young JC, Sussman MR.** T-DNA as an insertional mutagen in *Arabidopsis*. *Plant Cell.* 1999 Dec;11(12):2283-90
- Lametschwandtner G, Brocard C, Fransen M, Van Veldhoven P, Berger J, Hartig A.** The difference in recognition of terminal tripeptides as peroxisomal targeting signal 1 between yeast and human is due to different affinities of their receptor Pex5p to the cognate signal and to residues adjacent to it. *J Biol Chem.* 1998 Dec 11; 273(50):33635-43

- Larkindale J, Hall JD, Knight MR, Vierling E.** Heat stress phenotypes of *Arabidopsis* mutants implicate multiple signaling pathways in the acquisition of thermotolerance. *Plant Physiol.* 2005 Jun; 138(2):882-97
- Lazarow PB, Fujiki Y.** Biogenesis of peroxisomes. *Annu Rev Cell Biol.* 1985 1:489-530
- Leao AN, Kiel JA.** Peroxisome homeostasis in *Hansenula polymorpha*. *FEMS Yeast Res.* 2003 Nov; 4(2):131-9
- Lee GJ, Pokala N, Vierling E.** Structure and *in vitro* molecular chaperone activity of cytosolic small heat shock proteins from pea. *J Biol Chem.* 1995 May 5; 270(18):10432-8
- Lee GJ, Roseman AM, Saibil HR, Vierling E.** A small heat shock protein stably binds heat-denatured model substrates and can maintain a substrate in a folding-competent state. *EMBO J.* 1997 Feb 3; 16(3):659-71
- Lee GJ, Vierling E.** A small heat shock protein cooperates with heat shock protein 70 systems to reactivate a heat-denatured protein. *Plant Physiol.* 2000 Jan; 122(1):189-98
- Lee MS, Mullen RT, Trelease RN.** Oilseed isocitrate lyases lacking their essential type 1 peroxisomal targeting signal are piggybacked to glyoxysomes. *Plant Cell.* 1997 Feb; 9(2):185-97.
- Lin BL, Wang JS, Liu HC, Chen RW, Meyer Y, Barakat A, Delseny M.** Genomic analysis of the Hsp70 superfamily in *Arabidopsis thaliana*. *Cell Stress Chaperones.* 2001 Jul; 6(3):201-8
- Liepman AH, Olsen LJ.** Peroxisomal alanine: glyoxylate aminotransferase (AGT1) is a photorespiratory enzyme with multiple substrates in *Arabidopsis thaliana*. *Plant J.* 2001 Mar; 25(5):487-98
- Liepman AH, Olsen, LJ.** Alanine aminotransferase homologs catalyze the glutamate: glyoxylate aminotransferase reaction in peroxisomes of *Arabidopsis*. *Plant Physiol* 2003; 131, 215-227
- Lisenbee CS, Lingard MJ, Trelease RN.** Arabidopsis peroxisomes possess functionally redundant membrane and matrix isoforms of monodehydroascorbate reductase. *Plant J.* 2005 Sep; 43(6):900-14
- Leterrier M, Corpas FJ, Barroso JB, Sandalio LM, del Rio LA.** Peroxisomal monodehydroascorbate reductase. Genomic clone characterization and functional analysis under environmental stress conditions. *Plant Physiol.* 2005 Aug; 138(4):2111-23
- Lopez-Huertas E, Sandalio LM, del Rio LA.** Integral membrane polypeptides of pea leaf peroxisomes: Characterization and response to plant stress. *Plant Physiol Biochem* 1995, 33: 295-302
- MacRae TH.** Structure and function of small heat shock/alpha-crystallin proteins: established concepts and emerging ideas. *Cell Mol Life Sci.* 2000 Jun; 57(6):899-913. Review.
- Marzioch M, Erdmann R, Veenhuis M, Kunau WH.** PAS7 encodes a novel yeast member of the WD-40 protein family essential for import of 3-oxoacyl-CoA thiolase, a PTS2-containing protein, into peroxisomes. *EMBO J.* 1994 Oct 17; 13(20):4908-18
- Matsumura T, Otera H, Fujiki Y.** Disruption of the interaction of the longer isoform of Pex5p, Pex5pL, with Pex7p abolishes peroxisome targeting signal type 2 protein import in mammals. Study with a novel Pex5-impaired Chinese hamster ovary cell mutant. *J Biol Chem.* 2000 Jul 14; 275(28):21715-21
- Matsuzono Y, Kinoshita N, Tamura S, Shimozawa N, Hamasaki M, Ghaedi K, Wanders RJ, Suzuki Y, Kondo N, Fujiki Y.** Human PEX19: cDNA cloning by functional complementation, mutation analysis in a patient with Zellweger syndrome, and potential role in peroxisomal membrane assembly. *Proc Natl Acad Sci U S A.* 1999 Mar 2; 96(5):2116-21
- McCollum D, Monosov E, Subramani S.** The pas8 mutant of *Pichia pastoris* exhibits the peroxisomal protein import deficiencies of Zellweger syndrome cells--the PAS8 protein binds to the COOH-terminal tripeptide peroxisomal targeting signal, and is a member of the TPR protein family. *J Cell Biol.* 1993 May; 121(4):761-74
- McNew JA, Goodman JM.** An oligomeric protein is imported into peroxisomes *in vivo*. *J Cell Biol.* 1994 Dec; 127(5):1245-57

- Miernyk JA.** The 70 kDa stress-related proteins as molecular chaperones. *Trends Plant Sci* 1997; 2: 180-1878
- Miyagawa Y, Tamoi M, Shigeoka S.** Evaluation of the defense system in chloroplasts to photooxidative stress caused by paraquat using transgenic tobacco plants expressing catalase from *Escherichia coli*. *Plant Cell Physiol.* 2000 Mar;41(3):311-20
- Mizoguchi T, Hayashida N, Yamaguchi-Shinozaki K, Kamada H, Shinozaki K.** Two genes that encode ribosomal-protein S6 kinase homologs are induced by cold or salinity stress in *Arabidopsis thaliana*. *FEBS Lett.* 1995 Jan 23; 358(2):199-204
- Mogk A, Schlieker C, Strub C, Rist W, Weibezahn J, Bukau B.** Roles of individual domains and conserved motifs of the AAA+ chaperone ClpB in oligomerization, ATP hydrolysis, and chaperone activity. *J Biol Chem.* 2003 May 16; 278(20):17615-24
- Mogk A, Schlieker C, Friedrich KL, Schonfeld HJ, Vierling E, Bukau B.** Refolding of substrates bound to small Hsps relies on a disaggregation reaction mediated most efficiently by ClpB/DnaK. *J Biol Chem.* 2003 Aug 15; 278(33):31033-42
- Morrow G, Inaguma Y, Kato K, Tanguay RM.** The small heat shock protein Hsp22 of *Drosophila melanogaster* is a mitochondrial protein displaying oligomeric organization. *J Biol Chem.* 2000 Oct 6; 275(40):31204-10
- Motley AM, Hettema EH, Ketting R, Plasterk R, Tabak HF.** *Caenorhabditis elegans* has a single pathway to target matrix proteins to peroxisomes. *EMBO Rep.* 2000 Jul; 1(1):40-6
- Mukaiyama H, Oku M, Baba M, Samizo T, Hammond AT, Glick BS, Kato N, Sakai Y.** Paz2 and 13 other PAZ gene products regulate vacuolar engulfment of peroxisomes during micropexophagy. *Genes Cells.* 2002 Jan;7(1):75-90
- Mullen RT, Lee MS, Flynn CR, Trelease RN.** Diverse amino acid residues function within the type 1 peroxisomal targeting signal. Implications for the role of accessory residues upstream of the type 1 peroxisomal targeting signal. *Plant Physiol.* 1997 Nov; 115(3):881-9
- Nair DM, Purdue PE, Lazarow PB.** Pex7p translocates in and out of peroxisomes in *Saccharomyces cerevisiae*. *J Cell Biol.* 2004 Nov 22; 167(4):599-604
- Nair U, Klionsky DJ.** Molecular mechanisms and regulation of specific and nonspecific autophagy pathways in yeast. *J Biol Chem.* 2005 Oct 17; [Epub ahead of print]
- Neta-Sharir I, Isaacson T, Lurie S, Weiss D.** Dual role for tomato heat shock protein 21: protecting photosystem II from oxidative stress and promoting color changes during fruit maturation. *Plant Cell.* 2005 Jun;17(6):1829-38
- Neuberger G, Kunze M, Eisenhaber F, Berger J, Hartig A, Brocard C.** Hidden localization motifs: naturally occurring peroxisomal targeting signals in non-peroxisomal proteins. *Genome Biol.* 2004; 5(12):R97
- Neuberger G, Maurer-Stroh S, Eisenhaber B, Hartig A, Eisenhaber F.** Prediction of peroxisomal targeting signal 1 containing proteins from amino acid sequence. *J Mol Biol.* 2003 May 2;328(3):581-92
- Niedenthal RK, Riles L, Johnston M, Hegemann JH.** Green fluorescent protein as a marker for gene expression and subcellular localization in budding yeast. *Yeast.* 1996 Jun 30;12(8):773-86
- Noctor G, Foyer C.** Ascorbate and glutathione: keeping active oxygen under control. *Annu Rev Plant Physiol Plant Mol Biol.* 1998; 49:249-279
- Nover L and Miernyk JA.** A genomics approach to the chaperone network of *Arabidopsis thaliana*. *Cell Stress Chaperones.* 2001 July; 6(3): 175-176
- Nystrom T, Neidhardt FC.** Cloning, mapping and nucleotide sequencing of a gene encoding a universal stress protein in *Escherichia coli*. *Mol Microbiol.* 1992 Nov;6(21):3187-98
- Nystrom T, Neidhardt FC.** Isolation and properties of a mutant of *Escherichia coli* with an insertional inactivation of the uspA gene, which encodes a universal stress protein. *J Bacteriol.* 1993 Jul;175(13):3949-56
- Nystrom T, Neidhardt FC.** Expression and role of the universal stress protein, UspA, of *Escherichia coli* during growth arrest. *Mol Microbiol.* 1994 Feb;11(3):537-44

- Oatey PB, Lumb MJ, Danpure CJ.** Molecular basis of the variable mitochondrial and peroxisomal localisation of alanine-glyoxylate aminotransferase. *Eur J Biochem.* 1996 Oct 15; 241(2):374-85
- Oefner C, D'Arcy A, Winkler FK.** Crystal structure of human dihydrofolate reductase complexed with folate. *Eur J Biochem.* 1988 Jun 1; 174(2):377-85
- Oku M, Warnecke D, Noda T, Muller F, Heinz E, Mukaiyama H, Kato N, Sakai Y.** Peroxisome degradation requires catalytically active sterol glucosyltransferase with a GRAM domain. *EMBO J.* 2003 Jul 1; 22(13):3231-41
- Osakabe Y, Maruyama K, Seki M, Satou M, Shinozaki K, Yamaguchi-Shinozaki K.** Leucine-rich repeat receptor-like kinase1 is a key membrane-bound regulator of abscisic acid early signaling in *Arabidopsis*. *Plant Cell.* 2005 Apr; 17(4):1105-19
- Palma JM, Garrido M, Rodriguez-Garcia MI, del Rio LA.** Peroxisome proliferation and oxidative stress mediated by activated oxygen species in plant peroxisomes. *Arch Biochem Biophys.* 1991 May 15; 287(1):68-74
- Panaretou B, Prodromou C, Roe SM, O'Brien R, Ladbury JE, Piper PW, Pearl LH.** ATP binding and hydrolysis are essential to the function of the Hsp90 molecular chaperone *in vivo*. *EMBO J.* 1998 Aug 17; 17(16):4829-36
- Patharkar OR, Cushman JC.** A stress-induced calcium-dependent protein kinase from *Mesembryanthemum crystallinum* phosphorylates a two-component pseudo-response regulator. *Plant J.* 2000 Dec; 24(5):679-91
- Peltier JB, Emanuelsson O, Kalume DE, Ytterberg J, Friso G, Rudella A, Liberles DA, Soderberg L, Roepstorff P, von Heijne G, van Wijk KJ.** Central functions of the lumenal and peripheral thylakoid proteome of *Arabidopsis* determined by experimentation and genome-wide prediction. *Plant Cell.* 2002 Jan; 14(1):211-36
- Pearl LH, Prodromou C.** Structure and *in vivo* function of Hsp90. *Curr Opin Struct Biol.* 2000 Feb; 10(1):46-51. Review.
- Pires JR, Hong X, Brockmann C, Volkmer-Engert R, Schneider-Mergener J, Oschkinat H, Erdmann R.** The ScPex13p SH3 domain exposes two distinct binding sites for Pex5p and Pex14p. *J Mol Biol.* 2003 Mar 7; 326(5):1427-35
- Purdue PE, Lazarow PB.** Targeting of human catalase to peroxisomes is dependent upon a novel COOH-terminal peroxisomal targeting sequence. *J Cell Biol.* 1996 Aug; 134(4):849-62
- Purdue PE, Lazarow PB.** Peroxisome biogenesis. *Annu Rev Cell Dev Biol.* 2001; 17: 701-52
- Purdue PE, Zhang JW, Skoneczny M, Lazarow PB.** *Rhizomelic chondrodysplasia punctata* is caused by deficiency of human PEX7, a homologue of the yeast PTS2 receptor. *Nat Genet.* 1997 Apr; 15(4):381-4
- Rehling P, Brandner K, Pfanner N.** Mitochondrial import and the twin-pore translocase. *Nat Rev Mol Cell Biol.* 2004 Jul; 5(7):519-30
- Reumann S** (2002) The photorespiratory pathway of leaf peroxisomes. In *Plant Peroxisomes: Biochemistry, Cell Biology and Biotechnological Applications*, pp 141-189. Eds Baker A, Graham IA. Kluwer Academic Publishers, Dordrecht, The Netherlands
- Reumann S.** Specification of the peroxisome targeting signals type 1 and type 2 of plant peroxisomes by bioinformatics analyses. *Plant Physiol.* 2004 Jun; 135(2):783-800
- Reumann S, Ma C, Lemke S, Babujee L.** AraPeroX. A database of putative *Arabidopsis* proteins from plant peroxisomes. *Plant Physiol.* 2004 Sep; 136(1):2587-608
- Richmond TA, Bleecker AB.** A defect in beta-oxidation causes abnormal inflorescence development in *Arabidopsis*. *Plant Cell.* 1999 Oct; 11(10):1911-24
- Sakai Y, Koller A, Rangell LK, Keller GA, Subramani S.** Peroxisome degradation by microautophagy in *Pichia pastoris*: identification of specific steps and morphological intermediates. *J Cell Biol.* 1998 May 4; 141(3):625-36
- Sanders PM, Lee PY, Biesgen C, Boone JD, Beals TP, Weiler EW, Goldberg RB.** The *Arabidopsis* DELAYED DEHISCENCE1 gene encodes an enzyme in the jasmonic acid synthesis pathway. *Plant Cell.* 2000 Jul; 12(7):1041-61

- Sanger F, Nicklen S, Coulson AR.** DNA sequencing with chain-terminating inhibitors. *Proc Natl Acad Sci U S A.* 1977 Dec;74(12):5463-7
- Scharf KD, Siddique M, Vierling E.** The expanding family of *Arabidopsis thaliana* small heat stress proteins and a new family of proteins containing alpha-crystallin domains (Acid proteins). *Cell Stress Chaperones.* 2001 Jul; 6(3):225-37
- Schubert M, Petersson UA, Haas BJ, Funk C, Schroder WP, Kieselbach T.** Proteome map of the chloroplast lumen of *Arabidopsis thaliana*. *J Biol Chem.* 2002 Mar 8; 277(10):8354-65
- Schumann U, Wanner G, Veenhuis M, Schmid M, Gietl C.** AthPEX10, a nuclear gene essential for peroxisome and storage organelle formation during *Arabidopsis* embryogenesis. *Proc Natl Acad Sci U S A.* 2003 Aug 5; 100(16):9626-31
- Sharkey T.** Estimating the rate of photorespiration in leaves. *Physiologia Plantarum* 1988, 73: 147-152
- Soll J, Schleiff E.** Protein import into chloroplasts. *Nat Rev Mol Cell Biol.* 2004 Mar; 5(3):198-208
- Soukupova M, Sprenger C, Gorgas K, Kunau WH, Dodt G.** Identification and characterization of the human peroxin PEX3. *Eur J Cell Biol.* 1999 Jun; 78(6):357-74
- Sparkes IA, Baker A.** Peroxisome biogenesis and protein import in plants, animals and yeasts: enigma and variations? *Mol Membr Biol.* 2002 Jul-Sep; 19(3):171-85. Review.
- Sparkes IA, Brandizzi F, Slocombe SP, El-Shami M, Hawes C, Baker A.** An *Arabidopsis* pex10 null mutant is embryo lethal, implicating peroxisomes in an essential role during plant embryogenesis. *Plant Physiol.* 2003 Dec; 133(4):1809-19
- Stege GJ, Brunsting JF, Kampinga HH, Konings AW.** Thermotolerance and nuclear protein aggregation: protection against initial damage or better recovery? *J Cell Physiol.* 1995 Sep;164(3):579-86
- Stintzi A, Browse J.** The *Arabidopsis* male-sterile mutant, opr3, lacks the 12-oxophytodienoic acid reductase required for jasmonate synthesis. *Proc Natl Acad Sci U S A.* 2000 Sep 12; 97(19):10625-30
- Stone JM, Walker JC.** Plant protein kinase families and signal transduction. *Plant Physiol.* 1995 Jun; 108(2):451-7. Review.
- Stromer T, Fischer E, Richter K, Haslbeck M, Buchner J.** Analysis of the regulation of the molecular chaperone Hsp26 by temperature-induced dissociation: the N-terminal domain is important for oligomer assembly and the binding of unfolding proteins. *J Biol Chem.* 2004 Mar 19;279(12):11222-8
- Stromhaug PE, Bevan A, Dunn WA Jr.** GSA11 encodes a unique 208-kDa protein required for pexophagy and autophagy in *Pichia pastoris*. *J Biol Chem.* 2001 Nov 9;276(45):42422-35
- Studer S, Narberhaus F.** Chaperone activity and homo- and hetero-oligomer formation of bacterial small heat shock proteins. *J Biol Chem.* 2000 Nov 24;275(47):37212-8
- Studer S, Obrist M, Lentze N, Narberhaus F.** A critical motif for oligomerization and chaperone activity of bacterial alpha-heat shock proteins. *Eur J Biochem.* 2002 Jul; 269(14):3578-86
- Subramani S, Koller A, Snyder WB.** Import of peroxisomal matrix and membrane proteins. *Annu Rev Biochem.* 2000; 69:399-418
- Sun W, Bernard C, van de Cotte B, Van Montagu M, Verbruggen N.** At-HSP17.6A, encoding a small heat-shock protein in *Arabidopsis*, can enhance osmotolerance upon overexpression. *Plant J.* 2001 Sep; 27(5):407-15
- Sun W, Van Montagu M, Verbruggen N.** Small heat shock proteins and stress tolerance in plants. *Biochim Biophys Acta.* 2002 Aug 19;1577(1):1-9
- Swinkels BW, Gould SJ, Bodnar AG, Rachubinski RA, Subramani S.** A novel, cleavable peroxisomal targeting signal at the amino-terminus of the rat 3-ketoacyl-CoA thiolase. *EMBO J.* 1991 Nov; 10(11):3255-62
- Terlecky SR, Nuttley WM, McCollum D, Sock E, Subramani S.** The *Pichia pastoris* peroxisomal protein PAS8p is the receptor for the C-terminal tripeptide peroxisomal targeting signal. *EMBO J.* 1995 Aug 1; 14(15):3627-34

- Thomas G, Hall MN.** TOR signalling and control of cell growth. *Curr Opin Cell Biol.* 1997 Dec;9(6):782-7
- Thompson AR, Doelling JH, Suttangkakul A, Vierstra RD.** Autophagic nutrient recycling in *Arabidopsis* directed by the ATG8 and ATG12 conjugation pathways. *Plant Physiol.* 2005 Aug; 138(4):2097-110
- Thompson AR, Vierstra RD.** Autophagic recycling: lessons from yeast help define the process in plants. *Curr Opin Plant Biol.* 2005 Apr;8(2):165-73
- Tissieres A, Mitchell HK, Tracy UM.** Protein synthesis in salivary glands of *Drosophila melanogaster*: relation to chromosome puffs. *J Mol Biol.* 1974 Apr 15; 84(3):389-98
- Titorenko VI, Rachubinski RA.** Dynamics of peroxisome assembly and function. *Trends Cell Biol.* 2001 Jan; 11(1):22-29. Review.
- Todt D.** Recent advances in the study of Hsp90 structures and mechanism of action. *Trends Endocrinol Metabol* 1998 9: 238-243
- Tsukamoto T, Hata S, Yokota S, Miura S, Fujiki Y, Hijikata M, Miyazawa S, Hashimoto T, Osumi T.** Characterization of the signal peptide at the amino terminus of the rat peroxisomal 3-ketoacyl-CoA thiolase precursor. *J Biol Chem.* 1994 Feb 25; 269(8):6001-10
- Tuttle DL, Dunn WA Jr.** Divergent modes of autophagy in the methylotrophic yeast *Pichia pastoris*. *J Cell Sci.* 1995 Jan; 108 (Pt 1):25-35
- Tuttle DL, Lewin AS, Dunn WA Jr.** Selective autophagy of peroxisomes in methylotrophic yeasts. *Eur J Cell Biol.* 1993 Apr;60(2):283-90
- Vandenabeele S, Vanderauwera S, Vuylsteke M, Rombauts S, Langebartels C, Seidlitz HK, Zabeau M, Van Montagu M, Inze D, Van Breusegem F.** Catalase deficiency drastically affects gene expression induced by high light in *Arabidopsis thaliana*. *Plant J.* 2004 Jul; 39(1):45-58
- Vanderauwera S, Zimmermann P, Rombauts S, Vandenabeele S, Langebartels C, Gruissem W, Inze D, Van Breusegem F.** Genome-wide analysis of hydrogen peroxide-regulated gene expression in *Arabidopsis* reveals a high light-induced transcriptional cluster involved in anthocyanin biosynthesis. *Plant Physiol.* 2005 Oct;139(2):806-21
- van Montfort RL, Basha E, Friedrich KL, Slingsby C, Vierling E.** Crystal structure and assembly of a eukaryotic small heat shock protein. *Nat Struct Biol.* 2001 Dec;8(12):1025-30
- Veenhuis M, Komori M, Salomons F, Hilbrands RE, Hut H, Baerends RJ, Kiel JA, van der Klei IJ.** Peroxisomal remnants in peroxisome-deficient mutants of the yeast *Hansenula polymorpha*. *FEBS Lett.* 1996 Mar 25;383(1-2):114-8
- Veinger L, Diamant S, Buchner J, Goloubinoff P.** The small heat-shock protein IbpB from *Escherichia coli* stabilizes stress-denatured proteins for subsequent refolding by a multichaperone network. *J Biol Chem.* 1998 May 1;273(18):11032-7
- Vicentini F, Matile P** Gerontosomes, a multifunctional type of peroxisomes in senescent leaves. *J Plant Physiol* 1993 142, 50-56
- Vierling E.** The roles of heat shock proteins in plants. *Annu Rev Plant Physiol Plant Mol Biol* 1991 42: 579-620
- Walton PA, Wendland M, Subramani S, Rachubinski RA, Welch WJ.** Involvement of 70-kD heat-shock proteins in peroxisomal import. *J Cell Biol.* 1994 Jun; 125(5):1037-46
- Waters ER.** The molecular evolution of small heat-shock proteins in plants. *Genetics.* 1995 141: 785-795
- Waters ER, Lee GJ, Vierling E.** Evolution, structure and function of the small heat shock proteins in plants. *J Exp Bot.* 1996; 47: 325-338
- Webb MA, Newcomb EH.** Cellular compartmentation of ureide biogenesis in root nodules of cowpea (*Vigna unguiculata* (L.) Walp). *Planta* 1987 **172**: 162-175
- Wehmeyer N, Hernandez LD, Finkelstein RR, Vierling E.** Synthesis of small heat-shock proteins is part of the developmental program of late seed maturation. *Plant Physiol.* 1996 Oct;112(2):747-57
- Weigel D, Glazebrook J.** *Arabidopsis*: a laboratory manual. 2002. Cold spring harbor laboratory press, cold spring harbor, New York.

- Willekens H, Chamnongpol S, Davey M, Schraudner M, Langebartels C, Van Montagu M, Inze D, Van Camp W.** Catalase is a sink for H₂O₂ and is indispensable for stress defence in C3 plants. *EMBO J.* 1997 Aug 15;16(16):4806-16
- Wimmer B, Lottspeich F, van der Klei I, Veenhuis M, Gietl C.** The glyoxysomal and plastid molecular chaperones (70-kDa heat shock protein) of watermelon cotyledons are encoded by a single gene. *Proc Natl Acad Sci U S A* 1997 Dec 9; 94(25):13624-9
- Wimmer C, Schmid M, Veenhuis M, Gietl C.** The plant PTS1 receptor: similarities and differences to its human and yeast counterparts. *Plant J.* 1998 Nov; 16(4):453-64
- Woodward AW, Bartel B.** The *Arabidopsis* peroxisomal targeting signal type 2 receptor PEX7 is necessary for peroxisome function and dependent on PEX5. *Mol Biol Cell.* 2005 Feb; 16(2):573-83
- Yang T, Poovaiah BW.** Hydrogen peroxide homeostasis: activation of plant catalase by calcium/calmodulin. *Proc Natl Acad Sci U S A.* 2002 Mar 19; 99(6):4097-102
- Yang X, Purdue PE, Lazarow PB.** Eci1p uses a PTS1 to enter peroxisomes: either its own or that of a partner, Dci1p. *Eur J Cell Biol.* 2001 Feb;80(2):126-38
- Yoshimoto K, Hanaoka H, Sato S, Kato T, Tabata S, Noda T, Ohsumi Y.** Processing of ATG8s, ubiquitin-like proteins, and their deconjugation by ATG4s are essential for plant autophagy. *Plant Cell.* 2004 Nov; 16(11):2967-83
- Yu C, Huang AH.** Conversion of serine to glycerate in intact spinach leaf peroxisomes: role of malate dehydrogenase. *Arch Biochem Biophys.* 1986;245: 125-133
- Zantema A, Verlaan De Vries M, Maasdam D, Bol S, and van der Eb A.** Heat shock protein 27 and alpha B-crystallin can form a complex, which dissociates by heat shock. *J. Biol. Chem.* 1992; 267:12936-12941
- Zhang H, Wang J, Nickel U, Allen RD, Goodman HM.** A novel isoenzyme of ascorbate peroxidase localized on glyoxysomal and leaf peroxisomal membranes in pumpkin. *Plant and Cell Physiology* 1997; 36: 1157–1162
- Zimmermann P, Hirsch-Hoffmann M, Hennig L, Gruissem W.** GENEVESTIGATOR. *Arabidopsis* microarray database and analysis toolbox. *Plant Physiol.* 2004 Sep;136(1):2621-32
- Zolman BK, Silva ID, Bartel B.** The *Arabidopsis* pxa1 mutant is defective in an ATP-binding cassette transporter-like protein required for peroxisomal fatty acid beta-oxidation. *Plant Physiol.* 2001 Nov; 127(3):1266-78

7. APPENDICES

7.1 Primers used for gene cloning and subcloning

Constructs	Oligos	Sequences
AtHsp15.7 (At5g37670) in pGEMT	SR57f	CGG <u>TCTAGAA</u> TGGCAGACAGAGGAATATTCTTG
	SR58r	AAT <u>CCCGGGTCAA</u> AGCTTGCTAGTAAT
AtHsp15.7 in pGFP-N-FUS	SR57f	CGG <u>TCTAGAA</u> TGGCAGACAGAGGAATATTCTTG
	SR58r	AAT <u>CCCGGGTCAA</u> AGCTTGCTAGTAAT
EYFP-AtHsp15.7 in pCAT-Nfus	SR77f	ACATAAGATT <u>GCGGCCGCT</u> ATGGCAGACAGAGGAATATTC
	SR78r	CCT <u>TCTAGATCAA</u> AGCTTGCTAGTAAT
EYFP-AtHsp15.7ΔC pCAT-Nfus	SR77f	ACATAAGATT <u>GCGGCCGCT</u> ATGGCAGACAGAGGAATATTC
	SR102r	ATAT <u>TCTAGATCAC</u> GATGAAGTGTCTTAGG
AtHsp15.7 ΔC-EYFP pCAT-Cfus	SR103f	GAT <u>CCATGGCAGAC</u> AGAGGAATATT
	SR104r	AT <u>ACCATGGATGA</u> AGTGTCTTAGGAAC
AtHsp15.7ΔPTS1 in pYES2.1	SR236f	GAATATGGCAGACAGAGGAAT
	SR237r	GTATCAAGTAATATTAACATTCCTAAC
AtHsp15.7-pGBKT7	SR103f	GAT <u>CCATGGCAGAC</u> AGAGGAATATT
	SR58r	AAT <u>CCCGGGTCAA</u> AGCTTGCTAGTAAT
AtAc31.2 (At1g06460) in pGEMT	SR150f	ACT <u>GCGGCCGCT</u> ATGGAGCATGAATCTATCAC
	SR151r	TCAAAGCTTTGGAATTACTATTCTCAG
EYFP-AtAc31.2 pCAT-Nfus	SR150f	ACT <u>GCGGCCGCT</u> ATGGAGCATGAATCTATCAC
	SR151r	TCAAAGCTTTGGAATTACTATTCTCAG
AtAc31-EYFP pCAT-Cfus	SR186f	CACTA <u>ACCATGGAG</u> CATGAATCTATCAC
	SR187r	TGCTC <u>ACCATGGAA</u> AGCTTTGGAATTACTATTC
AtAc31.2ΔN-EYFP pCAT-Cfus	SR188f	CACTA <u>ACCATGGC</u> ATCTCTCGTCCCCTTG
	SR187r	TGCTC <u>ACCATGGAA</u> AGCTTTGGAATTACTATTC
EYFP-AtAc31.2ΔPTS1 pCAT-Nfus	SR150f	ACT <u>GCGGCCGCT</u> ATGGAGCATGAATCTATCAC
	SR239r	GATCAAATTACTATTCTCAGAATCC
AtAc31.2-EYFP(H11→D) pCAT-Cfus	SR316f	AGGCTCGCTGCCTTCGCCGCG <u>G</u> ACTTCCCGGCAACCAGTTACGATTC CG
	SR317r	CGGAATCGTAACTGTTGCCGGGAAGT <u>C</u> GCGGCGAAGGCAGCGAG CCT
AtAc31.2-EYFP(K284→E) pCAT-Nfus	SR318f	GGGATTCTGAGAATAGTAATTCAGAGCTCTGAGCGGCCG CTCTAGAG
	SR319r	CTCTAGAGCG GCCGCTCAGA GCTCTGGAAT TACTATTCTC AGAATCCC
EYFP-AtAc31.2ΔPTS1 pYES2.1	SR238f	AGAGATGGAGCATGAATCTATC
	SR239r	GATCAAATTA CTATTCTCAGAATCC
EYFP-AtAc31.2ΔPTS1+2 pYES2.1	SR188f	CACTA <u>ACCATGGC</u> ATCTCTCGTCCCCTTG

EYFP-PPP3	SR73f	GAATAAGATT <u>GCGGCCGCT</u> ATGGAAGAGGATTATCAAC
	SR74r	AGCTCTAGATCACAATGTGAACCGGA
EYFP-PTD _{ppk3}	SR157f	AAGTCCATGGTGAGCAAGGGCGAGGA
	SR204r	TATATCTAGATCACAATGTGAACCGGATGATGAGCCGTCATGCTTGT ACAGCTCGTCCATGCC
PPP4 (At3g61960)-pGEMT	SR19f	GTTTCTAGAATGGAGTCGGCACGACTTGTGGGTGA
	SR20r	GATCCCGGGCTAAAGATGAGACCGACGATG
GFP-PPP4	SR19f	GTTTCTAGAATGGAGTCGGCACGACTTGTGGGTGA
	SR20r	GATCCCGGGCTAAAGATGAGACCGACGATG
EYFP-PPP4	SR73f	ACATAAGTAAGCGGCCGCTATGGAGTCGGCACGACTTGTG
	SR74r	TGTTCTAGACTAAAGATGAGACCGACG
EYFP-PTD _{PPP4}	SR157f	AAGTCCATGGTGAGCAAGGGCGAGGA
	SR156r	TATATCTAGACTAAAGATGAGACCGACGATGCTGTAAGTTAGACTTGT ACAGCTCGTCCATGCC
EYFP-PTD _{ΔRPPP4}	SR157f	AAGTCCATGGTGAGCAAGGGCGAGGA
	SR282r	TATATCTAGACTAAAGATGAGATGCTCCATGCTGTAAGTTAGACTTGT CAGCTCGTCCATGCC
PPP4 (At3g61960)-pGEMT	SR19f	GTTTCTAGAATGGAGTCGGCACGACTTGTGGGTGA
	SR20r	GATCCCGGGCTAAAGATGAGACCGACGATG
GFP-PPP4	SR19f	GTTTCTAGAATGGAGTCGGCACGACTTGTGGGTGA
	SR20r	GATCCCGGGCTAAAGATGAGACCGACGATG
EYFP-PPP4	SR73f	ACATAAGTAAGCGGCCGCTATGGAGTCGGCACGACTTGTG
	SR74r	TGTTCTAGACTAAAGATGAGACCGACG
EYFP-PTD _{PPP4}	SR157f	AAGTCCATGGTGAGCAAGGGCGAGGA
	SR156r	TATATCTAGACTAAAGATGAGACCGACGATGCTGTAAGTTAGACTTGT ACAGCTCGTCCATGCC
EYFP-PTD _{PPP4ΔR}	SR157f	AAGTCCATGGTGAGCAAGGGCGAGGA
	SR282r	TATATCTAGACTAAAGATGAGATGCTCCATGCTGTAAGTTAGACTTGT CAGCTCGTCCATGCC
AtAtg1a (K72→R) in pGEMT	SR290f	GGTTTAGAAGTTGCCGTCAGAGAGATTGATAAGAAGCTTCTTAGCCCT AA AGTAAG
	SR291r	CTTACTTTAGGGCTAAGAAGCTTCTTATCAATCTCTCTGACGGCAACTT C TAAACC
AtAtg1a(1-300)-pGBKT7	SR258f	TATAGGATCCGTATGGAGTCGGCACGACTTG
	SR284r	TATACTGCAGCTAAAGTGAAGTTCGATGAAAC
AtAtg1a(1-300)-pGBKT7	SR258f	TATAGGATCCGTATGGAGTCGGCACGACTTG
	SR284r	TATACTGCAGCTAAAGTGAAGTTCGATGAAAC
AtAtg1a (300-623)-pGBKT7	SR260f	TATAGGATCCGTAACCGTTTTAAATCAAGTG
	SR261r	ATATACTGCAGCTACCGACGATGCTGTAAGTTAG
EYFP-PTD _{PPP5}	SR157f	AAGTCCATGGTGAGCAAGGGCGAGGA
	SR211r	TATATCTAGATCACAATCTAGAAGGCTGGATTTCGTTTCAGCAGCTTGT ACAGCTCGTCCATGCC
EYFP-PTD _{PPP6}	SR157f	AAGTCCATGGTGAGCAAGGGCGAGGA
	SR274r	TATATCTAGACTACAAGTTGGATGTGGTCCGATGAAGGAATGACTTGT ACAGCTCGTCCATGCC
EYFP-PTD _{PPP7}	SR157f	AAGTCCATGGTGAGCAAGGGCGAGGA

	SR212r	TATATCTAGATCAAATCTTTGCATCTGTTGTTATATCATTATCCTTGTAC AGCTCGTCCATGCC
EYFP-PPPK7	SR296f	AATT <u>GCGGCCGC</u> TATGACATCTCAGCTAAAACG
	SR229r	TGAT <u>CCCGGG</u> TCAAATCTTT GCATCTGTTG
PPPK7-pGBKT7	SR234f	AATT <u>CCCGGG</u> TATGACATCTCAGCTAAAACG
	SR235r	CTACAGTCGACTCAAATCTTTGCATCTGTTG
AtAtg13a (At3g49590) in pGEMT	SR248f	CACTA <u>ACCATGG</u> ATTTTCCAGAGAATTTG
	SR249r	ATATC <u>ACCATGG</u> AGTGGACGCGAGTTGGTCCAG
AtAtg13a(1-63) EYFP	SR248f	CACTA <u>ACCATGG</u> ATTTTCCAGAGAATTTG
	SR294r	TATA <u>CCATGG</u> CCATCACAAGATTAAACC
AtAtg13a(1-120) EYFP	SR248f	CACTA <u>ACCATGG</u> ATTTTCCAGAGAATTTG
	SR266r	TATA <u>CCATGG</u> AACGCTCAATCACAGTCTC
AtAtg13a (340-500)-pGADT7	SR277f	TATAG <u>AATCCT</u> CACCATCGG GTTCTCCA
	SR278r	TATAG <u>GATCC</u> TCAACTATGG CTGTACTGAA G
Pex5-TPR-pGADT7	SR225f	TATA <u>CCCGGG</u> TTATGTGGGTCACCCTGAAC
	SR226r	TATA <u>ATCGATT</u> CACAGCGGGAATTCTTTCTG

7.2 Abbreviations

Acd	α -crystallin domain
AD	activation domain
3-AT	3-amino-1,2,4-triazole
Amp	ampicillin
Amp ^R	ampicillin resistance
APS	ammonium peroxy disulfate
APX	ascorbate peroxidase
ASC	ascorbate peroxidase
ATP	adenosine 5' triphosphate
BD	binding domain
bp	base pair
CAT	catalase
cDNA	complementary DNA
CDPK	calcium-dependent protein kinase
CoxIV	cytochrome c oxidase subunit IV
dd H ₂ O	double distilled water
DHA	dehydroascorbate
DMSO	dimethyl sulfoxide
DNA	deoxyribonucleic acid
dNTPs	deoxyribonucleotides
DTT	dithiothreitol
ECFP	enhanced cyan fluorescence protein
EDTA	ethylenediamine tetraacetic acid
EST	expressed sequence tag
EYFP	enhance yellow fluorescence protein
GFP	green fluorescent protein
GR	glutathione reductase
HPR	hydroxypyruvate reductase
Hsp	heat shock protein
IPTG	isopropyl- β -D-thiogalactopyranoside

kb	kilobase pair
kDa	kilodalton
Km	kanamycin
Km ^R	kanamycin resistance
LB-medium	Luria-Bertani medium
MDH	malate dehydrogenase
MDHA	monodehydroascorbate
MDHAR	monodehydroascorbate reductase
MS medium	Murashige-Skoog medium
NLS	Nuclear localization signals
ORF	open reading frame
PAGE	polyacrylamide gel electrophoresis
PCR	polymerase chain reaction
Pex	peroxin
pl	isoelectric point
PMSF	phenyl methyl sulfonyl fluoride
PPPK	putative peroxisomal protein kinase
PTS	peroxisomal targeting signal
PTD	peroxisomal targeting domain
RNA	ribonucleic acid
ROS	reactive oxygen species
RT	reverse transcription
SEM	scanning electron microscopy
SOD	superoxide dismutase
<i>Taq</i>	<i>Thermus aquaticus</i>
TEMED	N,N,N',N'-tetramethylene diamine
T _m	melting temperature
TPR	tetratricopeptide repeat
USPA	universal stress protein A
v/v	volume to volume
w/v	weight to weight
w/w	weight to weight
X-Gal	5-bromo-4-chloro-3-indolyl-β-D-galactopyranoside
XOD	xanthine oxidase

7.3 List of figures and Tables

Figure 1.1: Model proposed for the production of ROS in plant peroxisomes and their subsequent detoxification by multiple scavenging systems (according to del Rio et al., 2002).

Figure 1.2: Import of peroxisomal matrix protein (according to Baker and Sparkes, 2005).

Figure 1.3: Overview of peroxisome sequestration via two distinct modes of pexophagy (according to Oku et al., 2003).

Figure 1.4: Oligomeric structure of sHsps (according to Haslbeck et al., 2005).

Figure 2.1: Biolistic PDS-1000/He Particle Delivery system

Figure 2.2 Diagram of the location of LP, RP and BP used for genomic PCR

Figure 3.1: Domain structure and predicted targeting signals of AtHsp15.7 and AtAc31.2.

Figure 3.2: Conservation of putative PTSs in plant homologs of AtHsp15.7 and AtAc31.2.

Figure 3.3: Diagram of constructed fusion proteins between AtHsp15.7 and EYFP.

Figure 3.4: Subcellular targeting analysis of AtHsp15.7 in onion epidermal cells (*Allium cepa* L.).

Figure 3.5: Identification of AtHsp15.7 in isolated leaf peroxisomes.

Figure 3.6: Diagram of constructed fusion proteins between AtAcd31.2 and EYFP.

Figure 3.7: Subcellular targeting analysis of AtAcd31.2 in onion epidermal cells (*Allium cepa*).

Figure 3.8 Complementation studies of single and double deletion strains of *S. cerevisiae* deficient in ScHsp42 and ScHsp26 with plant peroxisomal sHsps.

Figure 3.9: Reduction of protein aggregation in *S. cerevisiae* ScHsp42 and ScHsp26 deletion strains by plant peroxisomal sHsps.

Figure 3.10: Relative tissue-specific and developmental expression levels of *AtHSP15.7* and *AtACD31.2*.

Figure 3.11: The effects of temperature stress on *AtHSP15.7* and *AtACD31.2* mRNA levels.

Figure 3.12: Expression of *AtHSP15.7* and *AtACD31.2* under oxidative stress conditions.

Figure 3.13: Characterization of three mutant alleles of *AtHSP15.7*.

Figure 3.14: Identification and characterization of the *acd31.2-1* knock-out mutant by genomic PCR.

Figure 3.15: Identification of an *hsp15.7/acd31.2* homozygous knock-out mutant by genomic PCR.

Figure 3.16: Heat stress phenotype of *hsp15.7-3* during germination.

Figure 3.16: Heat stress phenotype of *hsp15.7-3* during germination.

Figure 3.18: Subcellular targeting analysis of PPPK1 to PPPK4 in *S. cerevisiae*.

Figure 3.19: Subcellular targeting analysis of PPPK1 to PPPK4 in onion epidermal cells (*Allium cepa* L.).

Figure 3.20: Subcellular targeting analysis of putative PTS1 targeting domains of PPPKs in onion epidermal cells.

Figure 3.21: Functional analysis of amino acid residues located upstream of PTS1 tripeptides.

Figure 3.22: Protein-protein interaction between PPPK7 and the PTS1 receptor, AtPex5 as detected by the yeast two-hybrid system.

Figure 3.23: Sequence comparison of the *Arabidopsis* Atg13 homologs with *S. cerevisiae* Atg13 protein.

Figure 3.24: Relative expression of *Arabidopsis* ATG1 and ATG13 homologs.

Figure 3.25: Subcellular localization analysis of AtAtg13a in onion epidermal cells.

Figure 3.26: Protein-protein interaction between AtAtg1a and AtAtg13a as detected by yeast two-hybrid assays.

ACKNOWLEDGEMENT

I am extremely thankful to Prof. Dr. H. W. Heldt for his constant support and invaluable suggestions and also for accepting to be on my doctoral committee as the referent.

I am deeply grateful to Prof. Dr. Ivo Feussner for giving an opportunity to do research in his lab and for provision of the nice scientific environment and also for his invaluable suggestions, encouragement, and continuous interest in my work.

I sincere thank to my supervisor, Dr. Sigrun Reumann, who provides me the opportunity to join her group, introduces me into the very exciting "peroxisome world" and guides me throughout my Ph.D thesis. During the last three and a half years, I have learned a lot from her, not only knowledge and science experiment, but only also how to be a good scientist. I thank her a second time for her taking care of my life in Germany.

I thank Dr. Martin Fulda for bring the transient onion epidermal cells expression system to the lab, and for giving me invaluable suggestion and also proof-reading this manuscript. I thank Dr. Ellen Hornung and Dr. Ingo Heilmann for their invaluable suggestions, help and proof-reading this manuscript.

I thank Prof. Dieter Heineke for give me advice on documents of my Ph.D study.

I thank for my colleague Dr. Lavanya babujee for working closely together and for her critical reading of the manuscript. I thank other group members, Gabriele Ertl, Caroline Meyer, Franziska Lueder, Dr. Xuan Wang and Dr. Olga Voiteskhovskaja for a great enjoyable working atmosphere.

I thank the lab members in the plant biochemistry department Jan-Gerrit Carsjens, Cornelia Göbel, Mareike Hoffmann, Danuta Kaczmarzyk, Sabine König, Martina Körner, Susan Kunze, Imke Lang, Alena Liavonchanka, Maike Rudolph, Michael Scharnewski, Irene Stenzel, Annett Struß, Michael Stumpe, Martin Wagner, Anna Zdyb for encouragement and support to finish this dissertation.

I thank Dr. M. Haslbeck for cooperation of the sHsp project and providing me the nice yeast complementation pictures.

I sincere thank Gerd Mader for his technical assistant and Heike Lott for helping prepare for all kinds of document. I thank to our gardeners Uwe Wedemeyer and Suzanne Mester.

This dissertation is dedicated to my parents, Litong Ma and Shulan Bi, who have given me all their love and unconditional support. Along the way, my sister Ma Xiaoling and brother Changjiang Ma have shared their caring thoughts. Without them, there is no way I could possibly have accomplished this. I sincerely thank my girl friend Pingping Wang for her support, for being with me and for her love.

LEBENS LAUF

NAME	Changle Ma
GEBURT	14.05.1978 in Zibo, Shandong Province, P.R. China
STAATSANGEHÖRIGKEIT	chinesisch
1992-1995	Oberschule in Zibo (No. 6), Shandong Province, P.R.
China 1995	Schulabschluß: Abitur-Equivalent

UNIVERSITÄTSSTUDIUM

1995-1999	Studium (undergraduate studies) an der Shandong Normal University (Jinan, Shandong Province, P.R. China), Fakultät für Biologie
1999-2002	Studium (graduate studies) am Key Laboratory of Plant Streß, Shandong Normal University (Jinan, Shandong Province, P.R. China)
2002	Studiumsabschluß: Master of Science; Thema der Masterarbeit: "Molecular cloning and characterization of salt stress related genes from <i>Suaeda salsa</i> ."
seit 6/2002	Promotion in der Abteilung Biochemie der Pflanze des Albrecht-von-Haller-Institut für Pflanzenwissenschaften, Universität Göttingen, Institutsleiter: Prof. I. Feußner, Gruppenleiterin: Dr. S. Reumann